

LI

LABORATORY INVESTIGATION

THE BASIC AND TRANSLATIONAL PATHOLOGY RESEARCH JOURNAL

VOLUME 99 | SUPPLEMENT 1 | MARCH 2019

 **USCAP 2019**

ABSTRACTS

**GASTROINTESTINAL
PATHOLOGY**
(578-775)

USCAP 108TH ANNUAL MEETING

 **UNLOCKING**
YOUR **INGENUITY**

MARCH 16-21, 2019

National Harbor, Maryland
Gaylord National Resort & Convention Center

Published by
SPRINGER NATURE
www.ModernPathology.org

 **USCAP**
Creating a Better Pathologist

AN OFFICIAL JOURNAL OF THE
UNITED STATES AND CANADIAN
ACADEMY OF PATHOLOGY

EDUCATION COMMITTEE

Jason L. Hornick, Chair
Rhonda K. Yantiss, Chair, Abstract Review Board
 and Assignment Committee
Laura W. Lamps, Chair, CME Subcommittee
Steven D. Billings, Interactive Microscopy Subcommittee
Shree G. Sharma, Informatics Subcommittee
Raja R. Seethala, Short Course Coordinator
Ilan Weinreb, Subcommittee for Unique Live Course Offerings
David B. Kaminsky (Ex-Officio)
Aleodor (Doru) Andea
Zubair Baloch
Olca Basturk
Gregory R. Bean, Pathologist-in-Training
Daniel J. Brat
Ashley M. Cimino-Mathews

James R. Cook
Sarah M. Dry
William C. Faquin
Carol F. Farver
Yuri Fedoriw
Meera R. Hameed
Michelle S. Hirsch
Lakshmi Priya Kunju
Anna Marie Mulligan
Rish Pal
Vinita Parkash
Anil Parwani
Deepa Patil
Kwun Wah Wen, Pathologist-in-Training

ABSTRACT REVIEW BOARD

Benjamin Adam
Michelle Afkhami
Narasimhan (Narsi) Agaram
Rouba Ali-Fehmi
Ghassan Allo
Isabel Alvarado-Cabrero
Christina Arnold
Rohit Bhargava
Justin Bishop
Jennifer Boland
Elena Brachtel
Marilyn Bui
Shelley Caltharp
Joanna Chan
Jennifer Chapman
Hui Chen
Yingbei Chen
Benjamin Chen
Rebecca Chernock
Beth Clark
James Conner
Alejandro Contreras
Claudiu Cotta
Timothy D'Alfonso
Farbod Darvishian
Jessica Davis
Heather Dawson
Elizabeth Demicco
Suzanne Dintzis
Michelle Downes
Daniel Dye
Andrew Evans
Michael Feely
Dennis Firchau
Larissa Furtado
Anthony Gill
Ryan Gill
Paula Ginter

Tamara Giorgadze
Raul Gonzalez
Purva Gopal
Anuradha Gopalan
Jennifer Gordetsky
Rondell Graham
Alejandro Gru
Nilesh Gupta
Mamta Gupta
Krisztina Hanley
Douglas Hartman
Yael Heher
Walter Henricks
John Higgins
Mai Hoang
Mojgan Hosseini
Aaron Huber
Peter Illei
Doina Ivan
Wei Jiang
Vickie Jo
Kirk Jones
Neerja Kambham
Chiah Sui (Sunny) Kao
Dipti Karamchandani
Darcy Kerr
Ashraf Khan
Rebecca King
Michael Kluk
Kristine Konopka
Gregor Krings
Asangi Kumarapeli
Alvaro Laga
Cheng-Han Lee
Zaibo Li
Haiyan Liu
Xiuli Liu
Yan-Chun Liu

Tamara Lotan
Anthony Magliocco
Kruti Maniar
Jonathan Marotti
Emily Mason
Jerri McLemore
Bruce McManus
David Meredith
Anne Mills
Neda Moatamed
Sara Monaco
Atis Muehlenbachs
Bitu Naini
Dianna Ng
Tony Ng
Ericka Olgaard
Jacqueline Parai
Yan Peng
David Pisapia
Alexandros Polydorides
Sonam Prakash
Manju Prasad
Peter Pytel
Joseph Rabban
Stanley Radio
Emad Rakha
Preetha Ramalingam
Priya Rao
Robyn Reed
Michelle Reid
Natasha Rekhtman
Michael Rivera
Michael Roh
Andres Roma
Avi Rosenberg
Esther (Diana) Rossi
Peter Sadow
Safia Salaria

Steven Salvatore
Souzan Sanati
Sandro Santagata
Anjali Saqi
Frank Schneider
Jeanne Shen
Jiaqi Shi
Wun-Ju Shieh
Gabriel Sica
Deepika Sirohi
Kalliopi Siziopikou
Lauren Smith
Sara Szabo
Julie Teruya-Feldstein
Gaetano Thiene
Khin Thway
Rashmi Tondon
Jose Torrealba
Evi Vakiani
Christopher VandenBussche
Sonal Varma
Endi Wang
Christopher Weber
Olga Weinberg
Sara Wobker
Mina Xu
Shaofeng Yan
Anjana Yeldandi
Akihiko Yoshida
Gloria Young
Minghao Zhong
Yaolin Zhou
Hongfa Zhu
Debra Zynger

578 Improved Risk Stratification with Gene Expression Testing in Gastrointestinal Stromal Tumors

Benjamin Adam¹, Klaudia Nowak¹, Iyare Izevbaye¹

¹University of Alberta, Edmonton, AB

Disclosures: Benjamin Adam: None; Klaudia Nowak: None; Iyare Izevbaye: None

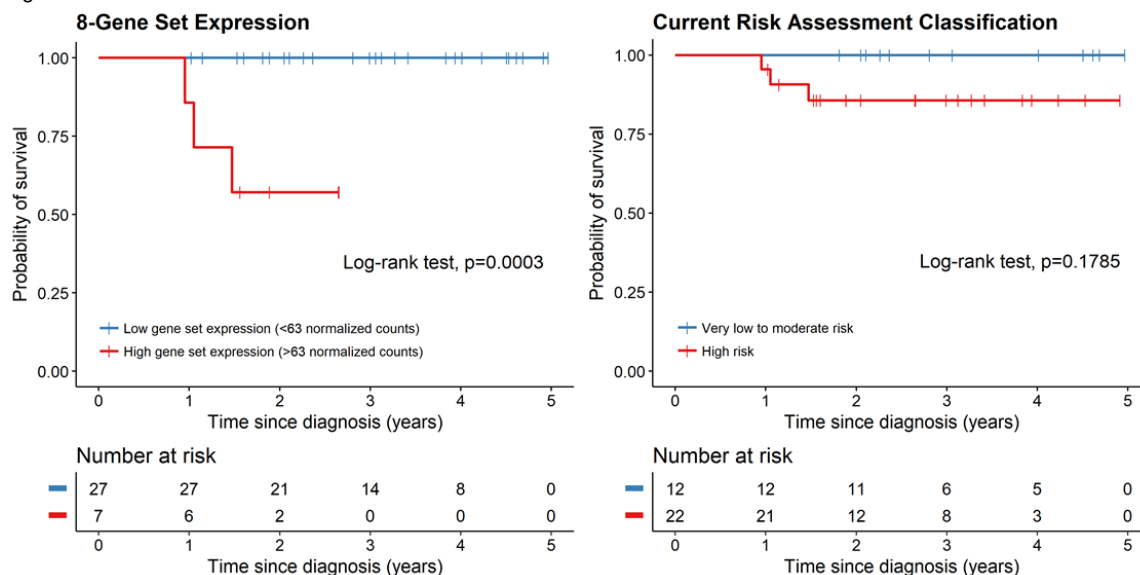
Background: The current risk assessment classification for gastrointestinal stromal tumors (GIST) includes tumor site, size and mitotic count. However, recent evidence suggests that up to 80-85% of patients currently classified as high risk may actually be at minimal to no risk of recurrence. Gene expression profiling has been shown to be a powerful tool for predicting risk of recurrence in other malignancies, such as breast carcinoma. Furthermore, multiple molecular alterations have been associated with worse prognosis in GIST patients. The aim of this study was to determine if gene expression testing can be used to provide more precise risk stratification in GIST patients.

Design: 56 GIST cases, confirmed with CD117/DOG1 immunohistochemistry, were analyzed using the NanoString GX Human Cancer panel, which includes 231 genes previously associated with human malignancy. Gene expression results were correlated with clinical and pathologic data to identify a molecular signal associated with traditional risk assessment parameters. The prognostic performance of this gene expression signal was then assessed in 34/56 patients with available survival data.

Results: Volcano plot analysis identified eight genes with significantly increased expression (FDR<0.05) in high risk vs. non-high risk tumors: TYMS, CDC2, TOP2A, CCNA2, E2F1, PCNA, BIRC5 and CHEK1. As an aggregate 8-gene set, these transcripts exhibited significantly higher expression in high risk tumors vs. intermediate (p<0.001), low (p<0.001) and very low (p=0.010) risk tumors. Receiver operating characteristic curve analysis demonstrated an AUC of 0.861 for the separation of high risk vs. non-risk tumors using 8-gene set expression. Cox proportional-hazards regression identified 8-gene set expression as the only variable with a statistically-significant association with patient death (p=0.039) (**Table 1**). Kaplan-Meier survival analysis demonstrated improved risk stratification with 8-gene set expression (log-rank test p<0.001) versus the current risk assessment classification (p=0.179) (**Figure 1**).

Table 1. Cox proportional-hazards regression model for death in patients with gastrointestinal stromal tumor (n=34*).		
Variable	HR (95% CI)	p-value
Age, yr	1.070 (0.982-1.166)	0.121
Gender		
Male	1 [Reference]	
Female	2.366 (0.214-26.12)	0.482
Tumor site		
Stomach	2.000 (0.181-22.056)	0.571
Duodenum	N/A ¹	N/A ¹
Jejunum/ileum	0.643 (0.058-7.094)	0.719
Tumor size, cm	0.943 (0.739-1.204)	0.638
Mitotic activity		
≤5 mitoses/50 high-power fields	1 [Reference]	
>5 mitoses/50 high-power fields	2.081 (0.189-22.97)	0.550
Exon 11 mutation	N/A ¹	N/A ¹
8-gene set expression, normalized counts	1.112 (1.006-1.229)	0.039
*3/34 patients died during study follow-up period.		
¹ N/A: unable to calculate (95% CI for hazard ratio = 0 to infinity).		

Figure 1 - 578



Conclusions: These results suggest that, compared with the current clinical and histology-based risk assessment classification for GIST patients, gene expression may offer superior prognostic performance. Further validation studies are warranted to confirm the utility of this molecular risk stratification approach.

579 The Frequency of Celiac Disease in Patients with Unexpected Intraepithelial Lymphocytosis in Duodenal Biopsy Specimen in a Tertiary Hospital.

Sunjida Ahmed¹, Ruliang Xu²

¹NYU Langone Health, New York, NY, ²New York University Medical Center, New York, NY

Disclosures: Sunjida Ahmed: None; Ruliang Xu: None

Background: The diagnosis of celiac disease (CD) is based on the combination of clinical, serological and histological findings. Patients with CD may not have classic clinical presentations but may have a variable degree of intraepithelial lymphocytes or lymphocytosis (IEL) irrespective of villous architecture in the duodenum. We analyze how frequent CD is diagnosed by clinical and/or serological testing correlation after reporting unexpected IEL in the biopsied specimen.

Design: We searched for cases with keywords "intraepithelial lymphocytosis" and "intraepithelial lymphocytes" in our departmental database (Powerpath) for a one-year period, from 25074 GI biopsy cases. All cases were divided into two groups: 1). known or suspicious CD cases; 2) cases with unexpected IEL. We reviewed all cases relevant clinical information in LIS system (Epic).

Results: Total 589 cases with increased IEL in duodenal biopsy were identified from 25074 cases (2.3%). Among 589 cases, 93 (15.7%) had a prior history of or serologically confirmed CD (group 1). Remaining 496 (84.2%) cases had unexpected IEL in the duodenum (Group 2). In group 2, 115 (23.1%) cases were tested by serology and 25 cases were diagnosed with CD (21.7%). The percentage of the unexpected CD in group 2 is 5.0%. Histologically, the alteration of villous architecture in unexpected CD (group 2) was variable. Normal villous architecture and villous blunting were reported in 9 of 25 cases (36%) and 16 cases (64%), respectively. In group 1 (93), the histological abnormality includes IEL with normal villous architecture in 24 cases (26%) and villous blunting in 69 cases (74%). There is no statistical difference of villous architectural changes between the two groups. A large number of cases with unexpected IEL have unknown etiology (N=204, 41%), many cases have strong association with H. pylori infection in the stomach (N=83, 17.6%), nonspecific gastritis (N=35, 7.1%), morbid obesity (N=20, 4%), duodenitis (N=19, 3.8%), gastroesophageal reflux disease (N=18, 6.1%), combined gastritis and duodenitis (N=10, 2%), irritable bowel syndrome (N=10, 2%), atrophic gastritis (N=4, 0.8%), NSAID use (N=3, 0.6%), and adenocarcinoma (N=2, 0.4%).<

Conclusions: A significant number of patients with unexpected IEL may have celiac disease. The degree of histological damage in those with the unexpected celiac disease is comparable to those with CD diagnosed before the biopsy. Thus, it is important to recognize IEL in a routine duodenal biopsy to prompt a further workup.

580 Radiofrequency Ablation Allows for Clonal Expansion of Highly Mutated Neosquamous Epithelium

Fahire Akarca¹, Nicholas Shaheen², Robert Odze³, Matthew Stachler³

¹Gazi University, Ankara, Turkey, ²University of North Carolina at Chapel Hill, Chapel Hill, NC, ³Brigham and Women's Hospital, Boston, MA

Disclosures: Fahire Akarca: None; Nicholas Shaheen: None; Robert Odze: None; Matthew Stachler: None

Background: Several endoscopic treatments are widely used for the treatment of dysplasia or early cancer in Barrett's esophagus, including radiofrequency ablation (RFA), endoscopic mucosal resection, etc. All of these procedures aim to denude the dysplastic Barrett's epithelium. After RFA, the ablated esophagus heals on acid suppressive therapy, and is re-populated with a stratified squamous epithelium, referred to as 'neosquamous epithelium (NSE)'. While histologically normal, the origin and clonal make-up of this NSE is unknown. This is especially important as there is some controversy in the field to whether this NSE has a higher incidence of developing squamous cell carcinoma. Also, given the unsure origin of Barrett's esophagus it is unknown how this NSE may be related to the previously ablated Barrett's.

Design: We therefore performed targeted (next-gen based) sequencing using a ~400 gene panel on a collection of patients who were diagnosed with dysplastic BE (either HGD or LGD) and then had RFA performed. Initially, to determine if genomic alterations could be found in the NSE using standard sequencing techniques, we sequenced 10 cases. We then sequenced an additional 14 patients with both the previous dysplastic BE, the paired NSE, and the recurrent BE if present. For control, we sequenced additional esophagitis biopsies and normal non-ablated squamous epithelium from the RFA patients.

Results: Within the NSE we identified multiple examples of samples containing pathogenic mutations in known esophageal adenocarcinoma and squamous cell carcinoma associated genes; including 33% patients with *TP53* mutations and 60% patients with *NOTCH1* mutations. On average, we identified 5.5 somatic mutations per NSE sample. When a mutation was present in *TP53* or *NOTCH1*, there were often more than one mutation identified in the same gene, suggesting either (or a combination) biallelic inactivation and multiple competing clones.

Conclusions: Previous reports, using deep sequencing, have shown *TP53* and other mutations in UV exposed skin. However, the presence of a high mutational burden, detected using standard approaches, in "normal" neosquamous suggests that basal/stem cells repopulating the denuded epithelium that harbor advantageous mutations may have a growth advantage and can clonally expand to a size detectable by routine sequencing. As more people who have had RFA performed age, future studies will need to determine if this mutated neosquamous is indeed at higher risk of neoplastic transformation.

581 Evaluation of a Fully Automated System for Use in Somatic Mutation Testing in Colorectal Cancer: a Prospective Study with Comparison to Next-Generation Sequencing

M. Rabie Al-Turkmani¹, Donald Green², Alicia Finney³, Michael Suriawinata⁴, Gregory Tsongalis²

¹Dartmouth-Hitchcock Medical Center and Geisel School of Medicine at Dartmouth, Lebanon, NH, ²Dartmouth-Hitchcock Medical Center, Lebanon, NH, ³Dartmouth-Hitchcock Medical Center, Andover, MA, ⁴Dartmouth-Hitchcock Medical Center, Hanover, NH

Disclosures: M. Rabie Al-Turkmani: None

Background: The management of colorectal cancer (CRC) has been aided by the advancement and increased usage of molecular testing. Mutational analysis of *KRAS* and *NRAS* is warranted for CRC patients considered for anti-EGFR therapy. *BRAF* codon 600 testing is also recommended in CRC for prognostic stratification. In this study, we evaluated a fully integrated, cartridge-based system that provides automated sample processing (deparaffinization, tissue digestion and DNA extraction) and real-time PCR-based mutation detection with all reagents included in a single-use cartridge.

Design: Fifty-five CRC tissue specimens which were ordered for next-generation sequencing (NGS) testing between January 2018 and August 2018 were also prospectively tested on the Idylla™ automated system (Biocartis, Belgium) using the *KRAS* and *NRAS*-*BRAF* cartridges (Research Use Only), which test for actionable mutations in *KRAS*, *NRAS* and *BRAF*. Two 10 µm formalin-fixed paraffin-embedded (FFPE) tissue sections (one for each cartridge) were used for each run on the cartridge-based system and all cases met the system's minimum tumor requirement of 10%. NGS testing was performed using the Ion AmpliSeq 50-gene Cancer Hotspot Panel v2 (Thermo Fisher Scientific). NGS results and turnaround times were compared to those obtained by the cartridge-based system.

Results: NGS testing detected *KRAS*, *NRAS* and *BRAF* mutations in 31%, 5% and 11% of the samples tested, respectively. The remaining samples (53%) had no detectable mutations in *KRAS*, *NRAS* or *BRAF* by NGS. The overall agreement between NGS and the cartridge-based system results was 91% (50/55) and the clinical concordance was 98% (54/55). The cartridge-based system detected an additional *NRAS* mutation in each of the 5 samples that had discrepant results with NGS. The average turnaround time for NGS testing from sample extraction to result reporting was 11.8 days (range: 8 - 20 days), compared to a turnaround time of 2.5 hours for the cartridge-based system testing.

Conclusions: The described cartridge-based system offers rapid and reliable testing of clinically actionable mutation in CRC specimens directly from FFPE tissue sections. Its simplicity and ease of use make it suitable for small centers that lack highly trained staff and infrastructure. It can also complement NGS and other molecular testing systems at larger diagnostic centers by providing rapid turnaround times that benefit time-sensitive decisions in the care of patients with CRC.

582 Tumor Heterogeneity in Gastroenteropancreatic Neuroendocrine Neoplasms do not Imply a Change in Grade at Metastatic Sites

Zahra Alipour¹, Iván González², Deyali Chatterjee³

¹Washington University in St. Louis, Clayton, MO, ²Washington University School of Medicine, St. Louis, MO, ³Washington University, St. Louis, MO

Disclosures: Zahra Alipour: None; Iván González: None; Deyali Chatterjee: None

Background: Ki-67 proliferative index (PI) prognostically stratifies gastroenteropancreatic neuroendocrine neoplasms (GEP-NEN), and is used in histologic grading. It is well-known that there is significant intratumoral heterogeneity in PI, but systematic studies comparing inter-tumoral heterogeneity between primary and metastatic sites are rare. The object of this study was to assess whether there is a change in histologic grade at the metastatic site as compared to the primary site.

Design: A retrospective cohort of 30 biopsy proven liver metastasis from 28 primary resections of GEP-NEN (2006-2018), were included. All slides were reviewed, and unless previously available, a Ki-67 immunohistochemical stain was performed on the tumor block which represented the most mitotically active region of the tumor. All the primary and metastatic tumors were graded based on WHO 2017 classification, adhering strictly to the current CAP guidelines of manually counting between 500-2000 cells in hot-spot areas. Spearman's Rank-Order Correlation was utilized to compare the PI between primary and metastatic tumors.

Results: The salient clinicopathologic features are detailed in Table 1. Primary tumor sites included stomach (n=2), duodenum (n=2), pancreas (n=9), ileum (n=12), small intestine (n=2) and rectum (n=1). Twenty-seven cases (93.1%) were well-differentiated neuroendocrine tumors, spanning grades 1-3 (G1-G3) and 2 cases were poorly differentiated neuroendocrine carcinomas (NEC-G3). Metastasis to liver was sampled synchronously in 12 cases, prior to primary resection in 3 cases, and the rest at a later time (5.5 – 52.2 mos.). PI in metastatic site compared to the primary tumor revealed no change in WHO tumor grades in any of the 30 cases. Greatest inter-tumoral heterogeneity was noted in G3 tumors, but while 4 cases from that group showed an increase in PI (by 10-40), 3 cases showed stable PI/ slight decrease (by 3-10) in the metastasis. G1 tumors showed the least change (PI remained same in 8 cases and increased by 1 in 1 case). For G2 tumors, 7 cases showed mild increase in PI (by 1-3), 2 cases remained the same, and 3 cases showed mild decrease (by 1-3). Statistical analysis confirmed significant correlation of PI between primary and metastatic tumors (p<0.001).

Table 1: Comparison of Primary and Metastatic Tumor Grades in GEP-NEN

Primary site	Sex	Age	Ki-67: primary (%)	WHO Grade in primary	Liver biopsy: days after primary	Ki-67 in metastatic focus (%)	WHO Grade in metastasis
Stomach #1	M	59	80	3*	2	95	3
Stomach #2	F	64	1	1	- 566	1	1
Duodenum #1	M	45	1	1	2489	1	1
Duodenum #2	F	61	10	2	0	12	2
Jejunum #1	M	63	4	2	0	4	2
Jejunum #2	F	56	<1	1	0	<1	1
Ileum #1	M	53	4	2	0	5	2
Ileum #2	F	52	1	1	1058	2	1
Ileum #3	F	65	4	2	0	3	2
Ileum #4	M	56	1	1	0	1	1
Ileum #5	M	59	10	2	0	11	2
Ileum #6	M	70	<1	1	0	1	1
Ileum #7	M	62	1	1	0	<1	1
Ileum #8	F	65	10	2	- 473	13	2
Ileum #9	F	54	<1	1	273	1	1
Ileum #9	F	54	<1	1	389	<1	1
Ileum #10	M	75	<1	1	167	1	1
Ileum #11	F	40	3	2	644	4	2
Ileum #12	F	55	3	2	- 57	5	2
Ileum #12	F	55	3	2	0	3	3
Rectum	M	47	8	2	490	8	2
Pancreas #1	F	56	25	3	447	40	3
Pancreas #2	M	48	30	3	762	70	3
Pancreas #3	M	76	50	3*	396	60	3
Pancreas #4	M	45	26	3	0	23	3
Pancreas #5	F	59	60	3	1681	50	3
Pancreas #6	M	45	30	3	2422	25	3
Pancreas #7	M	52	5	2	0	4	2
Pancreas #8	F	66	13	2	1477	10	2
Pancreas #9	M	64	7	2	1588	10	2

*Poorly-differentiated

Conclusions: Our study shows that a thoroughly performed PI accurately grades GEP-NEN in the primary tumor, and the metastatic focus recapitulates the biology of the primary tumor.

583 Appendiceal Neuroendocrine Neoplasms: Clinicopathologic Characteristics, Including Documentation of the Novel INSM-1 Immunohistochemical Staining: A Single Institution Experience With 80 Cases

Zahra Alipour¹, Iván González², Dengfeng Cao³, Deyali Chatterjee⁴

¹Washington University in St. Louis, Clayton, MO, ²Washington University School of Medicine, St. Louis, MO, ³Barnes Jewish Hospital/Washington University, St. Louis, MO, ⁴Washington University, St. Louis, MO

Disclosures: Zahra Alipour: None; Iván González: None; Dengfeng Cao: None; Deyali Chatterjee: None

Background: Well-differentiated appendiceal neuroendocrine tumors (A-NET) have an excellent prognosis, with some documentation that A-NET less than 2 cm almost never metastasize. Yet, the classification of A-NET is still part of the gastroenteropancreatic neuroendocrine neoplasms (GEP-NEN) as applied to any other site. In this study, we wanted to explore the clinicopathologic and prognostic parameters, as well as to assess the sensitivity of immunohistochemical staining with a novel marker INSM-1, that has recently been studied in other neuroendocrine tumors.

Design: A retrospective search for all A-NET was performed in the pathology database, with slides available for review and tissue blocks to perform immunohistochemical stains. All cases were subjected to INSM-1 immunohistochemical staining. Additionally, Ki-67 and chromogranin stains were performed on those cases which did not have those stains previously done. Grading was performed using WHO 2017 criteria for GEP-NEN, following the CAP guideline to determine the Ki-67 proliferative index (PI).

Results: We identified 80 patients with A-NET (30 males, 49 females, with the mean age of 42.1 years). 88.8% were grade 1, and the rest were grade 2 (with a maximum PI of 5%). 80% of cases were 1 cm or less in size. None of the tumors had any distant metastasis or local recurrence; mean follow up period was 113 mos. (1- 429 mos.). Tumor size showed a correlation to PI (Table 1). The predominant morphologic pattern was nested (52 cases), with a variable admixture of other morphologic types (tubular, trabecular, rosette) in 18 of them. 23 A-NET with pure tubular growth (tubular carcinoids) were identified in this cohort, all of which were 1 cm or less in size, and had a PI of <1%. 28 cases had lymph node sampling, of which 4 cases showed lymph node metastasis (2 of them were grade 1 with sizes 0.4 cm and 4 cm, and two were grade 2, 2.8 cm, and 1.5 cm). All tumors showed positive nuclear staining with INSM-1, including all tubular carcinoids.

Table 1: Comparison of Ki-67 proliferative Index to tumor size

Ki-67 proliferative index	Tumor size 0-1 cm	Tumor size 1.1 - 2 cm	Tumor size >2 cm
0-1%	58	7	1
1.1-2.9%	1	2	2
>=3%	5	2	2

Conclusions: Tumor size appears to be related to PI, but the range of PI is small, and overall prognosis of A-NET is excellent. WHO grading based on PI may not be entirely applicable for A-NET. Finally, to our knowledge, this is the first study, validating the sensitivity of INSM-1 immunohistochemical stain in A-NET, including in tubular carcinoids.

584 Early Onset Colorectal Adenocarcinomas are More Likely to Have Poor Prognostic Features: In Support of the New ACS Colorectal Cancer Screening Guidelines

Douglas Allison¹, Katherine Sun¹, Yvelisse Suarez¹, Gloria Young², Ruliang Xu¹, Wenqing Cao³, Suparna Sarkar¹

¹NYU Langone Health, New York, NY, ²New York, NY, ³New York University Langone Medical Center, New York, NY

Disclosures: Douglas Allison: None; Katherine Sun: None; Yvelisse Suarez: None; Gloria Young: None; Ruliang Xu: None; Wenqing Cao: None; Suparna Sarkar: None

Background: While the overall incidence of colorectal cancer (CRC) in the United States has been steadily declining over the past several decades, there has also been an unexpected increase in colorectal cancer in young and middle-aged adults over the same period. Recently, the American Cancer Society (ACS) issued new guidelines regarding screening for CRC, lowering the recommended age to begin screening from age 50 to 45. In this study, we reviewed the incidence of colorectal adenocarcinoma (CRAC) in patients under the age of 50 at our institution to further characterize the pathology of CRACs in this group.

Design: We retrospectively identified patients with CRAC in our pathology database (Powerpath) who underwent colectomy between January 2013 and August 2018. We reviewed the pathology reports, noting in particular the age, sex, tumor size, location, grade, pathologic TNM stage, and MSI status, as well as various other tumor parameters.

Results: A total 806 patients with CRAC were identified. The patient cohort consisted of 406 men and 400 women, ranging in age from 23 to 101 years (median 67). Patients under the age of 50 accounted for 12.5% (n=101), the majority of whom were male (58% vs. 49% of those age 50 and over) and who had predominantly left sided tumors (74% vs. 51%, p<0.001). Additionally, patients under 50 were more likely to have poor prognostic findings on pathologic examination, including higher stage disease (Stage III or IV; 58% vs. 43%, p=0.004), positive lymph nodes (51% vs. 36%, p=0.003), perineural invasion (52% vs. 35%, p=0.001), and presence of tumor deposits (34% vs. 25%, p=0.04). Similar adverse findings were also seen in the 50-54 year age group compared to patients 55 and over (Table 1).

Table 1.

	Under 50 (n=101)	50+ (n= 705)	50-54 (n=63)	55+ (n=642)
Male	58.4% (59)	49.2% (347)	44.4% (28)	49.6% (319)
<i>p-value</i>	0.087		0.427	
Left sided Tumor	74% (74)	50.6% (357)	69.8% (44)	48.8% (313)
<i>p-value</i>	<0.001		0.001	
Lymphovascular Invasion	63.3% (64)	57.6% (406)	65.1% (41)	56.9% (365)
<i>p-value</i>	0.27		0.21	
Perineural Invasion	51.5% (51)	35.0% (245)	44.4% (28)	34.0% (217)
<i>p-value</i>	0.001		0.002	
Tumor Deposits	34% (34)	24.5% (172)	33.9% (21)	23.6% (151)
<i>p-value</i>	0.042		0.072	
Positive Lymph Nodes	51.5% (52)	36.5% (257)	44.4% (28)	35.7% (229)
<i>p-value</i>	0.0037		0.168	
Stage III or IV Disease	58.4% (59)	43.4% (306)	55.6% (35)	42.2% (271)
<i>p-value</i>	0.0046		0.032	
MSI-H	16.2% (14/86)	18.6% (110/591)	8% (4/50)	19.6% (106/541)
<i>p-value</i>	0.589		0.044	

Conclusions: CRAC in patients under the age of 50 is not uncommon, accounting for 1 out of every 8 cases (12.5%) in our series. These tumors are more likely to be left sided, higher stage and demonstrate adverse prognostic histological features like perineural invasion and lymph node involvement. Similar adverse pathologic findings were also seen in patients aged 50-54, suggesting that patients in this age range may benefit from earlier screening and intervention. Both of these findings lend support to the new ACS recommendation to begin screening for CRC at age 45. Molecular analysis of these tumors is underway to better characterize these left-sided carcinomas presenting at a higher stage in the under 50 age group.

585 Smooth Muscle Tumors of the GI Tract: An Analysis of Prognostic Features in over 400 Cases

Lindsay Alpert¹, Ram Al-Sabti², Rondell Graham³, Rish Pai⁴, Raul Gonzalez⁵, Xuefeng Zhang⁶, Vanessa Smith⁶, Hanlin Wang⁷, Lindsey Westbrook⁷, John Goldblum⁸, Sindhu Shetty⁸, Ahmed Bakhshwin⁹, Jeanne Meis¹⁰, Sherry Tang¹¹, Marie Robert¹², Courtney Thomas¹³, John Hart¹, Sang Mee Lee¹, Rhonda Yantiss¹⁴, Erika Hissong¹⁵, Zu-Hua Gao¹⁶, Jingbo Wu¹⁶, Reetesh Pai¹⁷, Lei Zhao¹⁸, Leona Doyle¹⁹, Nicole Panarelli²⁰, Shaomin Hu²¹, Joseph Misdraji²², Angela Shih²³, Harry Cooper²⁴, Rajeswari Nagarathinam²⁴, Sanjay Kakar²⁵, Laura Lamps²⁶, Joel Greenson²⁷, Gregory Lauwers²⁸, Masoumeh Ghayouri²⁹, Mary Bronner³⁰, Zachary Dong³⁰

¹University of Chicago, Chicago, IL, ²University of Chicago Medical Center, Chicago, IL, ³Mayo Clinic, Rochester, MN, ⁴Mayo Clinic Arizona, Scottsdale, AZ, ⁵Beth Israel Deaconess Medical Center, Boston, MA, ⁶Duke University Medical Center, Durham, NC, ⁷David Geffen School of Medicine at UCLA, Los Angeles, CA, ⁸Cleveland Clinic, Cleveland, OH, ⁹Robert J. Tomsich Pathology & Laboratory Medicine Institute, Cleveland Clinic, Pepper Pike, OH, ¹⁰The University of Texas MD Anderson Cancer Center, Houston, TX, ¹¹Houston, TX, ¹²Yale University School of Medicine, New Haven, CT, ¹³Yale New Haven Hospital, Orange, CT, ¹⁴Weill Cornell Medical College, New York, NY, ¹⁵New York-Presbyterian/Weill Cornell Medical Center, New York, NY, ¹⁶Montreal, QC, ¹⁷UPMC-Presbyterian Hospital, Pittsburgh, PA, ¹⁸Brigham and Women's Hospital, Harvard Medical School, Boston, MA, ¹⁹Brigham and Women's Hospital, Boston, MA, ²⁰Montefiore Medical Center, Scarsdale, NY, ²¹Montefiore Medical Center, Bronx, NY, ²²Massachusetts General Hospital, Harvard Medical School, Boston, MA, ²³Massachusetts General Hospital, Boston, MA, ²⁴Fox Chase Cancer Center, Philadelphia, PA, ²⁵University of California, San Francisco, San Francisco, CA, ²⁶University of Michigan Hospital, Ann Arbor, MI, ²⁷University of Michigan Hospitals, Ann Arbor, MI, ²⁸H. Lee Moffitt Cancer Center & Research Institute, University of South Florida, Tampa, FL, ²⁹Moffitt Cancer Center, Tampa, FL, ³⁰University of Utah, Salt Lake City, UT

Disclosures: Lindsay Alpert: None; Ram Al-Sabti: None; Rondell Graham: None; Rish Pai: None; Raul Gonzalez: None; Xuefeng Zhang: None; Vanessa Smith: None; Hanlin Wang: None; Lindsey Westbrook: None; John Goldblum: None; Sindhu Shetty: None; Ahmed Bakhshwin: None; Jeanne Meis: None; Sherry Tang: None; Marie Robert: None; Courtney Thomas: None; John Hart: None; Sang Mee Lee: None; Rhonda Yantiss: None; Erika Hissong: None; Zu-Hua Gao: None; Jingbo Wu: None; Reetesh Pai: None; Lei Zhao: None; Leona Doyle: None; Nicole Panarelli: None; Shaomin Hu: None; Joseph Misdraji: None; Angela Shih: None; Harry Cooper: None; Rajeswari Nagarathinam: None; Sanjay Kakar: None; Laura Lamps: None; Joel Greenson: None; Gregory Lauwers: None; Masoumeh Ghayouri: None; Mary Bronner: None; Zachary Dong: None

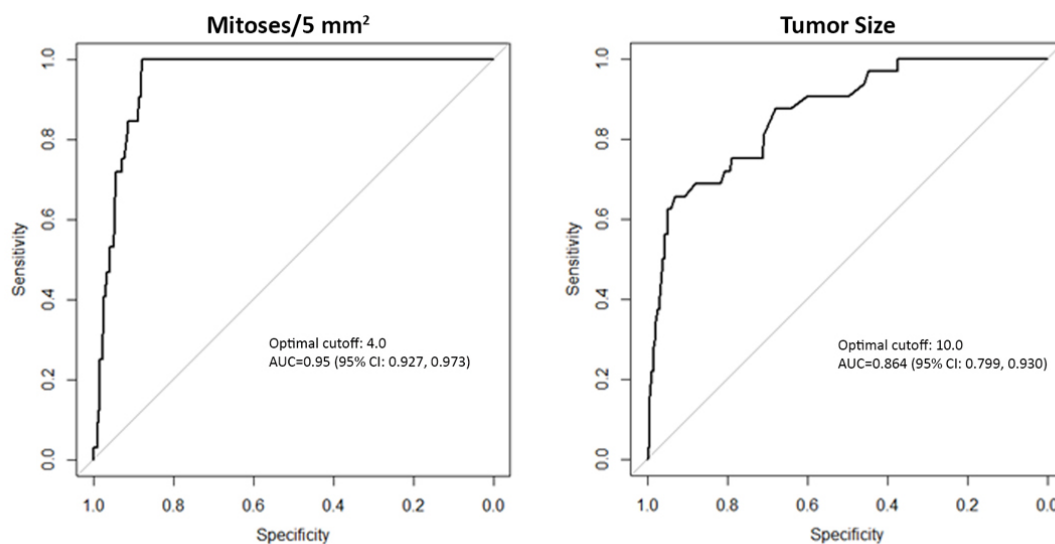
Background: Although classification systems exist for uterine and soft tissue smooth muscle tumors (SMTs), there are currently no established criteria for the diagnosis and prognosis of gastrointestinal SMTs. In this multi-institutional study, a large cohort of GI tract SMTs was analyzed to identify potential prognostic features.

Design: Resected GI tract SMTs of the esophagus, stomach, small bowel, and colorectum were identified from the pathology archives of 19 institutions. Muscularis mucosae tumors were excluded, as were suspected vascular tumors and metastases from other primary sites. Immunostains (SMA, desmin, CKIT, DOG1) were used to confirm the diagnoses. Pathologic features were assessed by expert GI or soft tissue pathologists in each center. Clinical data were retrieved from the electronic medical record. Disease progression was defined as tumor recurrence, metastasis, or disease-related death. Categorical variables were analyzed using χ^2 test; logistic regression and ROC analysis were performed for continuous variables.

Results: We identified 405 SMTs from the stomach (n=204, 50.4%), esophagus (n=83, 20.5%), small bowel (n=68, 16.8%), and colorectum (n=50, 12.3%). Patients were adults (mean: 56.2 years, range: 19-95 years) with a slight (52.6%) female predominance. Abdominal pain was the most common presentation (24%) in symptomatic patients, but 30% of cases were incidentally detected. Tumors measured up to 29 cm (mean: 4.7 cm). Follow-up data were available for 362 patients (mean: 52 months). Disease progression occurred in 35 (9.6%) patients and was strongly associated with colorectal location, size >10.0 cm, mitotic rate of >4/5 mm², increased cellularity, high-grade cytology, poor differentiation, necrosis, ulceration, and lamina propria and serosal involvement (Table 1 and Figure 1). None of the esophageal tumors recurred. Only one progressive SMT, a 20 cm colorectal tumor with local recurrence, was well differentiated and had low cellularity. Age, sex, and margin status were not significantly associated with progression (p=0.60, 0.30, and 0.16, respectively).

		No Progression n=327	Progression n=35	p-value
Site	Esophagus	78 (24%)	0 (0%)	<0.0001
	Stomach	180 (55%)	7 (20%)	
	Small bowel	44 (13%)	10 (29%)	
	Colon/rectum	25 (8%)	18 (51%)	
Atypia	None/mild	263 (81%)	2 (6%)	<0.0001
	Moderate	33 (10%)	8 (23%)	
	Severe	31 (9%)	25 (71%)	
Differentiation (1=resembles normal parenchyma, 2=abnormal but typing certain, 3=undifferentiated)	1	266 (81%)	1 (3%)	<0.0001
	2	43 (13%)	14 (40%)	
	3	18 (6%)	20 (57%)	
Tumor necrosis	Absent	279 (85%)	8 (23%)	<0.0001
	Present	48 (15%)	27 (77%)	
Cellularity (based on comparison with normal muscularis)	Low	254 (78%)	1/33 (3%)	<0.0001
	High	73 (22%)	32/33 (97%)	
Mucosal ulceration	Absent	275/317 (87%)	13/30 (43%)	0.0002
	Present	42/317 (13%)	17/30 (57%)	
Lamina propria involvement	No	258/283 (91%)	12/25 (48%)	<0.0001
	Yes	25/283 (9%)	13/25 (52%)	
Serosal involvement	No	192/249 (77%)	9/23 (39%)	0.0002
	Yes	57/249 (23%)	14/23 (61%)	
Size, mean, cm (SD)		4.01 (3.71)	11.77 (6.59)	<0.0001
Mitotic count/5 mm ² , mean (SD)		6.23 (26.20)	59.72 (61.65)	<0.0001

Figure 1 - 585



Conclusions: Disease progression was uncommon (9.6%) in this large series of GI tract SMTs and was more likely to occur in colorectal tumors, large tumors (>10 cm), and tumors with high mitotic activity (>4/5 mm²), moderate or severe atypia, necrosis, poor differentiation, and high cellularity.

586 Rosai-Dorfman Disease of Gastrointestinal Tract

Zainab Alruwaili¹, Yang Zhang², Tatianna Larman³, James Miller³, Elizabeth Montgomery¹

¹Johns Hopkins Medical Institutions, Baltimore, MD, ²Johns Hopkins Hospital, Baltimore, MD, ³Johns Hopkins University School of Medicine, Baltimore, MD

Disclosures: Zainab Alruwaili: None; Yang Zhang: None; Tatianna Larman: None; James Miller: None; Elizabeth Montgomery: None

Background: Rosai- Dorfman disease (RDD) is a histiocytic proliferation of unknown etiology. The classic form presents as cervical lymphadenopathy in children or young adults. The extra-nodal form can rarely affect the gastrointestinal (GI) system. Herein, we describe twelve cases of RDD in the GI.

Design: Twelve specimens from eleven patients with RDD involving the GI system were identified. H&E slides and immunohistochemical stains were reviewed. Clinical information was obtained from patients' electronic records.

Results: Patients were predominantly female (n=8). Age ranged from 17-76 years (mean 60 y). Abdominal pain was the most frequent symptom (n=5). Associated conditions included juvenile rheumatoid arthritis (n=1), monoclonal gammopathy of undetermined significance (n=1), asthma and diabetes (n=1) and rheumatoid arthritis (n=1). Of the 3 patients with multi-centric disease, 2 had nodal disease, and one had bone and soft tissue lesions. Affected sites were colon (appendix=1, right colon= 2, left colon=6), pancreas (n=2) and liver (n=1). Average sizes were 4.9 cm (colon) and 2.8 cm (pancreas). All cases consisted of polygonal to spindle-shaped histiocytes with eosinophilic to clear cytoplasm admixed with lymphoplasmacytic cells. Lesions had focal nodular (n=5) or storiform patterns (n=4). Other features included lymphoid aggregates (n=7), few neutrophils (n=6), thickened vessels (n=10), medium-sized arterial wall injury (n=5), and hemosiderin pigment (n=4). In the colon (resection=5, polypectomy=2, and biopsy=2), mucosal and submucosal lesions had entrapped crypts, little fibrosis, and prominent emperipolesis. In contrast, lesions in the subserosa, pericolonic or mesenteric fat showed marked fibrosis and inconspicuous emperipolesis. In one case the appendix was involved by RDD, low grade appendiceal mucinous neoplasm, and small lymphocytic lymphoma in the lymph nodes. Pancreatic cases displayed fairly defined margins, prominent fibrosis, and absence of entrapped parenchyma. The liver lesion involved the periportal area with fibrosis; emperipolesis was not identified. S100 protein immunostaining demonstrated strong staining in all cases. Of the five patients with follow up, one developed IgA nephropathy and died of renal failure.

Clinical features of 11 patients with Rosai- Dorfman disease of the GI								
Case	Age	Race	sex	Location	size	Presentation	Associated Autoimmune disease/ malignancy	Laboratory features
1	70	U	F	Sigmoid	U	Diarrhea	U	U
2	65	B	F	Right colon	4.5	U	U	U
3	74	B	F	Pancreas	2	Abdominal pain	Rheumatoid arthritis	Anemia
4	54	U	F	Rectum	U	Incidental Screening colonoscopy	U	U
5	46	B	F	Rectum	2	U	U	U
6	76	B	F	Appendix	6	Abdominal pain	CLL	Inc LDH, WBC (both neut and lymphocytes), anemia
7	68	W	M	Liver	Diffuse (non-mass forming)	Weight loss, Constitutional symptoms	IgA nephropathy	Inc ALT, AST, AP, neut, CRP, ESR, and ANA anemia
8	17	B	F	Rectum	6.5	Abdominal pain, gluteal mass	Juvenile rheumatoid arthritis	Inc ESR, Neut. Anemia
9	57	U	F	Pancreas	3.7	Abdominal pain	U	U
10	61	W	M	Mesentery around right colon	6.5	Abdominal pain	Asthma, Diabetes	Anemia Inc. WBC
11	69	B	M	Rectum	3.3	Weight loss Bleeding per rectum	MGUS	Anemia Inc. neut

B, black; M, male; F, female, W, White; Inc; increased; U, unknown; ALT: alanine aminotransferase; ANA, antinuclear antibodies; AST aspartate aminotransferase; CRP, C reactive protein ; ESR, erythrocyte sedimentation rate; neut, neutrophils; WBC, white blood cells.

Figure 1 - 586

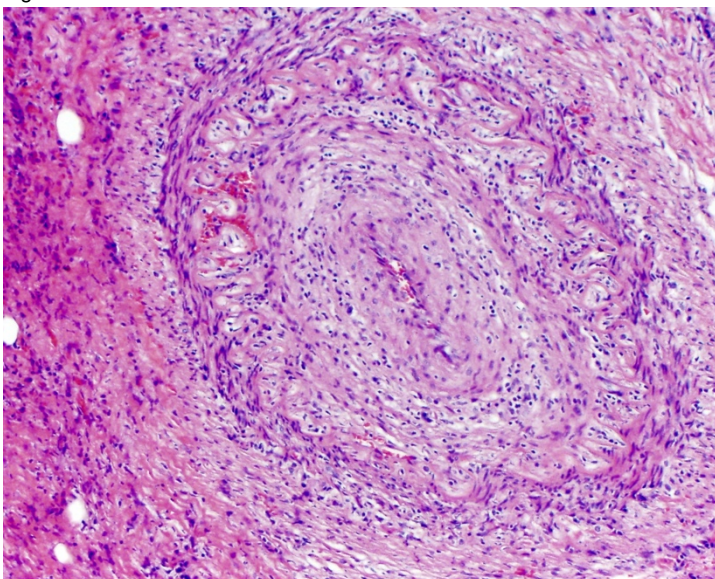
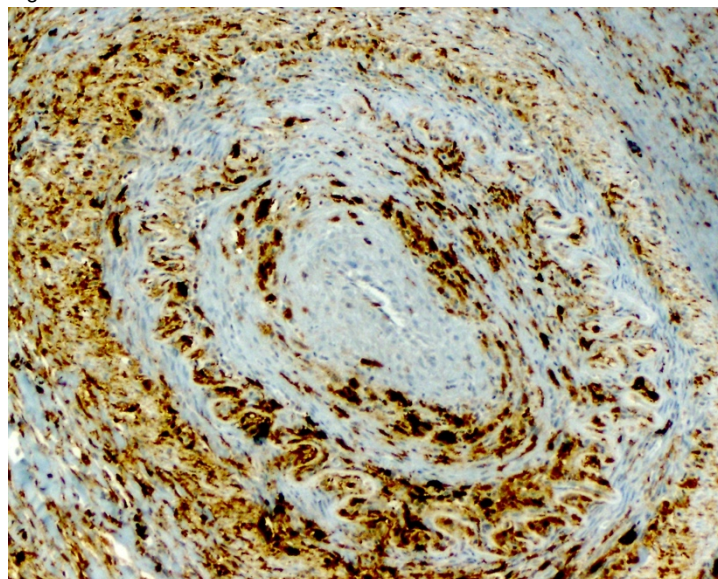


Figure 2 - 586



Conclusions: RDD is rare in the GI tract; the colon was the most affected organ. A previously unreported pattern of vasculopathy is described. Careful pathologic examination of the specimen is essential to rule-out associated neoplasms.

587 Age-associated clinicopathological characteristics of IBD-associated colorectal cancer

Manju Ambelil¹, Zongxian Cao², Samuel Ballentine¹, Qingqing Liu¹, Huaibin Mabel Ko¹, Hongfa Zhu³, Alexandros Polydorides¹, Noam Harpaz³

¹Icahn School of Medicine at Mount Sinai, New York, NY, ²Mount Sinai Health System, New York, NY, ³Mount Sinai Medical Center, New York, NY

Disclosures: Manju Ambelil: None; Zongxian Cao: None; Samuel Ballentine: None; Qingqing Liu: None; Huaibin Mabel Ko: None; Hongfa Zhu: None; Alexandros Polydorides: None; Noam Harpaz: None

Background: Patients with longstanding chronic inflammatory bowel disease (IBD) are at increased risk of developing colorectal cancer (CRC). They are disproportionately young, with a 15-20-year lower mean age at cancer diagnosis than their counterparts in the general population, but their risk extends into older age groups as well. Few systematic large-scale studies have focused on the age-associated clinicopathological features of these cancers.

Design: Our pathology database was searched for CRCs resected from patients with IBD between 1994-2018. Based on these records, patients were classified by age (expressed in years) and the pathological diagnosis of ulcerative colitis (UC), Crohn's colitis (CC) or indeterminate colitis (IC). Cancers were characterized by anatomical location, multiplicity, mucinous vs non-mucinous subtypes and presence or absence of proximate and distant dysplasia. Chi square analyses were performed with a significance level of $P \leq 0.05$.

Results: The search recovered 201 patients with CRC: 150 UC, mean age 54 (range, 22- 83 years); 38 CC, mean age 56 (range, 31- 83 years); 13 IC, mean age 47 (range, 30- 62 years). The cecum and ascending colon were the most common location in young patients with UC (20-29: 54.5%; 30-39: 38.9%), but accounted for only 30% of cancers in the 40 to >80 age groups. The rectosigmoid was the most common cancer site in the latter groups, whereas in CC, rectosigmoid cancers predominated in all age groups. Multiple cancers occurred in 11.3% of patients with UC, without age dependence, and in 13.2% of patients with CC but only in those below age 60. Mucinous cancers were more common in CC than UC (27.9% vs. 13.6%, $P=0.02$) and occurred in all age groups in CC but rarely below age 40 in UC (ages 20-29: 0%; 30-39: 4.2%). Dysplasia occurred in 80% of patients with UC independently of age, but distant dysplasia was correlated with younger age (<30: 72.7%; 70-79: 37.5%; >80: 14.3%; ($P=0.014$). No such age dependence was observed in CC.

Conclusions: In patients with IBD, age is significantly correlated with important clinicopathological features of CRC including anatomical location, tumor multiplicity, mucinous histology and association with proximate and distant dysplasia, however, there are significant differences between UC and CD with respect to these age-related characteristics.

588 International Tumor Budding Consensus Conference (ITBCC): Friend or Foe? An Institutional Interobserver Variability Study of 233 Colorectal Adenocarcinoma Cases

Mallorie Angert¹, Margaret Cho², Lili Lee³, Arvind Rishi⁴, Myriam Kline⁵, Rebecca Thomas⁶, Mansoor Nasim⁷

¹Donald and Barbara Zucker School of Medicine at Hofstra/Northwell, Lake Success, NY, ²Donald and Barbara Zucker School of Medicine at Hofstra/Northwell, Flushing, NY, ³Northwell Health Hofstra Northwell School of Medicine, New Hyde Park, NY, ⁴Northwell Health, New York, Lake Success, NY, ⁵Feinstein Institute for Medical Research, Manhasset, NY, ⁶Northwell Health System, New Hyde Park, NY, ⁷Northwell, Lake Success, NY

Disclosures: Mallorie Angert: None; Margaret Cho: None; Lili Lee: None; Arvind Rishi: None; Rebecca Thomas: None; Mansoor Nasim: None

Background: Given that tumor budding is considered to have clinical prognostic value, the accuracy and reproducibility of its assessment is essential. Recently, the International Tumor Budding Consensus Conference (ITBCC) created a 3-tier grading system to uniformly assess tumor budding in colorectal cancer. This is in contrast to the former practice that was based on a 2-tier system. Our study aims to look at interobserver variability using the current scoring system of tumor budding in colorectal cancer with comparison to the former 2-tier system.

Design: A total of 233 cases of colorectal carcinomas were retrospectively analyzed, and H&E stained slides of these cases were collected. A representative slide was selected per case. Randomized and blinded assessment of tumor budding scores was conducted by 4 investigators with different levels of experience and expertise. Tumor budding scores by individual investigator and by consensus were compared to data including patient survival, tumor grade, pathologic stage, and lymph node status.

Results: The mean age was 67 years, with ages ranging from 27 to 97. Average tumor size was 4.7 cm in greatest dimension, with sizes ranging from 0.2 cm to 15 cm in greatest dimension. The frequency of carcinomas was 50% in the right colon, 5% in the transverse colon, 21% in the left colon, 12% in the rectosigmoid colon, and 12% in the rectum. Gwet's Agreement Coefficient AC_1 (95% CI) showed higher interobserver agreement among the 4 pathologists for the 2-tier system with value of 0.329 than for the 3-tier system with value of 0.25. There was statistical significance comparing tumor budding score to pathologic stage in all individual investigators and the consensus

score. Higher budding was associated with higher tumor stage (Table 1) as well as lymph node metastasis. One investigator predicted survival status based on tumor budding score with statistical significance (p value 0.0175, OR 2.004).

Table 1: Tumor budding score vs Pathologic Tumor Stage, linear regression analysis

	Parameter estimate	Standard error	T value	P value
Observer 1	0.43848	0.10705	4.10	<.0001
Observer 2	0.55427	0.09596	5.78	<.0001
Observer 3	0.35013	0.09698	3.61	0.0004
Observer 4	0.39733	0.10433	3.81	0.0002
Consensus	0.41603	0.09524	4.37	<.0001

Conclusions: There is significant interobserver variability of the assessment of tumor budding in colorectal carcinoma. However, the 2-tier system of scoring was associated with less variation than the 3-tier grading system. We demonstrated that tumor budding score, both with individual observer and the consensus score, showed significant association with pathologic tumor stage and lymph node status. Given that tumor budding has significant clinical prognostic implications, it is important to improve accuracy and reproducibility with further study, training, and education.

589 Brown Bowel Syndrome: An Uncommon Diagnosis that can Simulate Malignancy

Christina Arnold¹, Edward Calomeni², Arvind Rishi³, Aatur Singhi⁴, Kristen Stashek⁵, Lysandra Voltaggio⁶, Rashmi Tondon⁷
¹The Ohio State University Wexner Medical Center, Columbus, OH, ²The Ohio State University, Columbus, OH, ³Northwell Health, New York, Lake Success, NY, ⁴University of Pittsburgh Medical Center, Sewickley, PA, ⁵University of Maryland School of Medicine, Baltimore, MD, ⁶Baltimore, MD, ⁷Hospital of the University of Pennsylvania, Philadelphia, PA

Disclosures: Christina Arnold: None; Edward Calomeni: None; Arvind Rishi: None; Aatur Singhi: None; Kristen Stashek: None; Lysandra Voltaggio: None; Rashmi Tondon: None

Background: Brown bowel syndrome (BBS) is associated with malnutrition, specifically vitamin E deficiency, and due to an accumulation of lipofuscin in smooth muscle.

Design: Six unique cases of BBS were retrospectively identified from 5 institutions. One case was subject to electron microscopy and special stains. Pertinent clinicopathologic features were studied.

Results: The study group consisted of 3 men and 3 women (mean age=59 years, range 45-67 years). All specimens were resections (terminal ileum with right colectomy=2; small bowel only, n=4). Surgical indications included inflammatory bowel disease (IBD)-related (n=2), mass concerning for malignancy based on wall thickening and abnormal insufflation (n=1), gastrointestinal bleed (n=1), small bowel obstruction (n=1), and dumping syndrome (n=1). Of these, two patients had a history of bariatric surgery, one other patient was described as severely malnourished, and another patient was eventually diagnosed with primary intestinal lymphangiectasia. Two of the 6 specimens were grossly described as mahogany, and the specimen removed for a presumed malignancy was grossly thickened. Histologic sections of all cases showed finely granular, brown cytoplasmic pigment in smooth muscle cells on H&E. The pigment was more conspicuous in the small bowel compared to the colon, and most easily appreciated in the muscularis propria, but could also be identified in the smooth muscle of intermediate-sized arteries in the submucosa. The pigment was not identified in the mucosa. The pigment was highlighted with Fontana Mason and PAS/d, and was negative on Prussian blue and von Kossa. EM studies showed pigment compatible with lipofuscin in the cytoplasm of the smooth muscle cells. None of the patients were known vitamin E deficient prior to the resection. Of the two patients with vitamin E studies, one was confirmed vitamin E deficient and demonstrated improved laboratory studies with vitamin E supplements. The other patient had normal vitamin E levels, but the lab was drawn after the patient had received vitamin E. The mean clinical follow-up was 208 weeks (range 10-770 weeks), and all patients were alive and well.

Conclusions: BBS is important to recognize because it is linked with malnutrition/vitamin E deficiency, and we report it can simulate malignancy. BBS was characterized by finely, granular cytoplasmic pigment in smooth muscle cells, and it was most easily identified in the muscularis propria of the small bowel.

590 Gastric Margin Status at Frozen Section: Discrepancies between Representative Vs. in Total Sections

Ahmed Bakhshwin¹, Rebecca Waters², Thomas Plesec³

¹Robert J. Tomsich Pathology & Laboratory Medicine Institute, Cleveland Clinic, Pepper Pike, OH, ²Cleveland Clinic, Manvel, TX, ³Cleveland Clinic, Cleveland, OH

Disclosures: Ahmed Bakhshwin: None; Rebecca Waters: None; Thomas Plesec: None

Background: Surgeons routinely submit esophagus and proximal stomach resections for intraoperative consultation to evaluate the gastric margin (GM); however, there is no gold standard on how to assess these specimens' margin status at frozen section (FS). Over time, our institution has submitted these for FS as both as representative sections and in total. In this study, we evaluated rates of discrepancy with final margin status between the two methods.

Design: All esophagogastrectomy cancer cases (2013-present) in which GM was submitted for frozen evaluation were retrieved. Cases were divided on the basis of whether or not the GM was entirely submitted for frozen examination. Those with total gastrectomy or lacking complete shave GM for permanent were excluded. Discrepancies between the FS and final diagnosis were identified and classified as sampling or interpretation error. Two-tailed Fischer's exact test was used to evaluate the data.

Results: There were 200 adenocarcinoma resection cases in which the GM was entirely submitted for permanent histological examination. In 140 cases, the GM was entirely submitted for frozen evaluation (3-17 sections, mean: 7.4). One case (0.7%) out of 140 had discordant diagnosis. Review of the frozen slides showed that the tumor was present on the FS slide, and thus this was classified as an interpretation error. Of the 60 cases in which only representative sections (1-4 sections, mean: 1.3) of the closest GM were submitted for frozen, 5 cases were discordant (8.3%). One of these 5 (20%) was categorized as an interpretation error and the remainder four (80%) as sampling error (table 1). Of the 6 total discordant cases, 5 (83%) had histological evidence of treatment effect, and 4 (67%) had poorly differentiated (signet ring) morphology. All 4 cases that had sampling error were either treated or poorly differentiated.

	Concordant	Discordant	Discordant rate	Sampling error	Interpretation error
Representative section(s)	55	5	8.3 %	4	1
Totally submitted	139	1	0.7%	0 (p=0.009)	1 (p=0.52)

Conclusions: Our data show that sampling errors are significantly more frequent when only submitting representative FS, but interpretation errors were not. This is especially true in cases of poorly differentiated or pre-treated cancers. Although more time consuming and labor intensive, the best method of evaluating GM of esophagogastrectomies at the time of FS is submission of the complete shave margin, particularly in cases with poorly differentiated/signet ring cell histology, neoadjuvant therapy, or if the status of is not known.

591 Low Grade Appendiceal Mucinous Neoplasms: A Large Cohort Study with Long Term Outcomes

Samuel Ballentine¹, Noam Harpaz², Hongfa Zhu², Huaibin Mabel Ko¹, Qingqing Liu¹, Manju Ambelil¹, Zongxian Cao³, Alexandros Polydorides¹

¹Icahn School of Medicine at Mount Sinai, New York, NY, ²Mount Sinai Medical Center, New York, NY, ³Mount Sinai Health System, New York, NY

Disclosures: Samuel Ballentine: None; Noam Harpaz: None; Hongfa Zhu: None; Huaibin Mabel Ko: None; Qingqing Liu: None; Manju Ambelil: None; Zongxian Cao: None; Alexandros Polydorides: None

Background: The study of low grade appendiceal mucinous neoplasms (LAMN) and pseudomyxoma peritonei (PMP) has been facilitated by the adoption of new consensus definitions by the American Joint Committee on Cancer. These include combining T1 and T2 tumor extension into Tis and reliance on acellular mucin as evidence of peritoneal invasion. We applied the new definitions to a large cohort of patients with LAMN and evaluated their long term outcomes.

Design: We searched our database for patients diagnosed with LAMN and/or PMP between 2000 and 2018 whose original pathology materials were available for review. Lesions deemed not to be LAMN or WHO grade 1 (G1) were excluded. Demographic and follow-up clinical data were obtained from electronic medical records. Statistical analysis utilized the chi square method with significance set at P<0.05.

Results: We identified 167 patients, 59 (35.3%) men and 108 (64.7%) women, with an average age of 57 years old (range: 19-91). Eighty LAMNs (47.9%) were confined to the appendix without serosal involvement, of which 69 (86.3%) were Tis and 11 (13.8%) were T3.

Thirteen cases (7.8%) had appendiceal serosal involvement by acellular mucin only (T4a), 21 (12.6%) had acellular mucin in the abdominal peritoneal cavity (M1a), and 53 (31.7%) had neoplastic epithelium in the peritoneum (M1b). There were no significant differences among the groups in terms of age and sex. No disease recurrence occurred among patients with LAMN confined to the appendix or with peri-appendiceal acellular mucin only (N=93) whereas recurrence occurred in 47% of patients with acellular mucin or neoplastic epithelium in the peritoneal cavity (N=74) after comparable follow up periods (median 27 vs. 43 months, respectively)($p < 0.001$). The former group had lower rates of therapy with HIPEC (12% vs 88%, $p < 0.001$), debulking surgery (4% vs 87%, $p < 0.001$), and systemic chemotherapy (0% vs 30%, $p < 0.001$). No patients in either group any had lymph node or visceral (systemic) metastases.

Conclusions: Based on the results of this large series, we conclude that LAMN confined to the appendix (Stage Tis or T3) or with only acellular peri-appendiceal mucin (T4a) has a low if not negligible likelihood of peritoneal recurrence compared to LAMN accompanied by neoplastic epithelium in the peritoneum or distant acellular mucin.

592 Signal Transducer and Activator of Transcription-3 (STAT3) expression concordance in paired primary and liver metastatic colorectal cancer (CRC)

Justin Bateman¹, Rachel Goodwin¹, Horia Marginean², Allen Gown³, Shelly Sud¹, Daniel Yokom⁴, Esmeralda Marginean⁵

¹The Ottawa Hospital Cancer Centre, Ottawa, ON, ²The Ottawa Hospital Research Institute, Ottawa, ON, ³PhenoPath Laboratories, PLLC, Seattle, WA, ⁴Princess Margaret Hospital, Toronto, ON, ⁵Ottawa Hospital, Ottawa, ON

Disclosures: Horia Marginean: None; Allen Gown: None; Daniel Yokom: None; Esmeralda Marginean: None

Background: STAT3 belongs to a family of transcription factors that mediate normal and pathological cellular functions. STAT3 inhibitors are currently being tested in various cancer types. The prognostic impact of activated STAT3 (pSTAT3) in CRC has been reported in multiple studies, albeit with conflicting result. Furthermore, the expression concordance for pSTAT3 between primary and metastatic sites is currently unknown. In this study we evaluated immunohistochemical (IHC) expression of pSTAT3 in a cohort of patients with paired primary and liver metastatic CRC in order to assess concordance, and association between pSTAT3 expression and clinicopathological features and overall survival.

Design: Retrospective study included patients with resected CRC and liver metastases, treated at The Ottawa Hospital from 1998-2016. Tissue microarrays were constructed using 2x2 mm cores from each tumor IHC was carried out with pSTAT3 (Tyr705). Two independent pathologists evaluated nuclear expression of pSTAT3. Intensity of staining was scored 0 [absent], 1-2+ [low], or 3+ [high]. Cohen's kappa was used to measure agreement between scores. Kaplan-Meier estimates were calculated for OS using Cox proportional hazard model.

Results: There was a lack of agreement between pSTAT3 staining of primary tumor and metastases, with calculated kappa-value of -0.02, 95% CI (-0.05 to 0.07). The expression of pSTAT3 on a 3-tier scale in primary CRCs showed significant association with lymphovascular invasion ($p = 0.01$). High pSTAT3 was not associated with overall survival in either the primary or metastatic tumors (median follow-up of 7.7 yrs; range: 0.1-19 yrs).

Table 1: Demographics and clinical characteristics		
Characteristic	Categories	N=103
Age at diagnosis, median (range)	Years	64 (30-89)
Sex	Female	47 (46%)
	Male	56 (54%)
Primary Site	Rectum	44 (43%)
	Left	22 (21%)
	Transverse	4 (4%)
	Right	33 (32%)
Synchronicity	Metachronous	38 (37%)
	Synchronous	65 (63%)
Grade	Well Diff	88 (85%)
	Moderately Diff	12 (12%)
	Poor Diff	3 (3%)
T Stage	T2	9 (9%)
	T3	76 (74%)
	T4 (4a and 4b)	17 (16%)
	TX	1 (1%)
N Stage	N0 and NX	40 (39%)
	N1 (1a, 1b, and 1c)	35 (35%)
	N2 (2a and 2b)	28 (27%)
LVI in primary CRC	Present	57 (55%)
	Absent	39 (38%)
Neoadjuvant Chemotherapy	Received	38 (37%)

Figure 1 - 592

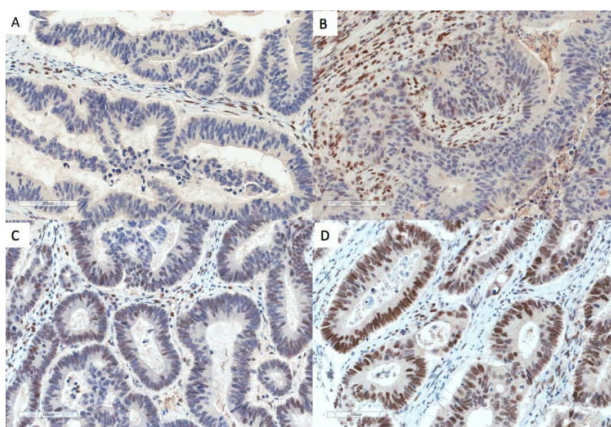


Figure 1: pSTAT3 staining intensity A=0 (absent) B=1+ (low) C=2+ (low) and D=3+ (high)

Conclusions: This study adds important new information to the existing literature on pSTAT3 in CRC, as lack of concordance between pSTAT3 expression in primary and liver metastases is important to recognize if pSTAT3 is to be used as a predictive or prognostic biomarker in the future. Furthermore, our study underlines the importance of concordance studies when developing a biomarker for clinical use. Activated pSTAT3 expression was not associated with a statistically significant difference in overall survival in either primary or metastatic CRC. However, pSTAT3 expression was significantly associated with lymphovascular invasion.

593 Endoscopic Mucosal Resection of Early Esophageal Adenocarcinoma: Clinical Outcomes and Metastatic Risk of a Cohort Stratified Based on Depth of Invasion, Histology, Lymphovascular Invasion and Deep Margin Status.

Varun Bhat¹, Saverio Ligato²

¹Hartford Hospital, Hartford, CT, ²Hartford Hospital, Canton, CT

Disclosures: Varun Bhat: None; Saverio Ligato: None

Background: Endoscopic mucosal resection (EMR) is a procedure used for the diagnosis and staging of early esophageal adenocarcinoma (pT1a and pT1b-EAC). In the absence of high risk histological factors (HRHFs), there exists some evidence that it may also be curative, obviating the need for surgical resection (SR). The aim of our study was to perform a retrospective clinicopathologic analysis of patients who underwent EMR at our institution for early EAC, and correlate with their clinical outcomes.

Design: From January 2010 to May 2018, 42 patients underwent 89 esophageal EMRs for clinical suspicion or biopsy-proven early EAC. The EMRs were reviewed and stratified according to the presence or absence of HRHFs including depth of tumor invasion (SM1 vs. SM2/SM3), histological grade/type, lymphovascular invasion (LVI) and tumor involvement of deep margin. The clinical records, follow-up pathological material and SRs were reviewed for evidence of residual local disease, lymph node metastasis (LNM) or metastatic disease.

Results: The median age of the 42 patients was 67 years (M=40,F=2). 25 (59.5%) had pT1a intramucosal carcinoma and 17(40.5%) had pT1b submucosal carcinomas (SM1=6, SM2=2, SM3=9). None of the pT1a EACs showed recurrence or progression on median follow up of 24 months. Due to the presence of one or more HRHFs, 6/17 (35.3%) pT1b EACs (SM1=1, SM3=5) underwent SR (Figure 1). The only case of SM1-invasive carcinoma that was selected for SR had a positive deep margin, LVI, and micropapillary histology, and was upgraded to SM3 on SR. This was the only case in our series that developed metastatic disease (16.7%). Interestingly, none of the 6 SR cases showed LNM. All 11 non-resected pT1b EACs (SM1=5, SM2=2, SM3=4) were negative for clinicoradiological evidence of LNM or metastatic disease on a median follow-up of 25 months. 3/11 had positive deep margins on EMR and were treated with additional EMRs and/or chemo-radiation therapy.

Figure 1 - 593

Pt. No.	Age	Sex	EMR				Resection		Non-surgical management	Follow-up	Follow-up duration (in months)
			Deep margin	LVI	High grade histology	Depth of invasion	Depth of invasion	Regional lymph node metastasis			
1	71	M	Positive	Present	Present (Micropapillary features)	SM1	pT1b (SM3)	0/30	Adjuvant chemotherapy	Distant metastatic disease*	61
2	66	M	Positive	Present	Present	SM3	pT1b (SM3)	0/21	None	NED	5
3	73	M	Positive	Present	Present (Micropapillary features with tumor budding)	SM3	No residual tumor	0/18	None	NED	30
4	64	F	Positive	Present, extensive	Absent	SM3	pT2	0/16	None	DUD	11
5	61	M	Negative	Absent	Present (Signet ring cell features with tumor budding)	SM3	pT1b (SM3)	0/15	None	NED	30
6	65	M	Close (<0.25 mm)	Absent	Absent	SM3	No residual tumor	0/14	None	DUD	15

* Biopsy proven lung metastases and widespread metastatic disease on clinicoradiologic follow-up

NED: No evidence of disease/progression
DUD: Died of unrelated disease

Conclusions: pT1a EAC, when adequately resected by EMR, can be considered completely cured, and endoscopic follow-up is sufficient. pT1b EACs with one or more HRHFs have metastatic risk (16.7%), but in our series no LNM, and should be considered for SR. pT1b EACs without HRHFs may be considered for conservative locoregional therapy, followed by vigilant endoscopic follow-up. Additional larger studies are needed to support these conclusions.

594 Gastrointestinal Tract Plasmablastic Lymphoma: Immunomorphologic Characterization of an Elusive Entity

Margaret Black¹, Esther Adler², Antonio Galvao Neto³

¹NYU, Long Island City, NY, ²NYU Langone Health, New York, NY, ³NYU Langone Health, Brooklyn, NY

Disclosures: Margaret Black: None; Esther Adler: None; Antonio Galvao Neto: None

Background: Plasmablastic lymphoma (PBL) has been reported in the gastrointestinal (GI) tract fewer than 40 times in the published English literature since its initial recognition as an HIV associated lymphoma in 1997. PBL has also been described in other immunocompromised states and rarely in immune competent individuals. Due to its rarity, unique morphology, and immunoprofile, it can be difficult to distinguish PBL from poorly differentiated carcinoma and other hematologic malignancies. This study seeks to identify key morphologic and immunophenotypic features to permit early diagnosis of PBL as it presents in the GI tract.

Design: The surgical pathology database at a large academic medical center was retrospectively searched for cases of PBL occurring from 2008 to 2018. A total of 13 cases were identified with 4 cases involving the GI tract (Table). Hematoxylin and Eosin, immunohistochemical, and in-situ hybridization slides were reviewed along with pathology reports and electronic medical record charts. A literature search was performed for published case reports and case series of PBL.

Results: All four patients with PBL presenting in the GI tract were adult males between 44 and 78 years (mean age 55). Three cases (cases 2 - 4) presented in the stomach and were associated with HIV and EBV. Case 1 presented in a surgically resected ileocolic anastomosis in an HIV and EBV negative patient with myelodysplastic syndrome and lung cancer. All four cases showed heterogeneous tumor cell morphology demonstrating areas with the classically described plasmablastic appearance including eccentrically placed nuclei, some prominent nucleoli, and a moderate amount of eosinophilic cytoplasm. Pleomorphic sheets of high grade tumor cells with non-specific morphologic appearance were seen in all cases, broadening the initial differential diagnosis. The immunoprofile (Table) supported the diagnosis of PBL with all cases expressing at least one plasma cell marker (CD138 and/or MUM 1), negativity for B-cell markers including CD20, and Ki-67 proliferation indices greater than 80%. IGH gene rearrangement was identified in all four cases.

Case	1	2	3	4
Age	78	50	47	44
Gender	Male	Male	Male	Male
Tumor Location	Ileocolic	Gastric	Gastric	Gastric
HIV status	Negative	Positive	Positive	Positive
1° Treatment	Surgery	EPOCH	EPOCH	LTF
1° Treatment Response	None	Remission	Remission	LTF
Relapse	No	Yes: 18 months	No	LTF
Outcome	DOD: 2 months	DOD: 19 months	NED: 21 months	LTF
Other Co-morbidities	Lung cancer, MDS	None	None	LTF
Immunoprofile				
CD20	Negative	Negative	Negative	Negative
CD138	Positive	Negative	Positive	Positive
MUM-1	Positive	Positive	N/A	Positive
HHV-8	Negative	Negative	N/A	N/A
Ki-67	80-90%	80-90%	> 80%	> 90%
EBER (ISH)	Negative	Positive	Positive	Positive
IgH gene rearrangement	Positive	Positive	Positive	Positive
Abbreviations: EPOCH = Chemotherapy regimen including Etoposide, Prednisolone, Oncovin, Cyclophosphamide and Hydroxydaunorubicin, LTF = loss to follow-up, DOD = died of disease, NED = no evidence of disease, MDS = myelodysplastic syndrome, N/A = Not available				

Conclusions: PBL is a rare and aggressive hematologic malignancy that can involve the gastrointestinal tract. The diagnosis can be confounded by its broad differential diagnosis. A high index of suspicion for PBL along with knowledge of its unique immunomorphology and clinical associations is essential for establishing this elusive diagnosis.

595 Distinctive Characteristics of Melanoma Metastatic to the Gastrointestinal Tract

Jayjay Blanco¹, Subramanya Sakaleshpura Mallikarjunappa¹, Paolo Gattuso², Shriram Jakate¹

¹Rush University Medical Center, Chicago, IL, ²Rush University Medical Center, Burr Ridge, IL

Disclosures: Jayjay Blanco: None; Subramanya Sakaleshpura Mallikarjunappa: None; Paolo Gattuso: None; Shriram Jakate: None

Background: Melanoma metastasis to the gastrointestinal (GI) tract may occur concurrent with the primary tumor or decades later and may be an isolated site of metastasis or one of the sites of disseminated tumor. The primary tumor may be mucosal or cutaneous, and in the case of late metastasis, may remain unknown and presumed to be a regressed cutaneous melanoma. We undertook a study to determine GI locations of melanoma metastases, type and locations of the primary and time intervals between the primary and metastases.

Design: We recovered 24 cases (16 males, 8 females, mean age of 61.3 years old) of GI metastases of melanoma in last 15 years (2003-2018) from the pathology databases in our medical center. Their electronic medical records (EMR) were reviewed for pertinent information regarding the primary and chronology of spread.

Results: Small bowel was the most common location in 18/24 (75%) followed by colon in 8/24 (33%) and stomach in only 3/24 (12%). Multiple GI organs, synchronously or metachronously, were involved in 8/24 cases (33%) and always included the small bowel. The most common known primary was cutaneous melanoma in 13/24 (55%), followed by presumed regressed cutaneous melanoma in 9/24 (37%) and only 2/24 cases (8%) of mucosal melanoma (vaginal and choroidal). The majority of the cases of known cutaneous primaries were located on the back or lower limbs (11/13 or 85% cases). The GI metastasis occurred early - 8 months or late - 15 years after the primary.

Conclusions: Unlike other metastatic tumors to the GI tract, melanoma is the least common in the stomach (12%) and most common in the small bowel (75%). The most common primary is cutaneous (92%) and the commonest primary sites are back and the lower limbs. Multiple synchronous or metachronous GI metastases occur in 33% of cases and always involve the small bowel. Both early and late metastases occur in the GI tract.

596 Quantitative, multiplexed analysis of the colorectal cancer microenvironment reveals prognostic significance for T cell subset densities and spatial distribution

Jennifer Borowsky¹, Koichiro Haruki², Andressa Dias Costa², Melissa Zhao³, Mai Chan Lau⁴, Annacarolina Fabiana Lucia Da Silva⁵, Tsuyoshi Hamada⁶, Kristen Felt², Jochen Lennerz⁷, Charles Fuchs⁸, Marios Giannakis², Jonathan Nowak⁵, Shuji Ogino⁵

¹The Royal Brisbane & Women's Hospital, Brisbane, QLD, Australia, ²Dana-Farber Cancer Institute, Boston, MA, ³Dana-Farber Cancer Institute, Somerville, MA, ⁴Boston, MA, ⁵Brigham and Women's Hospital, Boston, MA, ⁶The University of Tokyo, Boston, MA, ⁷Massachusetts General Hospital, Harvard Medical School, Boston, MA, ⁸Yale Cancer Center, New Haven, CT

Disclosures: Jennifer Borowsky: None; Koichiro Haruki: None; Andressa Dias Costa: None; Melissa Zhao: None; Mai Chan Lau: None; Annacarolina Fabiana Lucia Da Silva: None; Tsuyoshi Hamada: None; Kristen Felt: None; Jochen Lennerz: None; Charles Fuchs: Major Shareholder, Merck & Co., Inc.; Consultant, Eli Lilly; Advisory Board Member, CytomX; Consultant, Genentech; Consultant, Sanofi; Marios Giannakis: Advisory Board Member, Astra Zeneca; Jonathan Nowak: None; Shuji Ogino: None

Background: High T cell densities in the colorectal cancer (CRC) microenvironment are a well-established favorable prognostic factor. However, the specific T cell subsets that drive this association are not precisely defined, nor is the importance of the spatial relationship between T cell subsets, stroma and tumor epithelium. To address these questions, we developed a novel multiplex assay to enable deep T cell phenotyping in two nationwide prospective CRC cohorts with extensive clinical and molecular annotation.

Design: CRCs from stage I-IV patients in the Nurses' Health Study and Health Professionals' Follow-up Study were analyzed using a panel of antibodies directed against CD3, CD4, CD8, FOXP3, CD45RO, and cytokeratin. Multispectral immunofluorescent images of tissue microarrays were computationally processed to calculate T cell subpopulation densities in tumor and stroma. Multivariable inverse probability weighting (IPW)-adjusted Cox proportional hazard regression models were used to assess prognostic associations of quartile categories of T cell subset densities, adjusting for potential confounders, including stage, differentiation, microsatellite instability status, CpG island methylator phenotype (CIMP) status, LINE-1 methylation level, and KRAS and PIK3CA mutation status.

Results: Cumulatively, CRCs from 927 patients met image quality control criteria. Overall CD3⁺ T cell density was significantly associated with CRC-specific survival (tumor multivariate hazard ratio (HR) 0.54, 95% confidence interval (CI) 0.36-0.81, P for trend = 0.003 across quartile categories; stroma HR 0.58, CI 0.39-0.85, P for trend = 0.002). Additionally, intratumoral cytotoxic memory T cells (CD3⁺CD8⁺CD45RO⁺) (HR 0.45, CI 0.28-0.73, P for trend = 0.001), stromal naïve helper T cells (CD3⁺CD4⁺CD45RO⁻) (HR 0.60, 95% CI 0.40-0.90, P for trend = 0.004), and overall memory helper T cells (CD3⁺CD4⁺CD45RO⁺) (tumor HR 0.52, CI 0.34-0.80, P for trend < 0.001; stroma HR 0.54, CI 0.36-0.81, P for trend < 0.001) were also significantly associated with CRC-specific survival.

Conclusions: Tumor-infiltrating memory cytotoxic, stromal naïve helper, and overall memory helper T cell densities serve as prognostic biomarkers associated with longer survival of colorectal cancer patients, independent of clinical, pathological, and molecular features. Our

data provide a detailed view of the T cell landscape in the CRC microenvironment, revealing the importance of specific subpopulations and their spatial distributions.

597 Simple Three-Part Criteria for Diagnosing Sessile Serrated Polyps Versus Hyperplastic Polyps Validated by RNA Expression Profiling

Katherine Boylan¹, Priyanka Kanth², Don Delker², Mary Bronner³

¹University of Utah Hospital, Millcreek, UT, ²University of Utah Hospital, Salt Lake City, UT, ³University of Utah, Salt Lake City, UT

Disclosures: Katherine Boylan: None; Priyanka Kanth: None; Don Delker: None; Mary Bronner: None

Background: Sessile serrated polyps (SSPs) of the colon predispose to an estimated 20-30% of colonic adenocarcinomas. This increased cancer risk, relative to the little or no risk conferred by hyperplastic polyps (HPs), makes this a vital differential diagnosis. Currently, no gold standard diagnostic criteria exist to distinguish HPs and SSPs. Wide observer variability exists, due in part to the overlapping nature of current criteria based heavily on morphology, despite knowledge that polyp location and size are also important.

Design: We propose a simple three-part clinicopathologic scoring scheme to distinguish SSPs and HPs, respectively, based on: 1) colonic location (right or left), 2) size based on biopsy number (replacing two or more full biopsies versus one or less biopsy), and 3) morphology (SSP: minimum of two or more biopsies with at least one crypt each showing full thickness mucosal crypt dilation and/or lateral crypt extension at the base and/or crypt dysmaturation, versus HP: compact, non-dilated, hyperchromatic and non-serrated basal crypts with surface predominant serration). Using these criteria, an FFPE series of 104 serrated polyps (52 SSPs, 52 HPs) were correlated with our group's previously published 7-gene qRT-PCR expression profiling panel developed from RNA sequencing to distinguish HPs from SSPs (*Cancer Prev Res* 2016;9:456).

Results: ROC analysis of the three clinicopathologic categories in comparison to qRT-PCR data reveal the best correlation for polyp size followed by location and finally morphology (areas under the curves of 87.3%, 82.3% and 69.3%, respectively). Meeting 0 or 1 of these three pathologic criteria correlated best with an HP diagnosis by RNA profiling, whereas meeting 2 or 3 correlated best with an SSP diagnosis by RNA profiling. Data show high sensitivity (88.5%) and specificity (90%) for distinguishing SSPs and HPs when all three criteria are taken into account. When two out of three criteria are taken into consideration, the sensitivity (84.6%) and specificity (90%) remain high.

Conclusions: This simple three category system, further validated by RNA profiling, shows that serrated polyps meeting 2-3 criteria are SSPs and those meeting 0-1 are HP's. This diagnostic system provides a more objective, improved, and biologically validated approach to the accurate diagnosis of HPs and SSPs to assist colonic cancer risk assessment.

598 Serrated Lesions In Inflammatory Bowel Disease: Genotype-Phenotype Correlation

Iva Brcic¹, Heather Dawson², Hans Peter Gröchenig³, Christoph Högenauer¹, Karl Kashofer¹, Cord Langner¹

¹Medical University of Graz, Graz, Austria, ²Bern, Switzerland, ³Hospital Brothers of St. John of God, St. Veit/Glan, Austria

Disclosures: Iva Brcic: None; Heather Dawson: None; Hans Peter Gröchenig: None; Christoph Högenauer: None; Karl Kashofer: None; Cord Langner: None

Background: Patients with chronic inflammatory bowel disease (IBD) are at increased risk of developing colorectal cancer (CRC). Up to 30% of all sporadic CRCs arise through the serrated pathway. Recently, it has been identified that patients with IBD and hyperplastic/serrated polyposis have an increased risk of CRC. The aim of our study was to elucidate the nature of IBD-associated serrated lesions.

Design: Retrospectively, between 2005 and 2016, 39 adult IBD patients with clinical and endoscopic data, and 66 lesions with serrated morphology were analysed. Lesions were classified according to WHO criteria or were regarded as reactive. In addition, it was noted whether the lesion was arising in an area of current or previous inflammation. Immunostaining with Ki-67 and molecular analysis (Ion AmpliSeq™ Cancer Hotspot Panel) was performed.

Results: 82.1% of patients had ulcerative colitis, 17.9% Crohn's disease; 51.3% were female, mean age was 54.45 years. The duration of IBD from the first manifestation ranged greatly (16.73±11.40 months). Endoscopy showed polypoid lesions in 80.3% of cases. Size of the lesions ranged from 2 to 20 mm. One third of the lesions were located in the right colon. Five lesions were classified as inflammatory pseudopolyps, 27 as HP, 23 and 2 as SSA/P without and with low grade dysplasia, respectively, and 9 as TSA with low grade dysplasia. 35.4% of lesions were related to areas with signs of previous or recurrent inflammation. Ki-67 showed in majority of cases basal staining. Molecular analyses revealed 32 mutations in *KRAS* and 32 in *BRAF* gene (2 lesions with 2 *KRAS* mutations and one with *BRAF* non-V600E and *KRAS* mutation). In all inflammatory pseudopolyps no mutations were identified. In the right colon *BRAF* mutated lesions were more frequent than *KRAS* mutated ones (17 vs. 4), while *KRAS* mutations prevailed on the left side (28 vs. 15, p<0.001). 74.7% of IBD-associated serrated lesions harboured *KRAS* mutations.

Conclusions: In our study, Ki-67 was not helpful in the classification of serrated lesions. The molecular analysis could help to discriminate true serrated lesions (IBD-associated or not) from reactive pseudopolypoid mucosa with serrated epithelial change. These results should help pathologists to be more aware of serrated morphology in IBD patients in order to classify serrated lesions more accurately. Further studies should be performed in order to gather more evidence for developing surveillance guidelines for these patients.

599 Targeted DNA Sequencing Reveals Distinct Mutational Profiles in Polypoid Dysplasia of IBD versus Matched Colorectal Adenomas

Zongxian Cao¹, Zhenjian Cai², Samuel Ballentine³, Manju Ambelil³, Alexandros Polydorides³, Hongfa Zhu⁴, Huaibin Mabel Ko³, Qingqing Liu³, Noam Harpaz⁴

¹Mount Sinai Health System, New York, NY, ²The University of Texas Health Science Center at Houston, Houston, TX, ³Icahn School of Medicine at Mount Sinai, New York, NY, ⁴Mount Sinai Medical Center, New York, NY

Disclosures: Zongxian Cao: None; Zhenjian Cai: None; Samuel Ballentine: None; Manju Ambelil: None; Alexandros Polydorides: None; Hongfa Zhu: None; Huaibin Mabel Ko: None; Qingqing Liu: None; Noam Harpaz: None

Background: Inflammatory bowel disease (IBD)-associated colorectal cancers exhibit unique clinicopathological features that distinguish them from sporadic colorectal carcinomas and, based on the results of next generation sequencing studies, have distinct genetic profiles. To our knowledge, analogous comparisons between premalignant polypoid lesions in IBD and counterpart adenomatous polyps have not been reported.

Design: We analyzed 13 formalin fixed paraffin-embedded dysplastic polyps ranging from 0.5 to 2.5 cm in size from colonic resection specimens of patients with IBD (6 cases: 3 ulcerative colitis, 2 Crohn's disease, and 1 indeterminate colitis), and polypectomy specimens from non-IBD control patients (7 cases) which were matched by patient age, gender, anatomical location and size. DNA was extracted and next generation sequencing (NGS) was performed using the OncoPrint Comprehensive Assay (143 genes). Statistical comparisons utilized Fisher's exact test with significance set at $P \leq 0.05$.

Results: The IBD cases contained 13 mutations, 3 indels and 1 fusion whereas the controls contained 7 mutations, 2 indels and 1 fusion. The following genes were mutated exclusively in cases: *IDH1*, *CDKN2A*, *POLE*, *RNF43*, and *PTPRK-RSPO3* fusion, whereas *SETD2* mutation and *AGK-BRAF* fusion were only seen in controls. There were two hypermutated IBD cases, both with 5 genetic alterations and harboring a missense *POLE* mutation. The prevalence of *TP53* mutations trended higher in cases than controls (67% vs 14%, $p=0.10$, Fisher's exact test), whereas *KRAS* mutations were comparable in both groups (50% and 57%). *FBXW7* mutations were observed more commonly in IBD cases than controls but not significantly so (33% vs 14%, $p=0.56$). Our results are consistent with previous findings of early involvement of *TP53* mutation in IBD-associated carcinogenesis. In IBD-associated cancers *KRAS* mutations were reported to be relatively less frequent than sporadic CRC; here in our small series we found similar mutation rates in premalignant lesions of both conditions.

Conclusions: The mutational profiles of polypoid dysplastic lesions in IBD are genetically distinct from those of size, age, gender and location-matched sporadic colorectal adenomas reflecting their distinct histogenetic origins and potentially underscoring their divergent biologic behavior.

600 Molecular correlates of dysplasia subtypes in sessile serrated polyps and their relationship to invasive adenocarcinoma

Odise Cenaj¹, Masato Yozu², Michele Baltay³, Elizabeth Garcia³, Monica Devi Manam⁴, Neal Lindeman⁵, Joseph Misdraji⁶, Robert Odze³, Jonathan Nowak³

¹New York University Langone Medical Center, New York, NY, ²Middlemore Hospital, Auckland, New Zealand, ³Brigham and Women's Hospital, Boston, MA, ⁴Dana-Farber Cancer Institute, Natick, MA, ⁵Brigham and Women's Hospital Pathology, Boston, MA, ⁶Massachusetts General Hospital, Harvard Medical School, Boston, MA

Disclosures: Odise Cenaj: None; Masato Yozu: None; Michele Baltay: None; Elizabeth Garcia: None; Monica Devi Manam: None; Neal Lindeman: None; Joseph Misdraji: None; Robert Odze: None; Jonathan Nowak: None

Background: A subset of colorectal cancers (CRC) arise via the serrated neoplasia pathway, in which a sessile serrated polyp (SSP) develops dysplasia and then progresses to invasive carcinoma. Dysplasia in SSPs can show either a serrated or intestinal-type morphology. The molecular alterations associated with these types of dysplasia and their relationship to CRC have not been well characterized. We therefore sought to characterize the molecular features of these dysplasia subtypes in order to better define the biology of their neoplastic progression.

Design: DNA was isolated from macrodissected regions of SSPs containing either intestinal or serrated dysplasia. Massively parallel sequencing was performed using the OncoPrint platform, targeting 447 cancer-associated genes to provide mutation, copy number, tumor mutational burden (TMB) and mutational signature data. SSP molecular data were compared to prior CRCs analyzed using the same

OncoPanel version. Fisher's exact test and the Wilcoxon rank-sum test were used to evaluate correlations between dysplasia type and molecular features.

Results: In our multi-institutional cohort, 20 SSPs had intestinal dysplasia and 16 had serrated dysplasia. *BRAF* p.V600E mutation was common in both dysplasia types (75% intestinal, 93% serrated). There were no *KRAS* or *NRAS* mutations. Strikingly, intestinal dysplasia was characterized by a significantly higher rate of mismatch repair (MMR) deficiency (55% versus 13%, $p = 0.01$) and a higher TMB (median 15.3 versus 7.2 muts/mb, $p = 0.03$). Inactivating alterations in Wnt-signaling regulators *APC* and *FBXW7* were more common in intestinal dysplasia than in serrated dysplasia (65 versus 25%, $p = 0.03$; 30 versus 0%, $p < 0.01$), although other key CRC-associated genes did not show significantly different mutation patterns. Notably, the overall *TP53* mutation rate (25%) was significantly lower than in CRC (74%, $p < 0.001$) and there was minimal aneuploidy in both types of dysplasia. When stratified by proficient or deficient MMR status, the median TMBs of dysplastic SSPs (MMR-P: 6.8, MMR-D: 50.2) were similar to CRC (MMR-P: 6.8, MMR-D: 46.4).

Conclusions: MMR deficiency is significantly more common in SSPs with intestinal-type dysplasia, suggesting a partially distinct molecular progression pathway to CRC. While dysplastic SSPs have lower rates of *TP53* mutation and minimal aneuploidy compared to CRC, they nevertheless have a similar mutational burden, suggesting that they represent very proximal precursors to invasive cancer.

601 Distinguishing Hydrophilic Polymer-Associated Ischemic Enterocolitis (HPIE) from non-HPIE

Jesus Chavez¹, Michael Arnold², Wendy Frankel³, Wei Chen³, C. Eric Freitag³, Aatur Singhi⁴, Christina Arnold³

¹The Ohio State University, Columbus, OH, ²Nationwide Children's, Dublin, OH, ³The Ohio State University Wexner Medical Center, Columbus, OH, ⁴University of Pittsburgh Medical Center, Sewickley, PA

Disclosures: Jesus Chavez: None; Michael Arnold: None; Wendy Frankel: None; Wei Chen: None; C. Eric Freitag: None; Aatur Singhi: None; Christina Arnold: None

Background: Hydrophilic polymers coat intravascular medical devices to decrease friction and reduce device-related injury. When inadvertently dislodged, polymers can result in significant downstream thromboembolic events.

Design: A retrospective review conducted between 2011-2016 targeted patients status post aortic (n=797) and superior mesenteric artery (SMA) repair (n=42). All GI specimens within 3 months following the vascular repairs were retrieved: biopsies=72, resections=62. Ischemia was identified in 48 specimens (25 patients, all resections, SI=29, colon=19). Five of these specimens contained HPIE (4 patients, SI=1, colon=4). The morphology was compared to 15 non-HPIE ischemic resection controls.

Results: HPIE consisted of intravascular serpiginous polymers with stippled basophilia in the submucosa of ischemic zones. All aortic repair-related HPIE (n=3) underwent fenestrated endograft placement for unruptured juxtarenal or infrarenal aortic aneurysms, and these patients quickly developed complications (mean 1 day). For the SMA repair-related HPIE, the patient underwent an endovascular arteriography of the SMA and celiac trunk with celiac trunk stent placement using a hydrophilic coated guidewire and selective catheter (complication within 2 days of repair). In contrast, the non-HPIE controls all underwent open repairs for aortic aneurysms or dissections and presented with delayed complications (mean 65 days). Compared to the non-HPIE controls, characteristic features of HPIE included a lack of granulation tissue and macrophages at the ischemic border ($p=0.03$). Features exclusive to the non-HPIE controls (but not statistically significant) included architectural changes, perforations, transmural disease, smooth muscle hypertrophy of submucosal vessels, submucosal lymphocyte infiltrates, re-epithelization, and chronic serositis. Clinical follow-up was available up to 476 weeks. Of the 4 patients with HPIE, 2 died of multi-organ failure (mean 4.5 days). Of the non-HPIE patients, 7 patients died of more variable causes (cardiac arrest, septic shock, multi-organ failure, among others; mean 19.2 days).

Conclusions: In summary, HPIE occurs in ischemic enterocolitis resections status post aortic (19%) and SMA repair (4%). Timely recognition is important for accurate diagnosis and distinction from parasites. Clues to the diagnosis include a history of recent *endovascular* manipulation and acute ischemia (within 2 days).

602 Clinicopathologic and Molecular Investigation of Necrotizing Granulomas in Crohn's Disease

Sonja Chen¹, Evgeny Yakirevich¹, Albert Ross¹, Andres Matoso², Kara Lombardo², Shaolei Lu³, Shamlal Mangray⁴

¹Rhode Island Hospital, Providence, RI, ²Johns Hopkins Medical Institutions, Baltimore, MD, ³Providence, RI, ⁴Nationwide Children's Hospital, Providence, RI

Disclosures: Sonja Chen: None; Evgeny Yakirevich: None; Albert Ross: None; Andres Matoso: None; Kara Lombardo: None; Shaolei Lu: None; Shamlal Mangray: None

Background: Chronic active ileitis and non-necrotizing epithelioid granulomas (NNGs) are two key factors that assist in the diagnosis of Crohn's disease (CD). We have encountered examples of necrotizing granulomas (NGs) in CD which prompted further characterization of clinicopathologic features and etiology.

Design: 336 cases of Crohn's disease with granulomas diagnosed between 1997 and 2018 were retrospectively retrieved to identify cases with NGs. Demographic data, endoscopic and/or operative findings, morphologic features, treatment and follow-up data were reviewed. Acid fast, gram, GMS, and PAS/D special stains and PCR for bacteria, mycobacteria, and fungi were performed on FFPE tissue from all NG cases and 5 age-matched NNG cases. No testing for parasites was performed.

Results: Five of 336 (1.5%) cases had NG. There were 2 male, and 3 female patients with a median age 15 years (range 13-40) (Table 1). Three patients had ileo-colectomies, one had an ileal pouchectomy, with multiple prior bowel resections and one initially presented with abdominal lymphadenopathy and hypoechoic splenic lesions on imaging raising the concern for lymphoma. Diagnostic biopsies revealed florid NG of biopsied lymph nodes (LNs), granulomatous duodenitis and gastritis and mild right-sided active colitis. Four of 5 patients had established diagnoses of CD treated with either anti-inflammatory or immunosuppressive drugs at least 6 months prior to resection. Imaging of these 4 patients suggested periappendiceal inflammation or abscess, and all were treated with pre-surgical antibiotics. NGs were present in the ileocecal valve (2/4), periappendiceal fat (1/4) and LNs (2/4). On initial biopsy, no granulomas were identified in 3 of 5 patients. In the remaining 2 cases, NGs were identified in the ileum (1) and duodenum and stomach (1) respectively.

Special stains were negative in NG and NNG cases. PCR identified multiple bacterial templates in 1 case from each group, and was negative in all other cases. All NG patients improved with immunosuppressive therapy and none received anti-mycobacterial or anti-fungal therapy. Only one patient received metronidazole post-resection.

Table 1: Clinicopathologic features of CD patients with necrotizing granulomas

CASE	Age/ Sex	Duration of established CD diagnosis (mo)	Symptoms (duration in months)	Pre-resection therapy	Imaging	Location of NGs	Post-resection therapy	Follow up after NG diagnosis	Molecular findings		
									Mycobacterium (TB & non-TB)	Bacteria	Fungus
1	15/M	new	abd pain, fever, diarrhea, joint pain (1)	Prednisone	Enlarged LNs, hypoechoic lesions in spleen	LN	Steroid taper	Improved symptoms	Neg	Neg	Neg
2	13/F	21	abd pain (3)	Infliximab, Adalimumab	RLQ abscess, TI stricture, possible fistula	ICV	Adalimumab, Methotrexate	Improved symptoms	Neg	Multiple templates	Neg
3	15/F	6	abd pain (0.5)	Prednisone, mesalamine, metronidazole	RLQ inflammation	ICV	Prednisone, Mesalamine, Metronidazole then Infliximab	Partial small bowel obstruction, resection	Neg	Neg	Neg
4	18/M	24	abd pain (3)	Prednisone	RLQ abscess	ileum, periappend fat	6MP	Flare, resection	Neg	Neg	Neg
5	40/F	360	abd pain, diarrhea (3)	Prednisone, Azathioprine	Small bowel inflammation	LN	Prednisone	Multiple abscesses	Neg	Neg	Neg

Key: ICV- ileocecal valve, LN – lymph nodes, MTB- mycobacterium tuberculosis, Neg - no organism identified, PA – peri-appendiceal, RLQ – right lower quadrant, TI – terminal ileum, 6-MP – mercaptopurine

Conclusions: NGs are a rare, under-recognized finding mainly in patients with established CD, but may be identified at the initial manifestation of the disease. Recognition of this phenomenon allows for prompt treatment with appropriate immunosuppressive therapy once the special studies are done and potential risks for infection are ruled out.

603 Intraepithelial TCR delta+ Cells are Characteristic of Pediatric Celiac Disease

Sonja Chen¹, Ashlee Sturtevant², Kara Lombardo³, Murray Resnick¹

¹Rhode Island Hospital, Providence, RI, ²Brown University, Providence, RI, ³Johns Hopkins Medical Institutions, Baltimore, MD

Disclosures: Sonja Chen: None; Ashlee Sturtevant: None; Kara Lombardo: None; Murray Resnick: Consultant, PathAI

Background: Increased intraepithelial lymphocytes (IELs) in duodenal biopsies with villous blunting, may favor a diagnosis of celiac disease (CeID) in conjunction with clinical symptoms or serology. However, the differential diagnosis of duodenal IELs includes *Helicobacter pylori* infection (HP), Crohn's disease (CrD) and idiopathic/non-specific (INS), among others. We sought to identify and determine the pattern of expression of T lymphocyte subsets in CeID and its common differentials.

Design: As a pilot project, we identified 10 pediatric patients with CeID and three groups of 10 control cases (HP, CrD, INS) all with duodenal IELs (>30 CD3+ cells/100 enterocytes). Demographic, clinical data and histology were reviewed. Immunohistochemistry for CD3,

CD8, TCR delta, FOXP3 and IL-17 was performed on a representative formalin-fixed paraffin embedded block in each case and the number of T cells was calculated per 100 enterocytes as well as lymphocyte count per high power field in the lamina propria.

Results: The 10 CeID patients (6M, 4F; age range: 3-17years, median age:11 years) had mild to severe villous blunting, all had an elevated tissue transglutaminase (>20U) and presented with abdominal pain or failure to thrive. Control cases comprised three groups of 10 patients with IELs in CrD (5M, 5F; age range: 8-19yrs, median age:11yrs), HP (5M, 5F; age range: 5-17yrs, median age:11yrs), and INS (6M, 4F; age range: 7-18yrs, median age:16yrs); none of which showed villous blunting. Compared to control groups, CeID patients had a two-fold increase in intraepithelial CD3+T cells ($p<0.0001$), decreased CD8+ T cells and 6-10 times increased TCR delta expressing cells ($p<0.0001$ compared with CrD and INS; $p=0.0008$ compared with HP). Of controls, INS cases had the least number of TCR delta T cells (average 2.1 cells/100 enterocytes). IL-17+ cells were predominantly seen in the lamina propria however there was only a statistically significant difference between CeID and HP ($p=0.0286$). In addition, there were significantly increased FOXP3+ regulatory T cells present in the lamina propria of CeID compared with the other groups ($p=0.0223$ compared with HP, $p=0.0422$ compared with CrD and $p=0.0002$ INS).

Conclusions: Our findings demonstrate that CeID is characterized by increased intraepithelial TCR delta+ T cells and FOXP3+ regulatory T cells and increased lamina propria IL-17+ T cells. These may be useful adjunctive tools to aid in the differential diagnosis of duodenal IELs and inform the biology of CeID.

604 Retained Expression of Mismatch Repair Protein Is More Commonly Seen with Pathogenic Missense Than Other Mutations in Lynch Syndrome

Wei Chen¹, Heather Hampel¹, Rachel Pearlman¹, Dan Jones², Weiqiang Zhao², Mohammed Alsomali¹, Debbie Knight¹, Wendy Frankel¹

¹The Ohio State University Wexner Medical Center, Columbus, OH, ²The Ohio State University, Columbus, OH

Disclosures: Wei Chen: None; Heather Hampel: Grant or Research Support, Myriad Genetic Laboratories; Advisory Board Member, InVita Genetics; Advisory Board Member, Genome Medical; Advisory Board Member, Genome Medical; Rachel Pearlman: None; Dan Jones: None; Weiqiang Zhao: None; Mohammed Alsomali: None; Debbie Knight: None; Wendy Frankel: None

Background: Assessment of mismatch repair protein (MMR) expression by immunohistochemistry (IHC) is the cornerstone of universal Lynch syndrome (LS) screening. We expect expression of MMR protein will be lost for any MMR gene that has biallelic combinations of pathogenic germline mutation (LS), double somatic (DS) mutation, or methylation of the MLH1 promoter. However, occasionally these cases show retained expression of the corresponding MMR protein(s), and this has been speculated to be more frequent in LS cases due to pathogenic missense (MS) mutations due to expression of a nonfunctional protein with retained antigenicity. Our goal was to evaluate if colorectal cancer (CRC) cases with pathogenic MS mutations more frequently show retained MMR expression by IHC as compared with other pathogenic LS germline mutations and DS mutations.

Design: 3312 adults with CRC diagnosed from 1/1/2013 to 12/31/2016 were evaluated in our statewide initiative. MMR deficient tumors were identified by MMR IHC and MSI PCR. If MSI-high or absent MLH1, MLH1 methylation was analyzed by pyrosequencing. Select patients underwent germline next-generation sequencing (NGS) testing of 25 to 66 cancer genes including those patients with defective MMR without methylation (ColoSeq or BROCA, University of Washington). If no germline mutation was found in these cases, NGS of tumor MMR genes (MLH1, PMS2, MSH2, MSH6, EPCAM) was performed. Available MMR IHC slides from LS and DS mutation cases were reviewed and the expression level (strength and percent of tumor cells stained) was quantified manually.

Results: IHC slides were available on 80 patients with MMR deficiency (without methylation) and germline NGS results; 26 with absent germline mutation also had tumor sequencing. 16 of 80 MMR-defective cases showed retained MMR expression (Table). Unexpected MMR expression was present in 4 of 9 (44%) LS cases with MS mutation, 5 of 47 (11%) LS cases with non-MS pathogenic mutations, and 7 of 26 (27%) DS mutation cases.

Retained MMR Expression in Colorectal Cancers with Pathogenic MMR Mutation

Cases (n)	# Cases Retained MMR Expression	Mutation	MMR IHC (% staining)
LS, Missense (9)	1	PMS2	PMS2 Intact*
	1	PMS2	PMS2 WTC (75%)
	1	MSH6	MSH6 Intact
	1	MSH6	MSH6 WTC (30%)
	Total 4 (44%)		
LS, Others (47)	1	MLH1	MLH1 Intact
	1	PMS2	PMS2 Intact
	1	MSH6	MSH6 Intact
	2	MSH6	MSH6 WTC (20%, 50%)
	Total 5 (11%)		
Double Somatic (26)	5	MLH1	MLH1 WTC (10%, 10%,
	1	MLH1	10%, 20%, 75%)
	1	MSH2	MLH1 Intact
			MSH2 WTC (>95%)
	Total 7 (27%)		

* Intact = Diffuse Strong Staining >95%; LS=Lynch Syndrome; MMR=Mismatch Repair Protein; WTC=Weaker Than Control.

Conclusions: Retained expression of MMR proteins may occur in both LS cases and cases with MMR DS mutation. MMR protein expression is most commonly seen with pathogenic germline MS mutations. Cautious interpretation of MMR IHC is advised when dealing with tumor staining weaker than control regardless of the percentage of tumor staining, as these cases may harbor pathogenic MMR gene mutations. MS mutations appear to account for some, but not all CRC cases that may be missed in LS screening by IHC.

605 Gastric adenoma in Lynch syndrome: unique histomorphological features

Zongming Eric Chen¹, William Quinones¹, Iman Sarami¹, Fan Lin¹

¹Geisinger Medical Center, Danville, PA

Disclosures: Zongming Eric Chen: None; William Quinones: None; Iman Sarami: None; Fan Lin: None

Background: Lynch syndrome (LS) patients have increased risks for cancer development, particularly colonic and endometrial cancers, often at an early age. The prevalence of gastric cancer is highly variable. Although a recent study suggested pylori gland adenoma may be a precursor lesion for LS associated cancer in the stomach, gastric polyps including adenomas have not been well studied in these patients.

Design: 16 genetically confirmed LS patients were identified resulting from a universal screening program for colon and endometrial cancer at Geisinger from 2013-2018. 10 patients also had archived specimens for gastric polyps. All slides were reviewed and characteristic histomorphological findings were categorized and recorded. Immunostains of mismatch repair proteins (MLH1, MSH2, MSH6, PMS2) and mucin core proteins (MUC5AC and MUC6) were performed in some specimens to help characterize the lesions and confirm their molecular alteration.

Results: A total of 21 gastric polyps were examined from 10 patients (4 men, 6 women; age range from 23 to 81; average 53). 12 (57%) were gastric fundic gland polyps (FGP) and 2 (10%) were hyperplastic polyps (HP). There were 7 (33%) gastric adenomas found in 2 patients including 3 foveolar type, 2 pyloric type and 2 mixed type; no intestinal type was identified. 3 adenomas (2 mixed type and 1 foveolar type) showed high grade dysplasia and 1 foveolar type also harbored intramucosal adenocarcinoma. All adenomas demonstrated corresponding characteristic mismatch protein deficiency, while FGP and HP from the same patients did not. Increased intratumoral lymphocytes and prominent peritumoral lymphoid reaction were common features associated with these adenomas. For all patients, the background gastric mucosa was either normal or with mild non-specific chronic inflammation and reactive epithelial changes. No H pylori infection was found.

Conclusions: Gastric adenoma occurs at an increased rate in Lynch patients (20%) comparing to the general population. Instead of intestinal type, gastric type seems the predominant form in the studied cohort. Mismatch match protein deficiency appears responsible for tumorigenesis. These lesions are precursors for adenocarcinoma. Increased intratumoral lymphocytosis and prominent lymphoid reaction in surrounding tissue are helpful features for diagnosis.

606 Characterization of tumor buds and poorly differentiated tumor clusters at the invasive front of colorectal cancer by digital morphometry

Muhan Joyce Chen¹, Huaibin Mabel Ko¹, Hongfa Zhu², Qingqing Liu¹, Alexandros Polydorides¹, Noam Harpaz²

¹Icahn School of Medicine at Mount Sinai, New York, NY, ²Mount Sinai Medical Center, New York, NY

Disclosures: Muhan Joyce Chen: None; Huaibin Mabel Ko: None; Hongfa Zhu: None; Qingqing Liu: None; Alexandros Polydorides: None; Noam Harpaz: None

Background: Tumor buds (TBs) and poorly differentiated clusters (PDCs), defined as non-glandular cell groupings of ≥ 5 or >5 cells, respectively, at the invasive front of cancers, are adverse prognostic factors in resected colorectal cancer (CRC). TB was recently incorporated by American Joint Committee on Cancer (AJCC) as an optional synoptic report field in CRC. However, it is unclear if PDCs and TB coexist and share features of epithelial-mesenchymal transition (EMT). Also the upper limit of cell number for PDCs remains undefined. To this end, we sought to quantitatively characterize TB/PDCs utilizing a morphometric approach.

Design: The pathology records were searched for "tumor budding" and "colon" from Jan-July 2018. Resected CRCs were reviewed and the slide harboring the most TB/PDCs was selected for each case. Sections were stained for cytokeratin, E-cadherin and b-catenin, and subsequently scanned via Pannoramic 250 scanner. The cluster sizes and staining intensity were analyzed on digitalized slides utilizing the Halo Morphometry software (Indica Labs). Continuous variables were compared with the Student *t* test.

Results: 19 CRCs were identified. Visualizing by cytokeratin stains, TB and PDCs were simultaneously detected in all tumors ($n=19$, 100%) and they intermixed at the tumor invasive front. 63% of PDCs contained 6-10 cells and 37% contained 10-20 cells. The absolute count of PDCs per 3.9mm² was 9.8 ± 1.5 , and clusters of 6 and 9 cells were most common. The average number of TB was 30.5 ± 4.9 per 3.9mm², with single-cell, 2-cell, 3-cell, 4-cell and 5-cell buds composing 63%, 12%, 11%, 7.3% and 6.7% of the total. No correlation between TB/PDCs and tumor staging was identified. Stage III tumors ($n=9$) showed a 1.5-fold increase in TBs (37.6 ± 8.7 vs. 24.7 ± 4.8), and a 0.26-fold decrease in PDCs (8.3 ± 1.3 vs. 11.2 ± 2.5) compared to stage II tumors ($n=10$), however, these findings did not reach statistical significance. Compared with the intensity of E-cadherin staining of the main tumor, the TB/PDCs showed significantly impaired membranous expression, a hallmark of EMT ($p < 0.05$). No nuclear translocation of b-catenin was detected in any TB/PDCs, however they displayed decreased membranous b-catenin staining compared to main tumors ($p < 0.05$).

Conclusions: Morphometry, an unbiased quantitative approach, allows thorough examination of the invasive front of CRC. We demonstrated concurrent presence of TB and PDCs with overlapping partial EMT features in CRCs, and determined PDCs to be clusters of up to 20 cells.

607 High Frequency of Hes1 Loss in Colorectal Adenocarcinomas with RAS/BRAF mutations

Wei Chen¹, Amad Awadallah¹, Lan Zhou², Wei Xin³

¹University Hospitals Cleveland Medical Center, Cleveland, OH, ²Cleveland Medical Center, Case Western Reserve University, Solon, OH, ³Case Western Reserve University, Cleveland, OH

Disclosures: Wei Chen: None; Amad Awadallah: None; Lan Zhou: None; Wei Xin: None

Background: Hes1 is the downstream target of canonical Notch-signaling pathway, which plays an important role in maintaining intestinal proliferative crypts and regulating enterocyte differentiation. Hes1 is expressed in the nuclei of normal intestinal epithelial cells. We reported previously that loss of Hes1 expression is frequently found in the right-sided colon cancers, which commonly harbors RAS mutations, including KRAS and NRAS, as well as BRAF (V600E) mutation. Mutations in KRAS and BRAF genes as the key mediators in the EGFR signaling pathway play an important role in the colorectal pathogenesis. In this report, we explore the relationship between the dysregulated Notch pathway and the status of RAS or BRAF mutations.

Design: 43 cases of primary colorectal adenocarcinomas were collected in a tertiary teaching hospital. Hes1 expression is assessed by immunohistochemical stain. RAS (KRAS and NRAS), BRAF and APC status were determined by the next-generation sequencing or PCR-based mutation analysis. Clinical information including tumor diagnosis, staging and locations, were correlated in the data analysis.

Results: Overall, loss of Hes1 expression is found more frequently in colorectal cancer specimens with either RAS or BRAF mutation than cases that have the wild type RAS and BRAF status (78.6% vs 40.0%, $p < 0.05$ by χ^2 test). Further analysis showed that for tumors located at right side, all the cases with RAS or BRAF mutations show loss of Hes1 expression (12/12, 100%) ($p < 0.05$), while only 62.5% (10/16) of

left-sided tumors with *RAS* or *BRAF* mutation have lost Hes1 expression (Table 1). *APC* mutation was found in 25.6% cases, and was not related with Hes1 expression in our studies.

Table 1. *RAS* or *BRAF* mutation and Hes1 expression in right/left colorectal adenocarcinoma.

Right side (n=14)				Left side (n=29)			
Hes1	RAS/BRAF*		p	RAS/BRAF*		p	
	Wild type	Mutated		Wild type	Mutated		
Present	1 (50.0%)	0 (0)	0.01	8 (61.5%)	6 (37.5%)	0.19	
Loss	1 (50.0%)	12 (100%)		5 (38.5%)	10 (62.5%)		

**RAS/BRAF* wild type refers to cases with no mutations detected in *RAS* or *BRAF*; while Mutated refers to cases with either *RAS* or *BRAF* mutation.

Conclusions: High frequency of Hes1 loss in colorectal adenocarcinoma is associated with either *RAS* or *BRAF* mutation, suggesting that synergistic effects by dysregulated Notch and *RAS/BRAF* mutation may play an important role in colon carcinogenesis in some forms especially the right-sided tumors. This finding may help guide the future treatment for a subset of colon cancers.

608 A Multicenter Clinicopathologic Study of “Non-Conventional” Dysplasia in Patients with Inflammatory Bowel Disease

Won-Tak Choi¹, Masato Yozu², Gregory Miller³, Angela Shih⁴, Joseph Misdraji⁵, Gregory Lauwers⁶

¹University of California, San Francisco, San Francisco, CA, ²Middlemore Hospital, Auckland, New Zealand, ³Envoi Specialist Pathologists, Brisbane, QLD, Australia, ⁴Massachusetts General Hospital, Boston, MA, ⁵Massachusetts General Hospital, Harvard Medical School, Boston, MA, ⁶H. Lee Moffitt Cancer Center & Research Institute, University of South Florida, Tampa, FL

Disclosures: Won-Tak Choi: None; Masato Yozu: None; Gregory Miller: None; Angela Shih: None; Joseph Misdraji: None; Gregory Lauwers: None

Background: Various types of “non-conventional” dysplasia (NCD) are known to occur in patients with inflammatory bowel disease (IBD). However, there is limited information regarding their clinicopathologic features and whether they are more frequently associated with colorectal cancer (CRC) compared to traditional dysplasia (TD).

Design: 59 IBD patients with CRC were analyzed. All available prior biopsies showing dysplasia from each patient were also reviewed to classify different types of dysplasia. Hyper mucinous dysplasia was defined as a villous lesion with prominent mucinous differentiation. Serrated dysplasia was sub-classified into traditional serrated adenoma (TSA)-like, sessile serrated adenoma (SSA)-like, or serrated NOS. Goblet cell deficient (GCD) dysplasia was defined as a tubular lesion with a complete or near-complete absence of goblet cells, whereas dysplasia with terminal epithelial differentiation (TED) represents a tubular lesion with enterocyte-like cells showing hyperchromatic nuclei and occasional Paneth cell differentiation.

Results: 36 NCD cases were identified in 26 (44%) of the 59 patients and occurred with similar frequency in men and women (58 and 42%, respectively), with a mean age of 54 years and a long history of IBD (mean: 17 years). In comparison, 70 TD cases were identified in 46 patients (78%). Fourteen patients (24%) had both NCD (n = 20) and TD (n = 19), which were typically detected in the same colonic segment in all but 3 patients. NCD usually appeared as a polypoid lesion (61%) in the left colon (56%). Low-grade lesions (81%) were more common than high-grade (19%). Hyper mucinous dysplasia was the most common (42%), presenting as either a ‘pure type’ (14%) or a ‘mixed type’ (28%, with either TD or another type of NCD). Serrated dysplasia was also common (42%): TSA-like (28%), SSA-like (3%), and serrated NOS (11%). GCD (6%) and TED dysplastic lesions (11%) were relatively rare. When the exact location was available, NCD was detected in the vicinity of CRC in all but 4 patients. Similarly, TD was detected in the same colonic segment in all but 2 patients. Comparing CRC cases associated with NCD to those with TD only, no significant difference was noted in the characteristics of tumor (including size, grade, depth of invasion) or demographic factors (such as age, gender, type/duration of IBD).

Conclusions: NCD is common in IBD patients with CRC. It appears to develop in the same field of carcinomatous development, and it is not uncommonly associated with TD.

609 Tumor Heterogeneity Index to Detect HER2 Amplification by Next-Generation Sequencing: A Direct Comparison Study with Immunohistochemistry

Sangjoon Choi¹, Jinah Chu¹, Binnari Kim², Sang Yun Ha², Kyoung-Mee Kim²

¹Seoul, Korea, Republic of South Korea, ²Samsung Medical Center, Seoul, Korea, Republic of South Korea

Disclosures: Sangjoon Choi: None

Background: Intratumoral heterogeneity of HER2 is common in gastric cancer (GC) and poses a challenge for identifying patients who may benefit from anti-HER2 therapy. However, a direct comparison between the results of HER2 immunohistochemistry (IHC) and next-generation sequencing (NGS)-based cancer panel tests have not been explored in GC.

Design: This study included the data of 168 metastatic cases of GC with expression levels of HER2 obtained by IHC and the copy number alteration (CNA) of ERBB2 obtained by NGS test. To determine optimal thresholds of HER2 overexpression to be detected by NGS, we applied the Tumor Heterogeneity Index (the quantifiable value of H-score multiplied by tumor volume) and Receiver Operating Characteristic (ROC) curve.

Results: GC tissues were obtained via endoscopic biopsy (N=91), needle biopsy from metastases (N=8), peritoneal biopsy (N=4), and gastrectomy (N=65). HER2 3+ by IHC was observed in 27/168 (16%) cases, and 14/27 (52%) HER2 IHC 3+ cases showed intratumoral heterogeneity (<90% of tumor cells are HER2 3+). Out of 27 HER2 3+ cases, 19 (70%) were detected by NGS. All 8 cases with discrepant IHC and NGS results harbored intratumoral heterogeneity. The ROC curve analysis showed that the optimal value of the Tumor Heterogeneity Index to be detected by NGS was a score of 72 for biopsy specimens and 120 for resection specimens.

Conclusions: Intratumoral heterogeneity of HER2 expression is observed in 52% of metastatic GC cases. To accurately detect ERBB2 CNA by NGS, the optimal value obtained by the Tumor Heterogeneity Index can be used.

610 Frequency of sessile serrated adenoma/polyp diagnosis in a population based setting: Implications for colon cancer screening and surveillance

Alexander Christakis¹, Lynn Butterly², Christina Robinson², Joseph Anderson³, Amitabh Srivastava⁴

¹Brigham and Women's Hospital, Boston, MA, ²Dartmouth-Hitchcock Medical Center, Lebanon, NH, ³Dartmouth Geisel School of Medicine, Hanover, NH, ⁴Brigham and Women's Hospital, Harvard Medical School, Boston, MA

Disclosures: Alexander Christakis: None; Lynn Butterly: None; Christina Robinson: None; Joseph Anderson: None; Amitabh Srivastava: None

Background: Sessile serrated adenoma/polyp (SSA/P) was first proposed as an entity in 2003 but the morphological distinction of SSA/P from hyperplastic polyps (HP) remains problematic. Interobserver reproducibility studies from tertiary centers have been published but there is little data regarding pathologist performance in a population based setting. We evaluated the trends in frequency and factors associated with a diagnosis of SSA/P in a large population based colonoscopy registry.

Design: The New Hampshire colonoscopy registry has been collecting data from patient questionnaires, colonoscopy findings and pathology reports since 2006. We retrieved data from 15 pathology sites across the state and evaluated the frequency of SSA/P diagnosis across in low and high volume pathology laboratories during the tertile periods 2004-11, 2012-14, 2015-18 and also assessed factors associated with an SSA/P diagnosis on a multivariable analysis after adjusting for patient age, gender, BMI, family history and smoking.

Results: A total of 57,739 polyps were diagnosed as either HP or SSA/P between 2006-2018. Despite serving a relatively homogeneous patient population there was a wide variation in frequency of SSA/P diagnosis across various pathology sites (1.5% to 16.5%) during the entire study period. The frequency of SSA/P diagnosis increased with time in both low volume and high volume pathology centers (see table). Multivariable analysis showed that an SSA/P diagnosis was more likely to be associated with polyp size, proximal location, recent colonoscopy and high volume centers (see table).

	Serrated polyp diagnosis	Tertile 1	Tertile 2	Tertile 3
Low volume	SSP (n=)	3.1%	6.1%	12.8%
	HP	96.9%	93.9%	87.2%
	Total	1618	2532	3761
High volume	SSP	3.8%	10.1%	18.7%
	HP	96.2%	89.9%	81.3%
	Total	11923	17476	20757
		OR	95% CI	p
High versus low volume path center	1.73	1.55-1.94	0.0001	
Time period tertile	1	1.0	---	---
	2	4.01	3.50-4.59	0.0001
	3	8.65	7.58-9.86	0.0001
Size of serrated polyp	<5 mm	1.0	----	---
	5-9 mm	2.92	2.68-3.15	0.0001
	≥ 10 mm	8.44	7.49-9.51	0.0001
Proximal versus distal	11.88	10.92-12.92	0.0001	

Conclusions: Our data highlights the problems in using histologic distinction between HP and SSA/P for guiding surveillance intervals in patients undergoing colonoscopy. This issue may be even more challenging in low volume pathology centers. Using serrated polyp size and location, regardless of histologic diagnosis of HP or SSA/P, offers a more reproducible way of developing objective surveillance guidelines for patients undergoing colon cancer screening.

611 Noncanonical RAS Mutations in Colorectal Adenocarcinoma: Implication of Evolving Molecular Testing Patterns on Therapy Selection

Danielle Costigan¹, Jonathan Nowak², Lynette Sholl², Fei Dong²

¹Brigham and Women's Hospital, Harvard Medical School, Boston, MA, ²Brigham and Women's Hospital, Boston, MA

Disclosures: Danielle Costigan: None; Jonathan Nowak: None; Lynette Sholl: *Consultant*, Foghorn Therapeutics; *Speaker*, Astra Zeneca Pharmaceuticals; *Advisory Board Member*, Loxo Oncology; Fei Dong: None

Background: *KRAS* exon 2 mutation is a well-established predictor of resistance to anti-EGFR monoclonal antibody therapy in metastatic colorectal cancer. Updated consensus guidelines have recommended extended testing to include additional *RAS* mutations (in *KRAS* exons 3 and 4 and *NRAS* exons 2, 3 and 4) that are also predictive of resistance to anti-EGFR therapy. This study evaluates the impact of evolving molecular testing patterns by targeted next generation sequencing (NGS) on the detection of *RAS* mutations and examines the potential implications of extended *RAS* testing on therapy selection.

Design: At our institution, pyrosequencing for detection of *KRAS* codon 12/13 mutations was performed on 2096 colorectal cancers between 2008-2017, and clinical NGS was performed on 457 colorectal cancers between January 2017 and June 2018. Our institutional experience was correlated with the *RAS* mutation rates of 212 colorectal cancers from the Cancer Genome Atlas (TCGA) and 4335 colorectal cancers from the AACR Project Genomics Evidence Neoplasia Information Exchange (Project GENIE).

Results: The overall rate of *KRAS* codon 12/13 mutation detection by pyrosequencing in colorectal cancers at our institution was 36% (761/2096) over a 9-year period. This compared to a detection rate of 45% (204/457) for *KRAS* codon 12/13 mutations using NGS, which increased to a 57% (259/457) detection rate when all pathway activating *KRAS* and *NRAS* mutations were included in the analysis. 34% of TCGA and 36% of Project GENIE colorectal cancers contained *KRAS* codon 12/13 mutations, compared to 49% of TCGA and 46% of Project GENIE colorectal cancers when all activating *KRAS* and *NRAS* mutations were included.

Conclusions: In approximately 12% of all patients with colorectal cancer, an extended *RAS* testing strategy using NGS identified mutations in *KRAS* and *NRAS* that were not detectable by testing *KRAS* codons 12 and 13 only. The increasing availability and utility of NGS platforms has the potential for significant clinical impact by identifying a larger proportion of patients with colorectal cancer who are unlikely to respond to anti-EGFR therapy.

612 Assessment of the effectiveness of morphological criteria in distinguishing serrated lesions of the colon and rectum

Renata Coudry¹, Marcela Silva de Menezes², Pedro Popoutchi², Cristiane Ribeiro², Fábio Molinari¹, Luciana De Meirelles¹, Mariana Morini¹, Marianne de Castro², Melissa Fugimori³, Teoclito Sachetto², Thales Silveira¹, Laura López Claro⁴

¹São Paulo, SP, Brazil, ²Hospital Sírio Libanês, São Paulo, SP, Brazil, ³Hospital Sírio-Libanês, São Paulo, SP, Brazil, ⁴Irmandade da Santa Casa de Misericórdia de São Paulo, Santo André, SP, Brazil

Disclosures: Renata Coudry: None; Marcela Silva de Menezes: None; Pedro Popoutchi: None; Cristiane Ribeiro: None; Fábio Molinari: None; Melissa Fugimori: None; Thales Silveira: None; Laura López Claro: *Speaker*, Eli Lilly and Company

Background: Clinicopathological studies suggest that serrated polyps (SPs) are responsible for up a third of sporadically occurring colorectal cancer (CRC). For several years, the lack of consensus on definition, nomenclature and biology of serrated polyps (SPs) of the colon and rectum has created considerable confusion among pathologists and currently studies show that this difficulty is still present.

Design: Five gastrointestinal subspecialists and five generalists evaluated a total of 248 serrated polyps in order to establish the interobserver agreement through the Kappa (K) coefficient using whole slide imaging. Diagnostic analysis was conducted without clinical information and knowledge of the previous diagnosis. A consensus diagnosis was used to all concordance analysis and was defined when three or more gastrointestinal pathologists was in agreement with certain diagnosis. Cases without agreement were discussed with the five gastrointestinal subspecialists to achieve a final diagnosis.

Results: The interobserver agreement assessment among the ten pathologists was fair (K=0.28). Analysis between the two groups of pathologists indicated a fair agreement (K=0.34) among subspecialists and a slight agreement (K=0.19) among generalists. When comparing original versus consensus diagnosis, 33.5% of the sessile serrated adenoma (SSA) diagnosis were changed to hyperplastic polyps (HP) and 15.5% of the HPs were changed to SSAs. 19 cases did not reach a consensus diagnosis, 30% of them had a superficial orientation or fragmentation of the specimen. Concerning specimen acquisition, 87% of the polyps that showed a well-oriented basal portion of crypts were treated by mucosectomy.

Conclusions: The precision in the diagnosis of these lesions is essential for the prevention of CRC, thus the identification of factors that can pose challenges in diagnosis accuracy can help better solve this important matter.

613 Should Colectomy Size Be Considered When Assessing for Presence of 12 Lymph Nodes As A Quality Requirement For Laparoscopic Colectomies Performed For Colon Cancers?

Craig Cousineau¹, Samuel Gamsky², Mitul Amin³

¹Royal Oak, MI, ²Oakland University William Beaumont School of Medicine, Southfield, MI, ³William Beaumont Hospital, Royal Oak, MI

Disclosures: Craig Cousineau: None; Samuel Gamsky: None; Mitul Amin: None

Background: Current national guidelines recommend a minimum of 12 lymph nodes for adequate tumor staging of colorectal carcinoma (CRC). We have noticed a trend of decreasing lymph node counts found in specimens at our institution. This poses the question of whether the resultant tumor staging of these cases is adequate and accurately predicts patient outcomes. Also noticed in recent times is the increasing trend for performing laparoscopic colectomies (LC) as opposed to open colectomies (OC). We sought to systematically analyze the cause for this drift.

Design: We searched our in-house database for cases of CRC from the 2012-2015 period. We studied 465 cases of CRC; colectomies for adenomas were excluded. In cases where there was more than one tumor, we sought the tumor characteristics of the largest focus. We studied patient demographics, size and location of tumors, nodal counts, and type of surgical procedure.

56% of study patients were females and 44% were males. The mean age of presentation was 70 years. 59% of CRC were resected laparoscopically, and 41% by open colectomy. The mean size of resection for LC was 21.7 cm and 30.3 cm for OC. The mean size of tumor was 4.3 cm for LC, as opposed to 5.5 cm for OC. Pathology residents grossed 19% of LC and 29% of OC. The mean LN counts obtained were 24 for LC (range 3-75) and 27 for OC (range 0-100). Analysis with ROC curve and applying Youden's J Criteria yielded a resection size cutoff of 14 cm that reliably predicted finding 12 LNs. Applying this 14 cm cut-off, we found that 33% of LC and only 9% of OC that did not meet this requirement.

Type of surgery	Laparoscopic	Open
No. of cases (n=465)	274 (59%)	191 (41%)
Mean colectomy length	21.7 cm	30.3 cm
Mean tumor size	4.3 cm	5.5 cm
Mean lymph node count	24 (3 - 75)	27 (0 - 100)
Cases not meeting 14 cm cutoff	90 (33% of LC)	17 (9% of OC)
Resident grossing	52 (19% of LC)	55 (29% of OC)

Conclusions: We found that length of resections, size of tumors, and choice of laparoscopic procedure correlated with increased LN yields. The total LN count for OC vs LC was statistically significant. Larger resection sizes and larger tumor size correlated with higher LN yield. PAs consistently identified more LNs than pathology residents; this difference was also statistically significant. Only about one third (90/274) of all LC cases did not meet the required size of 14 cm. The increasing trend to perform laparoscopic surgeries has on many occasions yielded a very small resection, sometimes <10 cm in size, with short mesenteries; finding 12 LNs seems an unrealistic challenge. Submitting all the mesenteric fat may also not resolve the dilemma. Further work by other authors in this direction may resolve some of the vexing issues that we face today.

614 Prognostic Significance of Serrated Colorectal Carcinomas

Andrew Crabbe¹, Martin Taylor², Lieve Leijssen¹, Steffen Rickelt³, David Berger¹, Vikram Deshpande¹

¹Massachusetts General Hospital, Boston, MA, ²Boston, MA, ³David H. Koch Institute for Integrative Cancer Research, Cambridge, MA

Disclosures: Andrew Crabbe: None; Martin Taylor: None; Steffen Rickelt: None; Vikram Deshpande: None

Background: Serrated colorectal carcinomas represent an architectural subtype of colonic carcinomas characterized by serrated pattern of growth in the invasive component. Additionally, such tumors often feature abundant clear or eosinophilic cytoplasm, vesicular nuclei, minimal comedonecrosis, and a variable degree of mucin production. Though serrated colorectal carcinomas frequently arise in the setting of serrated precursor lesions, for many, no such precursor is identified. Although the subject of investigation in a few prior studies serrated colorectal carcinomas are not recognized by the World Health Organization. We evaluated a large series of colorectal carcinomas to assess the biologic significance of serrated colorectal carcinomas.

Design: We evaluated 542 cases of untreated colorectal carcinomas resected between 2004 to 2014. Serrated architecture was evaluated by 2 pathologists; we also assess the percentage of invasive tumor with a serrated pattern. We recorded the presence of the following histologic features: pTNM stage, tumor grade, lymphovascular and perineural invasion, lymph node metastasis. Survival data was recorded. We correlated the serrated pattern with survival using univariate (Log Rank test) and multivariate (Cox Regression) analysis.

Results: In this cohort, 11% (n=57 total) of patients demonstrated a serrated architecture (mean age: 68.2, M:F = 0.7, mean percentage of serrated component = 24%, ranging from 5-90%). At a cut point of 5%, the serrated phenotype was associated with decreased overall survival (p=0.005). The serrated phenotype was associated with low tumor grade (p=0.017), and it failed to show significant correlation with typical prognostic factors, including pT stage, pN stage, MSI-related protein status and the presence of lymphovascular invasion or perineural invasion. However, on multivariate Cox regression analysis, the presence of the serrated phenotype was associated with the highest hazard ratio (HR = 1.731, 95% CI of 1.153 – 2.559), and was one of three variables significant on multivariate analysis, along with pT stage (HR = 1.372, 95% CI 1.104 – 1.704) and pN stage (HR = 1.353, 95% CI 1.093 – 1.674).

Conclusions: Serrated colorectal carcinomas are associated with aggressive biologic behavior and our results support the recognition of this variant of colorectal carcinoma as a distinct subtype.

615 Pediatric Gastrointestinal Histopathology in Patients with Tetratricopeptide Repeat Domain 7A (TTC7A) Mutations: A Rare Condition Leading to Multiple Intestinal Atresia and Severe Combined Immunodeficiency

Katelyn Dannheim¹, Jay Thiagarajah¹, Bram Raphael¹, Daniel Kamin¹, Jeffrey Goldsmith²

¹Boston Children's Hospital, Boston, MA, ²Boston Children's Hospital, Harvard Medical School, Boston, MA

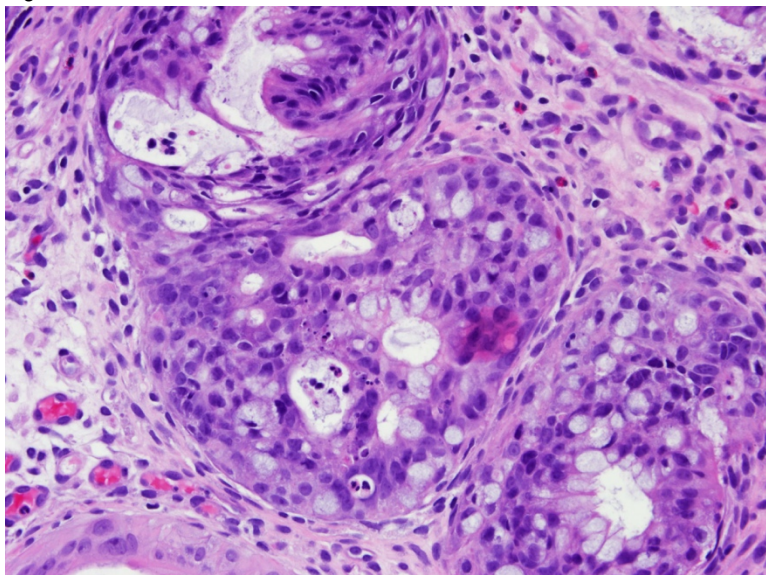
Disclosures: Katelyn Dannheim: None; Jay Thiagarajah: None; Bram Raphael: None; Daniel Kamin: None; Jeffrey Goldsmith: None

Background: Mutations in the TTC7A gene (2p21) are a rare cause of multiple intestinal atresia and severe combined immunodeficiency, a syndrome that can lead to early mortality. These mutations result in impaired immune cell homeostasis and disruption of enteric epithelium. Descriptions of the pathology of this condition have been published in case reports. We present an in depth examination of pediatric gastrointestinal pathology in the largest TTC7A mutation cohort to date.

Design: A retrospective chart review of six patients with TTC7A mutations was conducted. Endoscopically obtained mucosal biopsies and surgical resection specimens from five of the six patients were available for histopathologic examination. Comparison was made to twelve age-matched controls with intestinal atresia not associated with TTC7A.

Results: Patients with TTC7A mutations exhibited a spectrum of histologic phenotypes: Three were characterized predominantly by intestinal atresia, one had primarily microscopic epithelial changes, and the fifth showed combined features. The epithelial changes included varying degrees of cytologic abnormality, from "regenerative-like" change to marked nuclear pleomorphism that mimics high-grade dysplasia. Increased epithelial apoptosis was seen in all cases (figure). Architectural abnormalities included cribriform growth and patchy crypt degeneration. Lamina propria fibrosis and hypertrophy/disorganization of the muscularis mucosae were seen in all cases, and conspicuous submucosal spindle-cell condensations surrounding small vessels were noted in three of the four patients with available resection specimens. The inflammatory infiltrate appeared more pronounced and manifested as prominent lamina propria eosinophilia with a component of neutrophilic colitis. The epithelial changes in the colon were invariably more striking than those found in the stomach and small intestine. *Helicobacter pylori*-negative gastritis was seen in all four patients with available stomach biopsies. Three patients had gastric oxyntic atrophy, two of which also had associated squamous metaplasia and enterochromaffin-like cell hyperplasia, proven with immunohistochemistry. None of these findings were seen in the age-matched controls.

Figure 1 - 615



Conclusions: Unique gastrointestinal histopathologic findings were identified in the largest TTC7A mutation cohort to date. Additional investigation is needed to explore potential differences in these patients' mutations and correlation with clinical and histopathologic phenotypes.

616 Characteristic Morphologic Features of Eosinophilic Gastro-Duodenitis: A Single Institution Large Cohort Study

Audrey Deeken-Draisey¹, Edernst Noncent², Ryan Jones³, Katrina Krogh³, Maryam Pezhouh⁴, M. Sambasiva Rao³, Guang-Yu Yang³

¹Northwestern Memorial Hospital, Chicago, IL, ²Chicago, IL, ³Northwestern University, Chicago, IL, ⁴Northwestern University Feinberg School of Medicine, Chicago, IL

Disclosures: Audrey Deeken-Draisey: None; Edernst Noncent: None; Ryan Jones: None; Katrina Krogh: None; Maryam Pezhouh: None; M. Sambasiva Rao: None; Guang-Yu Yang: None

Background: Eosinophilic gastrointestinal diseases are an emerging diagnostic entity. Despite increase in recognition, only eosinophilic esophagitis (EoE) has established diagnostic criteria. Eosinophilic gastritis or duodenitis (EGD) is suggested with histologic eosinophilic infiltrate of ≥ 30 /HPF, although definitive diagnostic criteria haven't been established. The aims of this study are 1) to determine the characteristic histologic features for diagnosis and 2) to determine the association between the presence of EGD in conjunction to the presence of EoE.

Design: After searching our institution for cases with a diagnosis of eosinophilic gastritis or duodenitis within the past 5 years, 93 cases of EGD were identified including 70 eosinophilic gastritis (EG) and 23 eosinophilic duodenitis (ED). The characteristic morphologic features including number of eosinophils, associated epithelial injury, and lamina propria reaction were analyzed.

Results: For ED, the average number of eosinophils (eos) was 55/HPF (range 30-100+). 100% of cases had eos within lamina propria, while only 35% had presence of intraepithelial eos. 7/23 cases had diffuse involvement of ED in all fragments with an average 76 eos/HPF, while the other 16 cases had only focal involvement with an average of only 45 eos/HPF. 2/23 had lamina propria fibrosis. 19/23 cases (83%) had surface gastric foveolar metaplasia, with only 2 cases with surface erosions. Of cases with concomitant biopsies, 12/23 had associated eosinophilic gastritis (52%) and 17/23 had associated eosinophilic esophagitis (74%).

For EG, the average number of eos was 73/HPF (range 30-100+). 100% of cases had eos within lamina propria, while only 50% had intraepithelial eos. Only 8/70 had eos within muscularis mucosa, although this observation was limited due to depth of biopsy. 25 cases had diffuse involvement of EG in all fragments with an average of 85 eos/HPF, while the other 45 cases had focal involvement with an average of 65 eos/HPF. 42/70 had lamina propria fibrosis. 100% of cases had reactive epithelial change, while only half were associated with surface erosions. Of cases with concomitant biopsies, 44/62 had associated eosinophilic esophagitis (71%) and 15/56 had associated eosinophilic duodenitis (27%).

Conclusions: Diagnostic features of EGD include: ≥ 30 eos/HPF, with associated epithelial injury and/or lamina propria fibrosis. The findings of concurrent EoE with EGD is suggestive that these processes share similar etiology or pathogenic process.

617 Immune Microenvironment Characterization in Barrett Esophagus, Dysplasia, and Adenocarcinoma with Quantitative Multiplex Immunofluorescence Image Analysis

Armando Del Portillo¹, Sonya Purushothaman², Caitlin Hills¹, Elena Komissarova¹, Sarawut Kongkarnka³, Jorge Sepulveda¹, Antonia Sepulveda¹

¹Columbia University Medical Center, New York, NY, ²New York, NY, ³Chiang Mai University, Mueang, Thailand

Disclosures: Armando Del Portillo: None; Sonya Purushothaman: None; Caitlin Hills: None; Elena Komissarova: None; Sarawut Kongkarnka: None; Jorge Sepulveda: None; Antonia Sepulveda: None

Background: The incidence of esophageal adenocarcinoma (EAC) is rapidly increasing. EAC develops through progression of the pre-cancer lesions intestinal metaplasia (IM, Barrett esophagus) and dysplasia (DYS). There is limited knowledge of the immune microenvironment in esophageal pre-cancer and cancer. Multiplexed quantitative multispectral immunofluorescence (qmIF) provides the opportunity to characterize the temporo-spatial immune microenvironment of pre-cancer and cancer lesions. The aim of our study is to characterize the immune milieu in esophageal pre-cancer and EAC lesions to determine its potential role in the progression of esophageal carcinogenesis.

Design: Tissue microarrays (TMA) were constructed from FFPE resection specimens of IM (N=23), dysplasia (24), and esophageal adenocarcinoma (34) from 52 patients. TMA sections were stained using Opal multiplex 6-plex kits for DAPI, CD3, CD8, HLADR, FOXP3, CD68 and pan-cytokeratin. Multispectral images were captured with a Vectra platform and regions of interest were identified within each core of the TMA for qmIF analysis with custom algorithms developed with inForm to identify and quantitate cells within the esophageal lamina propria or tumor stroma. The numbers and relative proportions of positive cells for each marker and marker combinations relative to all stromal cells were captured and the results for each patient and lesion groups were analyzed using R custom algorithms.

Results: The number of macrophages (CD68+) was significantly higher (mean 6.0% \pm 5.6%) in tumor stroma than in IM (1.8% \pm 3.0%, p=0.002) and DYS (2.7% \pm 3.5%, p=0.02). In particular, the numbers of activated (CD68+HLADR+) macrophages were significantly higher in tumor stroma (4.0% \pm 4.9%) than in IM (0.4% \pm 0.7%, p=0.0002) and DYS (0.7% \pm 1.2%, p=0.0004). The overall number of CD3+ and of CD3+, FOXP3+ (Treg) lymphocytes was not significantly different in tumor stroma vs. IM and DYS. However, a small subset of EAC showed higher numbers of CD3+ lymphocytes. Further, the number of CD8+ T-cells was higher in tumor stroma (1.2% \pm 2.4%) vs. IM (0.1% \pm 0.2%, p=0.02).

Conclusions: Dynamic changes in the pre-cancer to EAC immune microenvironment involve increased HLADR+ macrophages and CD8+ T-cells infiltration in EAC vs. pre-cancer lesions. The presence of pro-inflammatory HLADR+ macrophages and cytotoxic CD8+ T-cells likely favors anti-tumor immunity. qmIF is a valuable tool to quantitatively and temporo-spatially define the immune microenvironment in esophageal carcinogenesis.

618 Morphological and molecular risk markers for coexistent adenocarcinoma in low-grade dysplastic areas of high-grade adenomatous polyps

Salvador Diaz-Cano¹, Andrew Emmanuel¹, Shraddha Gulati¹, Bu Hayee¹, Aryn Haji¹
¹King's College Hospital, London, United Kingdom

Disclosures: Salvador Diaz-Cano: None; Andrew Emmanuel: None; Shraddha Gulati: None; Bu Hayee: None; Aryn Haji: None

Background: Safe and effective endoscopic resection (ER) relies on the endoscopic diagnosis of large lesions to predict the risk of invasive cancer. However, a detailed evaluation of histopathological features and the molecular profile of the polypoid dysplastic mucosa to predict coexistent invasive neoplasm is not available.

Design: Data from endoscopic resection of colorectal superficial neoplastic lesions performed at a UK tertiary referral center (2011-2016) were analyzed. A subset of these lesions containing high-grade dysplasia (HGAP), intramucosal or invasive cancer was identified and subjected to a detailed analysis: endoscopic type, ulceration, distribution of high-grade dysplasia, dysplastic nuclear grade, presence and distribution of necrosis, and distribution of tumor-infiltrating lymphocytes (TIL). The two highest morphological grade were microdissected from each lesion and used for DNA extraction and next-generation sequencing using a 24-gene panel (Qiagen, Hilden, Germany). Genetic abnormalities for each locus were categorized by genetic impact according to its severity (low/moderate/high/modifier) and allele frequency.

Results: ER was performed for 418 large (≥ 20 mm) colorectal superficial neoplastic lesions (mean size 55.2mm, range 20mm-160mm), 81% being laterally spreading tumors (LST). The proportions harboring an area of invasive cancer by morphological subtype were as follows: LST (non-granular 30.8%, granular mixed 12.3%, granular homogeneous 0.9%) and Ls/Is 11.4%. There was no locoregional/distant recurrence in any patient deemed to have undergone curative ER.

The histopathological genetic evaluation was available in 70 cases; a coexistent adenocarcinoma significantly correlated with dysplastic adenomatous mucosa featuring ulceration, mixed interface/interstitial TIL, multifocal high nuclear grade, infiltrative edges, and multifocal intraluminal necrosis. Multifocal intraluminal necrosis and high nuclear grade in the low-grade dysplastic mucosa were driven by cooperative genetic abnormalities of high-impact (FLT4), moderate impact (KRAS/NRAS for infiltrative edges, FLT4, TP53, ERBB2), and low impact (FGFR3, PDGFA).

Conclusions: Low-grade areas of HGAP are characterized by cooperative genetic mutations. A subset of markers identifies a risk of coexistent adenocarcinoma, closely correlating with angiogenesis (FLT4), receptor activation (RAS/ERBB2), genome maintenance (TP53), stromal reaction (FGFR3, PDGFRA), and morphology (nuclear grade, necrosis, and inflammation).

619 Genetic Screening for Lynch Syndrome with IHC pMMR Subgroup of Chinese Familial Colorectal Cancer Patients

Lin Dong¹, Xianglan Jin², Shuangmei Zou¹, Jianming Ying¹

¹National Cancer Center/National Clinical Research Center for Cancer/Cancer Hospital, Chinese Academy of Medical Sciences and Peking Union Medical College, Beijing, China, ²Peking University Shenzhen Hospital, Shenzhen, China

Disclosures: Lin Dong: None; Xianglan Jin: None; Shuangmei Zou: None

Background: Lynch syndrome (LS) is associated with germline mutations in a class of genes involved in DNA mismatch repair (MMR), including *hMLH1*, *hPMS2*, *hMSH2*, *hMSH6*, and *EPCAM*. Immunohistochemistry (IHC) analysis to test MMR deficiency in tumor tissues all colorectal cancer (CRC) patients is routinely assessed for identifying LS in our center. However, there are still some cases with classic LS-like cancer family histories with well-defined IHC MMR proficiency (pMMR), tumors showing high level microsatellite instability (MSI-H) based on PCR based MSI analysis, which suggested the presence of hereditary predisposition is related with DNA replication and repair system.

Design: 4545 consecutive patients who had undergone surgery for CRCs between January 2015 and December 2017 in Chinese National Cancer Center were reviewed for pathological characteristics and tumor family histories. 206 patients with IHC pMMR and obvious tumor family histories were further analyzed in this study. The MSI status was evaluated by MSI PCR. Germline mutations were screening by Whole Exome Sequencing (WES) and target captured sequencing in normal and matched tumor samples. DNA mismatch repair assay verified the functional effects of the MMR mutants.

Results: Overall, 4.5% (206/4545) of patients showed obvious tumor family histories in whole CRCs cohort. 3.4% (7/206) of colorectal cancer samples presented MSI-H status in a subset of IHC pMMR with tumor family histories. The 7 cases had classic LS-like cancer family histories. Interestingly, germline analysis of the selected normal and matched tumor samples of the 7 cases with MSI-H and pMMR revealed pathogenic mutation of MMR gene. We also confirmed a dominant MLH1 missense mutation showing apparently reduced DNA mismatch repair efficiency in vitro assay.

Conclusions: Our results demonstrated that the MMR protein with rare pathogenic missense mutations, which abrogated MMR but not protein stability, could be well expressed in tumors. Genetic testing for Lynch Syndrome of rare cases with LS-like tumor family histories and IHC pMMR should not be neglected by routine IHC MMR through integrating MSI PCR technique with next generation sequencing.

620 Eosinophils in Gastrointestinal Smooth Muscle Tumors Appear Unique to the Esophagus and May Predict Benignancy

Zachary Dong¹, Lindsay Alpert², Raul Gonzalez³, John Hart², Lindsey Westbrook⁴, Hanlin Wang⁴, Mary Bronner¹

¹University of Utah, Salt Lake City, UT, ²University of Chicago, Chicago, IL, ³Beth Israel Deaconess Medical Center, Boston, MA, ⁴David Geffen School of Medicine at UCLA, Los Angeles, CA

Disclosures: Zachary Dong: None; Lindsay Alpert: None; Raul Gonzalez: None; John Hart: None; Lindsey Westbrook: None; Hanlin Wang: None; Mary Bronner: None

Background: Primary smooth muscle tumors (SMTs) of the gastrointestinal tract are rare, excluding benign incidental muscularis mucosae lesions. Little is known about features predicting outcome or the histologic differences at various gastrointestinal sites. This study further investigates esophageal SMTs of the muscularis propria.

Design: 162 (61 esophageal, 68 gastric, 14 small bowel, 19 colonic) consecutive gastrointestinal muscularis propria SMTs diagnosed between 2003 and 2017 were included, excluding muscularis mucosae SMTs, as they are known to be incidental and benign. SMT immunophenotypes were confirmed in all cases (SMA and/or desmin positive, CKIT and/or DOG1 negative). Patient demographics, pathologic features, and outcomes were evaluated. Differentiation scoring used the French Federation of Cancer Centers Sarcoma Group system. Bivariate analyses of pathologic variables, tumor site, and eosinophil infiltrates were performed using Stata software's Student's t, Pearson χ^2 , Fisher Exact, and Wilcoxon rank-sum tests.

Results: Of the 162 eligible tumors, 18 (11%) showed eosinophil infiltrates, ranging from 3 to 223/HPF (mean 49/HPF). Eosinophils were unique to esophageal tumors among all GI sites [$p < 0.001$]. Further, all esophageal SMTs with eosinophils were benign. Only 1 of 61 total esophageal SMTs appeared malignant with marked cytologic atypia, mucosal ulceration, high mitotic activity (17/5mm²), high cellularity, poor differentiation, and necrosis, but this patient was alive without disease at 35 months of follow-up. All of the remaining histologically benign esophageal tumors (n=60) revealed benign features in all of these characteristics except for 1 case with high cellularity, 2 cases with moderate atypia, and 5 cases with focal necrosis. All 60 of the histologically benign cases had long-term benign outcomes with no evidence of disease after resection at a mean of 40 months (range 1-167 months). When compared to esophageal SMTs without eosinophils, those with eosinophils (18 of 61) more often arose in females [$p = 0.039$], and none of the patients had histories of allergies, asthma, peripheral blood eosinophilia, or eosinophilic esophagitis. Interestingly, there was a strong positive correlation between tumor size and maximum eosinophil density [$r = 0.609$, $p = 0.007$].

Conclusions: A substantial subset of esophageal SMTs (30%) showed eosinophil infiltrates, a histologic feature unique to the esophageal SMTs and one that may predict a benign outcome.

621 Utility of INSM1 in the diagnosis in Goblet Cell Carcinoid Tumors and Adenocarcinoma-ex Goblet Cell Carcinoids of the Appendix

Erika Doxtader¹, Kelsey McHugh², Sanjay Mukhopadhyay³, Daniela Allende⁴

¹Cleveland Clinic, Pepper Pike, OH, ²Cleveland Clinic, Lakewood, OH, ³Cleveland Clinic, Cleveland, OH, ⁴Cleveland Clinic, Avon Lake, OH

Disclosures: Erika Doxtader: None; Kelsey McHugh: None; Sanjay Mukhopadhyay: None; Daniela Allende: None

Background: Goblet cell carcinoids (GCC) are neoplasms with dual neuroendocrine and glandular differentiation. Even though GCC reveals a characteristic morphologic appearance, the adenocarcinoma counterpart ("adenocarcinoma ex GCC", AGCC) is often subject to misclassification. The variable expression of traditional neuroendocrine markers (synaptophysin and chromogranin) seen in these tumors may contribute to the lack of recognition of their neuroendocrine differentiation. Insulinoma-associated protein 1 (INSM1) has recently been described as a sensitive and specific nuclear marker of neuroendocrine differentiation. Its utility in the diagnosis of GCC and AGCC remains unknown.

Design: Cases were identified through a retrospective pathology database search (2008-2018). A selected formalin fixed paraffin embedded block appendiceal neoplasms, including 3 pure GCC, 9 AGCC (8 with a GCC component), and 15 well differentiated neuroendocrine tumors (WDNET) and 47 controls were stained with INSM1 (mouse monoclonal, A-8, Santa Cruz Biotechnology), synaptophysin (mouse monoclonal, Snp88, BioGenex) and chromogranin (mouse monoclonal, DAK-A3, Agilent). The control group included non-neuroendocrine tumors (28 squamous cell carcinomas, 19 adenocarcinomas NOS) of the gastrointestinal tract. Any nuclear staining for INSM1 and cytoplasmic staining for synaptophysin and chromogranin was considered positive.

Results: INSM1 was positive in 8 of 11 GCC tumors (73%), 6 of 9 AGCC (67%), 11 of 15 WNET (73%), and 1 of 47 non neuroendocrine tumors (2%). INSM1 was negative in 46/47 of non-neuroendocrine tumors (98%). The sensitivity of INSM1 for GCC (73%) was less than that of synaptophysin (100%) and similar to chromogranin (82%). The sensitivity of INSM1 for AGCC (67%) and WNET (73%) was less than synaptophysin (100% and 93%) and chromogranin (89% and 87%). The specificity of INSM1 for appendiceal neoplasms with neuroendocrine differentiation (98%) exceeded that of synaptophysin (92%) and chromogranin (92%). The summarized findings are detailed in Table 1.

Table 1. Sensitivity and Overall Specificity of INSM1, SYN, and CHR for Primary Appendiceal Neoplasms with Neuroendocrine Differentiation

		Positive/Total, n/N (%)	
	INSM1	SYN	CHR
Overall Sensitivity	26/36 (72)	35/36 (97)	31/36 (86)
Overall Specificity	46/47 (98)	43/47 (92)	43/47 (92)
Sensitivity, GCC	8/11 (73)	11/11 (100)	9/11 (82)
Sensitivity, Adeno-ex GCC	6/9 (67)	9/9 (100)	8/9 (89)
Sensitivity, WNET	11/15 (73)	14/15 (93)	13/15 (87)

Abbreviations: INSM1, insulinoma-associated protein 1; SYN, synaptophysin; CHR, chromogranin.

Conclusions: When compared to traditional neuroendocrine markers synaptophysin and chromogranin, INSM1 demonstrates high specificity for neuroendocrine differentiation in both GCC and AGCC. However, in cases of AGCC, the sensitivity of INSM1 is lower than synaptophysin and chromogranin, which should warrant caution regarding the use of INSM1 as an isolated neuroendocrine marker in this setting.

622 The Predictive Value of Linear Spiculation for Elastin-Detected Venous Invasion in Colorectal Cancer: A Prospective Analysis

Kai Duan¹, Aysegul Sari¹, Sameer Shivji¹, Brian Chow², Emily Almeida², Colin Elliot², Nadia Saito², William Tsui², Richard Kirsch², James Conner²

¹Toronto, ON, ²Mount Sinai Hospital, Toronto, ON

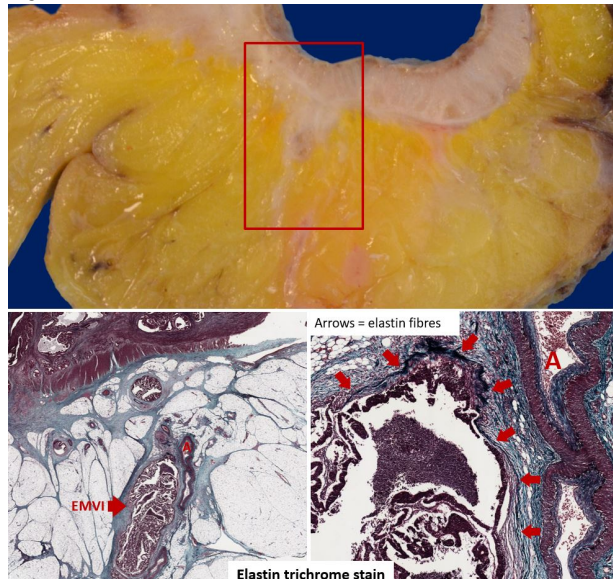
Disclosures: Kai Duan: None; Aysegul Sari: None; Sameer Shivji: None; Brian Chow: None; Emily Almeida: None; Colin Elliot: None; Nadia Saito: None; William Tsui: None; Richard Kirsch: None; James Conner: None

Background: Extramural venous invasion (EMVI) is a powerful predictor of adverse outcome in colorectal cancer (CRC) yet remains widely under-reported. Careful gross inspection for linear spiculation at the advancing edge of the tumor has been recommended since it may indicate the presence of EMVI (RCPATHUK CRC dataset 2017, Odze and Goldblum, 3rd ed, 2015). However, the relationship between linear spiculation and EMVI has never been studied prospectively. We sought to address this question in a cohort of 168 consecutive CRC resection specimens.

Design: A standardized tumor sampling protocol for all CRC specimens was designed: careful gross inspection for areas of linear spiculation at the advancing edge of the tumor was performed and, when present, such areas were recorded and identified for sampling. A minimum of 8 tumor-containing blocks were submitted for histologic examination and stained with both H&E and elastin trichrome to assess for EMVI. Tumors that were too small to yield 8 tissue blocks were submitted in their entirety.

Results: The 168 CRC resections (stage 1, n=24; stage 2, n=47; stage 3, n=56; stage 4, n=4; post-neoadjuvant cases, n=37) included 63 right sided, 41 left sided and 64 rectal cancers. The mean tumor size was 4.9 cm (range 0.5-13.7 cm). An average of 7.4 blocks were submitted from each specimen. Linear spiculation (Figure 1) was identified in 35 tumors (21%) and EMVI in 71 (42%). In 131 cases without neoadjuvant therapy, the rate of EMVI was 75% in tumors with linear spiculation compared to 32% in tumors without (p<0.001). Of those with EMVI detected histologically, 35% showed linear spiculation. No statistically significant relationship was observed in post-neoadjuvant cases, but analysis of this group was limited by small sample size.

Figure 1 - 622



Conclusions: This prospective study is the first to confirm a significant association between linear spiculation and EMVI. The positive predictive value of linear speculation for EMVI was high (75%), although the low sensitivity (35%) implies that its absence does not reliably exclude EMVI. These findings support careful gross inspection for linear spiculation and ensuring that these areas are sampled histologically (with consideration given to elastin stains if EMVI is not detected on H&E) to increase detection of this important risk factor.

623 Gynecologic Malignancies Presenting as Gastrointestinal Malignancies

Andrew Dunn¹, Aaron Huber¹, Raul Gonzalez²

¹University of Rochester Medical Center, Rochester, NY, ²Beth Israel Deaconess Medical Center, Boston, MA

Disclosures: Andrew Dunn: None; Aaron Huber: None; Raul Gonzalez: None

Background: Malignancies that cause gastrointestinal signs (e.g., mass identified on colonoscopy) or symptoms (e.g., bloody stools) are typically gastrointestinal in origin. However, female patients may rarely have a gynecologic malignancy (ovarian or uterine) initially masquerading as a gastrointestinal primary. In these situations, the malignancy metastasizes or directly spreads into the gastrointestinal tract, where it is first discovered in a biopsy or resection sample. This phenomenon has, to our knowledge, not been systematically evaluated in the literature.

Design: We retrospectively identified 16 cases of a gynecologic malignancy manifesting as a gastrointestinal lesion. We recorded radiologic and endoscopic findings when available. We evaluated tumor type, surface involvement, desmoplastic response, psammoma bodies, and "colonic-type" dirty necrosis.

Results: The 16 cases included 13 biopsies and 3 resections, arising in the rectosigmoid (13, 81%), right (2, 13%), and transverse (1, 6%) colon. Gastrointestinal-type complaints included abdominal pain, weight loss, hematochezia, and obstruction; one case was asymptomatic and was found on screening colonoscopy. Among the 13 biopsy cases, colonoscopy showed a mass in 9 (69%) and colonic narrowing in 4 (31%). Imaging showed abnormal bowel wall thickening (5, 31%), obstruction (1, 6%), and mass lesion (4, 25%). Nine patients (56%) had no known prior gynecologic malignancy, and in only two cases was there clinical suspicion for a non-colonic primary prior to pathology results. Most cases (12, 75%) were ovarian or primary peritoneal serous carcinoma; the remainder were ovarian carcinoma NOS (2, 13%), clear cell carcinoma (1, 6%), and endometrial endometrioid adenocarcinoma (1, 6%). Six cases (38%) directly extended into the colon, and seven (44%) metastasized; route of spread was unclear in the other 3. Most cases showed no surface involvement (1, 6%), desmoplasia (0%), or dirty necrosis (0%). Three of the twelve serous carcinomas (25%) contained psammoma bodies. Confirmatory immunostains included Pax-8, WT-1, CK7, and p53, with negativity for CK20 and CDX2.

Conclusions: Advanced gynecologic malignancies can rarely manifest as gastrointestinal lesions; this underreported phenomenon can be both clinically and histologically deceptive. Serous carcinoma appears to be the most common type of tumor presenting in this way. Clues to non-colonic origin on biopsy include lack of surface involvement/dysplasia, desmoplasia, or dirty necrosis.

624 Multicenter retrospective evaluation of fundic gland polyps of various etiologies

Reima El Naili¹, Daniela Pereira², Ryoji Kushima³, Priyanthi Kumarasinghe⁴, Gregory Lauwers¹, W. Bastiaan De Boer⁵
¹H. Lee Moffitt Cancer Center & Research Institute, University of South Florida, Tampa, FL, ²Lisboa, Portugal, ³Shiga University of Medical Science, Otsu, Japan, ⁴Queen Elizabeth II Medical Centre, Nedlands, WA, Australia, ⁵PathWest Laboratory Medicine, QE2 Medical Centre, Perth, WA, Australia

Disclosures: Reima El Naili: None; Daniela Pereira: None; Ryoji Kushima: None; Priyanthi Kumarasinghe: None; Gregory Lauwers: None; W. Bastiaan De Boer: None

Background: Fundic gland polyps (FGPs) represent 77% of all gastric polyps. FGPs can be sporadic, usually secondary to PPI use or syndromic, associated with FAP or Gastric Adenocarcinoma & Proximal Polyposis of the Stomach (GAPPS). Few studies have compared FGPs in these settings. This study evaluated the features of FGPs detected in various settings using Kushima's classification.

Design: We performed a retrospective analysis of 89 FGPs [68 patients]. Retrieved data included age, gender, history of PPIs, FAP or GAPPS. Blinded to the etiology, all FGPs were evaluated according to the criteria set forth by Kushima: disordered architecture of fundic glands (cellular glandular buds, stellate or irregular tortuous glands), presence of microcysts, parietal cell hyperplasia, foveolar epithelial changes (shortened or hyperplastic) & detection of inflammation.

Results: The patients included 26 M & 42 F [13-82 years old]. 41 cases (46%) had a history of PPIs, 15 (17%) were associated with FAP & 33 (37%) were associated with GAPPS. 3 patterns were observed:

Pattern A: prominent, irregular & disordered fundic glands. The cysts measured 0.06-0.7mm & were lined by fundic & foveolar type epithelium (79%). Parietal cell hyperplasia (97%), foveolar surface hyperplasia (100%) & chronic inflammation (100%) were common. This pattern was identified in most cases of PPIs (83%) and few cases of FAP related FGPs (20%)

Pattern B: small microcysts [0.01-0.3mm] lined by pure fundic epithelium (74%) with limited parietal cell hyperplasia (15%). Foveolar hyperplasia and inflammation were uncommon (21% & 26% respectively). 80% of FAP & 17% of PPI related FGPs displayed this pattern

Pattern C: FGPs arising in GAPPS were large [up to 8 mm] with microcysts measuring 0.2-1.9 mm. The lining epithelium were a mixture of fundic & foveolar type (79%) and inverted foveolar hypermaturation. Parietal cell hyperplasia (12%) & inflammation (6%) were uncommon

Conclusions: Despite association with diverse clinical presentations, molecular alterations, and risk of neoplastic transformation, FGPs share – in general – similar morphologic features. However, the distinctive features of the underlying etiology/associations are not well recognized with only one case series originating from Japan. Therefore, it is critical to establish set criteria in order to organize a classification of polyps to tailor clinical management. Our review shows some distinctive features particularly in the setting of GAPPS.

625 Characterizing the Cytotoxic Lymphocyte Antigen-4 (CTLA-4) and Programmed Cell Death Ligand 1 (PD-L1) Expression Landscape in High-grade Neuroendocrine Carcinomas Compared to Neuroendocrine Tumors of the Digestive System: implications for prognosis and treatment

David Escobar¹, Jessica Nguyen², Audrey Deeken-Draisey³, Katrina Krogh⁴, Jennifer Pincus³, Guang-Yu Yang⁴, Maryam Pezhoh²
¹McGaw Medical Center of Northwestern University, Chicago, IL, ²Northwestern University Feinberg School of Medicine, Chicago, IL, ³Northwestern Memorial Hospital, Chicago, IL, ⁴Northwestern University, Chicago, IL

Disclosures: David Escobar: None; Jessica Nguyen: None; Audrey Deeken-Draisey: None; Katrina Krogh: None; Jennifer Pincus: None; Guang-Yu Yang: None; Maryam Pezhoh: None

Background: High grade neuroendocrine carcinomas (NEC) of the gastrointestinal tract (GI) and pancreas are aggressive tumors with poor outcomes. Patients with NEC often present at advanced stages not amenable to surgical resection. Currently no targeted therapies strategies exist for these tumors. The recent emergence of immune checkpoint inhibitor agents is offering new therapeutic options for patient with advanced malignancies. The complex interplay between proteins such as cytotoxic lymphocyte antigen-4 (CTLA-4) or programmed cell death protein (PD-1/PD-L1), expressed on both tumor cells (TCs) and tumor infiltrating lymphocytes (TILs) has not been fully explored in GI NECs.

Design: Through searching our pathology database for NECs of the GI tract and pancreas, 14 NEC cases were identified, and 14 well differentiated neuroendocrine tumors (NET) of GI tract and pancreas were included as a control group. PD-L1 and CTLA-4 expression were assessed in TCs and TILs and expression in ? 1% was considered positive. CTLA-4 immunolabeling was scored by extent (1= >1%, 2= >25%, 3= >50% and 4= >75%) and intensity (0= none, 1= weak, 2= moderate, 3= strong). A composite score (CS) was computed by multiplying extent and intensity scores. PD-L1 expression was scored as follows: 0= 0%, 1= >1%, 2= >10%, 3= >25%, and 4= >50%.

Results: The NECs in colon (n=5) was the most common primary site followed by pancreas, ampulla, small bowel and stomach. PD-L1 was expressed in TCs in 57% of NEC, compared to 14% in NET (Table1, $p < 0.05$). TILs expressed PD-L1 in 64% of NEC, compared to 28% of NETs ($p=0.058$). 14% of NECs expressed PD-L1 above a score 2 in TCs, while none of the NETs expressed PD-L1 above a score 2. CTLA-4 was expressed in TCs in 5 out of 14 NECs (36%) versus 14% of NETs ($p=0.19$), with a mean CS of 3 and 1, respectively. CTLA4 expression in TILs was present in 35% compared to 21% of NETs with a mean CS of 4 and 1, respectively ($p=0.4$). Tumor size, growth pattern, necrosis or presence of lymphovascular invasion did not show any significant association with PD-L1 and CTLA-4 expression. One of the NECs with a CS of 12 was associated with shorter survival time (less than 6 months).

Table 1. Comparison of PD-L1 and CTLA-4 expression in TCs of NECs and NETs at cut off >1%.

	PD-L1+ (% of cases)	PD-L1- (%of cases)
NEC	8/14 (57%)	6/14 (43%)
NET	2/14 (14%)	12/14 (86%)
The chi-square statistic is 5.6 ($p=0.017$).		
	CTLA-4+ (%)	CTLA-4- (%)
NEC	5/14 (36%)	9/14 (64%)
NET	2/14 (14%)	12/14 (85%)
The chi-square statistic is 1.7143 ($p= 0.19$).		

Conclusions: These findings suggest that PD-L1 and CTLA-4 expression is a common finding in NECs and indicate it is a potential target for immune-modulation therapy to improve survival. Analysis of additional cases is underway to further evaluate the role of CTLA-4 expression in NECs as a prognostic marker.

626 Microscopic Esophageal Sloughing is not Specific to Sloughing Esophagitis

Mark Ettel¹, Raul Gonzalez²

¹University of Rochester, Rochester, NY, ²Beth Israel Deaconess Medical Center, Boston, MA

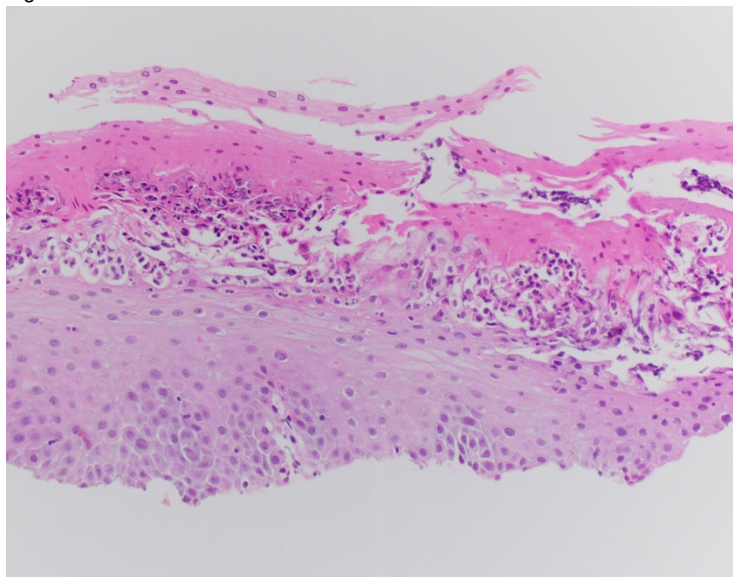
Disclosures: Mark Ettel: None; Raul Gonzalez: None

Background: Sloughing esophagitis (SE) is a histologic pattern of injury characterized by a “two-toned” appearance to the squamous epithelium, with a superficial necrotic layer overlying a viable deeper layer; the two layers are often separated from each other, causing a sloughing appearance. It is unknown how cases clinically diagnosed as SE differ from cases with other clinical diagnoses despite a histologic appearance suggestive of sloughing. We compared histologic findings in cases clinically considered SE to those with histologic sloughing but a different clinical diagnosis.

Design: We searched departmental archives for esophageal biopsies from 2001 to 2018 with histologic features of sloughing. For each case, endoscopic and clinical findings were reviewed, and histologic appearance was assessed. We compared findings between cases of clinically confirmed SE and cases with a different or unclear ultimate clinical diagnosis. Statistics were performed using *t*-test for continuous variables and Fisher’s exact test for categorical variables, with significance set at $P < 0.05$.

Results: We identified 52 patients (median follow-up: 15 months), of whom 10 (17%) were clinically deemed to have SE and 18 (35%) were deemed to have another diagnosis; in 24 (46%) patients, findings were not specifically addressed or were treated as “esophagitis NOS.” The 18 other diagnoses included reflux (n=8), motility disorders (n=3), medication injury (n=2), *Candida* (n=2), or a combination of multiple factors (n=3). Endoscopic sloughing tended to be reported more often in SE cases ($P=0.07$) than in cases with a different or unclear diagnosis. Histologic features, including neutrophilic microabscesses ($P=0.72$), eosinophils per high-power field ($P=0.50$), a “two-toned” appearance ($P=0.58$), and sloughed/stripped epithelium ($P=0.15$) (Fig.), did not discriminate between SE and other etiologies. The esophagitis resolved in 18 of 31 patients with follow-up, with no difference between SE and non-SE cases ($P=0.69$).

Figure 1 - 626



Conclusions: While SE has a “classic” microscopic appearance, including epithelial sloughing/stripping, its findings are not specific and do not necessarily translate to a clinical diagnosis of SE. Endoscopic evidence of sloughing appears to be the most likely factor influencing a clinical diagnosis of SE. Therefore, in histologically SE-like cases where clinical information is unclear or not readily available, SE should be suggested among other differential diagnoses, rather than singled out as a sole diagnostic possibility.

627 De Novo Ulcerative Colitis Can Occur in the Immunosuppressed Setting of Transplantation

Jiayun Fang¹, Laura Lamps², Jerome Cheng³, Amoah Yeboah-Korang¹, Maria Westerhoff³

¹University of Michigan Hospitals, Ann Arbor, MI, ²University of Michigan Hospital, Ann Arbor, MI, ³University of Michigan, Ann Arbor, MI

Disclosures: Jiayun Fang: None; Laura Lamps: None; Jerome Cheng: None; Amoah Yeboah-Korang: None; Maria Westerhoff: None

Background: Chronic idiopathic inflammatory bowel disease (IBD) is treated by immunosuppression; hence it is highly unexpected for *de novo* IBD to develop after solid organ or stem cell transplantation (BMT), given the immunosuppressive therapy used to prevent allograft rejection. A few reports suggest tacrolimus use as a risk factor for *de novo* IBD in the setting of transplant (tx). Most reports of post-tx *de novo* IBD describe liver tx patients, some with PSC, which already has a known association with developing IBD. We sought to determine whether post-tx *de novo* IBD can occur beyond known associations such as PSC as well as the potential promoting role played by tacrolimus.

Design: The medical electronic database was searched for any tx patients who underwent colon biopsies. PSC or patients with known IBD prior to tx were excluded. Chart reviews were performed, including symptoms, medications, and follow up.

Results: 197 patients who underwent colon biopsy for diarrhea after a solid organ tx or BMT were identified. After exclusion of pts with PSC or known IBD prior to tx, and identifying those with available chart review information, 88 were evaluated. 5 developed ulcerative colitis (UC) after tx, 3 of whom had >1 endoscopy with biopsies showing more active disease as more time passed after tx. 4 had kidney tx and 1 had undergone lung tx. All were on tacrolimus and 4 of the 5 were also on mycophenolate. The mean time from tx to UC development was 2.6 years (range 1-7 years). In contrast, 73 patients also on tacrolimus had colon biopsies, which showed GVHD (22), no abnormality (21), polyps (7), mycophenolate toxicity (6), neoplasm (colon cancer or lymphoma, n=5), ischemia (5), chronic colitis of uncertain etiology (4), and infection (3). Of these tacrolimus patients without IBD, BMT (25), kidney (17), liver (9), lung (8), and heart (5) tx were represented, with 9 additional patients having more than one organ tx. 6 other tx patients without IBD on biopsy had no documentation of tacrolimus use.

Conclusions: De novo UC accounted for 2.5% of the diagnoses for tx patients undergoing colon biopsy for diarrhea. Unlike other studies, our cohort excludes known associated risk factors, such as PSC. The role of tacrolimus is unclear, considering the majority of tx patients undergoing colon biopsy used tacrolimus and did not develop IBD. Although in the tx setting, pathologists may be conditioned against the possibility of *de novo* IBD, they should be aware that it can occur in immunosuppressed tx patients.

628 Validation of a Novel Histologic Scoring System for Gastrointestinal Graft-Versus-Host Disease

Ayesha Farooq¹, Christopher Hartley¹, Catherine Hagen¹

¹Medical College of Wisconsin, Milwaukee, WI

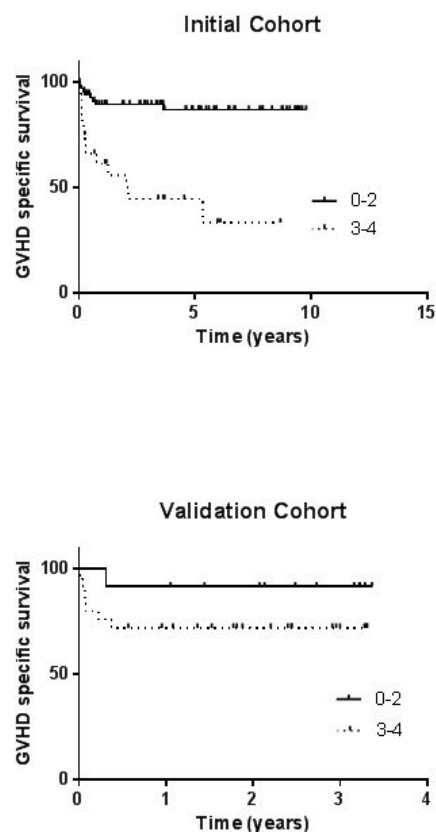
Disclosures: Ayesha Farooq: None; Christopher Hartley: None; Catherine Hagen: None

Background: The Lerner system is the most commonly used histologic grading system for gastrointestinal graft-versus-host disease (GVHD) but fails to provide prognostic stratification. We previously proposed a novel grading system for GVHD, which provided prognostic stratification in our initial study group. The aim of this study was to validate our grading system on a separate cohort of patients.

Design: Colon biopsies taken to assess for GVHD from 2008-2014 (initial cohort) and 2015-2016 (validation cohort) were retrospectively reviewed for the maximum number of apoptotic bodies per 10 contiguous crypts (ap/10), crypt dropout, and ulceration. Our histologic scoring system was applied by combining a score for mucosal irregularities (No crypt dropout or ulceration – 0; crypt dropout without ulceration – 1; ulceration – 2) and crypt apoptotic counts (No apoptosis – 0; 1-6 ap/10 – 1; >6ap/10 – 2). Clinical information was collected from chart review.

Results: Our initial study group consisted of 122 colonic biopsies from 84 patients (M:F 1:1.3; mean age 53.6) while our validation group consisted of 78 colonic biopsies from 48 patients (M:F 1.2:1; mean age 60.3). Patients with >6 ap/10 also had significantly worse GVHD specific survival compared to patients with 1-6 ap/10 in the initial cohort (HR 4.6, 95%CI 2.0-13.1, p=0.004) and showed a trend of worse GVHD specific survival in the validation cohort (HR 3.7, 95%CI 0.7-19.0, p=0.11). Using our newly proposed scoring system, patients with an overall histologic score of 3-4 had significantly worse GVHD specific survival compared to patients with a score of 0-2 in the initial cohort (HR 6.2, 95% CI 4.4-36.1, p<0.0001) and showed a trend of worse GVHD specific survival in the validation cohort (HR 2.7, 95%CI 0.6-11.7, p=0.17) (Figure 1).

Figure 1 - 628



Conclusions: Our current study suggests that our proposed histologic scoring system utilizing apoptotic count and mucosal irregularities provides prognostic stratification. A larger validation cohort is necessary to provide prognostic significance for the trends we report here.

629 KRAS Amplifications in Metastatic Colorectal Carcinoma (mCRC) are Frequently Detected in Younger Patients with a History of Inflammatory Bowel Disease and May Confer Resistance to Anti-EGFR Therapy

Laura Favazza¹, Lucas Santana-Santos¹, Abigail Wald¹, Somak Roy¹, Marina Nikiforova¹, Michael Landau¹, Aatur Singhi²
¹University of Pittsburgh Medical Center, Pittsburgh, PA, ²University of Pittsburgh Medical Center, Sewickley, PA

Disclosures: Laura Favazza: None; Lucas Santana-Santos: None; Abigail Wald: None; Somak Roy: None; Marina Nikiforova: None; Michael Landau: None; Aatur Singhi: None

Background: Mutations in *KRAS* and *NRAS* occur in 30-50% of mCRCs and are known to be associated with resistance to anti-EGFR therapy. Consequently, CRC biomarker guidelines by the ASCP, CAP, AMP and ASCO state patients being considered for anti-EGFR therapy must receive *RAS* mutational testing. However, in addition to *KRAS* mutations, a small subset of mCRCs harbor a *KRAS* amplification. In order to evaluate the clinicopathologic features and anti-EGFR treatment response associated with *KRAS* amplification, we prospectively screened mCRC samples that were submitted clinically for molecular biomarker studies.

Design: Between April 2017 and September 2018, 485 consecutive mCRCs from 473 patients were prospectively submitted for targeted next-generation sequencing (NGS) and mismatch repair (MMR) immunohistochemistry. The patient cohort ranged in age from 18 to 81 yrs (mean, 64.9 yrs) with a female-to-male ratio of 1:1.2. A history of Lynch syndrome and inflammatory bowel disease (IBD) was noted for 3 (1%) and 7 (2%) patients, respectively. Primary tumor sites were predominantly left-sided (n=294, 61%) with the majority in the rectum (n=115, 24%). Targeted NGS included both hotspot and copy number analysis (CNA) for *KRAS*, *NRAS*, *HRAS*, *BRAF* and *PIK3CA* using the Ion Torrent Proton with >300X coverage for each genomic region. Molecular results were correlated with clinicopathologic features, MMR status and treatment data.

Results: Amplifications in *KRAS* were detected in 5 (1%) mCRCs with concomitant *KRAS* mutations in 3 of 5 tumors. Patients with a *KRAS*-amplified mCRC were more likely to be younger (mean age, 46.2 yrs vs. 65.0 yrs, p<0.001) and have a history of IBD (80% vs. 1%, p<0.001). No significant differences were found between *KRAS* copy number and patient gender, history of Lynch syndrome, primary tumor site, MMR status and other genetic alterations. In comparison, *KRAS* mutations were more likely to be seen in MMR-proficient mCRCs (95% vs. 86%, p=0.001), but other clinicopathologic associations were not identified. An analysis of treatment data revealed 1 of 5 patients with amplifications in *KRAS* and no concomitant mutations received anti-EGFR therapy, but did not demonstrate a radiographic or biochemical response.

Conclusions: *KRAS* amplifications in mCRC are uncommon but are often seen in younger patients with a history of IBD. Further, its presence may confer resistance to anti-EGFR therapy and, therefore, expansion of *RAS* mutational testing to include *KRAS* CNA should be of consideration.

630 Gastrointestinal Tract Injury by Yttrium-90 Appears Restricted to Resin Microspheres: A Multi-institutional Experience of 10 Cases

Michael Feely¹, Numbereye Numbere², Aaron Huber³, Brian Geller¹, Ashwani Sharma³, Safia Salaria⁴, Raul Gonzalez⁵
¹University of Florida, Gainesville, FL, ²Pittsford, NY, ³University of Rochester Medical Center, Rochester, NY, ⁴Vanderbilt University Medical Center, Nashville, TN, ⁵Beth Israel Deaconess Medical Center, Boston, MA

Disclosures: Michael Feely: None; Numbereye Numbere: None; Aaron Huber: None; Brian Geller: *Consultant*, BTG; Ashwani Sharma: None; Safia Salaria: None; Raul Gonzalez: None

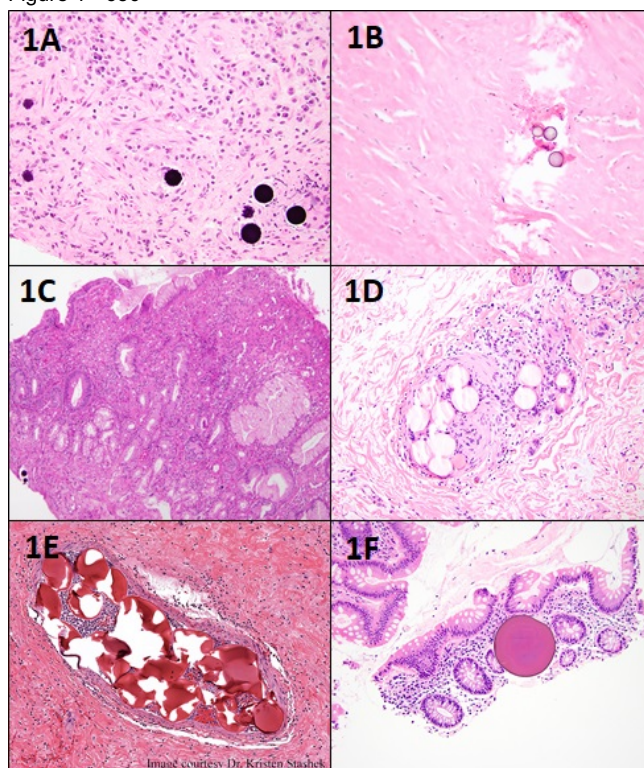
Background: While medication-induced injury in the gastrointestinal (GI) tract is not uncommon, cases secondary to treatment with yttrium-90 (Y-90) have rarely been reported. This therapy utilizes Y-90-impregnated resin (SIR-Spheres) or glass (TheraSpheres) microspheres to selectively target hepatic lesions via trans-arterial radioembolization. We examined cases from multiple institutions to assess corresponding clinical and pathologic sequelae.

Design: We queried the pathology archives at our 4 institutions for GI specimens containing Y-90 microspheres. Cases were reviewed for histologic findings, and corresponding clinical and endoscopic data were collected. We additionally performed a retrospective review of GI tissue obtained post-procedure from all patients treated with Y-90 microspheres over a 13-year period at one institution.

Results: Among 548 patients undergoing Y-90 therapy at the single institution, 135 received resin microspheres, 408 received glass microspheres, and 5 received both. Thirty-eight of these patients had subsequent upper GI biopsies, with three (0.5%) containing resin microspheres (Fig. 1A) and none containing glass microspheres (Fig. 1B). Combined, our institutions identified 10 cases showing Y-90 microspheres, from 7 patients (5 women, 2 men). The mucosal biopsies were obtained from 2 to 88 months following Y-90 therapy (median 6.5 months). Most cases (7; 70%) were gastric; the others were duodenal. Endoscopic ulceration was seen in 6 cases, and mucosal erythema in the other 4. Histologically, all cases showed rounded, dark blue to purple microspheres measuring 4-28 µm, consistent with resin microspheres. Two cases showed intravascular microspheres, and 5 showed vascular congestion or ectasia. Histologic evidence of

ulceration was appreciated in 5 cases (Fig. 1C). A foreign body giant cell reaction to the microspheres was rarely observed (2 cases). Glass microspheres were not seen in any case.

Figure 1 - 630



Conclusions: Y-90 microspheres rarely cause subsequent GI tract injury (<1%). Based on our findings, this damage appears to be limited to resin microspheres. This increased risk of non-target embolization may be due to the increased number of particles required per activity for resin versus glass microspheres. Resin microspheres may be encountered years after initial therapy and, when present, are often associated with mucosal ulceration. Microspheres should not be confused with TACE beads (Fig. 1D), bland embolization beads (Fig. 1E), or bile acid sequestrant granules (Fig. 1F).

631 Prognostic Implications of Histologic Findings in Mismatch Repair-Deficient Colorectal Carcinomas

Jennifer Findeis-Hosey¹, Justin Cates², Karina Hiroshige³, Meenal Sharma⁴, Rebecca Amorese⁵, Elena Gupta⁶, Laura Frado⁷, Caitlin Foor-Pessin⁸, Qi Yang⁹, Danielle Marino³, Raul Gonzalez¹⁰

¹University of Rochester Medical Center, Rochester, NY, ²Vanderbilt University Medical Center, Nashville, TN, ³University of Rochester, Rochester, NY, ⁴Unity Hospital, Rochester Regional, Rochester, NY, ⁵University of Rochester, Mohegan Lake, NY, ⁶Cornell University, Ithaca, NY, ⁷University of Rochester, New York, NY, ⁸University of Rochester Medical Center, Ithaca, NY, ⁹Pittsford, NY, ¹⁰Beth Israel Deaconess Medical Center, Boston, MA

Disclosures: Jennifer Findeis-Hosey: None; Justin Cates: None; Karina Hiroshige: None; Meenal Sharma: None; Rebecca Amorese: None; Elena Gupta: None; Laura Frado: None; Caitlin Foor-Pessin: None; Qi Yang: None; Danielle Marino: None; Raul Gonzalez: None

Background: Mismatch repair (MMR)-deficient colorectal carcinomas (CRCs) generally have a better prognosis than CRC arising through other molecular pathways, though they sometimes have high-risk features such as signet ring cells and “poor differentiation” in medullary carcinoma. While such histologic factors have been compared to prognosis in CRC in general, there are few series examining their role solely within MMR-deficient CRC.

Design: We retrospectively identified 134 MMR-deficient CRC resection specimens (defined as immunohistochemical loss of expression of MLH1, MSH2, MSH6, and/or PMS2). Cases receiving neoadjuvant therapy were excluded. For each case, we recorded patient age and sex; gross appearance (sessile/ulcerated/fungating/polypoid/rounded); tumor site and size; grade; mucinous, signet ring, medullary, or micropapillary features; infiltrating/pushing edge; microscopic ulceration or necrosis; tumor budding (using ITBCC criteria); tumor-infiltrating and tumor-adjacent lymphocytes, plasma cells, and eosinophils; adjacent Crohn-like reaction; intraepithelial lymphocytes; small and large vessel invasion; perineural invasion; *BRAF* mutation status; nodal and tumor deposit status; AJCC TNM staging parameters; and

recurrence-free and disease-specific survival. Clinicopathologic factors were compared to patient outcome using Cox regression stratified for AJCC eighth edition stage, with statistical significance set at $P < 0.05$.

Results: Average patient age was 70 years; average tumor size was 5.7 cm. Mucinous features were seen in 76 (57%) cases, and medullary features in 38 (28%). Fifteen (11%) cases showed signet ring cells, always floating in mucin pools (rather than invading tissue). Bd2/Bd3 budding was seen in 30 (22%) cases. AJCC stages were as follows: 31 Stage I (23%), 56 Stage II (42%), 40 Stage III (30%), 7 Stage IV (5%). Nineteen (14%) patients had recurrent disease, and 23 (17%) died of disease (overall median follow-up: 34.5 months). Statistically significant and near-significant prognostic factors are summarized in the Table. Mucinous features and Bd2 budding were significant histologic indicators of shorter recurrence-free survival; only patient age was associated with decreased disease-specific survival.

Variables influencing recurrence-free survival, stratified for AJCC stage:	Hazard Ratio	95% Confidence Interval	P-value
Mucinous features	0.35	0.12-0.98	0.047
Bd2 tumor budding score	4.14	1.47-1.66	0.007
Bd3 tumor budding score	3.90	0.80-19.02	0.092
Small vessel lymphovascular invasion	3.77	0.95-14.92	0.059
Perineural invasion	2.93	0.92-9.31	0.068
Variables influencing disease-specific survival, stratified for AJCC stage:			
Age (per year; as continuous variable)	1.04	1.00-1.07	0.040
Perineural invasion	2.49	0.88-7.07	0.086

Conclusions: In the context of MMR-deficient CRC, several histologic factors, including mucinous features and tumor budding, influenced stage-adjusted recurrence-free survival. No histologic factors significantly impacted stage-adjusted disease-specific survival.

632 Composite Intestinal Adenoma-Microcarcinoid (CIAM) in Surgically Removed Polyps Associated With Benign Squamous Morule (SM): Potential Common Pathogenesis

Zhiyan Fu¹, Rayan Saade¹, Brandon Koo², Hwajeong Lee¹

¹Albany Medical Center, Albany, NY, ²Albany Medical College, Albany, NY

Disclosures: Zhiyan Fu: None; Rayan Saade: None; Brandon Koo: None; Hwajeong Lee: None

Background: CIAM is a rare colorectal lesion consisting of adenoma and small well-differentiated neuroendocrine cell clusters at its base. Benign SM is seen in 0.4% of adenomas, which may demonstrate a neuroendocrine phenotype by immunohistochemistry (IHC). We investigated the incidence and clinicopathologic features of CIAM in endoscopically unresectable, surgically removed colorectal adenomas and evaluated its association with SM.

Design: Archived pathology materials (2003-2018) from surgically removed colorectal adenomas were reviewed. Representative sections in selected cases were subject to IHC for synaptophysin and cytokeratin 5/6 (CK5/6). Additional chromogranin and CD56 IHC were performed when indicated. Electronic medical records were reviewed for clinical data. Fisher's exact test was performed to compare frequencies of two parameters ($p < 0.05$ is considered statistically significant).

Results: 164 cases were retrieved wherein 90% of the polyps were entirely submitted for microscopic examination (mean number of slides examined 5.2/polyp). All lymph nodes were negative for adenocarcinoma and neuroendocrine tumor. CIAM was identified in 8 (4.9%) cases, of which 7 were in the right colon and one in the rectum. The microcarcinoid (MC) components were at the base of full-thickness adenomatous components in myxoinflammatory lamina propria with conspicuous eosinophils. The mean size of MC was 0.43 cm (range 0.2 to 1.2 cm), and were multifocal in 4 cases. The IHC for synaptophysin/CK5/6 in MC was (+/+) in 3, (+/focal +) in 2, (+/-) in 2 and (-/focal +) in one. In the last CIAM, the MC was negative for chromogranin and positive for CD56. 4 of 8 (50.0%) CIAM showed concurrent SM in the adenoma components compared to 3.8% (6 of 156) of adenomas without MC ($p < 0.001$). At the end of the follow-up (mean follow-up duration 45.5 (range: 5 to 114) months), 7 patients were free of disease and one with previous history of pulmonary large cell neuroendocrine carcinoma had a recurrence of the same disease.

		Adenoma (without MC)	CIAM
Number of cases		156	8
Mean age (range), years		61.1 (34 to 94)	66.8 (50 to 82)
Gender (M:F)		78:78	5:3
Procedure	Right hemicolectomy	103	7
	Segmental resection	39	1
	Low anterior resection	9	0
	Transanal excision	5	0
Mean size of adenoma (range), cm		2.9 (0.5-11)	4.1 (2.5-6.3)
Adenoma component (%)	Tubulovillous	64.2	100
	Tubular	30.0	0
	Villous	3.4	0
	Sessile serrated	2.3	0
	Traditional serrated	1.1	0
High grade dysplasia (%)		41.0	62.5
Submucosal invasive adenocarcinoma (%)		3.2	0.0
Squamous morule (%)		3.8	50.0

Conclusions: The incidence of CIAM in surgically removed colorectal adenomas is 4.9%, with an indolent clinical course. Frequent co-expression of CK5/6 in MC combined with common co-existence of SM in the same polyp suggests shared pathogenesis of MC in CIAM and SM, likely representing basal/stem cell phenotype.

633 Nonrandom associations of Gastrointestinal Stromal Tumors (GISTs) with other colonic soft tissue tumors

Caterina Fumagalli¹, Eva Chenu², Juan Carlos Pernas², Vicens Artigas², Antonio Lopez Pousa², Jaume Llauger², Silvia Bagué³, Justyna Szafranska²

¹Barcelona, Spain, ²Hospital de la Santa Creu i Sant Pau, Barcelona, Spain, ³The Royal Marsden HNS Foundation Trust, London, United Kingdom

Disclosures: Caterina Fumagalli: None; Eva Chenu: None; Juan Carlos Pernas: None; Vicens Artigas: None; Antonio Lopez Pousa: None; Jaume Llauger: None; Silvia Bagué: None; Justyna Szafranska: None

Background: GIST is the most common mesenchymal tumor in the digestive tract. Sporadic GISTs typically occur during the middle-age and are most commonly located in the stomach (60%) followed by the small intestine (35%). In 70-80% of cases there are mutations in the c-kit gene and in 7-15% of cases in the PDGFRA gene, whilst in the other cases these genes are wild-type. The last group includes GISTs with other genes' mutation (such as BRAF, SDHB, RAS, NF1 or unknown) that usually affect young patients. The aim of the study was to analyze the characteristics of the GISTs resected at our institution and their mutational state in order to gain insight in our epidemiology and find nonrandom associated soft tissue tumors.

Design: We reviewed histological, clinical and molecular findings of 48 GISTs diagnosed during the period 2012-2017

Results: The study included 23 males and 25 females with a median age of 65yrs and a median tumor size of 9cm subdivided in 3 groups depending on the presence of mutations in c-kit gene (A), PDGFRA gene (B) or absence of mutations (C). The characteristics of each group are shown in the table. As described in the literature, most GISTs (group A in this study) harbored mutations in c-kit. Group B was characterized by gastric location and epithelioid morphology of the lesions. Group C consisted of younger patients with low prognostic grade-tumor and smaller median size of the lesion compared to the other groups. Interestingly, in group A one patient (53yo woman) was diagnosed of a desmoid tumor (DT) 3 years after GIST's resection. Furthermore, in two cases belonging to group C, coexisting lesions typical for neurofibromatosis type 1 (NF1) were found. The first patient was a 47yo female affected by multiple dermic neurofibromas and a single, low grade GIST (4,3cm). The second case was a 74yo male with multiple, very low grade GISTs measuring between 0,5 and 5cm, concurrently with diffuse colonic ganglioneuromatosis. Both GISTs were localized in the small bowel and had low prognostic grade, as typically occurs in NF1-associated GISTs.

Group	Mutational state	N. of cases	Sex	Median age	Median size (cm)	N. of lesions	Localization	Prognostic grade (AFIP)	Morphology
A	c-kit mutation	33	16Male 17Female	66	9.6	32 single 1 multifocal	13Stomach mall bowel colon 18S 1Sigmoid 1Rectum	3 very low low intermediate high 14 2 14	28spindle cell type 1e pithelioid type 4mixt type
B	PDGFRA mutation	6	4Male 2Female	70	13.7	5single 1multifocal	5Stomach mall bowel 1S	3low 2intermediate 1high	1spindle cell type 4e pithelioid type 1mixt type
C	c-kit y PDGFRA wild type	9	3Male 6Female	60	5	8single 1multifocal	1Esophagus mach bowel 4Sto 4Small	3very low 1intermediate 5low	8spindle cell type 1 epithelioid type

Conclusions: Wild type GISTs and their associated lesions can be linked to genetic syndromes and have a strong impact on therapeutic options. Despite the known connection between GIST and NF1, its prevalence in NF1 is low (3.9-25%) and its diagnostic recognition is prone to be missed by non-specialists. Furthermore, there are other nonrandom GISTs-related lesions, such as DT, that must be taken into account when examining colonic soft tissue tumors.

634 Clinician Driven GI Biopsy Case Routing: Using Social Media Constructs to Modify the Specialization Model and Deliver Quality Care in the "Volume To Value" Era of Medicine

Gretchen Galliano¹, Mona Bansal²

¹Ochsner Health System, New Orleans, LA, ²New Orleans, LA

Disclosures: Gretchen Galliano: None; Mona Bansal: None

Background: We are a group practice of employed physicians in a community health system and from 2010 to 2017 there was an addition of 6 hospitals and numerous clinics into our health system with consolidation of Anatomic Pathology (AP) processing labs and without full time staffing of AP at the low volume hospitals. There was an increase in endoscopists (ENDO), including advanced ENDO, IBD ENDO, and pediatric ENDO at the main tertiary hospital (TCH) with an overall case volume increase of 44%. Liver AP was the only specialization in place due to the high liver transplant volume. With the increased demand of the clinicians, we identified a need for specialized GI AP services but were constrained by the speed and process of the budget cycle.

Design: Initial plan. Inspired by the hashtag(#) in social media we developed a # list we wanted the ENDO to use in the AP order and planned to educate all ordering and receiving staff. The # would trigger a specimen code (CODE) selection in the AP LIS. Within the AP LIS, we created an internal group (GI AP), and cases with the new CODE would be routed to the GI group. Roll out: 1.We met with endoscopy nurses and followed the work flow. 2.Nurse case documentation burden was high, therefore we simplified our list to only 2 (#ROUTINE and #SPECIAL). 3.Met with the ENDO to review and get support/feedback. 4.Met with AP LIS to create new CODE. 5.We gave an in-service to the endoscopy nurses and made badge cards (figure 1). 6. Trained the AP accession staff. 7. Survey sent to the ENDO at 20 months.

Results: Since go live 12/2016, TCH surgical volume was 120,751 specimens with 9,845 specimens routed to GI AP out of 40,087 GI biopsy specimens (figure 2). 67% of the ENDO responded to the survey and 62.5% said the project exceeded expectations and 37.5% said it met expectations. 75% answered they would recommend expanding to system wide use. 75% answered that routing all their cases to GI AP specialists was not necessary.

Figure 1 - 634

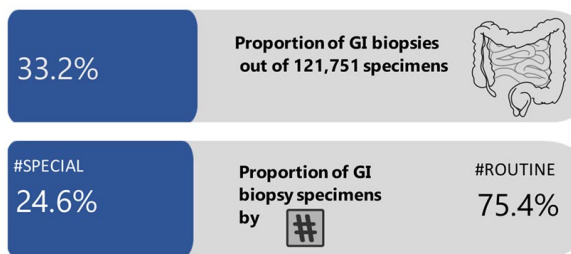
Figure 1. Badge Card

#ROUTINE	#SPECIAL
ESOPHAGUS	ESOPHAGUS
GERD	Known esophagus dysplasia
R/O EOE	Long segment Barrett's (multiple biopsies)
R/O Barrett's (single biopsy)	Mass
STOMACH	STOMACH
Gastritis	Known gastric dysplasia
R/O H. pylori	Mass
Fundic gland polyps	Known adenoma/FAP
SMALL BOWEL	SMALL BOWEL
R/O celiac	Ampulla mass
COLON	COLON
Colon polyps	Colon mass and rectal mass
Diarrhea, NOS	
MISC	MISC
Endoscopically normal	IBD (Crohn or UC any biopsy)
	Polyposis syndromes (FAP)
	Pediatric
	History of transplant (any type)
	Anything unusual

Figure 2 - 634

Figure 2.

Relative Volume of GI Cases in Clinician Directed Case Routing



	Total	% of Total	% of GIBx
Total Specimen Volume	120,751	100.0%	
GI Biopsy Volume	40,087	33.2%	
GI #Routine Volume	30,242	25.0%	75.4%
GI #Special Volume	9,845	8.1%	24.6%

BX = number of biopsy specimens

Conclusions: The project met our goals to route cases from the most complex patients to the GI group using only our ability to communicate, flexibility, and creativity with no investment of capital. The hashtag allowed us to communicate our goals very clearly to all parties which helped with buy in and compliance. The pressures on hospital based specialties are a reality that we will all continue to face. As pathologists we need to publish more projects that show how different groups are using processes to navigate the current practice environment.

635 SATB2 Expression in Hindgut Well Differentiated Neuroendocrine Tumors: Is It Specific?

Jatin Gandhi¹, Yongchao Li¹, Jorge Solares¹, Mahul Amin², Ian Clark¹

¹University of Tennessee Health Science Center, Memphis, TN, ²Methodist University Hospital, Memphis, TN

Disclosures: Jatin Gandhi: None; Yongchao Li: None; Jorge Solares: None; Ian Clark: None

Background: Special AT-rich sequence binding protein-2 (SATB2), is a recently described transcription factor and an epigenetic regulator. The proteomic expression of SATB2 is seen in 1) epithelium of lower gastrointestinal tract mucosa 2) colorectal adenocarcinoma and 3) tumors with osteoblastic differentiation. The major objective of this study was to investigate the expression of SATB2 in well-differentiated neuroendocrine tumors, and to explore its potential as a diagnostically useful marker specifically for NETs of hindgut origin.

Design: Cases of previously diagnosed gastrointestinal well differentiated neuroendocrine tumor (NET), grades 1 and 2, were selected and divided into 3 groups depending on site of origin: foregut, midgut and hindgut. Immunohistochemical staining with a polyclonal antibody to SATB2 (Sigma polyclonal rabbit antibody) was performed on Ventana platform using full tissue blocks in 45 well-differentiated neuroendocrine tumors (15 each from foregut, midgut and hindgut). The staining pattern was quantitatively scored as 0 (no nuclear staining), 1+ (1-33%), 2+ (33-66%), 3+ (67-100%) and qualitatively graded as weak (+), moderate (++) and strong (+++) based on the intensity of nuclear expression.

Results: Among the hindgut NET tumors all 14/14 cases were positive for SATB2 with most of them quantitatively expressing 3+ staining (moderate to strong nuclear expression). The midgut (0/11) and the foregut (0/8) well differentiated neuroendocrine tumors were completely negative. Of further interest was the strong homogeneous expression in the hindgut mucosa.

Conclusions: Our results indicate that SATB2 is a sensitive and specific marker for hindgut well-differentiated neuroendocrine tumors, and has a potential utility in assessment of metastatic NETs of unknown origin. However, the utility of SATB2 needs further exploration in terms of identifying/predicting the behaviour of hindgut NETs.

636 Modified Becker Tumor Regression Grading of Rectal Adenocarcinoma After Neoadjuvant Therapy Predicts Distant Recurrence and Supports Total Submission of Residual Tumor Bed

Paulo Garcia¹, Kaitlyn Wieditz¹, Melissa Contos², Michael Idowu¹

¹Virginia Commonwealth University Health System, Richmond, VA, ²VCU Health, Richmond, VA

Disclosures: Paulo Garcia: None; Kaitlyn Wieditz: None; Melissa Contos: None; Michael Idowu: None

Background: In neoadjuvant treated rectal adenocarcinoma (NATRA), there are cases where minute focal groups of residual tumor (RT) are present with little fibrosis, the significance of which is unclear. In these cases, tumor regression grading systems (TRGS) like the Becker TRGS (BTRGS), which estimate the amount of tumor without comparison to the amount of fibrosis, are advantageous. However, the BTRGS does not delineate between minute foci of RT (<1%) and subtotal tumor regression (<10%). To our knowledge, there are no studies determining prognostic end-points with regard to overall survival or disease free survival of a modified Becker TRGS score that delineates residual tumor of <1% in the setting of NATRA.

Design: Patients with resected RA from 2006 to 2017, ages 18-80, histologically confirmed RA, AJCC stage 2 or 3, neoadjuvant chemoradiotherapy, and low-anterior or abdominoperitoneal resection were retrospectively selected for further study. Cases with distant metastases at time of resection or only chemotherapy or radiotherapy treatment were excluded. Primary resection specimens were scored for histopathologic evidence of tumor regression according to Becker et. al. To evaluate the importance of rare tumor cells inclusion of a grade 1b was created to capture RT <1%. Additionally, combinations of grades were created to assess <1% vs >1% RT and <10% vs >10% RT. Kaplan-Meier plots and log-Rank, comparison test were used for statistical analysis.

Results: Of the 118 patients selected, 91 resection specimens were available for evaluation. As expected, increasing RT burden was correlated with decreased disease free survival with regard to distant recurrence ($p<0.05$) in all grading combinations examined (see Figure 1). Overall survival and disease free survival (local recurrence) was also correlated with increasing RT burden, but did not reach statistical significance ($p=0.35$ and 0.48 , respectively).

Figure 1 - 636

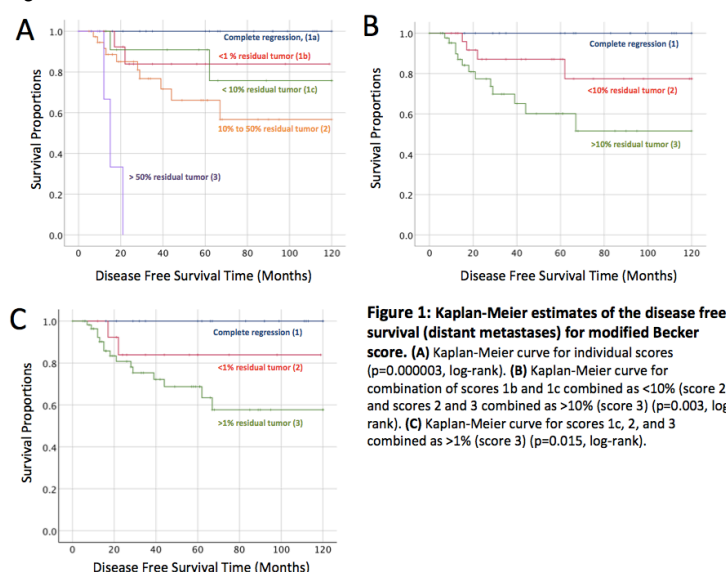


Figure 1: Kaplan-Meier estimates of the disease free survival (distant metastases) for modified Becker score. (A) Kaplan-Meier curve for individual scores ($p=0.000003$, log-rank). (B) Kaplan-Meier curve for combination of scores 1b and 1c combined as <10% (score 2), and scores 2 and 3 combined as >10% (score 3) ($p=0.003$, log-rank). (C) Kaplan-Meier curve for scores 1c, 2, and 3 combined as >1% (score 3) ($p=0.015$, log-rank).

Conclusions: Overall, the data suggests that the modified Becker tumor regression grading system predicts distant recurrence, and shows that focal tumor deposits (<1%) are significantly linked to lower time-to-local recurrence. Thus, submission of the entire tumor bed may be necessary for evaluation of residual disease in NATRA. However, further studies with a larger cohort and additional observers will be needed to further evaluate the significance of these findings.

637 Tumor-Infiltrating Lymphocytes at the Invasive Edge are Predictive of Distant Recurrence in Neoadjuvant Rectal Adenocarcinoma

Paulo Garcia¹, Kaitlyn Wieditz¹, Michael Idowu¹, Melissa Contos²

¹Virginia Commonwealth University Health System, Richmond, VA, ²VCU Health, Richmond, VA

Disclosures: Paulo Garcia: None; Kaitlyn Wieditz: None; Michael Idowu: None; Melissa Contos: None

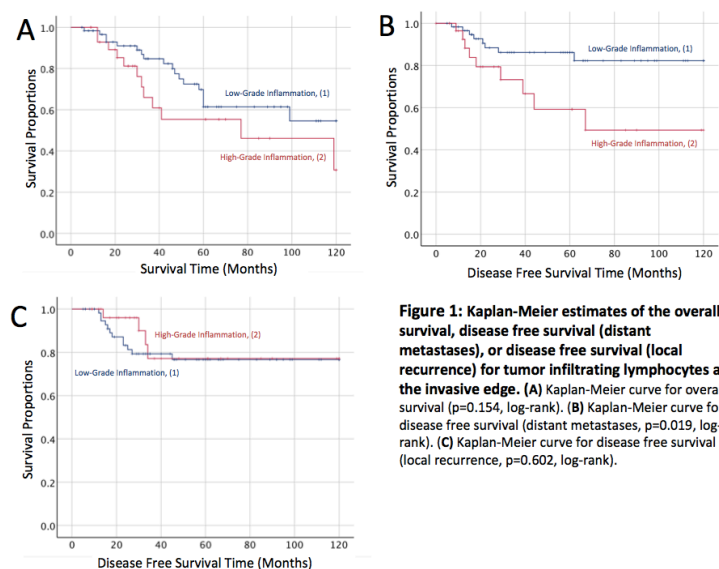
Background: The grading of tumor-infiltrating lymphocytes (TILs) has been recognized by the TILs Working Group 2017 to have significant prognostic implications in rectal adenocarcinoma (RA). However, assessment of TILs using semi-quantitative methods, like the Klintrup-Mäkinen score (KMS), in neoadjuvant treated rectal adenocarcinoma (NATRA) with regard to prognostic endpoints, such as overall survival and disease free survival has yet to be done.

Design: Patients from 2006 to 2017 with low-anterior or abdominoperitoneal resection, histologically confirmed RA, AJCC stage 2 or 3, ages 18-80, and chemoradiation were retrospectively selected for further study. Cases with distant metastases at the time of resection were excluded. Primary resection specimens were scored for histopathologic evidence of TILs at the invasive edge according to Klintrup et al; overall TILs present was also assessed. Kaplan-Meier plots, Log-Rank, Breslow, and Tarone-Ware comparison tests were used for statistical analysis.

Results: Out of 118 patients, 91 resection specimens were available for evaluation. Invasive edge TILs (IETILs) correlated with decreased disease free survival with regard to distant recurrence ($p < 0.05$), but was not significantly correlated with decreased 10 year survival ($p = 0.15$) (see Figure 1). Evaluation and grading of overall TILs present did not show statistical significance with 10-year survival or distant or local recurrence ($p = 0.75, 0.45, 0.40$, respectively) (see Table 1).

Table 1: Distribution of inflammatory cell scores							
	Score ^a				Combined scores ^b		
	0	1	2	3	1	2	
Invasive edge (N=91)	25	36	27	3	61	30	
Overall (N=91)	3	45	39	4	48	43	
Overall survival ^c							p-value
Invasive edge (N=91)	7 (18)	11 (25)	11 (16)	1 (2)	18 (43)	12 (18)	0.154
Overall (N=91)	1 (2)	15 (30)	14 (25)	0 (4)	16 (32)	14 (29)	0.85
Disease free survival (distant recurrence) ^c							
Invasive edge (N=91)	1 (24)	7 (29)	8 (19)	1 (2)	8 (53)	9 (21)	0.019
Overall (N=91)	0 (3)	10 (35)	7 (32)	0 (4)	10 (38)	7 (36)	0.404
Disease free survival (local recurrence) ^c							
Invasive edge (N=91)	5 (20)	7 (29)	4 (23)	0 (3)	4 (26)	12 (49)	0.602
Overall (N=91)	1 (2)	9 (36)	6 (33)	0 (4)	10 (38)	6 (37)	0.445
^a Inflammation for invasive was graded using: 0 = no increased inflammation, 1 = patchy increase of inflammatory cells at invasive edge, 2 = band-like inflammation at invasive edge, 3 = prominent cup-like inflammation at invasive edge. Inflammation for overall TILs present was graded using: 0 = absence of inflammatory reaction, 1 = weak inflammatory reaction, 2 = moderate inflammatory reaction, 3 = severe inflammatory reaction							
^b Absent and patchy inflammation scores (scores 0 and 1) were combined into low-grade inflammation (score 1). Band-like inflammation and prominent cup-like inflammation (scores 2 and 3) were combined into high-grade inflammation (score 2).							
^c Numbers in parenthesis indicate amount of censored cases with that score							
p-values (Log-rank) calculated on combined scores							

Figure 1 - 637



Conclusions: The data suggests that grading of IETILs in NATRA using the KMS may predict distant recurrence and shows that increased inflammation at the tumor edge is significantly linked to lower time-to-distant recurrence. However, further studies, especially with a larger cohort, are needed to further evaluate the significance of these findings.

638 Basaloid Carcinoma of the Anus: A Comprehensive Genomic Profiling Study

Laurie Gay¹, Julia Elvin², Jo-Anne Vergilio², J. Keith Killian², Nhu Ngo², Shakti Ramkissoon³, Eric Severson³, Amanda Hemmerich³, Siraj Ali¹, Alexa Schrock², Jon Chung², Venkataprasanth Reddy², Vincent Miller², Jeffrey Ross⁴

¹Cambridge, MA, ²Foundation Medicine, Cambridge, MA, ³Foundation Medicine, Morrisville, NC, ⁴Upstate Medical University, Syracuse, NY

Disclosures: Laurie Gay: *Employee*, Foundation Medicine, Inc.; Julia Elvin: *Employee*, Foundation Medicine, Inc.; Nhu Ngo: *Employee*, Foundation Medicine, Inc.; Eric Severson: *Employee*, Foundation Medicine, Inc.; Amanda Hemmerich: *Employee*, Foundation Medicine, Inc.; Alexa Schrock: *Employee*, Foundation Medicine, Inc.; Vincent Miller: *Employee*, Foundation Medicine, Inc.; *Advisory Board Member*, Revolution Medicines; Jeffrey Ross: *Employee*, Foundation Medicine, Inc.

Background: Basaloid squamous cell carcinoma (BSCC) of the anus, also known as cloacogenic carcinoma, is an uncommon clinically aggressive form of malignancy. Although clinically considered to be a variant of conventional anal SCC (CSCC), a comparison of genomic alterations (GA) between these 2 tumor types has not been previously performed.

Design: FFPE tissues from clinically advanced BSCC (31 cases) and CSCC (442 cases) underwent hybrid-capture based comprehensive genomic profiling (CGP) to evaluate all classes of genomic alterations. Tumor mutational burden (TMB) was determined on up to 1.1 Mbp of sequenced DNA and microsatellite instability (MSI) was determined on 114 loci.

Results: The BSCC and CSCC patients have a similar median age (59 years) and female preponderance (Table). The BSCC were more often HPV16 positive (90% vs 79%). GA per tumor was higher in the CSCC group. The frequencies of GA in both groups was similar, with non-clinically relevant (CR) GA in *KMT2D* and *SOX2* common in both types, and *TP53* GA relatively infrequent. CR GA in both tumors were most frequent in the PI3K/mTOR pathway with only rare kinase gene targets identified (*ERBB2* in BSCC and *FGFR3* in CSCC, both at 4%). Using various metrics, TMB was higher in the CSCC than BSCC samples. MSI high status was virtually absent in both groups.

	Basaloid Carcinoma	Squamous Cell Carcinoma
Number of Cases	31	442
Males/Females	M 16% F 84%	M 31% F 69%
Median age (range)	59 (46-80)	59 (25-88)
HPV16	90%	79%
HPV18	6%	4%
HPV6/11	3%	<1%
HHV8	3%	3%
HHV4	<1%	<1%
GA/tumor	2.45	4.6
Top Non-CR GA	<p><i>CYLD</i> 35%</p> <p><i>KMT2D</i> 20%</p> <p><i>SOX2</i> 10%</p> <p><i>CTNNB1</i> 10%</p> <p><i>KMT2C</i> 8%</p> <p><i>MSH2</i> 7%</p> <p><i>TP53</i> 7%</p> <p><i>RB1</i> 7%</p>	<p><i>KMT2D</i> 20%</p> <p><i>FBXW7</i> 17%</p> <p><i>KMT2C</i> 14%</p> <p><i>SOX2</i> 10%</p> <p><i>TP53</i> 10%</p> <p><i>CYLD</i> 10%</p> <p><i>FAT1</i> 10%</p>
Top CRGA	<p><i>PIK3CA</i> 23%</p> <p><i>NF1</i> 4%</p> <p><i>ERBB2</i> 4%</p>	<p><i>PIK3CA</i> 33%</p> <p><i>PTEN</i> 16%</p> <p><i>STK11</i> 4%</p> <p><i>FGFR3</i> 4%</p>
MSI-High	0%	1%
Mean TMB	4.8	6.8
Median TMB	3.6	5.2
TMB>10 mut/Mb	13%	19%
TMB>20 mut/Mb	3%	5%
PD-L1 IHC Positive	NA	29%

Conclusions: This study confirms well-established clinical similarities between BSCC and CSCC of the anus including female preponderance and association with HPV infection. The distribution of GA in the 2 tumor types is also similar, further confirming that BSCC is a variant of CSCC and not a distinct tumor type. The identification of targetable alterations and tumors with higher TMB in both subtypes suggests that CGP could play a role in personalizing therapies for these patients and extending their survival.

639 SDHC Promoter Hypermethylation In SDH Deficient GIST - Experience From The United Kingdom National Paediatric And Adolescent Wild Type And Syndromic (PAWS)-GIST Clinic

Olivier Giger¹, Rogier ten Hoopen², Venkata Bulusu³, Eamonn Maher², Ruth Casey²

¹University of Cambridge, Cambridge, CAbridgeshire, United Kingdom, ²University of Cambridge, Cambridge, United Kingdom, ³Cambridge University Hospitals, Cambridge, United Kingdom

Disclosures: Olivier Giger: None; Rogier ten Hoopen: None; Eamonn Maher: None

Background: Gastrointestinal stromal tumours (GIST) are the most commonly occurring sarcomas. 15% of GIST harbour germline variants or epimutations involving genes encoding for the SDH protein complex, *NF1* and other rare mutations. SDH deficient (dSDH) GIST account for up to 7.5% of gastric GISTs and mainly affect individuals below the age of 40. Up to 20% of these dSDH GIST are caused by silencing of the SDHC gene by promoter hypermethylation (SDHCmet). Diagnosis of tumours with SDHCmet has proven difficult as often only sparse FFPE material is available for testing. Here we describe our clinic experience on SDHCmet analysis in 15 patients. We also propose an altered testing algorithm for dSDH GIST.

Design: Fifteen patients (7f / 8m) were enrolled in a study for SDHCmet analysis. Germline analysis for *SDHA*-, *D*, *KIT*, *PDGFRA* and *NF1* was performed on all patients. SDHB expression was assessed by immunohistochemistry. Tumours and

adjacent normal tissue was investigated for SDHCmet by pyrosequencing and for SDHC expression by RT-qPCR. Multiple ligation dependent probe analysis (MLPA) analysis was performed on all cases with SDHC promoter hypermethylation.

Results: Ten patients showed to be dSDH (8f / 2m). Of these 7 had germline variants in one of the *SDHx* genes. Six (all f) showed a median SDHCmet of 51% in their tumours compared to less than 3% in the others. One pathogenic and one benign variant was detected in two of the SDHCmet tumours, whereas no pathogenic variant or copy number variation was detected by MLPA in any of the other four. SDHCmet was co-occurring with lowered SDHC mRNA levels. SDHCmet was associated with female gender (6/6), metastatic disease (5/6), young age at diagnosis (average age 24 years, range 15-27) and multiple primary tumours (3/6). Constitutional SDHC promoter hypermethylation was not detected in any patient.

Conclusions: Our work shows that SDHC promoter methylation analysis can reliably be performed on FFPE material in dSDH GIST. Our data is in keeping with published array and methylation sequencing data, however our method does not require fresh frozen material. Identification of dSDH GIST harbouring epigenetic SDHC silencing will help guide genetic testing algorithms and better categorise these tumours. It may also provide therapeutic options with epigenetic drugs in the future for patients with metastatic dSDH GIST.

640 Clinicopathologic Determinants of Pathologic Treatment Response in Neoadjuvant Treated Rectal Adenocarcinomas

Iván González¹, Philip Bauer¹, William Chapman¹, Rehan Rais², Zahra Alipour³, Esther Lu⁴, Deyali Chatterjee⁵

¹Washington University School of Medicine, St. Louis, MO, ²Washington University in St. Louis, St. Louis, MO, ³Washington University in St. Louis, Clayton, MO, ⁴St. Louis, MO, ⁵Washington University, St. Louis, MO

Disclosures: Iván González: None; Philip Bauer: None; William Chapman: None; Rehan Rais: None; Zahra Alipour: None; Esther Lu: None; Deyali Chatterjee: None

Background: Neoadjuvant treatment (NAT) followed by total mesorectal excision is currently considered the standard of treatment for rectal adenocarcinoma (RA). It has been shown that the degree of pathologic response correlates with survival. However, it is still unclear, which patients would respond to NAT, including showing pathologic complete response (CR). In this study, we sought to evaluate if any pathologic feature in the diagnostic biopsy, or any treatment related parameters predicted tumor response to NAT.

Design: 91 patients with RA were retrospectively identified (2008 to 2016) who had a biopsy-proven diagnosis of RA, received NAT and underwent surgical resection, and all pathology material was available at our institution. All the archival biopsy slides were evaluated for various histopathologic parameters such as tumor differentiation, tumor budding (TB), tumor infiltrating lymphocytes (TIL), lymphovascular invasion (LVI), perineural invasion (PNI), and mitotic index. All the archival slides from the resection specimens were reviewed for standardized scoring of treatment response (TR) according to the current CAP guideline (version 4.0.0.1). Accordingly, TR was scored as 0 (CR), 1 (near CR), 2 (partial response), and 3 (poor or no response). The relevant clinical information was obtained from a prospectively maintained database.

Results: The mean age of presentation was 58.2 years, with a M:F ratio of 1.4:1. All patients received a standardized NAT. The mean duration of NAT was 46.1 days (1 - 243 days), and the mean time lapse from end of NAT to resection was 96.3 days (1 - 614 days). 16.5% of the cases had a TR score 0, 20.9%: score 1, 30.8%: score 2, and 31.9%: score 3. Higher pre-treatment cT stage ($p=0.0191$) and clinical AJCC stage ($p=0.0038$), were significantly associated with a poor TR. A longer duration of NAT ($p=0.0088$), time lapse from end of NAT to resection ($p=0.0217$), and the presence of TIL ($p=0.0193$) were significantly associated with TR. The clinicopathologic associations with TR are summarized in Table-1 respectively.

Table-1. Correlation of Clinicopathologic features with Pathologic Treatment Response					
N = 91	Group 0	Group 1	Group 2	Group 3	P
	(n = 15)	(n = 19)	(n = 28)	(n = 29)	
Clinical T Stage					
T1 (n = 2)	0	2, 100%	0	0	0.0191
T2 (n = 11)	3, 27.3%	5, 45.5%	1, 9.1%	2, 18.2%	
T3 (n = 67)	11, 16.4%	8, 11.9%	23, 34.3%	25, 37.3%	
T4 (n = 11)	1, 9.1%	4, 36.4%	4, 36.4%	2, 18.2%	
Clinical N Stage					
N0 (n = 34)	5, 14.7%	6, 17.6%	7, 20.6%	16, 47.1%	0.2953
N1 (n = 44)	9, 20.5%	10, 22.7%	15, 34.1%	10, 22.7%	
N2 (n = 13)	1, 7.7%	3, 23.1%	6, 46.2%	3, 23.1%	
Clinical AJCC Stage					
I (n = 9)	1, 11.1%	6, 66.7%	0	2, 22.2%	0.0038
II (n = 23)	5, 21.7%	1, 4.3%	8, 34.8%	9, 39.1%	
III (n = 49)	9, 18.4%	11, 22.4%	18, 36.7%	11, 22.4%	
IV (n = 10)	0	1, 10%	2, 20%	7, 70%	
Pretreatment CEA levels (mean, SD)	8.4, 23.11	3.3, 3.6	6.3, 10.2	23.4, 55.5	0.1197
Duration of NAT, days (mean, SD)	38.4, 14.6	50.8, 22.5	57.3, 40.4	35.1, 55.3	0.0088
Time Lapse from end of NAT to Resection, days (median, SD)	83, 34.3	72.5, 86.9	91, 122.9	47, 68.5	0.0217
Tumor Budding					
No (n = 62)	12, 19.4%	12, 19.4%	21, 33.9%	17, 27.4%	0.4211
Yes (n = 29)	3, 10.3%	7, 24.1%	7, 24.1%	12, 41.4%	
TILs					
No (n = 74)	11, 14.9%	12, 16.2%	27, 36.5%	24, 32.4%	0.0193
Yes (n = 17)	4, 23.5%	7, 41.2%	1, 5.9%	5, 29.4%	
Abbreviations: CEA - Carcinoembryonic Antigen; SD - Standard Deviation; NAT - Neoadjuvant Treatment; TIL - Tumor Infiltrating Lymphocyte.					

Conclusions: Of the several histopathologic parameters studied in the diagnostic biopsy material, only TILs, along with clinical parameters such as duration of NAT and time from end of NAT to resection, showed significant correlation with TR. Clinical T and AJCC stage were inversely associated with TR.

641 Clinicopathologic Correlation of CXCR4 Expression and Treatment Response in Neoadjuvant Treated Rectal Adenocarcinoma

Iván González¹, William Chapman¹, Philip Bauer¹, Esther Lu², Rehan Rais³, Deyali Chatterjee⁴

¹Washington University School of Medicine, St. Louis, MO, ²St. Louis, MO, ³Washington University in St. Louis, St. Louis, MO, ⁴Washington University, St. Louis, MO

Disclosures: Iván González: None; William Chapman: None; Philip Bauer: None; Esther Lu: None; Rehan Rais: None; Deyali Chatterjee: None

Background: The anatomic location of the rectum, coupled with frequent deep extension of the tumor, makes primary surgical resection for rectal adenocarcinoma (RA) challenging, and leads to a high locoregional recurrence. Therefore, neoadjuvant treatment (NAT) followed by total mesorectal excision is currently considered the standard of therapy. It has been shown that the degree of pathologic response correlates with survival. However, it is still unclear which patients would respond to NAT, moreover achieve a complete response (CR). Chemokine receptor 4 (CXCR4) is a membrane bound heptahelical receptor. CXCR4 over-expression predicts an unfavorable overall survival (OS) in several malignancies including colorectal cancer. In this study, we sought to evaluate the expression of CXCR4 in RA and its correlation with treatment response (TR) and survival.

Design: 88 patients with RA were retrospectively identified (2008 to 2016) who had an endoscopic biopsy diagnostic of RA, received NAT, and underwent surgical resection at our institution. All the resection slides were reviewed to assess for TR according to the latest CAP guideline (version 4.0.0.1), into scores 0 (CR), 1 (near CR), 2 (partial response), and 3 (poor or no response). The clinical information was obtained from a prospective maintained database. CXCR4 IHC (R&D System, clone #44716) was performed on all the diagnostic biopsies, and the slides were reviewed blinded to clinical information.

Results: The mean age of presentation was 58.2 years, with a M:F ratio of 1:1.5. 15.9%, 77.3%, and 6.8% of the cases were well-, moderately-, and poorly-differentiated respectively. The mean duration of NAT was 46.1 days (1 - 243 days), and the mean time lapse from end of NAT to resection was 96.3 days (1 - 614 days). 15.3% of the cases had a TR score 0, 22.4%: score 1, 31.7%: score 2, and 30.6%: score 3. Cytoplasmic, cytoplasmic and nuclear, and only nuclear CXCR4 expression was identified in 52.3%, 36.3%, and 11.4% of the cases respectively. CXCR4 expression was not associated with CR (p=0.1894), TR (p=0.3545), pT- (p=0.4211) or pN-stage (p=0.4244).

OS and recurrent free survival (RFS) were not associated with CXCR4 expression. The clinicopathologic characteristics and associations with CXCR4 expression are summarized in Table-1.

Table-1. Clinicopathologic features and CXCR4 Expression				
N = 88	Cytoplasmic (n = 46)	Cytoplasmic and Nuclear (n = 32)	Nuclear (n = 10)	P
Complete Response				
No (n = 74)	41, 55.4%	24, 32.4%	9, 12.2%	0.198
Yes (n = 13)	5, 38.5%	7, 53.8%	1, 7.7%	
Treatment Response (n=85)				
Group 0 (n = 13)	5, 38.5%	7, 53.8%	1, 7.7%	0.354
Group 1 (n = 19)	7, 36.8%	8, 42.1%	4, 21.1%	
Group 2 (n = 27)	16, 59.3%	9, 33.3%	2, 7.4%	
Group 3 (n = 26)	17, 65.4%	7, 53.8%	2, 7.7%	
Percentage Residual Tumor (mean, SD)	44.7%, 37.6	29.9%, 37.6	27.3%, 36.8	0.111
Pathologic T Stage				
T0 (n = 13)	5, 38.5%	7, 53.8%	1, 7.7%	0.421
T1 (n = 5)	2, 40%	2, 40%	1, 20%	
T2 (n = 21)	12, 57.1%	6, 28.6%	3, 14.3%	
T3 (n = 40)	19, 47.5%	16, 40%	5, 12.5%	
T4 (n = 9)	8, 88.9%	1, 11.1%	0	
Pathologic N Stage				
N0 (n = 61)	29, 47.5%	23, 37.7%	9, 14.8%	0.424
N1 (n = 18)	12, 66.7%	6, 33.3%	0	
N2 (n = 9)	5, 55.6%	3, 33.3%	1, 11.1%	
Pathologic AJCC Stage				
0 (n = 12)	4, 33.3%	7, 58.3%	1, 8.3%	0.635
I (n = 19)	9, 47.4%	6, 31.6%	4, 21.1%	
II (n = 29)	15, 51.7%	10, 34.5%	4, 13.8%	
III (n = 19)	12, 63.2%	6, 31.6%	1, 5.3%	
IV (n = 9)	6, 66.7%	3, 33.3%	0	

Conclusions: Although some studies have shown that CXCR4 expression is a poor prognostic marker for colonic adenocarcinoma, it probably does not hold true for rectal adenocarcinoma.

642 Ileocolonic Lipomas Larger than 3.5 cm Have Ulcers, Symptoms, and/or Features of Chronic Mucosal Injury Resembling Inflammatory Bowel Disease

Sara Hall¹, Scott Owens²

¹Michigan Medicine, Ann Arbor, MI, ²University of Michigan, Ann Arbor, MI

Disclosures: Sara Hall: None; Scott Owens: None

Background: Ileocolonic lipomas (IL) are uncommon. They may be found incidentally on colonoscopy performed for other reasons or targeted for examination, particularly if they cause signs or symptoms. In our experience, large IL can clinically mimic malignancy such as adenocarcinoma and biopsy diagnosis biopsy may be difficult, as the submucosal tumor may go unsampled. If clinical suspicion of malignancy is high and a diagnosis isn't made on biopsy, or if there is obstruction or intussusception, patients may undergo resection. We reviewed ILs resected at our institution to characterize the patient population and to seek micro- or macroscopic features that may aid in pre-surgical diagnosis of IL.

Design: Our laboratory information system was searched for the words 'resection', 'colon' and 'lipoma' between 2003 and 2011. Slides from identified cases were reviewed for diagnostic confirmation and for histologic features, including whether or not there was/were: ulcer; features of atypical lipomatous tumor/liposarcoma; and/or other findings of note. The electronic medical record was reviewed for each patient's age, gender, and details of clinical presentation.

Results: We found 13 resected ILs in the study period. Of the 13, 8 were female and 5 male. Two IL involved the terminal ileum and 9 of the other 11 occurred in the right or transverse colon. Nine presented with intussusception/obstruction, confirmed by imaging, while 4 were asymptomatic and found incidentally on screening or surveillance colonoscopy. The two groups were separable based on size, with symptomatic tumors ≥ 3.5 cm (mean 4.7) while asymptomatic tumors were < 3.5 cm (mean 2.4; $p=0.002$). Ulcers and inflammatory bowel disease (IBD)-like changes (Paneth cell hyper-/metaplasia; pseudopyloric metaplasia, mucosal distortion, muscularis mucosae

hypertrophy, inflammatory pseudopolyps) were found only in symptomatic patients, none of which had a pre-existing diagnosis of IBD. No case had features suggesting atypical lipomatous tumor/liposarcoma. Data summarized in Table 1.

Clinical presentation	Mean Size	Mean Age	Gender (F:M)	Ulcer	IBD-like changes
Symptomatic	4.7 cm	49	(5:4)	67%	67%
Asymptomatic	2.4 cm	55	(3:1)	0%	0%

Conclusions: In prior studies, IL >2 cm had symptoms but we found only IL ≥ 3.5 cm were symptomatic. A predilection for occurrence in the right colon is similar to prior studies. IBD-like mucosal changes in a patient with no known IBD history and a mass can reasonably lead to suspicion of IL. Compatible imaging findings with these histologic mucosal features may obviate resection in some patients, as endoscopic removal techniques have been described.

643 Inter-Observer Variability Among Pathologists in the Diagnosis of Challenging Serrated Colonic Polyps and the Diagnostic Utility of Agrin Immunostaining

Cynthia Harris¹, Ian Brown², Gregory Lauwers³, Anthony Mattia⁴, Deepa Patil⁵, Omer Yilmaz⁶, Qing (Grace) Zhao⁷, Lawrence Zukerberg⁸, Vikram Deshpande¹, Richard Hynes⁹, Steffen Rickelt⁹

¹Massachusetts General Hospital, Boston, MA, ²Brisbane, QLD, Australia, ³H. Lee Moffitt Cancer Center & Research Institute, University of South Florida, Tampa, FL, ⁴Newton-Wellesley Hospital, Sudbury, MA, ⁵Cleveland Clinic, Cleveland, OH, ⁶Massachusetts Institute of Technology, Cambridge, MA, ⁷Boston Medical Center, Boston, MA, ⁸Auburndale, MA, ⁹David H. Koch Institute for Integrative Cancer Research, Cambridge, MA

Disclosures: Cynthia Harris: None; Ian Brown: None; Gregory Lauwers: None; Anthony Mattia: None; Deepa Patil: None; Omer Yilmaz: None; Qing (Grace) Zhao: None; Lawrence Zukerberg: None; Vikram Deshpande: None; Richard Hynes: None; Steffen Rickelt: None

Background: Sessile serrated adenoma/polyps (SSA/P) are precursors to colorectal carcinoma. There are no universally accepted diagnostic criteria for SSA/P and distinguishing them from other serrated polyps, including hyperplastic polyps (HP), can be difficult. In this study, diagnostically challenging serrated polyps were evaluated by academic gastrointestinal (GI) pathologists and the inter-observer agreement in the diagnosis was assessed. We then compared these results with an immunostain for agrin, a sensitive and specific marker for SSA/P.

Design: We identified 255 formalin-fixed, paraffin-embedded polypectomies. Of those 255 polyps, 50 were deemed diagnostically challenging. The polyps were evaluated by nine GI pathologists in three countries and classified as: 1) SSA/P, 2) HP, 3) traditional serrated adenoma (TSA), and 4) unclassified, per current WHO criteria (2010). The pathologists were blinded to endoscopic size, endoscopic appearance, and location of the individual samples. We used Fleiss' kappa statistics to determine the inter-observer agreement in this cohort. An agrin immunostain was performed on the polyps and deemed positive in cases with staining of the muscularis mucosa, independently evaluated by 3 non-pathologists.

Results: The majority opinion (at least 5/9 pathologists) was used as the gold-standard diagnosis. The polyps were classified as follows: 25 SSA/P, 14 HP, 4 TSA, and 3 samples which did not yield a majority. Four samples were excluded due to insufficient tissue for agrin staining. Complete diagnostic concordance among the experts was achieved in only 12 cases (24%) and in 1 case, no majority agreement was reached. Fleiss' kappa statistics showed a weak overall agreement (kappa value = 0.493). Agrin staining was positive in 24/25 SSA/P and negative in 19/21 non-SSA/P. The sensitivity and specificity of agrin in this cohort of challenging polyps was 96% and 90%, respectively.

Conclusions: Our results show that there is continued and significant inter-observer variability in the diagnosis of SSA/P. Agrin staining in the muscularis mucosa is a powerful tool in differentiating challenging examples of SSA/P from HP and TSA.

644 Tumor Mutational Burden, Immunoscore and PD-L1 Expression in Patients with Epstein-Barr virus-associated Gastric Cancer

Lu He, Nanjing, China

Disclosures: Lu He: None

Background: Epstein-Barr virus (EBV)-associated gastric cancer (EBVaGC) is a unique subtype of gastric adenocarcinoma with frequent overexpression of programmed death ligand-1 (PD-L1) and good prognosis. Tumor mutation burden (TMB), defined as the number of non-synonymous coding mutations per megabase of genome examined, has been found to be positively linked to clinical benefit to the immune checkpoint blockade in non-small cell lung cancer (NSCLC), metastatic melanoma, colorectal cancer and other solid tumors. Nevertheless, data regarding immunoscore, TMB and PD-L1 expression in EBVaGC is limited. This study was aimed to tentatively explore the possible landscape of TMB in EBVaGC as well as to assess the immunoscores of the cohort.

Design: We employed whole-exome sequencing (WES) in 12 patients with EBVaGC using tumor paraffin-embedded sections. Somatic TMB were calculated from WES results and compared with TMB of unselected non-EBV⁺ gastric cancer samples from TCGA database. We also performed immunohistochemistry to evaluate expression of PD-L1(SP142), CD3 and CD8. The densities of CD3⁺ and CD8⁺ T cells in tumor core and invasive margin regions were measured at 200 magnification in 5 respective areas.

Results: The clinical characteristics of all 12 patients with EBVaGC are shown in Table 1. The median age of patients at diagnosis was 55 years old. The heatmap showed significantly mutated genes as identified by the analysis and the number of samples with each mutation (Figure 1). The median TMB of 12 EBVaGC patients were remarkably higher than that of unselected non-EBV⁺ gastric cancers (GCs) in asian cohort (data from TCGA): 28.05vs 8.87mutations/megabase ($P=0.0003$, $n=12$ vs 80) (Figure 2). There seemed to be an association between PD-L1 expression and TMB, despite correlation coefficient is not quite strong ($P=0.032$, $R^2=0.618$) (Figure 2). The analysis showed that PD-L1 expression was positively associated with Immunoscores ($P=0.043$, $R^2=0.591$) (Figure 2), but no significant correlation was observed between Immunoscores and TMB.

Clinical Characteristics	No. (%) (N=12)
Age, median (range), years	55.3(27-67)
Maximum diameter?cm?	5.5(2.5-12)
Sex	
Male	11(91.7)
Female	1(8.3)
Location	
Cardia	3(25.0)
Corpora	4(33.3)
Sinuses	5(41.6)
Stage at diagnosis	
I	3(25)
II	3(25)
III	6(50)
IV	0
Prognosis	
Alive	11(91.7)
Dead	1(8.3)

Figure 1 - 644

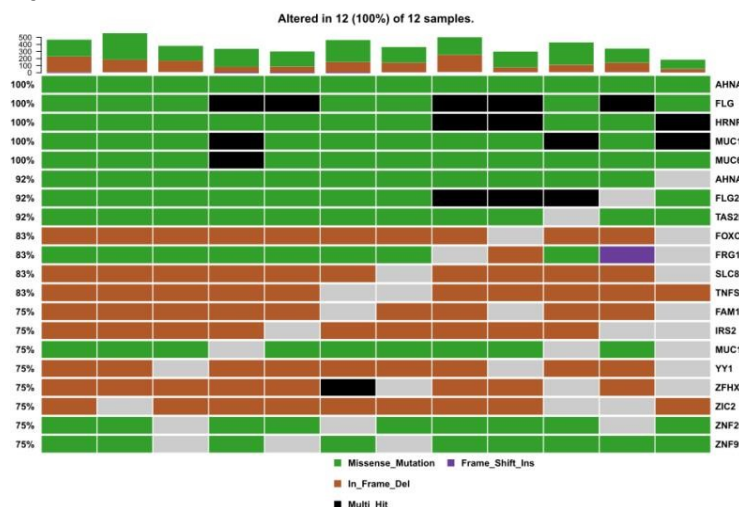
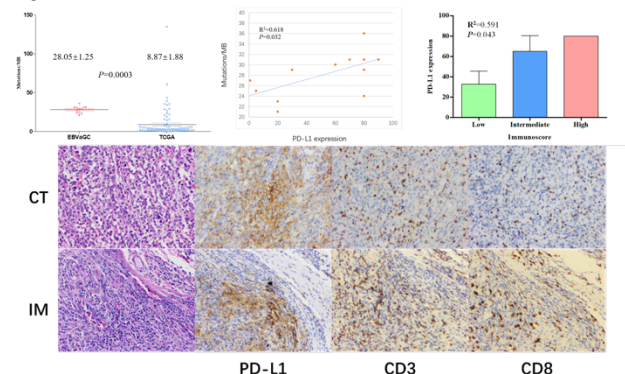


Figure 2 - 644



Conclusions: A substantial proportion of EBVaGCs express PD-L1, and the median TMB is much higher compared with unselected GCs. An elevated level of Immunoscore was also observed in this study. We render that high TMB is probably a unique characteristic of EBVaGCs. Generally speaking, PD-L1 overexpression in tumors predicts poor outcome. Considering the favorable prognosis of EBVaGCs, we hypothesize that high TMB may overcome survival disadvantage of PD-L1 overexpression.

645 Aberrant SATB2 Expression Is A Novel Marker of Inflammatory Bowel Disease-Associated Colorectal Neoplasia

Patrick Henn¹, Dane Olevian², Douglas Hartman², Changqing Ma³, Reetesh Pai¹

¹UPMC-Presbyterian Hospital, Pittsburgh, PA, ²Pittsburgh, PA, ³University of Pittsburgh, Pittsburgh, PA

Disclosures: Patrick Henn: None; Dane Olevian: None; Douglas Hartman: None; Changqing Ma: None; Reetesh Pai: None

Background: SATB2 is a sensitive marker of colorectal carcinoma and non-neoplastic colorectal epithelium (PMID 30001238). This study examines SATB2 expression in inflammatory bowel disease-associated colorectal carcinoma (IBD-CRC) and assesses its utility as a marker of IBD-associated dysplasia (IBD-dysplasia).

Design: Tissue microarrays of 385 CRCs, including 349 sporadic CRCs and 36 IBD-CRCs, were evaluated for SATB2 and CDX2 by immunohistochemistry using a modified H-score (intensity multiplied by percent of positive cells). Thirty-six cases of IBD-dysplasia from 28 patients were evaluated. Aberrant SATB2 expression was defined as an H-score of ≤ 10 with concurrent strong SATB2 in adjacent non-neoplastic colorectal crypt epithelium. SATB2 expression in IBD-CRC was correlated with clinicopathologic features; survival; molecular alterations (*KRAS*, *IDH1*, *HER2*, and *c-MYC*); and CDX2 and p53 expression. SATB2 expression in IBD-dysplasia was correlated with clinicopathologic features and endoscopic findings.

Results: Only 42% of IBD-CRC demonstrated SATB2 expression compared to 88% of sporadic CRC ($p < 0.001$). There was no difference in CDX2 expression between IBD-CRC and sporadic CRC (84% vs. 81%, $p = 1.0$). In IBD-CRCs, negative SATB2 expression was associated with abnormal (strong) p53 expression ($p = 0.02$) but not IBD type (UC vs. CD), tumor location, tumor grade, tumor stage, any of the evaluated molecular alterations, or disease-specific and recurrence-free survival (all with $p > 0.05$).

Of the 36 cases of IBD-dysplasia, 15 (42%) demonstrated aberrant SATB2 expression including 5 cases with negative SATB2 (H-score 0) and 10 cases with weak and focal SATB2 (H-score ≤ 10). Aberrant SATB2 expression was seen in cases of invisible (4/8, 50%) and visible (11/28, 39%) dysplasia ($p = 0.6$), more often identified in high-grade dysplasia (12/21, 57%) compared to low-grade dysplasia (3/15, 20%) ($p = 0.03$), and more frequently identified in non-polypoid (7/9, 78%) compared to polypoid (4/19, 21%) visible dysplasia ($p = 0.004$). There was no association between aberrant SATB2 expression and dysplasia location or IBD type (UC vs. CD).

Conclusions: IBD-CRCs more often lack SATB2 expression compared to sporadic CRCs. Aberrant SATB2 expression is observed in 42% of IBD-dysplasia and is more frequently observed in high-grade dysplasia and non-polypoid visible dysplasia. Aberrant SATB2 expression is a potential marker of IBD-associated colorectal neoplasia and may be a helpful ancillary marker when evaluating for IBD-dysplasia.

646 Gastric Carcinomas Arising In Autoimmune Metaplastic Atrophic Gastritis Are Associated With Increased Frequency Of DNA Mismatch Repair Deficiency And EBV Infection

Patrick Henn¹, Changqing Ma²

¹UPMC-Presbyterian Hospital, Pittsburgh, PA, ²University of Pittsburgh, Pittsburgh, PA

Disclosures: Patrick Henn: None; Changqing Ma: None

Background: Autoimmune metaplastic atrophic gastritis (AMAG) caused by immune-mediated destruction of gastric parietal cells is an early manifestation of pernicious anemia. It is associated with metaplastic processes which lead to a significant increased risk of carcinoma. This study examines the histopathologic and molecular characteristics of carcinomas arising in AMAG and pernicious anemia patients.

Design: Forty-six gastric carcinoma cases (study group), including 40 patients with AMAG and 6 patients with pernicious anemia and positive anti-intrinsic factor and/or antiparietal cell antibodies, were identified through a retrospective review of medical and pathology records between 2004 and 2018. Twenty-eight and 25 carcinomas with available material were tested for DNA mismatch repair (MMR) proteins by immunohistochemistry and EBV by in situ hybridization, respectively. Demographic, clinicopathologic, and molecular characteristics were compared to 152 consecutive gastric carcinomas from patients without pernicious anemia or AMAG (control group).

Results: The mean age at diagnosis of carcinoma for study group patients was 73 years old (range 54-91). Half (23/46) were men; 80% (37/46) were White. Age, gender, and race distributions were similar to those of the control group ($P>0.05$ for all). Of the 46 cases, 5 (11%) had concurrent well-differentiated neuroendocrine tumors (NETs), while 4 (9%) had more than one synchronous gastric carcinoma. In contrast, only 1 (1%) control group case had a synchronous carcinoma ($P=0.01$) and none had concurrent NETs ($P<0.01$). The majority of study group carcinomas (35/46, 76%) were identified in the body, fundus, and/or cardia while only 42% of control group cases arose in the proximal stomach ($P<0.01$). Histologically, study group cases were more frequently classified as carcinoma with lymphoid stroma (5/46 11% vs. 3/152 2%, $P=0.02$) and less often as diffuse-type carcinoma (9/46 20% vs. 65/152 43%, $P<0.01$) when compared with controls. Furthermore, significantly higher proportions of study group carcinomas were MMR deficient (6/28 21% vs. 12/152 8%, $P=0.04$) or EBV positive (3/25 12% vs. 1/152 1%, $P<0.01$) than controls.

Conclusions: Gastric carcinomas in pernicious anemia and AMAG patients have notable differences compared to carcinomas in patients without AMAG. They often affect proximal stomach and are associated with increased frequencies of DNA MMR deficiency and EBV infection. These findings warrant further systemic histopathologic and molecular characterization.

647 Diagnosing Clinically Significant Esophageal Candida Infection: A Clinicopathologic Reappraisal

Erika Hissong¹, Shula Schechter², Jonathan Mowers³, Rhonda Yantiss⁴, Tomas Slavik⁵, Jerome Cheng², Laura Lamps⁶

¹New York-Presbyterian/Weill Cornell Medical Center, New York, NY, ²University of Michigan, Ann Arbor, MI, ³Ann Arbor, MI, ⁴Weill Cornell Medical College, New York, NY, ⁵Ampath Pathology Laboratories and University of Pretoria, Pretoria, South Africa, ⁶University of Michigan Hospital, Ann Arbor, MI

Disclosures: Erika Hissong: None; Shula Schechter: None; Jonathan Mowers: None; Rhonda Yantiss: None; Tomas Slavik: None; Jerome Cheng: None; Laura Lamps: None

Background: Distinguishing true esophageal *Candida* infections from oral contaminants is a common diagnostic issue. Several histologic parameters have been conveyed through generations as indicators of true infection, including the presence of pseudohyphae, epithelial invasion, and intraepithelial neutrophils. Whether these features actually correlate with endoscopic lesions, symptoms, and response to therapy has never been tested in a large cohort. The goal of this study was to determine if specific histologic features correlate with clinical and endoscopic findings when *Candida* is found in esophageal biopsies.

Design: 271 consecutive biopsies in which *Candida* was detected were reviewed (from 3 institutions, 2012-2018). Cases were evaluated for the presence of desquamated epithelial cells, location of fungi (intact epithelium vs. debris), fungal form (budding yeast or pseudohyphae), neutrophils, and ulceration. Medical records were reviewed for clinical history, endoscopic lesions, and response to antifungal therapy. Statistical analysis was performed to determine if any histologic features significantly correlated with clinical variables.

Results: There were 120 males and 151 females, with mean age of 42 (range: 1-91 years). 48% of patients had comorbidities predisposing them to *Candida* infection. 197/271 patients (73%) had abnormal endoscopies showing plaques (139), ulcers (23), or esophagitis (35). 57% had symptoms referable to the esophagus (38% did not, 5% unknown). 55% of patients had a documented response to antifungal therapy (13% did not; 32% unknown). The only statistically significant histologic variable was ulceration, which significantly correlated with response to antifungal therapy ($p<0.05$). None of the other histologic variables significantly correlated with any of the clinical parameters. Budding yeast without pseudohyphae were identified in only 9 cases; 6 of these had abnormal endoscopies (3 plaques, 1 ulcer, 2 grade D esophagitis).

Conclusions: Other than the presence of ulceration, no histologic feature, including the presence of pseudohyphae, significantly correlated with endoscopic lesions, clinical symptoms, or response to antifungal therapy. Our data indicate that esophageal *Candida* infections have variable histologic appearances that do not correlate well with clinical or endoscopic findings. This study also suggests that detection of *Candida* in esophageal biopsy samples is very rarely a clinically insignificant finding, even when only budding yeast are identified.

648 Clinical and Pathologic Features of EBV-Positive Gastric and Gastroesophageal Carcinomas

Erika Hissong¹, Clifton Fulmer², Rhonda Yantiss³

¹New York-Presbyterian/Weill Cornell Medical Center, New York, NY, ²Weill Cornell Medicine, New York, NY, ³Weill Cornell Medical College, New York, NY

Disclosures: Erika Hissong: None; Clifton Fulmer: None; Rhonda Yantiss: None

Background: Published data suggest that 10-15% of gastric cancers are EBV-related. Although most fall in the category of gastric carcinoma with lymphoid stroma, a substantial number reportedly display conventional (i.e intestinal-type) morphology. Given that EBV-positive tumors often express PD-L1, one may consider screening all gastric carcinomas for EBV-encoded RNAs (EBER), particularly in an era of checkpoint inhibitor therapy. We performed this study to determine the prevalence of EBV-positivity in gastric carcinomas at our institution and identify morphologic features that may aid their detection. We also assessed extent and distribution of PD-L1 immunostaining in these tumors compared with a cohort of EBV-negative tumors.

Design: We retrospectively identified gastric and gastroesophageal resection specimens from 2009-2018, including all carcinomas with lymphoid stroma. Diffuse-type carcinomas were excluded due to the infrequent occurrence of EBV-positivity in this tumor subtype. We subjected 150 cases to EBER *in situ* hybridization. Positive cases were evaluated for clinicopathologic features and subjected to PD-L1 immunohistochemistry using standard techniques. A combined positivity score (CPS) was calculated for each case and results compared with EBV-negative controls.

Results: There were no statistical differences between the clinical features of patients with EBV-positive and EBV-negative tumors (Table 1). Six (4%) tumors were EBV-positive, all of which showed variable amounts of solid tumor growth, as well as prominent lymphoid stroma at the advancing tumor edge and numerous tumor infiltrating lymphocytes. Areas of glandular differentiation were seen in 4 (66%) cases; they also displayed numerous tumor infiltrating lymphocytes (Figure 1). All 6 cases showed strong PD-L1 staining of tumoral and inflammatory cells (mean CPS: 56, range: 40-70), which was significantly higher than controls (mean CPS: 14, range: 0-40, $p < 0.01$) and often striking (Figure 2).

Clinicopathologic features of EBV-positive gastric carcinomas compared with EBV-negative controls			
	EBV-positive (N=6)	EBV-negative (N=144)	P value
Sex Ratio (male/female)	1/1	103/41	0.26
Age (mean, years)	73	67	0.41
Tumor location			0.26
Proximal	3 (50%)	103 (72%)	
Distal	3 (50%)	41 (28%)	

Figure 1 - 648

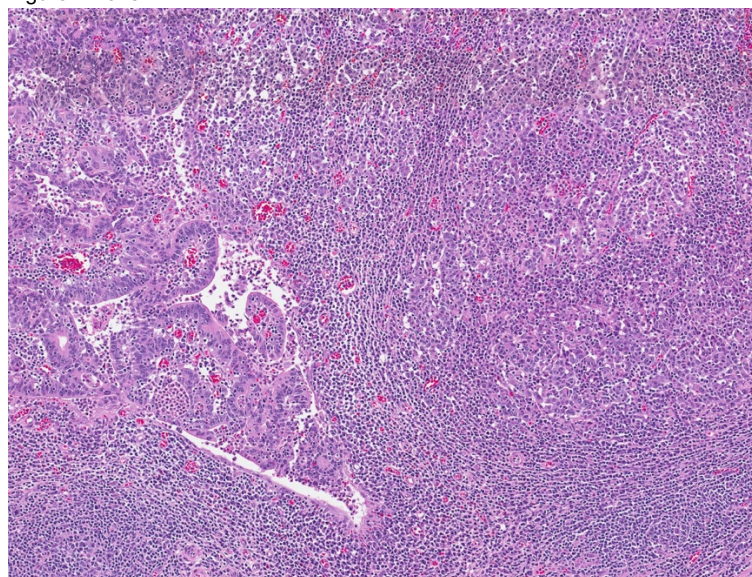
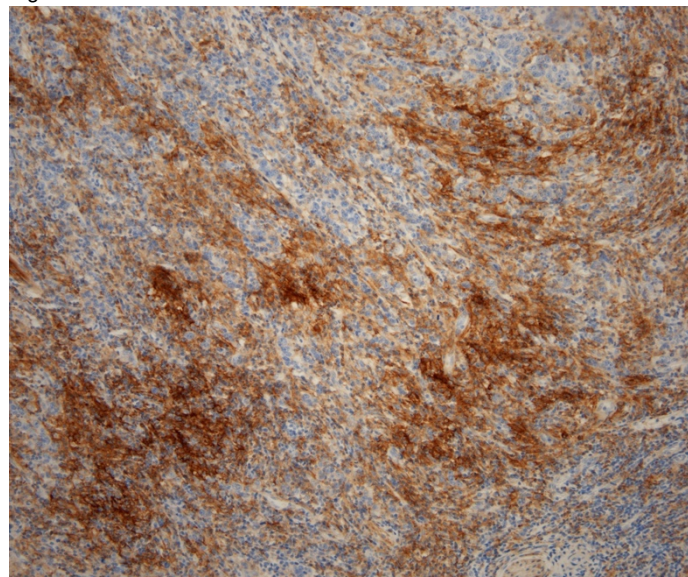


Figure 2 - 648



Conclusions: We found the prevalence of EBV-positivity among gastric and gastroesophageal carcinomas to be much lower than previously reported. Although glandular differentiation is common in these lesions, other features are sufficiently characteristic to allow their recognition and, thus, up-front evaluation of all gastric and gastroesophageal carcinomas for EBV is unnecessary. EBV-positive carcinomas show high levels of PD-L1 staining and may represent another cancer subgroup susceptible to immune checkpoint inhibitor therapy.

649 Post-Inflammatory Mucosal Hyperplasia and Appendiceal Diverticula Simulate Features of Low-Grade Appendiceal Mucinous Neoplasms

Erika Hissong¹, Wei Song², Rhonda Yantiss³

¹New York-Presbyterian/Weill Cornell Medical Center, New York, NY, ²Weill Cornell Medical College, Short Hills, NJ, ³Weill Cornell Medical College, New York, NY

Disclosures: Erika Hissong: None; Wei Song: None; Rhonda Yantiss: None

Background: One of the most problematic issues in appendiceal pathology is distinguishing between low-grade appendiceal mucinous neoplasms (LAMN) and non-neoplastic mimics, namely post-inflammatory mucosal hyperplasia of the “interval appendix” and diverticulosis with hyperplasia and abundant mucin. This distinction is particularly important since there is a movement to eliminate “mucinous adenoma” as a diagnostic category and consider all mucinous neoplasms to be potentially malignant. The purpose of this study is to identify any clinical, pathologic, or molecular features that distinguish LAMN from non-neoplastic mimics.

Design: We retrospectively identified all hypermucinous appendiceal lesions from 2006-2018. Those confined to the appendix and mesoappendix were categorized as non-neoplastic (i.e. mucosal hyperplasia/diverticula) or LAMN and evaluated for appendiceal diameter; atrophy of lymphoid tissue; preserved lamina propria; non-neoplastic crypts containing goblet cells, Paneth cells, and/or endocrine cells; fibrous obliteration of non-lesional appendix; fibrosis of the lamina propria, muscularis mucosae, or submucosa; and mural mucin. Eleven non-neoplastic lesions were subjected to *KRAS* mutational testing. Follow-up data were obtained from the electronic medical record.

Results: 90 cases were identified, including 54 non-neoplastic lesions and 36 LAMN, and their features are summarized in Table 1. Compared with LAMN, non-neoplastic lesions were smaller ($p < 0.05$) and more often presented with appendicitis ($p < 0.05$), and contained non-neoplastic crypts ($p < 0.05$) supported by lamina propria. LAMN showed striking loss of lamina propria ($p < 0.05$) and less conspicuous lymphoid tissue ($p < 0.05$). Sequencing revealed *KRAS* codon 12 mutations in 4 (36%) non-neoplastic lesions (Figures 1 and 2) with variant allele frequencies ranging from 5-22%. None of the patients in either group developed pseudomyxoma peritonei.

Clinicopathologic features of non-neoplastic appendiceal lesions and LAMNs			
	Non-neoplastic (N=54)	LAMN (N=36)	p value
Male/female ratio	11/16	1/2	0.45
Age	53 years	59 years	0.12
Presenting symptoms			
Appendicitis	37	3	$p < 0.05$
Mass on imaging	13	32	$p < 0.05$
Incidental	4	1	$p = 0.64$
Pathologic features			
Appendiceal diameter (mean)	1.2 cm	2.4 cm	$p < 0.05$
Markedly reduced/absent lamina propria	0	36	$p < 0.05$
Submucosal fibrosis	36	32	$p = 0.20$
Non-neoplastic crypts	37	0	$p < 0.05$
Acellular mucin within wall	26	25	$p = 0.06$
Lymphoid tissue	34	3	$p < 0.05$
Fibrous obliteration of nonlesional appendix	16	9	$p = 0.63$

Figure 1 - 649

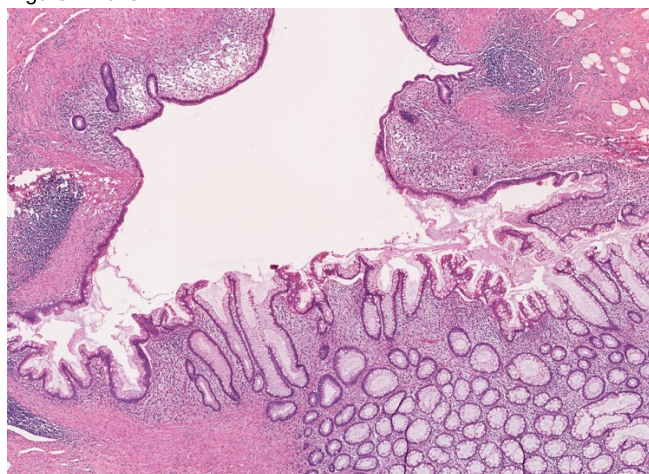
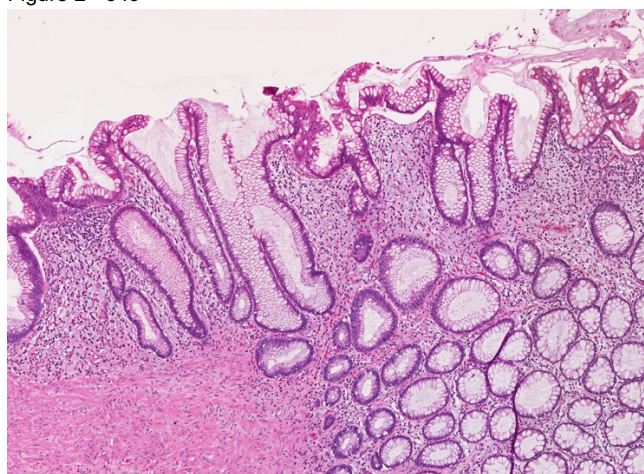


Figure 2 - 649



Conclusions: LAMN consistently show reduced or absent lamina propria and lack normal crypts compared with non-neoplastic lesions that feature hyperplastic mucinous epithelium. Submucosal fibrosis and mural mucin pools do not distinguish between LAMN and non-neoplastic mimics. Importantly, *KRAS* mutations are frequent (36%) in mucosal hyperplasia and appendiceal diverticula; their detection does not necessarily imply biologic risk or the presence of a neoplasm.

650 SATB2 Expression by Immunohistochemistry is a Marker of Neuroendocrine Neoplasms of Hindgut Origin

Deepthi Hoskoppal¹, Jonathan Epstein², Allen Gown³, Chanjuan Shi⁴, Giovanna A Giannico⁵

¹Memphis Pathology Group, Memphis, TN, ²Johns Hopkins Medical Institutions, Baltimore, MD, ³PhenoPath Laboratories, PLLC, Seattle, WA, ⁴Nashville, TN, ⁵Vanderbilt University Medical Center, Nashville, TN

Disclosures: Deepthi Hoskoppal: None; Jonathan Epstein: None; Allen Gown: None; Chanjuan Shi: None; Giovanna A Giannico: None

Background: Neuroendocrine neoplasms (NN)s range from well differentiated tumors to poorly differentiated carcinomas, and have a wide range of biologic behavior from relatively indolent to malignant with potential to metastasize. Determining the site of origin in a metastatic NN has important therapeutic and prognostic implications. SATB2 is a transcriptional regulator involved in osteoblastic and neuronal differentiation, and has been shown to be a highly sensitive and specific marker of normal colorectal epithelium and colorectal adenocarcinoma. The primary aim of this study was to evaluate the expression of SATB2 in NNs from various primary sites, and the utility of this marker in determining the site of origin of these neoplasms.

Design: A total of 180 NNs, including lung small cell carcinomas (N=40), and carcinoids (N=29), urinary bladder (N=21) and prostate (N=31) small cell carcinomas and GIT well differentiated neuroendocrine tumors (WDNET)s (stomach, N=11, small bowel, N=4, rectum, N=14, and pancreas, N=30) were selected. SATB2 immunohistochemistry was performed on whole-slides in all cases except 13 bladder small cell carcinomas, 31 prostate small cell and 15 lung small cell carcinomas, for which a tissue microarray containing 1-mm cores in triplicate was used.

Results: All rectal WDNETs (14/14) (100%) but none of the other GIT tumors (stomach, 0/11; small bowel, 0/4; pancreas, 0/30) showed SATB2 expression. Among rectal WDNETs, 13/14 cases had moderate to strong nuclear staining. In the genitourinary tract, SATB2 was expressed in 10/31 (32%) small cell carcinomas of the prostate, and 8/21 (38%) small cell carcinomas of the urinary bladder. In the lung, 8/40 (20%) small cell carcinomas and 1/29 (3.4%) carcinoid tumors were positive for SATB2. When comparing NETs of GIT and pancreatic origin, SATB2 had high sensitivity, ranging from 100% to 93% at intensity cutoffs of 0.5-2.5, and 100% specificity at all cutoffs in identifying primary rectal origin [area under the curve (AUC) 1.00±0.0, P<0.0001]. SATB2 had similar sensitivity but lesser specificity (81-88% at intensity cutoffs 1.5->2.5) when comparing rectal origin to all primary site analyzed, GIT and non-GIT (AUC 0.9391±0.01974, P<0.0001).

Conclusions: SATB2 is a sensitive and specific marker for rectal origin in the differential diagnosis of GIT NNs. However, due to limited expression in NNs from bladder, prostate and lung, sensitivity and specificity decrease when these sites of origin are considered in the differential diagnosis.

651 Markedly Thickened Muscularis Mucosae and Submucosa in the Gastric Cardia

Qin Huang¹, Lingchuan Guo², Jiong Shi³, Yuqing Cheng⁴, YH Wang⁵, Mingzhan Du⁶, Xiangshan Fan³, XL Zhou⁴, YiFen Zhang⁵, Xiaoping Zou³, Tianyun Liu³

¹VA Boston/Harvard Medical School, West Roxbury, MA, ²Suzhou, China, ³Nanjing Drum Tower Hospital, Nanjing, China, ⁴Changzhou Second Hospital, Changzhou, China, ⁵Jiangsu Provincial Hospital of Traditional Chinese Medicine, Nanjing, China, ⁶Soochow University First Hospital, Suzhou, China

Disclosures: Qin Huang: None; Yuqing Cheng: None; YH Wang: None; Mingzhan Du: None; YiFen Zhang: None

Background: The gastric cardia is a narrow region below the gastroesophageal junction (GEJ). Carcinoma arising in this region is common in the Chinese population with unknown mechanisms. Our recent multicenter study demonstrated a significantly lower risk for lymph node metastasis in 495 early gastric cardiac carcinomas (EGCC), compared to its distal counterparts (Mod Pathol. 2018 May 25. doi: 10.1038/s41379-018-0063-1.). We hypothesized that histomorphology of muscularis mucosae (MM) and submucosa in the gastric cardia might be different from that of the adjacent oxyntic or distal esophageal mucosa, especially in EGCC patients.

Design: The study was conducted in 110 consecutive radical resection cases with at least one slide showing an intact gastric cardiac wall for evaluation of histopathology of MM and submucosa in two groups of patients: the study group with 60 resection cases for EGCC and the control group with 50 cases of distal esophagectomy with proximal gastrectomy for esophageal squamous cell carcinoma. The GEJ line was defined as the distal end of squamous epithelium, multi-layered epithelium, or deep esophageal glands/ducts. The gastric cardia was defined as the presence of cardiac and cardio-oxyntic mucosae below the GEJ line. The oxyntic mucosa was defined as the presence of only oxyntic glands distal to the cardiac mucosa. The distal esophageal mucosa within 1 cm above the GEJ was also analyzed. The MM thickness was measured microscopically between the uppermost and the lowermost horizontal smooth muscle fibers of MM. The depth of submucosa was measured from the lowest MM fiber to the surface of muscularis propria. The following changes were also assessed: the growth pattern of MM (thickened, frayed, and double-layered), the presence of entrapped glands, lymphoid follicles, and microcysts, as well as submucosal changes such as fibrosis, fatty changes (defined as over 33% of the submucosal space filled with fat), and abnormal artery (defined as separation of the external smooth muscle layer of an artery). On the same slide, the changes in MM and submucosa of the adjacent oxyntic mucosa (N=36) and the distal esophageal mucosa (N=92) were compared statistically. A p value of < 0.05 was considered as statistically significant.

Results: Overall, there was no significant difference in demographic data and the frequency of H. pylori infection between groups. The average thickness of MM and submucosa was 1.04 mm and 1.4 mm in cardiac mucosa, respectively, significantly thicker than in oxyntic mucosa (0.22 mm and 0.99 mm) or distal esophageal mucosa (0.6 mm and 1.15 mm) ($p < 0.0000$, $p < 0.05$), respectively. In the gastric cardia, the thickened MM displayed primarily frayed smooth muscle fibers (81.8%) and the double-layer change was observed in 1 case; in addition, MM demonstrated a significantly higher prevalence of entrapped glands, microcysts, and lymphoid follicles than the oxyntic or distal esophageal mucosa ($p < 0.0000$). In the submucosa, the presence of fatty changes ($p < 0.0000$), abnormal artery ($p < 0.0000$), and microcysts ($p < 0.0001$) was also significantly more common in the cardiac mucosa than in the oxyntic or esophageal mucosa. Compared to the control group, the EGCC group showed significantly thicker MM (average: 1.31 mm, vs. 0.72mm in controls, $p < 0.0000$) and submucosa (average: 1.61 mm, vs. 1.16mm, $p < 0.0000$), more frequent presence of the frayed growth pattern of MM (93.3%, vs. 60.0%, $p < 0.05$) or microcysts (26.7%, vs. 4%, $p < 0.01$).

Conclusions: The results displayed significantly thickened MM and submucosa in the gastric cardia, especially in patients with EGCC, which may have both physiologic and pathologic implications for protecting the distal esophagus against gastric juice reflux and for dampening the infiltration of intramucosal carcinoma into deeper layers of the gastric cardiac wall and perigastric lymph nodes.

652 Autoimmune Metaplastic Atrophic Gastritis (AMAG): Assessment of Correlation with Serology and Adequacy of Clinical Follow-Up

Sarah Imam¹, Mary Wong², Deepti Dhall³, Kevin Waters³

¹Cedars-Sinai Medical Center, North Hollywood, CA, ²Arcadia, CA, ³Cedars-Sinai Medical Center, Los Angeles, CA

Disclosures: Sarah Imam: None; Mary Wong: None; Deepti Dhall: None; Kevin Waters: None

Background: AMAG is a chronic inflammatory disease affecting predominantly older females which results in the immune-mediated destruction of gastric parietal cells. Serology and clinical follow up are recommended with a diagnosis of AMAG as pernicious anemia is a late manifestation and studies have shown that AMAG confers a greater risk for gastric malignancy. We evaluated the clinical and serologic follow up of the diagnosis of AMAG due to the clinically important consequences of the disease.

Design: 226 cases were identified with a diagnosis of AMAG in the surgical pathology archives between 2006 and 2018. Of these, 122 had adequate clinical records to assess follow-up. Clinical and medication history, prior and current biopsy results, and serologic findings were recorded and tabulated for each case.

Results: Of the 122 cases evaluated, the median age was 69 and 70% were female. 61% were Caucasian 23% Hispanic, 11% African American, and 5% Asian. 13 (11%) had a history of *Helicobacter pylori* infection. 14 (11%) had a concurrent type-1 gastric neuroendocrine tumor. 14% had prior upper gastrointestinal (GI) biopsies without sampling of the gastric body in the last 10 years. Serology was performed on 44 (36%) patients, (14 anti-parietal cell antibody (PCA), 10 anti-intrinsic factor antibody (IFA), 20 both). 54% of PCA and 38% of IFA tests were positive. Overall, 64% of patients tested had at least one positive serology. 61% (n=75) of the patients had a history of anemia. Of these patients, 80% received iron supplementation, but only 53% (40/75) received vitamin B12. In patients with both anemia and a positive serology, 82% received B12 therapy.

Conclusions: AMAG is a relatively common and under recognized disease with important clinical morbidities. Our finding that it was not uncommon (14%) for patients with AMAG to have recent upper GI biopsies without sampling of the gastric body, perhaps delaying diagnosis, emphasizes the importance of sampling the gastric body, especially in older women. Serologic testing was not entirely sensitive for AMAG pattern on biopsy as 64% of cases tested had positive serology. Our finding that many (47%) anemic patients with AMAG did not receive vitamin B12 suggests the need for increased clinical awareness of this association. This raises the question of whether the association with pernicious anemia should be explicitly stated in pathology reports to ensure clinical awareness and proper follow-up.

653 Expression of CD47 in Gastroenteropancreatic Neuroendocrine Tumor is Related to Lymph Node Metastasis, a Potential Indicator for Poor Prognosis

Rami Imam¹, Margaret Black², Ruliang Xu³, Wenqing Cao⁴

¹New York University, New York, NY, ²NYU, Long Island City, NY, ³New York University Medical Center, New York, NY, ⁴New York University Langone Medical Center, New York, NY

Disclosures: Rami Imam: None; Margaret Black: None; Ruliang Xu: None; Wenqing Cao: None

Background: Gastroenteropancreatic neuroendocrine tumors (GEP-NETs) are relatively rare tumors that arise from the diffuse neuroendocrine system. In the past four decades, the incidence of GEP-NETs has increased steadily in the United States. Although many therapeutic options are available, prediction of prognosis in GEP-NETs is still difficult. CD47 is a transmembrane glycoprotein that is ubiquitously expressed in normal tissues and mediates a "self/don't-eat-me" signal on normal cells by inhibiting macrophage phagocytosis. The enhanced expression of CD47 has been reported in various malignancies and is associated with poor prognosis of a variety of cancers. Currently, there is lack of studies on the role of CD47 expression in GEP-NETs progression and prognosis. Here, we investigate the expression patterns of CD47 in small intestinal NETs (SI-NETs) and pancreatic NETs (PNETs), and evaluate its role in lymph node metastasis.

Design: 80 well differentiated GEP-NETs (33 SI-NETs and 47 PNETs) resection specimens were selected and analyzed using CD47 immunohistochemistry. H-score method was used to evaluate both staining intensity (0-3) and percentage of positive cells. One-way analysis of variance or Student's t-test was utilized to correlate mean H-score with various clinical parameters.

Results: Diffuse membranous and cytoplasmic CD47 staining was seen in all GEP-NETs. Compared to the adjacent non tumorous tissue, CD47 was overexpressed in both SI-NETs and PNETs. The expression of CD47 in SI-NETs was significantly higher than that in PNETs (205.0±10.7 versus 148.8±7.9, P=0.001). In the cases with lymph metastasis, a relatively lower CD47 expressions in SI-NETs as well as in PNETs were seen, compared to the cases without lymph node metastasis (191.5±12.1 versus 241.1±18.5, P=0.036 in SI-NET; 160.5±9.9 versus 128.2±9.0, P=0.034 in PNETs). Overexpression of CD47 inversely associated with lymph node metastasis in both SI-NETs and PNETs.

Conclusions: This is the first study to investigate CD47 expression in pNETs and correlate the expression of CD47 with clinicopathologic characteristics including currently used prognostic factors. Data suggested that CD47 was overexpressed in all pNETs. CD47 expression significantly correlated with lymph node metastasis, perineural invasion, lymphovascular invasion, and mitosis, suggesting it is a promising marker for predicting prognosis of pNETs.

654 Expression analysis of CD70, CD27 and FOXP3 with an evaluation of their prognostic values in colorectal cancer

Shingo Inaguma¹, Satoshi Inoue¹, Hideaki Ito¹, Takumi Tsunoda¹, Hideki Murakami¹, Kunio Kasugai¹, Kenji Kasai¹, Hiroshi Ikeda¹

¹Aichi Medical University, School of Medicine, Nagakute, Japan

Disclosures: Shingo Inaguma: None

Background: The promising anticancer effects of immune checkpoint inhibitors against CTLA4 and CD274-PDCD1 axes are evident. However, these immunotherapies for colorectal cancers (CRCs) are now limited to a small subset of patients with microsatellite instable (MSI) tumours. Thus, therapeutics targeting other types of CRCs are desired.

The CD70-CD27 axis plays a co-stimulatory role in promoting T-cell expansion and differentiation through the NF κ B pathway under physiological conditions. FOXP3, a master transcription factor of regulatory T-cells (Tregs), plays crucial roles for the differentiation, maintenance, and function of Tregs. Aberrant CD70-CD27 axis activation accelerates tumour cell proliferation, survival, and immune evasion through ERK-activation and Tregs-induction. Based on these observations, drugs modulating the CD70-CD27 axis have been developed with expectation of anticancer effects.

Design: In this study, 270 well-characterized primary colorectal cancers (CRCs) were evaluated immunohistochemically for CD70, CD27 and FOXP3 expression. A 4.5 mm single core from tumor samples was assembled to multitumor blocks. Immunohistochemistry was performed using the Ventana BenchMark XT automated immunostainer (Roche Diagnostics, Basel, Switzerland). Any CD70 immunoreactivity (luminal/membranous or cytoplasmic) was evaluated as positive in the present study. CD27+ and FOXP3+ tumour-infiltrating lymphocytes (TILs) were counted in high-power field (HPF).

Results: CRC tumour cells rarely (2.2%, 6/270) expressed CD70 (tCD70). In contrast, tumour-associated fibroblasts showed various CD70 expressions (fCD70) in 40.3% (109/270) of cases. The logistic regression analysis revealed significant association between fCD70 expression and fewer CD27+ tumour-infiltrating lymphocytes (TILs) (OR, 1.73; 95% CI, 1.02-2.95; P=0.044), younger age (OR, 1.88; 95% CI, 1.11-3.18; P=0.019), incomplete resection (OR, 2.47; 95% CI, 1.05-5.83; P=0.039), or tubular-forming histology (OR, 5.33; 95% CI, 1.71-16.6; P=0.0039). Overall survival was decreased in the cohort of the patients carrying CRC with a higher fraction of fCD70 (P=0.09). Significantly more CD27+ TILs were detected within the primary CRCs without metastases (P=0.026).

Conclusions: The CD70-CD27 axis may have several roles in CRCs independent from their mismatch repair system (MMR) status. CD70-CD27 pathway-modulating therapies may be applied to CRC patients regardless of their tumour MMR status.

655 Immune Checkpoint Inhibitor Induced Upper Gastrointestinal Tract Inflammation Shows Morphologic Similarities to, but is Immunologically Distinct from H. Pylori Gastritis and Celiac Disease

Lina Irshaid¹, Marie Robert², Xuchen Zhang³

¹Yale New Haven Hospital, New Haven, CT, ²Yale University School of Medicine, New Haven, CT, ³Yale University School of Medicine, Orange, CT

Disclosures: Lina Irshaid: None; Marie Robert: None; Xuchen Zhang: None

Background: Immune checkpoint inhibitor (CPI) therapies are increasingly being utilized in the treatment of malignancies, with the unfortunate side effect of multi-organ immune-related adverse events. Morphologic changes due to CPI therapy in the upper gastrointestinal tract have not been well characterized. We analyzed the morphologic and immunophenotypic effects of CPI therapy on gastric and duodenal mucosa with comparisons to H. pylori gastritis (HPG) and Celiac disease (CD).

Design: The morphology and immune cell content of gastric and duodenal biopsies in patients treated with anti-CTLA-4 or anti-PD1/PD-L1 antibodies were compared with that of HPG (n=8), CD (n=6) and normal gastric (n=6)/duodenal (n=8) biopsies. H&E slides were scored blindly by 2 pathologists for degree of lamina propria (LP) inflammation, lymphoid aggregates (LA), activity, apoptosis, intraepithelial lymphocytes (IELs) and villous blunting (duodenum). B- and T-cell subsets were counted in 2 hotspots (LP and IEL) using CD4, CD8 and CD20 immunostains.

Results: Malignancies treated by CPIs included metastatic melanoma, breast, renal cell, urothelial and non-small cell lung carcinomas. Compared to anti-CTLA-4 (n=8), patients on anti-PD1/PD-L1 therapy (n=7) received more doses over a longer period of time before upper GI biopsies were obtained. Gastric biopsies in patients on CPIs all showed active chronic gastritis mimicking HPG (Fig 1A-B). However compared to HPG, CPI gastritis showed higher IELs, less LP inflammation and fewer LA. Immunophenotypically, CPI gastritis showed fewer LP CD20 B cells and a reduced LP CD4/8 ratio. There were no differences between anti-CTLA-4 and anti-PD1/PD-L1 therapy in gastric biopsies. Duodenal biopsies in patients on CPIs (n=8 anti-CTLA-4 and n=3 anti-PD1/PD-L1) all showed sprue-like active chronic duodenitis with villous blunting mimicking CD (Fig 1C-D). Compared to CD, neutrophilic infiltrates with ulceration were more likely in CPI cases. Immunophenotypically, CPI duodenitis showed reduced CD4/8 ratio compared to CD. There were no differences between anti-CTLA-4 and anti-PD1/PD-L1 therapy, except less IELs in anti-PD1/PD-L1 group (Fig 2).

Figure 1 - 655

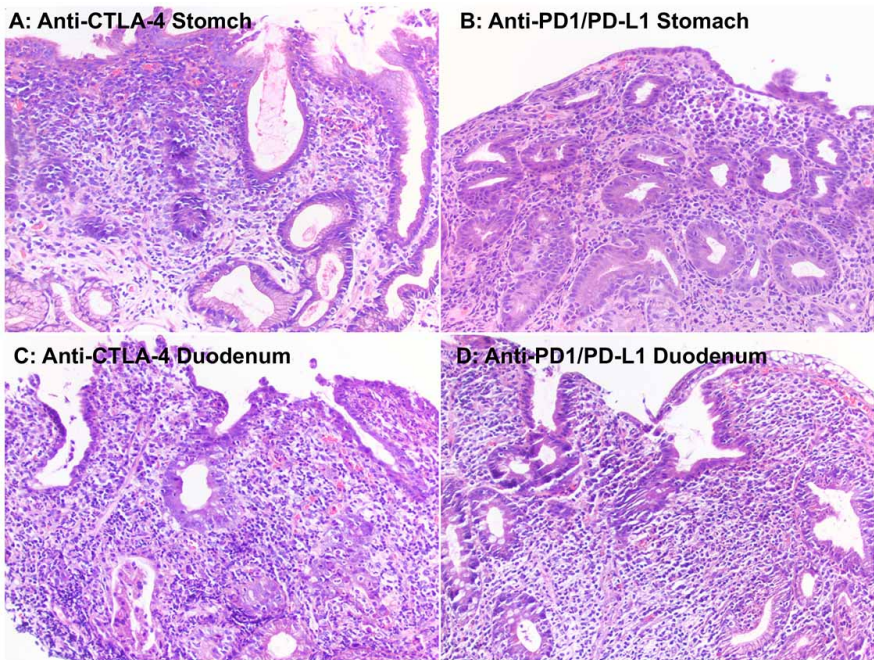


Figure 2 - 655

Stomach								
	Morphology					CD4:CD8	CD20	
	LP inflammation (0-3)	IELs/100 enterocytes	Activity (%)	Apoptosis (0-2)	Lymphoid aggregate (%)	LP	LP	
HPG vs. Control	2.86 ± 0.14 vs 0 ± 0*	7.43 ± 1.04 vs. 3.67 ± 0.80**	100% vs. 0%*	1.43 ± 0.20 vs. 0.50 ± 0.22**	85.7% vs. 0%*	2.21 ± 0.35 vs. 2.19 ± 0.27	37.14 ± 3.92 vs. 3.5 ± 0.89**	
CPI vs. Control	1.73 ± 0.15 vs. 0 ± 0*	22.87 ± 1.88 vs. 3.67 ± 0.80*	86.7% vs. 0%*	1.33 ± 0.13 vs. 0.50 ± 0.22*	13.3% vs. 0%	1.32 ± 0.18 vs. 2.19 ± 0.27*	14.4 ± 2.88 vs. 3.5 ± 0.89*	
CPI vs. HPG	1.73 ± 0.15 vs. 2.86 ± 0.14 *	22.87 ± 1.88 vs. 7.43 ± 1.04*	86.7% ± 100%	1.33 ± 0.13 vs. 1.43 ± 0.20	13.3% vs.85.7%*	1.32 ± 0.18 vs. 2.21 ± 0.35*	14.4 ± 2.88 vs. 37.14 ± 3.92**	
Anti-CTLA-4 vs. anti-PD(L)-1	1.75 ± 0.16 vs. 1.71 ± 0.29	23.75 ± 3.25 vs. 21.86 ± 1.83	88.9% vs. 85.7%	1.38 ± 0.18 vs. 1.29 ± 0.18	0% vs. 28.6%	1.03 ± 0.15 vs. 1.66 ± 0.31	14.13 ± 3.13 vs. 14.71 ± 5.34	
Duodenum								
	Morphology					CD4:CD8	CD20	
	LP inflammation (0-3)	IELs/100 enterocytes	Activity (%)	Apoptosis (0-2)	Lymphoid aggregate (%)	Villous blunting (0-3)	LP	LP
CD vs. Control	2.83 ± 0.17 vs. 0 ± 0*	48.83 ± 6.41 vs. 22.89 ± 2.91*	16.7% vs. 0%	1.5 ± 0.22 vs. 0.44 ± 0.18**	50% vs. 0% **	2.67 ± 0.21 vs. 0 ± 0**	2.24 ± 0.39 vs. 2.96 ± 0.21	16.33 ± 1.71 vs. 9.67 ± 1.76*
CPI vs. Control	2.60 ± 0.27 vs. 0 ± 0*	32.67 ± 3.55 vs. 22.89 ± 2.91**	100% vs. 0%*	1.5 ± 0.17 vs. 0.44 ± 0.18**	20% vs. 0%*	2.3 ± 0.26 vs. 0 ± 0**	0.97±0.09 vs. 2.96 ± 0.21*	19.7 ± 3.28 vs. 9.67 ± 1.76*
CPI vs. CD	2.60 ± 0.27 vs. 2.83 ± 0.17	32.67 ± 3.55 vs. 48.83 ± 6.41**	100% vs. 16.7%*	1.5 ± 0.17 vs. 1.5 ± 0.22	20% vs. 50%	2.3 ± 0.26 vs. 2.67 ± 0.21	0.97±0.09 vs. 2.24 ± 0.39*	19.7 ± 3.28 vs. 16.33 ± 1.71
Anti-CTLA-4 vs. anti-PD(L)-1	2.43 ± 0.37 vs. 3 ± 0	32.67 ± 3.55 vs. 25.67 ± 0.88**	100% vs. 100%	1.43 ± 0.20 vs. 1.67 ± 0.33	14.3% vs. 33.3%	2.29 ± 0.29 vs. 2.33 ± 0.67	1.12 ± 0.10 vs. 1.48 ± 0.06	21.71 ± 4.35 vs. 15.0 ± 3.61

Table 1 – Morphologic and immunophenotypic characterization of CPI effect on the stomach and duodenum, with comparison to HPG and CD.

Conclusions: Increased CD8 lymphocyte infiltration with reduced CD4/CD8 ratio is present in CPI gastroduodenitis compared to HPG and CD, consistent with drug mechanisms. The morphologic distinctions noted between these entities may provide useful discriminators when confronted with gastric and duodenal inflammatory changes in patients undergoing CPI therapy.

656 Loss of SATB2 expression in a subset of IBD-associated dysplasias

Mai Iwaya¹, Robert Riddell², James Conner³
¹Shinshu University Hospital, Matsumoto, Nagano, Japan, ²Mt. Sinai Hospital, Toronto, ON, ³Mount Sinai Hospital, Toronto, ON

Disclosures: Mai Iwaya: None; Robert Riddell: None; James Conner: None

Background: SATB2 is expressed in colonic epithelium and has diagnostic utility as a relatively specific marker for colorectal cancer (CRC). Colitis associated colorectal adenocarcinomas are frequently associated with loss of SATB2 expression (Iwaya et. al 2018). However, SATB2 status in IBD associated dysplasia (ID), and by extension its potential value as a diagnostic marker in this often challenging diagnosis, has not been investigated. We examined the expression of SATB2, as well as p53, a marker used in some settings to support a diagnosis of dysplasia, in a series of ID cases.

Design: 39 ID from 32 resections between 2011 and 2018 were examined. 22 resections had synchronous CAC and 10 were performed for dysplasia only. Immunohistochemistry for SATB2 was scored semi-quantitatively in areas of dysplasia and non-dysplastic control mucosa as follows: extent – 0%; 1–5%; 5–25%; 26–50%; 51–75%; 76–100% and intensity – negative; weak; moderate; strong. For binary analyses, cases with 5% or more cells showing moderate or strong intensity were considered positive. Expression of p53 was classified as wild type (variable weak to moderate staining) or mutant (either diffuse strong staining or complete absence of staining). Dysplasia morphology was classified using a modified version of the scheme proposed by Harpaz et al (2017): conventional, serrated, hypermucinous, goblet cell deficient and terminally differentiated.

Results: SATB2 was negative in 12 of 39 (31%) IDs. Staining was retained in all control areas of non-dysplastic colitic mucosa ($p=0.0002$). There was a nonsignificant association between SATB2 expression and dysplasia morphology: expression was retained in 11 of 12 (92%) conventional-type dysplasias, compared to 16 of 27 (59%) in all other subtypes ($p=0.063$). Sixteen of 23 (41%) IDs had a p53 mutant pattern of staining and there was no association between p53 and SATB2 status.

Conclusions: Although the sensitivity is low (31%), loss of SATB2 expression has a high positive predictive value (100%) for discriminating IBD associated dysplasia from background non-dysplastic colitic mucosa. SATB2 loss is more common in unconventional (serrated, hypermucinous, goblet cell deficient, terminally differentiated) morphologic subtypes of dysplasia, some of which can be challenging to distinguish from background reactive changes. If this effect is confirmed in larger cohort analyses, loss of SATB2 expression could be a useful, and sorely needed, adjunctive marker to support a diagnosis of ID.

657 Most colitis associated carcinomas lack expression of Lgr5: implications for unique pathways of carcinogenesis compared to sporadic colorectal carcinoma

Mai Iwaya¹, Hiroyoshi Ota², Tomoyuki Nakajima³, Robert Riddell⁴, James Conner⁵

¹Shinshu University Hospital, Matsumoto, Nagano, Japan, ²Shinshu University School of Health Sciences, Matsumoto, Japan, ³Shinshu University Hospital, Matsumoto, Japan, ⁴Mt. Sinai Hospital, Toronto, ON, ⁵Mount Sinai Hospital, Toronto, ON

Disclosures: Mai Iwaya: None; Hiroyoshi Ota: None; Tomoyuki Nakajima: None; Robert Riddell: Non; James Conner: None

Background: Lgr5, a component of the Wnt receptor complex, is thought to lineage-label gastric and intestinal stem cells. Lgr5 expression is increased in colorectal carcinoma (CRC) compared to normal tissue. Colitis associated colorectal adenocarcinoma (CAC) often shows distinct morphologic and molecular phenotypes compared to sporadic cases. However, the expression profile of Lgr5, and by extension the potential role of an intestinal stem cell phenotype, has not been described in a series of colitis associated colorectal carcinoma in human.

Design: The study group consisted of 30 CACs from 29 resections between 2011 and 2016; 10 sporadic CRCs were used as controls. RNA in situ hybridization (ISH) was performed for Lgr5 expression and quantified according to the five-grade scoring system previously described (Baker et al., 2015): 0 = no staining or less than one dot per cell; 1 = 1 to 3 dots per cell; 2 = 4 to 10 dots per cell and no or very few dot clusters; 3 = >10 dots per cell and <10% positive cells overall; and 4 = >10 dots per cell and >10% positive cells with dot clusters. For a binary analysis, Lgr5 status was considered positive if the ISH score was >2 (Jang et al., 2018). CAC tumor morphology was classified as conventional, mucinous, serrated and low grade tubuloglandular subtypes.

Results: Lgr5 was positive in 30% (9/30) of CAC cases and 90% (9/10) of sporadic CRCs ($p=0.002$). Of the 9 positive CAC cases, 67% showed had a limited extent of staining, with < 10% of tumor cells positive (ie. score 3), whereas 67% of the nine positive sporadic cases were graded as score 4. A large majority (89%) Lgr5 positive CACs were of the conventional histologic type, while morphologies were much more variable in the Lgr5 negative group, where only 19% of cases were conventional ($p<0.001$). Lgr5 positive CACs were more likely to be located in the rectum ($p=0.03$). There was no significant difference in pT stage, pN stage, IBD phenotype, age, or sex between Lgr5 positive CACs and negative CACs.

Conclusions: Lgr5 expression is significantly less frequent in CAC compared to sporadic CRC and is associated with conventional morphology. These findings suggest that the wider spectrum of tumor morphology in CAC may be associated with absence of an intestinal stem cell phenotype.

658 The Morphological Spectrum of Immune-Checkpoint Inhibitor Associated Gastritis

Melanie Johncilla¹, Xuchen Zhang², Dhanpat Jain³, Amitabh Srivastava⁴

¹New York-Presbyterian Hospital/Weill Cornell Medical Center, New York, NY, ²Yale University School of Medicine, Orange, CT, ³Yale University School of Medicine, New Haven, CT, ⁴Brigham and Women's Hospital, Harvard Medical School, Boston, MA

Disclosures: Melanie Johncilla: None; Xuchen Zhang: None; Dhanpat Jain: None; Amitabh Srivastava: None

Background: Immune checkpoint inhibitors, including ipilimumab, nivolumab and pembrolizumab, are now frequently used in solid tumor chemotherapy. The mechanism of action of these drugs involve upregulation of cytotoxic T cells, which can lead to lack of self-tolerance

and immune-related adverse events. Gastrointestinal complaints are common among patients on these drugs but the histologic features of immune-checkpoint inhibitor associated gastritis have not been well characterized and was the purpose of this study.

Design: Patients who underwent endoscopic evaluation with gastric biopsy under clinical suspicion of drug-associated gastrointestinal injury while receiving immune-checkpoint inhibitor therapy were identified. Patients with an infectious etiology were excluded. The predominant histologic pattern and distribution (antral or corpus predominant or pangastritis) of injury, presence of prominent eosinophils, and apoptotic bodies was recorded. Patient presenting symptoms, treatment and follow up data was obtained by medical chart review.

Results: 11 patients (7M: 4F) with a mean age of 54 (range 33-76) years formed the study group. Immune-checkpoint inhibitor therapies administered included ipilimumab, nivolumab, pembrolizumab and Lag-3 inhibitors. Metastatic malignant melanoma (n=7) was the most common indication for treatment. Common symptoms at presentation included nausea, vomiting and diarrhea. The histopathologic features are summarized in Table 1. Six patients showed a pangastritis. The presence of chronic active gastritis with intraepithelial lymphocytosis and prominent apoptosis was the most useful combination in predicting drug-induced gastritis. Three patients had focally enhancing lesions with a lymphohistiocytic cuff around inflamed glands reminiscent of Crohn's disease, while three showed prominent eosinophils suggestive of drug induced mucosal injury. The majority of patients responded to medication withdrawal and steroids. However, one patient with focal enhancing gastritis was steroid resistant but responded to infliximab therapy.

Case	Predominant pattern of injury	Distribution	Degree of Inflammation	Intraepithelial Lymphocytes	Other Inflammatory Cells	Apoptosis
1	Chronic Active Gastritis	Antrum	Severe	Absent	Eosinophils	Absent
2	Chronic Active Gastritis	Antrum	Mild	Present	None	Absent
3	Chronic Active Gastritis	Corpus	Mild	Present	None	Present
4	Chronic Active Gastritis	Antrum and Corpus	Severe	Present	None	Present
5	Chronic Active Gastritis	Corpus	Moderate	Absent	Eosinophils	Present
6	Chronic Active Gastritis and Focal Enhancing Lesions	Antrum and Corpus	Mild	Present	None	Absent
7	Lymphocytic Gastritis	Antrum and Corpus	Moderate	Present	Eosinophils	Present
8	Chronic Active Gastritis	Antrum and Corpus	Severe	Present	None	Present
9	Focal Enhancing Gastritis	Antrum and Corpus	Focal	Absent	None	Absent
10	Focal Enhancing Gastritis	Corpus	Focal	Absent	None	Absent
11	Chronic Active Gastritis	Antrum and Corpus	Moderate	Present	None	Present

Conclusions: Immune checkpoint inhibitor therapy associated gastritis shows a variety of morphological patterns. The combination of chronic active gastritis with intraepithelial lymphocytosis and apoptosis is helpful in making this diagnosis. Some patients may show features reminiscent of gastritis seen in patients with Crohn's disease. Awareness of these features is helpful for accurate diagnosis and prompt management of these patients.

659 Unique Pathologic and Molecular Characterization of FBXW7-Mutant Colorectal Adenocarcinomas: A Large Single Institution Cohort

Ryan Jones¹, Audrey Deeken-Draisey², Katrina Krogh¹, Haonan Li³, Edernst Noncent⁴, Leyu Sun¹, Jie Liao¹, Juehua Gao², Guang-Yu Yang¹

¹Northwestern University, Chicago, IL, ²Northwestern Memorial Hospital, Chicago, IL, ³Northwestern University Feinberg School of Medicine, Chicago, IL, ⁴Chicago, IL

Disclosures:

Ryan Jones: None; Audrey Deeken-Draisey: None; Katrina Krogh: None; Haonan Li: None; Edernst Noncent: None; Leyu Sun: None; Jie Liao: None; Juehua Gao: None; Guang-Yu Yang: None

Background: The cell cycle regulatory molecule F-box/WD repeat-containing protein 7 (FBXW7) is a tumor suppressor promoting exit from the cell cycle. FBXW7 is commonly mutated in cancers and genetic profiling using next generation sequencing (NGS) indicates that FBXW7 mutation occurs in about 6-8% of colorectal adenocarcinomas (CRC). The morphologic features, location within the colon, co-occurring mutations, and prognosis of FBXW7-mutant CRC are not fully known. In this study, we comprehensively analyzed a large cohort of FBXW7 mutant CRC using NGS and immunohistochemical (IHC) approaches.

Design: Genetic alterations of 564 cases of CRC at a single institution were analyzed using next generation sequencing (NGS) approach on an Ion Torrent platform targeting 22 cancer-related gene panels including *FBXW7*, *KRAS*, *EGFR*, *BRAF*, *PIK3CA*, *AKT1*, *ERBB2*, *PTEN*, *NRAS*, *STK11*, *MAP2K1*, *ALK*, *DDR2*, *CTNNB1*, *MET*, *TP53*, *SMAD4*, *NOTCH1*, *ERBB4*, *FGFR1/2/3*. FBXW7 IHC was performed on these CRC with proper controls.

Results: FBXW7 mutations were identified in 44 CRCs (7.8%). Among these i) there were 84% missense mutations, 14% nonsense mutations, and 2% frameshift; and ii) frequently mutated codons were 465 (13), 505 (10), 479 (5), and 582 (5). The most frequent co-mutations were p53 (52%), KRAS (52%), PIK3CA (18%), and SMAD4 (18%). Pathologic features were: i) tumor location was 34% right colon, 36% left colon, 27% rectum, and 2% small bowel; ii) tumor stage was 19 stage 0-II, 20 stage III-IV, and 5 unresectable; iii) 6 were microsatellite instable, 17 mucinous, 5 micropapillary, and 3 signet ring cell carcinoma; and iv) most cases showed absent or mild peri- and intra-tumoral lymphoid responses. FBXW7 IHC expression patterns were i) mostly nuclear staining in tumor cells, ii) occasionally with a subtle perinuclear dot-like pattern, ii) 5 cases showed absent staining, 2 of which have stop codons and 1 frameshift, and iii) staining intensity was faint to moderate.

Conclusions: Our data indicate that 1) FBXW7 mutation is common in CRC, particularly its missense mutation is a dominant pattern that leads to mutant FBXW7 nuclear expression, 2) FBXW7 mutation combined with other key gene mutations, particularly KRAS and p53, lead to CRC carcinogenesis, 3) FBXW7 mutant CRCs display aggressive pathologic histologic types, including mucinous/micropapillary/signet ring cells with less peri- and intra-tumoral lymphoid responses. This study is an important first step towards characterizing FBXW7 mutant CRCs.

660 PD-L1, LAG-3, and GAL-3 Expression in Anal Squamous Cell Carcinoma

Jennifer Ju¹, Anne Mills², Edward Stelow¹

¹University of Virginia Health System, Charlottesville, VA, ²University of Virginia, Charlottesville, VA

Disclosures: Jennifer Ju: None; Anne Mills: None; Edward Stelow: None

Background: High-risk human papillomavirus (HR-HPV) is associated with approximately 68-88% of anal squamous cell carcinomas (ASCC), creating a strong immune response in many of these tumors. Many cancers evade host immune response through upregulation of normal T-cell inhibitory checkpoint proteins. Novel immunotherapies targeting these pathways have been emerging, particularly those targeting programmed cell death-1 (PD-1) and its ligand (PD-L1). However, only a subset of ASCC patients with PD-L1 positive tumors on immunohistochemistry (IHC) experience clinical benefit to corresponding monoclonal antibodies. Lymphocyte-activation gene-3 (LAG-3) can act synergistically with PD-1/PD-L1, and patients may benefit from dual therapy. Furthermore LAG-3 interacts with galectin-3 (GAL-3) to suppress CD8 T-cells. Subsequently, we compare IHC staining patterns of these different proteins to evaluate the possible role of dual target immunotherapy.

Design: A tissue microarray was created with 48 cases of ASCC. HPV status was determined using in situ hybridization (ISH) (RNAscope technique by Advanced Cell Diagnostics) and p16 IHC (CINtec by Ventana). The cases were then stained for PD-L1 (Spring Biosciences), LAG-3 (Abcam), and GAL-3 (Cell Marque). PD-L1 (membranous) and LAG-3 (cytoplasmic and/or membranous) were scored on tumor infiltrating lymphocytes (TIL), and GAL-3 (cytoplasmic) was scored on tumor cells. PD-L1 was considered positive with at least mild staining, LAG-3 was considered positive with at least one stained TIL per high-power field, and GAL-3 with at least 1% of tumor cells staining.

Results: Thirty-eight (79%) cases of ASCC were HR-HPV-associated, 5 (10%) low risk (LR)-HPV-associated, and 5 (10%) HPV-negative. Of the HR-HPV cases, 28 (74%) were positive for PD-L1 and 31 (82%) were positive for LAG-3 within the TIL. Of the LR-HPV cases, 2

(40%) were positive for PD-L1 and 3 (60%) were positive for LAG-3. Of the HPV-negative cases, 2 (40%) were positive for PD-L1 and 2 (40%) were positive for LAG-3. Twenty-seven (71%) HR-HPV, 0 (0%) LR-HPV, and 2 (40%) HPV-negative cases were GAL-3 positive. (See Table).

Tumor infiltrating lymphocyte staining for PD-L1 and LAG-3				
	PD-L1 Positive		PD-L1 Negative	
	LAG-3 Positive	LAG-3 Negative	LAG-3 Positive	LAG-3 Negative
HR-HPV	66% (25/38)	8% (3/38)	16% (6/38)	11% (4/38)
LR-HPV	0% (0/5)	40% (2/5)	60% (3/5)	0% (0/5)
HPV-Negative	20% (1/5)	20% (1/5)	20% (1/5)	40% (2/5)
GAL-3 tumor cell and LAG-3 tumor infiltrating lymphocyte staining pattern				
	GAL-3 Positive		GAL-3 Negative	
	LAG-3 Positive	LAG-3 Negative	LAG-3 Positive	LAG-3 Negative
HR-HPV	63% (24/38)	8% (3/38)	18% (7/38)	11% (4/38)
LR-HPV	0% (0/5)	0% (0/5)	60% (3/5)	40% (2/5)
HPV-Negative	20% (1/5)	20% (1/5)	20% (1/5)	40% (2/5)

Conclusions: Dual staining patterns of PD-L1 and LAG-3 within TIL is common, particularly in HR-HPV ASCC. Concomitant GAL-3 tumor expression and LAG-3 TIL expression is also frequent, especially in HR-HPV ASCC. Subsequently, multidrug immunotherapy techniques may be of benefit.

661 PD-L1, LAG-3, and GAL-3 Expression in Mismatch Repair Deficient and Intact Colorectal Carcinomas

Jennifer Ju¹, Anne Mills², Edward Stelow¹

¹University of Virginia Health System, Charlottesville, VA, ²University of Virginia, Charlottesville, VA

Disclosures: Jennifer Ju: None; Anne Mills: None; Edward Stelow: None

Background: Immune-based therapies are a new and promising approach to cancer treatment, particularly those targeting the programmed cell death protein (PD-1) and ligand (PD-L1) pathway. However, anti-PD-1/PD-L1 immunotherapies have not been as effective in colorectal carcinomas (CRC), with better responses in the minority of CRC that are mismatch repair deficient (MMR-d). Moreover, PD-L1 positive staining by immunohistochemistry does not correlate well with outcome. This may be due to the presence of other immune modulatory molecules. Lymphocyte-activation gene-3 (LAG-3) can act synergistically with PD-1/PD-L1 to cause immune cell exhaustion. Additionally, LAG-3 can interact with galectin-3 (GAL-3) to cause T-cell suppression. Here, we compare immunohistochemical staining patterns of PD-L1, LAG-3, and GAL-3 to evaluate the possible role of combination immunotherapy.

Design: Tissue microarrays were made of 65 cases of mismatch repair intact (MMR-i) CRC and 48 cases of MMR-d CRC (comprised of 25 likely Lynch Syndrome (LS), 4 possible LS, and 19 likely sporadic cases as determined by MMR protein status and BRAF/MLH1 testing). Tumor infiltrating lymphocytes (TIL) were scored semi-quantitatively based on membranous CD3 staining (Leica). Membranous PD-L1 (Spring Biosciences) and cytoplasmic/membranous LAG-3 (Abcam) were scored on TIL, and cytoplasmic GAL-3 (Cell Marque) was scored on tumor cells. Positive staining was called as follows: PD-L1 with at least mild staining, LAG-3 with at least one stained TIL per high-power field, and GAL-3 with stronger staining than normal colonic mucosa.

Results: MMR-d cases were much more likely to have TIL [77% (37/48) vs 35% (23/65), $p=0.00001$]. The majority of CRC cases showed dual PD-L1 and LAG-3 staining within TIL, and this was significantly more likely in MMR-d cases ($p=0.02$). Similarly, the majority of CRC showed dual tumor GAL-3 staining and TIL LAG-3 staining, with MMR-d being more likely to show this pattern ($p=0.07$). (See Table).

Tumor infiltrating lymphocyte staining for PD-L1 and LAG-3				
	PD-L1 Positive		PD-L1 Negative	
	LAG-3 Positive	LAG-3 Negative	LAG-3 Positive	LAG-3 Negative
MMR-Deficient	81% (39/48)	10% (5/48)	4% (2/48)	4% (2/48)
<i>Likely LS</i>	72% (18/25)	16% (4/25)	8% (2/25)	4% (1/25)
<i>Possible LS</i>	100% (4/4)	0% (0/4)	0% (0/4)	0% (0/4)
<i>Likely Sporadic</i>	89% (17/19)	5% (1/19)	0% (0/19)	5% (1/19)
MMR-Intact	60% (39/65)	18% (12/65)	3% (2/65)	18% (12/65)

GAL-3 tumor cell and LAG-3 tumor infiltrating lymphocyte staining pattern				
	GAL-3 Positive		GAL-3 Negative	
	LAG-3 Positive	LAG-3 Negative	LAG-3 Positive	LAG-3 Negative
MMR-Deficient	75% (36/48)	15% (7/48)	10% (5/48)	0% (0/48)
<i>Likely LS</i>	76% (19/25)	20% (5/25)	4% (1/25)	0% (0/25)
<i>Possible LS</i>	75% (3/4)	0% (0/4)	25% (1/4)	0% (0/4)
<i>Likely Sporadic</i>	74% (14/19)	11% (2/19)	16% (3/19)	0% (0/19)
MMR-Intact	57% (37/65)	35% (23/65)	5% (3/65)	3% (2/65)

Conclusions: Patients with CRC may benefit from multidrug therapy targeting combinations of PD-L1, LAG-3, and GAL-3. This may be of particular benefit to some MMR-i patients who have not had as strong of a response to anti-PD-1/PD-L1 therapy.

662 Prognostic significance of stromal and intra-epithelial tumor-infiltrating lymphocytes in small intestinal adenocarcinoma

Sun-Young Jun¹, Eun Su Park², Jae Jun Lee³, Heekyung Chang⁴, Eun Sun Jung⁵, Young-Ha Oh⁶, Seung-Mo Hong⁷

¹Incheon St. Mary's Hospital, Incheon, Korea, Republic of South Korea, ²Incheon St. Mary's Hospital, The Catholic University of Korea, Incheon, Korea, Republic of South Korea, ³Good Morning Hospital, Pyeongtaek-si, Korea, Republic of South Korea, ⁴Kosin University Gospel Hospital, Busan, Korea, Republic of South Korea, ⁵The Catholic University of Korea College of Medicine, Seoul, Korea, Republic of South Korea, ⁶Hanyang University, Guri, Korea, Republic of South Korea, ⁷Asan Medical Center, Songpa-gu, Korea, Republic of South Korea

Disclosures: Sun-Young Jun: None; Eun Su Park: None; Jae Jun Lee: None; Heekyung Chang: None; Eun Sun Jung: None; Young-Ha Oh: None; Seung-Mo Hong: None

Background: Assessment of tumor-infiltrating lymphocytes (TILs) may provide valuable information in predicting the prognosis and therapeutic benefit for immunotherapy in patients with small intestinal adenocarcinomas (SIACs).

Design: TILs were evaluated in 231 surgically resected SIACs and compared with microsatellite instability (MSI) and clinicopathologic variables, including overall survival. After counting TILs in 10 high-power fields (HPFs) in intra-tumoral areas, average number of intraepithelial-TILs (iTILs)/HPF and average stromal-TIL (sTIL) density (%) on x200 magnification were independently calculated. High levels of iTIL and sTIL were categorized as iTIL > 1 and sTIL > 20%, respectively.

Results: The median iTIL and sTIL were 1.1 and 16.0% (range, 0 to 26.9 and 0 to 74.0%), respectively. High iTIL and sTIL were observed in 51.1% (118/231) and 42.0% (95/226), respectively and MSI-high was observed in 21.7% (50/230). High iTIL was associated with MSI-high ($P < 0.001$), while high sTIL was not ($P = 0.312$). High iTIL and sTIL were more frequently presented in SIACs with polypoid growth ($P = 0.001$ and $P = 0.040$, respectively), medullary feature ($P = 0.029$ and $P = 0.005$, respectively), and high Crohn-like lymphoid reaction counts ($P = 0.038$ and $P = 0.009$, respectively). SIACs with high iTIL or sTIL showed less aggressive clinicopathologic behavior, including less pancreatic ($P = 0.007$ and $P = 0.011$, respectively) and lower T category ($P = 0.013$ and $P = 0.001$, respectively). On multivariate analysis, high sTIL ($P = 0.012$), lower stage grouping ($P = 0.001$), and the absence of lymphovascular invasion ($P = 0.003$) remained as better independent prognostic predictors.

Conclusions: High sTIL can be used as a good prognostic indicator and provide potential basis for the clinical use of targeted immunotherapy in SIAC patients.

663 Tumour Stroma As a Prognostic Marker in Colorectal Cancer: Novel Relationship With Tumour Budding And Poorly Differentiated Clusters

Iphshita Kak¹, Sameer Shivji², Kai Duan², Aysegul Sari², Rossi Tomin³, Mantaj Brar⁴, Erin Kennedy³, Richard Kirsch³, James Conner³

¹McMaster University, Hamilton, ON, ²Toronto, ON, ³Mount Sinai Hospital, Toronto, ON, ⁴Mount Sinai Hospital, University of Toronto, Toronto, ON

Disclosures: Iphshita Kak: None; Sameer Shivji: None; Kai Duan: None; Aysegul Sari: None; Rossi Tomin: None; Mantaj Brar: None; Erin Kennedy: None; Richard Kirsch: None; James Conner: None

Background: The role of the tumor microenvironment in colorectal cancer (CRC) progression has received increasing attention in recent years. Emerging evidence suggests that peritumoral stroma, and in particular the presence of an immature/myxoid morphology, may exert a powerful influence on clinical outcomes in CRC, rivalling other established adverse prognostic factors. We evaluated the relationship between peritumoral stroma and several new and established prognostic factors.

Design: 372 CRC resection specimens were evaluated for TNM stage as well as for venous invasion (using elastin stains), tumor budding (ITBCC 2016 criteria), poorly differentiated clusters (PDC, Ueno classification 2012) and peritumoral stroma type (mature, intermediate, immature; Ueno et al 2017). The proportion of immature stroma at the invasive front was scored semiquantitatively as absent, <10% or ≥10%.

Results: The study group included 77 Stage I (20.7%), 136 Stage II (36.6%), 146 Stage III (39.2%) and 13 Stage IV (3.5%) CRC. Overall, 38% of cases had a mature stroma, 16% an intermediate stroma, and 21% an immature stroma; in 25% of cases tumour stroma designation was not possible (Ueno et al 2017). Tumor stroma type was significantly associated with T-stage ($p < 0.0001$), N-stage ($p = 0.0003$), venous invasion ($p = 0.001$), extramural venous invasion ($p = 0.001$), high-grade tumor budding [Bd3] ($p < 0.00001$) and grade 3 PDC ($p = 0.004$), with a stepwise progression from mature to intermediate to immature stroma. Moreover, the extent of immature stroma was significantly associated with both high-grade tumor budding [Bd3] ($p < 0.0001$) and grade 3 PDC ($p < 0.005$), with a stepwise progression from absent to <10% to ≥10% immature stroma.

Conclusions: Immature stroma was significantly associated with all stage and non-stage related prognostic factors evaluated in this study. The relationship between immature stroma and loss of tumor differentiation (i.e. tumor budding and PDC) as well as major pathways of tumor dissemination (i.e. venous invasion and lymph node metastasis) suggests important biologic relationships that merit further investigation.

664 Oh My... Struggles and Disagreements in Staging Treatment-Naïve Colorectal Carcinomas

Dipti Karamchandani¹, Tonya King², Runjan Chetty³, Xiuli Liu⁴, Maria Westerhoff⁵, Rhonda Yantiss⁶, Zhaohai Yang⁷

¹Penn State Health Milton S. Hershey Medical Center, Hershey, PA, ²Pennsylvania State University College of Medicine, Hershey, PA, ³University Health Network, Toronto, ON, ⁴University of Florida, Gainesville, FL, ⁵University of Michigan, Ann Arbor, MI, ⁶Weill Cornell Medical College, New York, NY, ⁷Penn State Hershey Medical Center, Hershey, PA

Disclosures: Dipti Karamchandani: None; Tonya King: None; Runjan Chetty: None; Xiuli Liu: None; Maria Westerhoff: None; Rhonda Yantiss: None; Zhaohai Yang: None

Background: The American Joint Committee on Cancer (AJCC) staging is widely used to stage colorectal carcinomas (CRC). Even with the adoption of the newest 8th edition, there are still less well-defined parameters that are subject to each pathologist's interpretation. The aim of this study was to assess practice trends among pathologists in staging treatment-naïve CRC.

Design: A web-based survey with multiple hypothetical case scenarios pertaining to staging of untreated CRC was circulated amongst pathologists, and the results were analyzed using SAS v9.4 software.

Results: 118 pathologists [49% academic subspecialized (AS); 27% academic general (AG); 19% private practice (PP); 5% fellows] from different countries [America 56% (mostly US), Europe 19%, others 25%] with varied years of clinical experience (0-5 years: 32%; 5-10 years: 25%; >10 years: 43%) completed the survey. For T3 vs T4a: when CRC is > 1mm from serosal surface but continuous with it via inflammation, 49% respondents assigned pT3 and 51% assigned pT4a. In addition, 30% considered this as tumor perforation, and 42% included granulation tissue in this scenario. In pT3 CRC < 1mm from the serosa, 53% respondents would report distance from the serosa and/or comment on likely higher risk of peritoneal recurrence. The practice setting, years of experience, or country of practice had no significant impact on the above responses ($p > 0.05$). 33% pathologists considered acellular mucin in untreated lymph node (LN) as positive. There was no significant difference in practice setting or years of experience; however European pathologists were more bound to call these positive ($p = 0.015$). For tiny LN metastatic focus (< 0.2mm), 48% pathologists staged as positive node (pN1), 47% staged as pN0(i+), and 5% staged as pN0. There was no significant difference in years of experience or country of practice; however, AG diagnosed significantly more pN1 in this setting ($p = 0.02$).

Conclusions: There is significant discordance among pathologists worldwide, irrespective of practice setting, clinical experience or country of practice for certain staging parameters. Many believe tumor >1 mm from the serosa continuous via inflammation is pT4a. Many reject AJCC criteria of N0 for deposits <0.2 mm, probably because this recommendation is not data driven. In light of significant implications on treatment selection and patient outcome, better-defined criteria regarding these commonly encountered challenging scenarios are needed, to ensure consistency in CRC staging.

665 A Survey of Challenges and Issues in staging Rectal Carcinoma post Neoadjuvant Therapy

Dipti Karamchandani¹, Tonya King², Runjan Chetty³, Xiuli Liu⁴, Maria Westerhoff⁵, Rhonda Yantiss⁶, Zhaohai Yang⁷
¹Penn State Health Milton S. Hershey Medical Center, Hershey, PA, ²Pennsylvania State University College of Medicine, Hershey, PA, ³University Health Network, Toronto, ON, ⁴University of Florida, Gainesville, FL, ⁵University of Michigan, Ann Arbor, MI, ⁶Weill Cornell Medical College, New York, NY, ⁷Penn State Hershey Medical Center, Hershey, PA

Disclosures: Dipti Karamchandani: None; Tonya King: None; Runjan Chetty: None; Xiuli Liu: None; Maria Westerhoff: None; Rhonda Yantiss: None; Zhaohai Yang: None

Background: Accurate staging of neoadjuvantly treated rectal carcinomas (RC) is crucial to assess therapeutic response and determining prognosis. Despite current American Joint Committee on Cancer (AJCC) / College of American Pathologists (CAP) guidelines, there are still ambiguous issues that pose diagnostic challenges to surgical pathologists. This study aimed to assess current staging practices by pathologists worldwide in different settings.

Design: A web-based questionnaire was circulated among an international group of surgical pathologists, with selected case scenarios pertaining to tumor staging and radial margin assessment in the neoadjuvant setting. The responses were analyzed using SAS v9.4.

Results: 118 pathologists [49% academic subspecialized (AS), 27% academic general (AG), 19% private practice (PP), 5% fellows] from different countries [America (mostly US) 56%, Others 34%] completed the survey. The clinical experience ranged from 0-5 years (32%), 5-10 years (25%), to >10 years (43%). For treated RC with viable tumor cells floating in mucin pool: 65% respondents ignored the mucin and assigned a T stage based on the deepest invasion by viable tumor only, while others used the deepest extent of mucin which resulted in a higher T stage. Similar percentage of respondents considered acellular mucin at radial margin as negative margin. There were significant differences between US pathologists versus those from other countries with the former choosing lower stage (p=0.03) and negative margin (p=0.003). More AS and PP also chose the lower stage (p=0.04) and negative margin (p=0.02), as compared to AG. The years of experience did not have significant impact. For treated RC with nodal metastasis <0.2 mm: 61% assigned ypN1 irrespective of the size in post-therapy setting (ypN1neo), 15% assigned ypN1 irrespective of the size/treatment, and 24% assigned ypN0(i+). Pathologists with < 5 years and >10 years of experience favored ypN1neo as compared to those with 5-10 years' experience (p=0.02), and no difference was associated with practice setting or country. Also, 62% respondents did not diagnose mucinous carcinoma or report tumor budding in treated RC. The overall responses were grouped into 2 clusters (Table 1).

Table 1: Cluster analysis of response to practice trend questions

Question/Response	Cluster 1	Cluster 2	p value
America(A)/Other (O)	O>A	A>O	0.002
Practice setting	AG>AS>PP	AS>AG=PP	0.0078
Deepest invasion for T stage	Count acellular mucin	Count viable tumor cells only	<0.001
Acellular mucin at margin as positive radial margin	Yes>No	No>Yes	<0.001
Diagnose mucinous carcinoma in treated RC	Yes=No	No>Yes	0.032
Report tumor budding in treated RC	Yes=No	No>Yes	0.022
Lymph node stage	ypN1neo > ypN1> ypN0(i+)	ypN1neo> ypN0(i+)> ypN1	0.0019

Conclusions: Despite the AJCC/ CAP guidelines, discordance remains amongst pathologists in staging RC in neoadjuvant setting. Further studies are needed to provide consensus guidelines in these areas, which may have important implications in treatment selection and patient outcome.

666 Histopathology of Diversion Colitis in Inflammatory Bowel Disease Patients: Longitudinal Examination of Pre- and Post-Diversion Specimens

Roula Katerji¹, Raul Gonzalez², Aaron Huber¹, Jennifer Findeis-Hosey¹

¹University of Rochester Medical Center, Rochester, NY, ²Beth Israel Deaconess Medical Center, Boston, MA

Disclosures: Roula Katerji: None; Raul Gonzalez: None; Aaron Huber: None; Jennifer Findeis-Hosey: None

Background: Diversion colitis (DC) may occur when the fecal stream has been surgically diverted with subsequent inflammation of the de-functioned segment. A large proportion of patients with DC are those with inflammatory bowel disease (IBD) who have been surgically diverted. In these patients, the diagnosis of DC may be challenging due to histologic similarities between IBD and DC, including the presence of lymphoid aggregates and ulceration, as well as the potential for DC to be superimposed on active IBD. We compared the histologic features of IBD and DC and examined post-diversion changes.

Design: We retrospectively identified 19 cases of adult patients with IBD who underwent surgical diversion and subsequently developed DC between 1998 and 2018. Cases were included if there were slides available for review from (1) before/at time of surgical diversion, and (2) following diversion with the clinicopathologic diagnosis of DC. Clinicopathologic features were reviewed and pathologic features were compared using two-tailed Fisher's exact test with statistical significance set at $P < 0.05$.

Results: Specimens from before/at time of diversion were all resections, with the original diagnoses of ulcerative colitis (11 cases, 58%), Crohn disease (1, 5%), or indeterminate colitis/IBD not otherwise specified (7, 37%). Post-diversion specimens with diversion colitis included 15 resections and 4 biopsies, with a median patient age of 44 years; 5 (26%) were classified as DC and 14 (74%) were classified as diagnostic of concurrent DC and IBD based on overall clinicopathologic features. Comparative histologic features between the pre- and post-diversion specimens are summarized in the Table. Germinal centers were significantly more common in post-diversion specimen (90% vs. 42%, $P = 0.0051$), while crypt abscesses (84% vs. 42%, $P = 0.017$), mural inflammation in pre-diversion resection specimens (47% vs. 7%, $P = 0.0098$), and Paneth cell metaplasia (53% vs. 16%, $P = 0.0382$) did not appear as frequently in the post-diversion specimens.

	Pre-diversion/at time of diversion (%)	Post-diversion (%)	P value
Lymphoid aggregates	19 (100.0)	18 (94.7)	1.0000
Germinal centers	8 (42.1)	17 (89.5)	0.0051
Lamina propria expansion	17 (89.5)	19 (100.0)	0.4865
Cryptitis	14 (73.7)	9 (47.4)	0.1837
Crypt abscesses	16 (84.2)	8 (42.1)	0.0170
Ulceration	17 (89.5)	13 (68.4)	0.2320
Paneth cell metaplasia	10 (52.6)	3 (15.8)	0.0382
Crypt dropout	12 (63.2)	11 (57.9)	1.0000
Branching	13 (68.4)	7 (36.8)	0.1031
Reactive epithelium	18 (94.7)	16 (84.2)	0.6039
Granulomas	1 (5.3)	0 (0.0)	1.0000
Mural inflammation (resections only)	9 (47.4)	1 (6.7)	0.0098
Withering crypts	8 (42.1)	5 (26.3)	0.4951
Microthrombi	3 (15.8)	0 (0.0)	0.2297
Fibrosis	3 (15.8)	0 (0.0)	0.2297

Conclusions: The identification of overlapping DC in a diverted IBD patient can be diagnostically challenging. In this retrospective longitudinal study, we identified that germinal centers occur more frequently in post-diversion specimens with DC, while crypt abscesses, mural inflammation and Paneth cell metaplasia do not occur as frequently in DC as compared to pre-diversion IBD specimens.

667 Significance of Novel Immunotherapy Target CD73 in Primary Colorectal Adenocarcinoma

Riham Katkhuda¹, Anuj Verma¹, Atin Agarwal², Nastaran Neishaboori³, Ignacio Wistuba¹, Michael Overman¹, Scott Kopetz¹, Zhi-Qin Jiang¹, Barbara Mino¹, Luisa Solis Soto¹, Dipen Maru¹

¹The University of Texas MD Anderson Cancer Center, Houston, TX, ²Irving, TX, ³Portland, OR

Disclosures: Riham Katkhuda: None; Anuj Verma: None; Nastaran Neishaboori: None; Ignacio Wistuba: None; Michael Overman: *Consultant*, MedImmune, Inc.; *Primary Investigator*, MedImmune; Zhi-Qin Jiang: None; Barbara Mino: None; Luisa Solis Soto: None; Dipen Maru: None

Background: Because of its immunosuppressive properties and interaction with PD-1, CD73 is identified as a novel target of immunotherapy in solid tumors. Prior studies have shown that higher expression of CD73 correlates with higher stage and poor outcome in colon cancer patients. However, cellular distribution of CD73 protein and its relation to molecular subtypes of colorectal cancer is not known and is needed to prioritize patients who can be targeted for antiCD73 antibody therapy

Design: We evaluated CD73 expression by immunohistochemistry (clone D7F9A, Cell Signaling) on tissue microarray of colorectal cancer samples from 136 patients with matching non-neoplastic colon from 44 patients. The membranous immunohistochemistry staining was scored as the H-score (%tumor cells with intensity 1x1+%tumor cells with intensity 2x2+%tumor cells with intensity 3x3). The immunohistochemistry staining score was correlated with clinicopathological features, mutational profile and consensus molecular subtype.

Results: Luminal membranous staining was observed in non-neoplastic colon from all samples, while basolateral membranous staining was identified only in tumor cells in 38% (51/136) patients. Median H-score was 10 in the entire population. Table shows the comparison of clinicopathological features and molecular features and consensus molecular subtypes between patients with high CD73 expression and low CD73 expression.

CHARACTERISTICS		CD73 IHC expression					P value
		Total	Negative/Low <10		High >=10		
			N	%	N	%	
ALL		136	109	80%	27	20%	
SEX							0.006
	Female	59	41	69.49%	18	30.5%	
	Male	77	68	88.31%	9	11.68%	
STAGE	AJCC 7th						0.064
	II	67	58	86.6%	9	13.4%	
	III	69	51	73.9%	18	26.1%	
Pathological T stage							0.482
	1	2	1	50.0%	1	50.5%	
	2	6	4	66.7%	2	33.3%	
	3	103	85	82.52%	18	17.47%	
	4	25	19	76%	6	24%	
Pathological N stage							0.064
	N0	67	58	86.56%	9	13.43%	
	others	69	51	73.91%	18	26.08%	
LOCATION							0.195
	Left	73	62	84.93%	11	15.06%	
	Right	62	46	74.19%	16	25.80%	
	Left&Right	1	1	100	0		
CMS SUBTYPE							0.018
	CMS1	16	10	62.50%	6	37.50%	
	CMS2	45	40	88.88%	5	11.11%	
	CMS3	7	7	100%	0	0%	
	CMS4	16	9	56.25%	7	43.75%	
Microsatellite instability by Immunohistochemistry							0.007
	MSI-H	18	10	55.6%	8	44.4%	
	MSS	116	97	83.62%	19	15.96%	
PIK3CA Mutation Status							0.325
	Wild Type	91	68	74.72%	23	25.27%	
	Mutant	20	17	85%	3	15%	
BRAF Mutation Status							0.070
	Wild Type	100	79	79%	21	21%	
	Mutant	11	6	54.5%	5	45.5%	
KRAS Mutation Status							0.034
	Wild Type	75	53	70.66%	22	29.33%	
	Mutant	36	32	88.88%	4	11.11%	

Conclusions: Higher CD73 expression in CMS4 subtype, KRAS wild type and /or MSI-H colorectal cancer support prioritising patients with these subgroups of CRC for AntiCD73 therapies.

668 Tumor Infiltrating CD8 Lymphocytes Correlate with Residual Tumor Following Neoadjuvant Chemoradiation for Rectal Adenocarcinoma

Rossana Kazemimood¹, Namita Agrawal², Sunil Badve³, Susannah Ellsworth¹, Romil Saxena⁴

¹Indiana University, Pathology & Laboratory Medicine, Indianapolis, IN, ²Indiana University, Indianapolis, IN, ³Indiana University Medicine, Indianapolis, IN, ⁴Indiana University School of Medicine, Indianapolis, IN

Disclosures: Rossana Kazemimood: None; Namita Agrawal: None; Susannah Ellsworth: None; Romil Saxena: None

Background: Neoadjuvant chemoradiation is a standard therapy for non-metastatic locally advanced rectal adenocarcinoma (LARC). However, complete response (CR) to neoadjuvant therapy is rare (<20%), and the factors contributing to CR are not well understood. We hypothesized that the numbers of tumor infiltrating lymphocytes (TILs), especially CD3 and CD8 cells, correlates with tumor necrosis, and therefore the amount of residual tumor.

Design: All patients with non-metastatic LARC treated with a uniform neoadjuvant chemoradiation protocol between 2008 and 2017 were identified from a registry-based database. Archived slides of pre-treatment biopsies and post-treatment surgical specimens were retrieved from pathology files. Immunohistochemical stains for CD3 and CD8 were performed on 4-micron sections of the pre-treatment biopsies by a standard procedure. Percentages of CD3 and CD8 cells were quantified by a standard technique (*Adv Anat Pathol.* 2017; 24: 311-335). Surgical resection specimens were evaluated for presence of residual tumor, and the amount recorded as a percentage of total tumor area. $P < 0.05$ was considered to be statistically significant.

Results: Of 332 patients treated for LARC in our institution during the study period, 109 received uniform neoadjuvant chemoradiation. Paired pre-treatment biopsies and post-treatment resection specimens were available in 38 patients. There were 21 (55%) males and 17 (45%) females; mean age was 60 years (range 36-85). Twenty-three (60%) patients were clinical stage 3 and only one patient was stage 1. Eight patients (21%) showed pathologic CR; 22 (58%) patients had $\leq 10\%$ residual tumor; 6 patients (16%) had 10-50% residual tumor and 2 (5%) showed more than 50% residual tumor. The percentage of CD3 TILs on pre-treatment biopsy specimens ranged from 1-20% (mean 8%) and CD8 from 1-10% (mean 3.5%). Correlation between the percentages of CD8 TILs in the pre-treatment biopsies and the amount of residual tumor was statistically significant ($p < 0.05$). There was no statistically significant difference between the percentages of CD3 TILs in the pre-treatment biopsies and the amount of residual tumor.

Conclusions: CD8 TILs may serve as a predictive marker of response of rectal adenocarcinoma to neoadjuvant chemoradiation.

669 Ki-67 expression and FDG uptake in Colorectal Adenomas and Adenocarcinoma

Osama Khan¹, Sergey Pyatibrat², Wanzhen Zeng³, Ran Klein³, Lionel Zuckier³, Jeremy Gardner³

¹University of Ottawa, Ottawa, ON, ²Royal Columbian Hospital, New Westminster, BC, ³The Ottawa Hospital - University of Ottawa, Ottawa, ON

Disclosures: Osama Khan: None; Sergey Pyatibrat: None; Wanzhen Zeng: None; Ran Klein: None; Lionel Zuckier: None; Jeremy Gardner: None

Background: Focal uptake in the colon is an incidental finding in FDG PET scans for patient cancer staging. The significance of colorectal FDG uptake and its relation to architectural types, degree of polyp dysplasia and Ki67 has not been elucidated in the literature. We assessed the relationship between adenomatous polyps and adenocarcinoma (AC) with regard to FDG uptake and Ki-67.

Design: Patients referred for FDG PET/CT staging over 2 years with colorectal FDG uptake and polypectomies were included. 29 subjects (age: 72.3 ± 9.1 , M:F=18:11) and 61 specimens were included. FDG PET images were acquired on a Discovery 710 Scanner and reconstructed and interpreted on HERMES workstation. Maximum Standard Uptake Values (SUV_{max}) were measured and correlated to pathohistological findings including malignancy, degree of dysplasia, adenoma types, gross size and Ki-67 index. Data were reported as median \pm inter-quartile range. Cut-off SUV_{max} values were determined using receiver operator curves (ROC) analysis. Ki-67 quantification was performed by two experienced readers blinded to patient data. A minimum of 500 cells were counted manually on each slide at $\times 400$ magnification. Ki67 index was obtained from the ratio of stained nuclei cells and total counted nuclei.

Results: SUV_{max} measured 4.8 ± 6.3 for adenomas and 11 ± 10.5 for AC ($p = 0.006$). The degree of dysplasia SUV_{max} was 5.7 ± 7.7 , 9.2 ± 6.4 and 9.2 ± 12.3 for low ($n = 34$), high ($n = 12$) and invasive ($n = 7$) adenomas respectively. The FDG uptake was highest in tubulovillous (TV) (9.8 ± 8.8 , $p = 0.01$) as compared to villous (V) (8.7 ± 8.1 , $p = 0.1$) and tubular adenomas (TA) (4.7 ± 4.8). The ROC analysis demonstrated that SUV_{max} can distinguish benign from malignant (AUC = 0.83) and TV adenomas (AUC=0.76) versus poor ability for dysplasia and architectural types. No significant correlation with Ki-67 was identified for adenomas vs. ACs ($p = 0.9$) or dysplasia ($p = 0.2$). Ki-67 did not differ between TA ($46 \pm 18\%$), V ($55 \pm 38\%$) TV ($51 \pm 27\%$) adenomas ($p > 0.4$). No correlation between FDG uptake and Ki-67 ($p = 0.63$) nor gross size ($p > 0.05$) was seen.

Figure 1 - 669

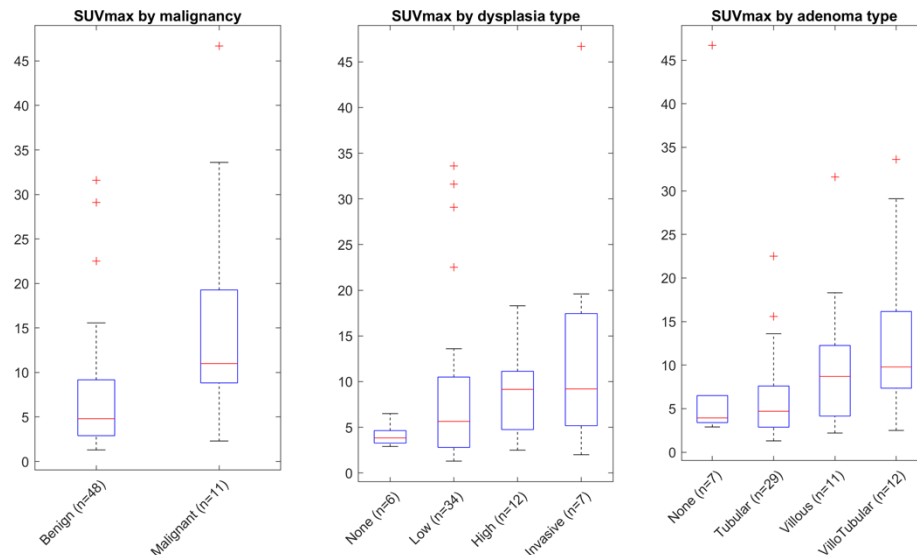
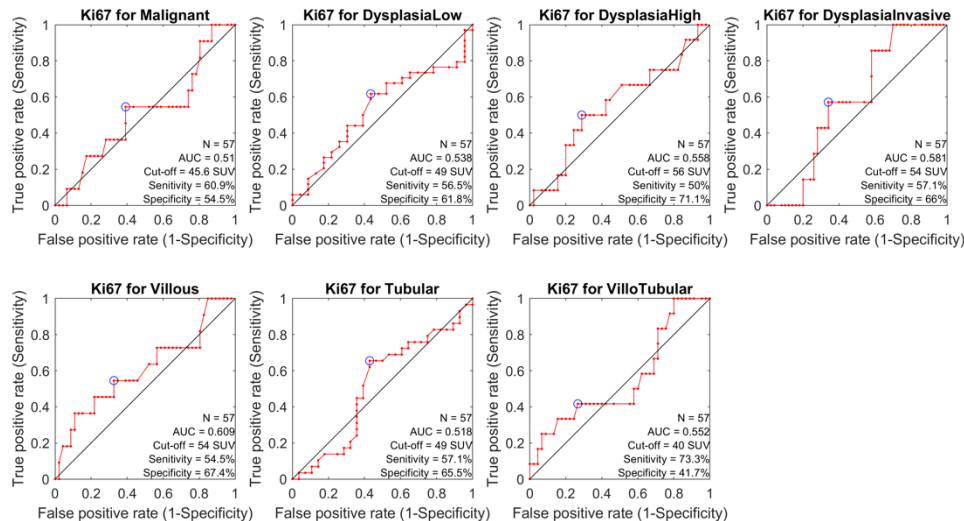


Figure 2 - 669



Conclusions: Increased FDG uptake was identified in V and TV adenomas and in high grade dysplasia. Higher FDG uptake was present in AC versus adenomas. No correlation between FDG uptake and Ki-67 expression or gross size was seen. Ki-67 did not correlate to malignancy, grade of dysplasia or architectural type. Focal FDG uptake is likely to be associated with malignancy with intense FDG uptake. Ki-67 index may not be a reliable index for colon cancer.

670 Upregulation of Peritumoral Stromal Plasminogen Activator Inhibitor-1 (PAI-1) in Colorectal Cancer (CRC) Correlates with High Grade Tumor Budding (TB) and Mismatch Repair Proficiency (MMR-P)

Brandon Koo¹, Saleh Najjar², Kavita Umrau¹, Christine Sheehan³, Steven Higgins¹, Hwajeong Lee²

¹Albany Medical College, Albany, NY, ²Albany Medical Center, Albany, NY, ³Albany Medical College, Averill Park, NY

Disclosures: Brandon Koo: None; Saleh Najjar: None; Kavita Umrau: None; Christine Sheehan: None; Steven Higgins: None; Hwajeong Lee: None

Background: PAI-1, a constituent of the urokinase plasminogen system, promotes tumorigenesis by epithelial to mesenchymal transition (EMT). The combination of upregulated PAI-1 and TB is associated with synergistic adverse prognoses in CRC patients. Cellular origin of PAI-1 and association with MMR status have not been elucidated. This study assessed the localization of the PAI-1 protein and its association with TB and MMR status in CRCs.

Design: 96 cases of resected CRC were retrieved and reviewed. TB was graded (low-1, intermediate-2, high-3) according to the recently published consensus paper. MMR status was determined by immunohistochemistry (MLH1, MSH2, MSH6 and PMS2) in 94 cases and by PCR in 2 cases. Tissue microarrays (TMA) were constructed (3 mm core, Simport M473 Mold Kit; Newcomer, Middleton, WI) with 2 cores per case to separately capture tumor and tumor-stroma interface at the leading edge. PAI-1 immunostain was performed (rabbit polyclonal, developed in-house) on TMAs and representative whole sections from 6 cases. Cytoplasmic and/or partial/complete membranous stain was considered positive. The staining extent was assessed in tumor cells (T(L) <50% ; T(H) >=50%) and peritumoral stroma (S(L) inconspicuous staining; S(H) conspicuous staining). Two tailed Student's t-test and Fisher's exact test were performed to correlate parameters (p<0.05 was considered statistically significant).

Results: 53 CRCs were MMR-P and 43 were MMR-deficient (D). PAI-1 expression was consistent in whole section vs. TMA in the 6 representative cases. There were 72 T(L) and 24 T(H), and 44 S(L) and 52 S(H) cases. 62% of T(L) vs. 33% of T(H) were MMR-P (p = 0.0176), and higher grade TB was observed in T(L) compared to T(H) cases (mean TB grade = 1.9 vs. 1.4, p=0.004). 47 cases were T(L)+S(H), while 19 were T(H)+S(L), with higher grade TB in T(L)+S(H) vs. T(H)+S(L) cases (mean TB grade =1.9 vs 1.4, p=0.016). MMR-P tumors showed higher grade TB as compared to MMR-D (mean TB grade = 2.0 vs 1.5, p=0.002). Neither TB grade nor MMR status significantly differed between S(L) and S(H).

Conclusions: High grade TB and MMR-P correlated with high peritumoral stromal and low intratumoral PAI-1 expression. High PAI-1 activity may play a role in increased EMT at the leading edge of CRC invasion when its upregulation is derived from stromal, and not tumor cells. PAI-1 may serve as a biomarker to stratify CRCs with EMT and high grade TB pathway vs. MMR-D and high mutation burden pathway, with potential therapeutic implication.

671 How good are we in Diagnosing Anal Squamous Intraepithelial Lesions with and without p16-an Inter-observer Variability Study?

Uma Krishnamurti¹, Ashley Monsrud², Mohammad Mohammad³, Mario Mosunjac⁴, Gabriela Oprea-Ilie⁵, Krisztina Hanley¹, Tadros Talaat¹, Lisa Flowers¹, Marina Mosunjac⁶

¹Emory University, Atlanta, GA, ²Morehouse SOM, McDonough, GA, ³Atlanta Clinical and Translational Science Institute, Atlanta, GA, ⁴Emory University Medicine, Atlanta, GA, ⁵Emory University Medical School/Grady Memorial Hospital, Atlanta, GA, ⁶Atlanta, GA

Disclosures: Uma Krishnamurti: None; Ashley Monsrud: None; Mohammad Mohammad: None; Mario Mosunjac: None; Gabriela Oprea-Ilie: None; Krisztina Hanley: None; Tadros Talaat: None; Lisa Flowers: None; Marina Mosunjac: None

Background: Morphologic diagnosis and grading of anal squamous intraepithelial lesions (SIL) are challenging. p16 positivity is useful in determining high grade squamous intraepithelial lesion (HSIL). There are limited studies investigating interobserver variability and p16 utility in accurately grading anal SIL.

Design: 146 consecutive anal biopsies were extracted from the pathology database. In 89 cases p16 was not used and in 57cases p16 had been used to render a diagnosis. Six pathologists first blindly evaluated only the hematoxylin and eosin (H&E) slides and rendered a diagnosis of negative for SIL (NSIL), low grade SIL (LSIL/AIN 1) or HSIL encompassing AIN 2 and AIN 3. They were also asked to record if they would order a p16 or not. Subsequently, they were given the p16 immunostained and H&E slides in cases where p16 had been performed and asked to render a diagnosis of NSIL, LSIL/AIN 1, or HSIL (AIN 2 or AIN 3). Fleiss kappa values were calculated for three groups: All cases HE diagnosis only; Diagnosis after reviewing p16; H&E diagnosis on cases without p16. For each of these groups kappa was calculated for a 4 tier diagnosis (NSIL, AIN1, AIN2, AIN3); 3 tier diagnosis-A (NSIL/AIN 1(pooled), AIN 2, AIN 3); 3 tier diagnosis-B (NSIL, LSIL, HSIL); 2 tier diagnosis (No HSIL, HSIL) .

Results: There is only moderate agreement with a 4 tier diagnosis with or without p16. Agreement is improved with a 3 tier diagnosis, with substantial agreement when AIN2 and AIN3 are pooled as just HSIL both in cases where p16 was used and where it was not required. Most discrepancies were in a stratification of HSIL as AIN 2 or AIN3 and due to cases interpreted as NSIL by some and as LSIL by others. There is almost perfect agreement with a 2 tier diagnosis in cases where p16 was used and also where p16 was not required with the best agreement with a 2 tier diagnosis and concurrent p16 review. The p16 request rate ranged from 25-55% with a median of 30%.

Kappa (k) values in Anal SIL				
Cases	Diagnosis			
	4 tier	3 tier (A)	3 tier (B)	2 tier
All cases	0.48	0.54	0.61	0.68
HE only (146)				
p16 cases (57)	0.50	0.57	0.75	0.87
Non- p16 cases (89)	0.54	0.63	0.72	0.82

Conclusions: This study highlights the importance of a judicious use of p16 for diagnosis. Inter-observer agreement was substantial to almost perfect when there is no need for p16; however, when its use is indicated but not reviewed, agreement is much lower even with a 2 tier diagnosis. p16 should be ordered where HSIL is a possibility such as in cases where there is increased nuclear atypia, increased mitoses with abnormal surface keratinization, and abnormal mitoses at any level. This will ensure diagnostic accuracy and best possible patient care.

672 Prevalence of Cytomegalovirus, Adenovirus and Epstein-Barr Virus Infection in Patients with Immune Checkpoint Inhibitor-induced Colitis

Carissa LaBoy¹, Audrey Deeken-Draisey², Lily Marsden³, Guang-Yu Yang⁴, Maryam Pezhouh¹

¹Northwestern University Feinberg School of Medicine, Chicago, IL, ²Northwestern Memorial Hospital, Chicago, IL, ³Utah Office of the Medical Examiner, Salt Lake City, UT, ⁴Northwestern University, Chicago, IL

Disclosures: Carissa LaBoy: None; Audrey Deeken-Draisey: None; Lily Marsden: None; Guang-Yu Yang: None; Maryam Pezhouh: None

Background: One of the most common and clinically significant immune related adverse events (irAEs) of check point inhibitors is immune related colitis (irColitis). The immune dysregulation of the gastrointestinal (GI) mucosa caused by these medications and the immunosuppressants administered to treat the colitis can predispose such patients to viral infections leading to refractoriness to medical therapy. In the present study, we analyzed the frequency of cytomegalovirus (CMV), adenovirus and Epstein Barr virus (EBV) infections in GI biopsies from patients with irColitis.

Design: We evaluated 36 GI biopsies of 21 patients with irColitis. A group of age and sex matched patients with diarrhea without any exposure to checkpoint inhibitors was included as a control. Biopsies were scored for presence of active inflammation, lymphocytic like pattern of injury, distorted crypt architecture, ulceration and crypt epithelial apoptosis. Highly sensitive EBV-encoded RNA1 (EBER-1) in situ hybridization and immunohistochemical staining (IHC) for adenovirus and CMV were performed on all the samples.

Results: The patients had been treated for metastatic melanoma (14/21; 67%) and lung carcinoma (2/21; 10%) followed by urothelial carcinoma, renal cell carcinoma, ovarian carcinoma and Hodgkin lymphoma (1/21; 5% each). Other encountered irAEs included immune thrombocytopenia and hypothyroidism (5% each). Most of the patients were on combination of ipilimumab/nivolumab (11/21; 52%) followed by pembrolizumab (5/21; 24%), ipilimumab (4/21; 19%) and nivolumab (1/21; 5%), with an average regimen of 3 cycles of treatment. Endoscopic evidence of colitis were seen in 79% of the cases. Although the endoscopic evaluation was normal in 23% of the cases (5/21), histologic evaluation identified pathologic findings in 40% of them (2/5). Histologically, active inflammation was present in 91% (33/36) followed by lymphocytic-like injury in 63% of biopsies (23/36). Only 13% of cases show mild architectural distortion (5/36). Adenovirus was detected by IHC in 3 out of 36 GI biopsies (8%). Rare EBER-1 positivity was present in 17% of cases (6/36). CMV was detected in one patient (3%). The CMV viral cytopathic effects was appreciated prior to IHC staining. The control group did not show any staining for adenovirus, CMV and EBV.

Conclusions: Our results indicate that routine Hematoxylin and Eosin stained slides should be evaluated for presence of concurrent viral infections in irColitis, followed by confirmatory IHC in suspected cases.

673 Functional loss of ARID1A is the main mechanism boosting PD-L1 expression in gastric cancer

Dakeun Lee¹, Young-Bae Kim²

¹Suwon, Korea, Republic of South Korea, ²Ajou University School of Medicine, Suwon, Korea, Republic of South Korea

Disclosures: Dakeun Lee: None; Young-Bae Kim: None

Background: Notwithstanding the remarkable treatment success of anti-PD-1 monoclonal antibody, the oncogenic mechanism of PD-L1 regulation in gastric cancer (GC) remains poorly understood.

Design: We performed PD-L1 (SP263) and ARID1A for immunohistochemistry, EBV in situ hybridization, and microsatellite instability (MSI) tests in a large cohort of experimental set (N = 276) and in the validation set (n = 157). Furthermore, using ARID1A knockdown experiments, we checked the PD-L1 levels by Western blot, qRT-PCR, and FACS in GC cell lines. After treating PI3K inhibitor, we tested PD-L1 expression levels along with other nodes in the PI3K/AKT signaling pathways.

Results: PD-L1 positivity was associated with loss of ARID1A and better patients' survival in various molecular subtypes (tissue microarray blocks, n = 276). Considering the heterogeneous expression of ARID1A, we validated this using whole tissue sections (n = 159) and found that loss of ARID1A was correlated with microsatellite instability-high (MSI-H), Epstein-Barr virus (EBV), and PD-L1 positivity. Furthermore, especially in MSI-H tumors, the degree of PD-L1 expression was significantly greater in ARID1A-deficient tumors. After ARID1A knockdown in GC cell lines, the total and membranous PD-L1 as well as PD-L1 mRNA was increased by Western blot, flow cytometry, and qRT-PCR, respectively. IFN- γ -mediated PD-L1 upregulation was more amplified in ARID1A-deficient cancer cells. Conversely, ectopic ARID1A overexpression decreased PD-L1 expression in ARID1A-deficient SNU216 cells. Loss of ARID1A increased PD-L1 via activating AKT signaling, while LY294002 (PI3K inhibitor) decreased PD-L1 levels in various GC cell lines.

Conclusions: These results strongly indicate that loss of ARID1A is the main underlying mechanism of PD-L1 regulation in GC, and also provide an explanation why MSI and EBV types show higher PD-L1 expression and better clinical response to anti-PD-1 treatment, at least in part. ARID1A-deficient tumor may become a potential candidate for PD-1 or AKT signaling inhibition in future clinical trials.

674 Neuroendocrine cells are commonly absent in the intestinal crypts in autoimmune enteropathy

Hee Eun Lee¹, Lin Yuan², Tsung-Teh Wu³

¹Rochester, MN, ²Shanghai, China, ³Mayo Clinic, Rochester, MN

Disclosures: Hee Eun Lee: None; Lin Yuan: None; Tsung-Teh Wu: None

Background: Absence of neuroendocrine (NE) cells of intestinal mucosa in autoimmune enteropathy (AIE) has been occasionally reported. However, the status of NE cells in the intestinal mucosa in AIE has not been evaluated in detail.

Design: Small bowel and colonic biopsies were retrospectively collected from 19 AIE patients (34 duodenum and 15 colon; 28 initial available and 21 follow-up biopsies from 12 patients). 33 common variable immunodeficiency (CVID) patients (34 duodenum, and 19 colon), 13 IgA deficiency patients (13 duodenum and 5 colon), and 10 normal (5 colon and 5 duodenum) were used as control groups. Histologic features (villous atrophy/crypt distortion, intraepithelial lymphocytes (IELs), acute inflammation, crypt apoptosis, and absence or presence of goblet cells, Paneth cells and plasma cells) were recorded. Chromogranin immunostain was performed to assess quantity of NE cells in the intestinal crypts and graded as absence, marked decrease, or intact; and was correlated with histologic features.

Results: Median age of AIE patients was 40 years (range of 11-74) and 15 of 19 patients were male. 18 (12 duodenum and 6 colon) initial available biopsies from 15 of 19 (79%) patients showed absence (n=14) or markedly decreased (n=4) NE cells in the crypts. The remaining 4 patients with intact NE cells were treated with steroid before the biopsies were taken. On follow-up biopsies, 6 patients with initial absent or markedly decreased NE cells regained them, 2 with intact NE cells initially showed absence or markedly decreased NE cell, and the remaining 4 showed no change. Absence or markedly decreased NE cells were significantly associated with increased IELs (p=0.006), increased crypt apoptosis (p=0.004), and absence of goblet cells (p=0.001), but not with other histological features. 2 patients (1 duodenum and 2 colon) showed absence or markedly decreased NE cells while goblet cells and/or Paneth cells were intact. 4 (3 colon and 1 duodenum) biopsies from 3 of 33 (9%) patients showed absent (n=1) or markedly decreased (n=3) NE cells in CVID patients. Intact NE cells were present in biopsies from all 13 patients with IgA deficiency and 10 normal controls.

Conclusions: Absence or markedly decreased NE cells in the intestinal crypts were common (79%) in AIE while being only occasionally found (9%) in CVID and absent in IgA deficiency. Absence of NE cells can be present with intact goblet cells or Paneth cells in a small subset (11%) of AIE patients.

675 Insulinoma-associated protein 1 (INSM1) is a sensitive and specific marker of neuroendocrine neoplasia in the gastrointestinal tract

Hee Eun Lee¹, Tsung-Teh Wu², Samar Said¹, Lizhi Zhang¹, Andrew Bellizzi³, Rondell Graham²

¹Rochester, MN, ²Mayo Clinic, Rochester, MN, ³University of Iowa Hospitals and Clinics, Iowa City, IA

Disclosures: Hee Eun Lee: None; Tsung-Teh Wu: None; Samar Said: None; Lizhi Zhang: None; Andrew Bellizzi: None; Rondell Graham: None

Background: The aim of this study was to determine the utility of INSM1 immunostain as a diagnostic marker of neuroendocrine neoplasm focusing on gastrointestinal (GI) and liver tumors using whole tissue sections.

Design: Whole sections from well-differentiated neuroendocrine tumor (WD NET; n=60) from gastrointestinal primaries; poorly-differentiated neuroendocrine carcinoma (PD NEC; n=30); and gangliocytic paraganglioma (GPG; n= 4) were stained for INSM1, synaptophysin, and chromogranin. As a control group to determine specificity, potential morphologic mimics including hepatocellular carcinoma (n=20), intrahepatic cholangiocarcinoma (n=22), acinar cell carcinoma (n=5), adrenocortical carcinoma (n=10), melanoma (3 rectal and 6 non-GI), diffuse large B cell lymphoma (n=5), Ewing sarcoma (n=3), rhabdomyosarcoma (n=5), and squamous carcinoma (n=5) were stained for the same markers on whole sections. PD NECs with negative synaptophysin and chromogranin were either small cell type or positive for CD56. Nuclear staining with at least moderate intensity was considered positive for INSM1. Immunostains for all 3 markers were graded as 0 = no staining, 1+ = 1-10% of tumor cells, 2+ = 11-25% of cells, 3+ = 26-50% of cells, 4+ = >50% of tumor cells.

Results: Immunostain results of INSM1, synaptophysin, and chromogranin are listed in Table. Synaptophysin and chromogranin stains were unavailable for 2 (intrahepatic cholangiocarcinoma and adrenocortical carcinoma) and 1(intrahepatic cholangiocarcinoma) cases, respectively. The 7 WD NETs negative/1+ chromogranin were from the rectum; all were positive for INSM1. INSM1 was positive (2+) in 1 of 3 PD NECs which were negative/1+ for both synaptophysin and chromogranin. 3 cases of non-NETs, rhabdomyosarcoma, adrenocortical carcinoma and rectal melanoma (n=1 each), showed diffuse (3+ or 4+) positivity for INSM1. When immunoreactivity in >10% of tumor cells is considered positive, the sensitivity (%) / specificity (%) of INSM1, synaptophysin, and chromogranin immunostains for diagnosing WD NET were 100/90, 100/85, and 88/100, respectively; and 87/90, 90/85, and 60/100 for diagnosing PD NEC.

Table: A table showing the expression of each of the 3 assayed markers in the cohort of whole tissue sections.

Tumor type	Total	N =178											
		Negative			1+			2+			3+ - 4+		
		INSM1	Syn	Chrom	INSM1	Syn	Chrom	INSM1	Syn	Chrom	INSM1	Syn	Chrom
WD NET	60	0	0	1	0	0	6	1	0	1	59	60	52
PD NEC	30	2	0	9	2	3	3	2	2	1	54	25	17
GPG	4	0	0	0	0	0	0	1	0	0	3	4	4
Acinar cell carcinoma	5	2	2	2	2	3	3	1	0	0	0	0	0
Adrenocortical carcinoma	10	8	1	10	1	0	0	0	0	0	1	8	0
DLBCL	5	4	5	5	1	0	0	0	0	0	0	0	0
Ewing sarcoma	3	2	2	3	0	0	0	1	0	0	0	1	0
HCC	20	19	19	20	1	0	0	0	1	0	0	0	0
Intrahepatic CC	22	16	21	21	6	0	0	0	0	0	0	0	0
Melanoma	9	6	8	9	1	0	0	1	0	0	1	1	0
Rhabdomyosarcoma	5	2	3	5	1	1	0	1	0	0	1	1	0
Squamous cell carcinoma	5	0	5	5	4	0	0	1	0	0	0	0	0

INSM1 - Insulinoma-associated protein 1; Syn – Synaptophysin; Chrom – Chromogranin; WD NET, well-differentiated neuroendocrine tumor; PD NEC, poorly-differentiated neuroendocrine carcinoma; GPG, gangliocytic paraganglioma; DLBCL, diffuse large B cell lymphoma; HCC, hepatocellular carcinoma; intrahepatic CC, intrahepatic cholangiocarcinoma

Conclusions: INSM1 is a useful marker in making a diagnosis of a neuroendocrine neoplasm in GI pathology practice with better sensitivity than chromogranin and better specificity than synaptophysin. In particular, INSM1 highlighted all hindgut WD NETs.

676 Her2 expression and amplification of Colorectal Adenocarcinomas: a prospective study of 1046 cases

Sun Mi Lee¹, Chang Ohk Sung²

¹Jeju National University Hospital, Jeju-si, Korea, Republic of South Korea, ²University of Ulsan College of Medicine, Asan Medical Center, Seoul, Korea, Republic of South Korea

Disclosures: Sun Mi Lee: None; Chang Ohk Sung: None

Background: Her2/neu overexpression and/or amplification are known to be associated with clinical outcome and enables to predict the response to chemotherapy in some carcinomas including colorectal carcinomas (CRCs). However, Her2/neu positivity rates are not consistent and controversial in prior studies, ranging from 2.7% to 47.7%. We prospectively assessed the prevalence and clinicopathologic significance of HER2 overexpression/amplification in a series of 1046 primary CRC samples revealed by immunohistochemistry and silver in situ hybridization (SISH) and further performed a next-generation sequencing (NGS) and microsatellite instability testing on tumors with Her2 amplification to analyze molecular characteristics.

Design: We have prospectively performed immunohistochemistry for cerbB2 on all surgically resected primary CRCs from 2016 and detected 242 positive tumors. We evaluated HER2 amplification using SISH in a whole tissue section of 86 positive tumors (2+ and 3+ tumors) after reviewed. Tumors with Her2 amplification confirmed by SISH subject to molecular profiling using NGS on the Ion Torrent PGM (Thermo Fisher Scientific) and were examined substitution, small indels and variations of copy numbers of amplified gene in 409 cancer-related

Results: Of 1046 surgically resected primary CRCs, 242 tumors showed expression of cerbB2, consisting of 155 CRCs with 1+ positivity, 52 tumors with 2+ positivity and 35 tumors with 3+ positivity. All 35 tumors with 3+ expression showed HER2 amplification on SISH. Ten of fifty-two tumors with 2+ positivity showed HER2 amplification on SISH. In total, 44 of 1046 primary CRCs were HER2 amplified (4.2%) on SISH and 41 tumors arose from the rectosigmoid colon. Sequence variations of HER2 amplified 44 tumors were observed in TP53, KRAS, APC, SMAD4, PIK3CA and ERBB2/3. Eleven (25%) of Her2 amplified 44 tumors harbor KRAS mutations in codon 12 and 13. Her2 amplification were found in all 44 cases on NGS showing 2 to 39 copy numbers. All Her2 amplified tumors were microsatellite stable. Six (85.7%) of seven metastatic tumors showed Her2 amplification on SISH.

Conclusions: In our cohort study, Her2 amplification was identified in 4.2% of 1046 primary CRCs and predominantly left colon. Main oncogenic mutations including TP53, KRAS, APC and PIK3CA were observed in Her2 amplified 44 CRCs showing a relative low frequency of KRAS mutations. These findings suggest that anti-HER2 therapy is beneficial for approximately 4-5% of patients with CRC.

677 Clinicopathological features and metastatic patterns of patients with gastroenteropancreatic mixed adenoneuroendocrine carcinoma

Zhong Wu Li¹, Panpan Zhang², Ming Lu²

¹Peking University, Beijing, China, ²Department of Gastrointestinal Oncology, Beijing, China

Disclosures: Zhong Wu Li: None

Background: Gastroenteropancreatic mixed adenoneuroendocrine carcinoma (GEP-MANEC) is a rare and aggressive neoplasm with worse prognosis. We aim to evaluate the clinicopathologic characteristics and metastatic patterns of GEP-MANECs.

Design: Clinical data of patients with a pathological diagnosis of GEP-MANEC and radiological evaluation of lymph nodes or distant metastases were retrospectively analyzed.

Results:

20 patients with MANEC received surgery and had regional lymph node metastasis. 70% (14/20) patients had lymph nodes with pure adenocarcinoma (AC) or neuroendocrine (NE) component, 15% (3/20) patients had both of the two components separately metastasizing to different lymph nodes, and only 15% (3/21) patients had both two components coexisted in the same lymph nodes. The characteristics of lymph node metastasis were not correlated with the differentiation but may be related to the proportion of the two components. 20 patients with distant metastasis performed biopsy of both primary and metastatic lesions. 40% (8/20) distant metastases had two components, and 60% (12/20) metastases showed pure NEC component. 65% (13/20) patients had liver metastases (4 cases of mixed component, 9 cases of NEC component), 1 case had lung metastasis of two components, 2 cases had peritoneal nodules metastases (1 case of NEC component, 1 case of both components), 4 cases had supraclavicular lymph node metastases (2 cases of both components, 2 cases of NEC). Component accounting for less than 30% can still metastasize to the distant lesions.

Table1 Clinical and pathological features of MANEC with lymph nodes metastasis after surgery

Case	Gender	Age	Tumor Site	Exocrine component	NEN component	Exocrine /NEN (%)	Ki67	Lymph nodes	Exocrine	NEN	mixed	recurrent	DFS (mo)	vital	OS (mo)
1	Male	72	Stomach	PD AC	NEC	40/60	30%	12/40	0	12	0	0	51.1	0	51.5
2	Female	78	Stomach	MD AC	NEC	50/50	80%	2/37	2	0	0	0	3.2	0	3.2
3	Female	64	Stomach	PD AC	NEC	70/30	80%	6/27	6	0	0	0	6.9	0	11.4
4	Male	52	Stomach	PD AC	NEC	10/90	75%	5/20	0	5	0	0	60.7	0	63.4
5	Male	59	Esophagus	MD SC	NEC	/	75%	5/36	0	0	5	1	1.5	0	14.0
6	Male	46	Esophagus	PD AC	NEC	/	75%	1/30	0	0	1	1	0.9	0	17.4
7	Female	69	Stomach	PD AC	NEC	50/50	70%	16/30	8	8	0	/	/	/	/
8	Male	69	Stomach	MD AC	NEC	15/85	60%	17/21	0	17	0	0	5.3	0	5.9
9	Male	48	Rectal	MD AC	NEC	10/90	60%	19/23	5	14	0	0	8.6	0	9.2
10	Male	46	Stomach	MD AC	NEC	/	75%	6/19	0	6	0	0	1.0	0	1.0
11	Female	57	Gallbladder	WD AC	NEC	/	80%	1/1	0	1	0	0	26.0	0	26.3
12	Male	63	Stomach	PD AC	NEC	20/80	80%	3/12	0	3	0	1	9.9	0	18.6
13	Male	51	Esophagus	MD SC	NEC	/	80%	2/17	0	0	2	1	1.9	0	30.5
14	Male	79	Esophagus	MD SC	NEC	/	90%	2/5	0	2	0	1	18.8	1	20.3
15	Male	60	Stomach	MD AC	NEC	70/30	75%	7/76	7	0	0	0	/	/	/
16	Male	63	Colon	PD AC#	NEC	60/40	90%	9/20	9	0	0	0	5.3	0	5.3
17	Male	48	Gallbladder	MD AC	NEC	30/70	/	1/1	0	1	0	0	6.3	0	7.9
18	Male	77	Colon	MD AC	NEC	/	/	2/2	2	0	0	/	/	/	/
19	Male	64	Rectal	PD AC	NEC	40/60	30%	7/14	0	7	0	0	9.8	0	11.7
20	Male	56	Stomach	MD AC	NEC	5/95	70%	11/24	2	9	0	0	8.6	0	9.9

AC, adenocarcinoma; SC, squamous carcinoma; # the case was mucinous adenocarcinoma;

Conclusions: Lymph node and distant metastases have different metastatic patterns in patients with GEP-MANEC. Regional lymph nodes mostly showed NE or AC component only; distant metastases at diagnosis or recurrence are dominated invaded by NE component, which is independent of the proportion of two components of the primary lesions. The component less than 30% of the tumor can still metastasize to the distant lesions, indicating that the threshold should be reevaluated and defined.

678 Lymphocytic Gastritis in Children: Report of 23 Cases

Yongchao Li¹, Anas Bernieh², Yaohong Wang¹, Jie Zhang¹, Siraj El Jamal³, Ali Saad⁴

¹University of Tennessee Health Science Center, Memphis, TN, ²University of Mississippi Medical Center, Jackson, MS, ³Icahn School of Medicine at Mount Sinai, New York, NY, ⁴Methodist/LeBonheur Health System, Memphis, TN

Disclosures: Yongchao Li: None; Anas Bernieh: None; Yaohong Wang: None; Jie Zhang: None; Siraj El Jamal: None; Ali Saad: None

Background: Lymphocytic gastritis (LG), defined as the presence of ≥ 25 intraepithelial lymphocytes (IELs)/100 epithelial cells regardless of the inflammation in the lamina propria, is uncommon in children and has not been well studied. We report the largest series of LG in children with clinical follow-up.

Design: Pediatric LG cases were collected from multiple institutions. Serology for celiac disease was performed on all patients (tissue transglutaminase antibodies). Slides were reviewed and a representative block from the stomach was immunostained with CD3, CD4, CD8, CD20 and H. pylori antibodies. Clinical follow-up information was retrieved from the patients' medical records.

Results: The search resulted in 23 pediatric patients with LG (13 males and 10 females). Median age was 9.6 years (range 3-18 years). The most common clinical presentations were abdominal pain in 13 patients (56.5%) and diarrhea in 7 patients (30.4%). The number of gastric IELs ranged from 27-66/100 epithelial cells (median: 41). Lamina propria cellularity was normal in 10 patients (43.5%) and increased in 11 patients (47.8%). Two patients (8.7%) showed chronic active gastritis. In the duodenum, 9 patients (39.1%) showed < 40 IELs/100 enterocytes and 14 (60.9%) patients showed > 40 /100 enterocytes.

By immunohistochemistry, gastric IELs were predominantly CD3-positive T-cells with very minor CD20-positive B-cells. CD4 and CD8 were expressed in 20% and 30% of gastric IELs, respectively.

Follow-up showed that 11 patients (47.8%) were diagnosed with celiac disease, 5 patients (21.7%) with Crohn's disease, 4 patients (17.4%) had no definitive diagnosis, 2 patients (8.8%) were diagnosed with H. pylori gastritis and 1 patient (4.3%) was found to have lymphocytic colitis. Statistical analysis showed no correlation between gastric IELs and a particular disease. Interestingly, 2 patients with > 40 IELs in duodenum were diagnosed with Crohn's disease and H. pylori gastritis, respectively, and both showed negative celiac serological studies.

Conclusions: In pediatric patients, LG is frequently associated with the presence of other gastrointestinal disorders, particularly celiac disease or Crohn's. The number of gastric IELs is not disease specific. We conclude that the presence of ≥ 25 gastric IELs/100 epithelial cells should trigger additional work up including, but not limited to, H. pylori immunostain, serology for celiac disease and colonoscopy/biopsy.

679 C-myc expression helps distinguish intestinal-type dysplasia from reactive changes in the stomach antrum

Yuanxin Liang¹, Natalie Ciomek²

¹Boston, MA, ²Tufts Medical Center, Boston, MA

Disclosures: Yuanxin Liang: None

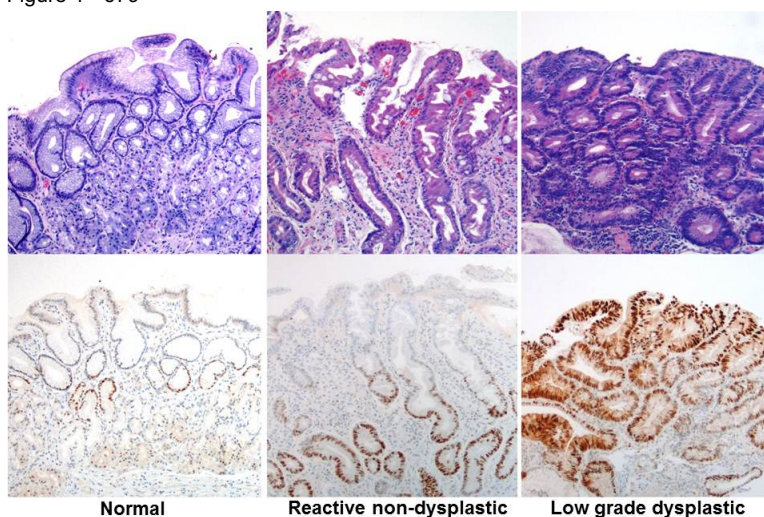
Background: Diagnosing gastric dysplasia is often difficult in patients with dysplasia-associated reactive changes due to gastritis, the latter of which can mimic dysplasia both cytologically and architecturally. Dysregulation of the oncogene C-myc has been described in gastric cancer. An increase in MYC copy number has been noted during the sequential steps of intestinal-type gastric carcinogenesis. The purpose of this study was to evaluate the expression pattern, frequency, and utility of c-myc immunohistochemistry in distinguishing true gastric dysplasia from dysplasia-like reactive changes.

Design: C-myc immunohistochemistry was performed on gastric biopsies of 41 biopsies with intestinal metaplasia from 18 patients. Twenty-five (25) non-dysplastic biopsies had chronic gastritis with intestinal metaplasia and 16 had dysplasia. Immunohistochemistry was also performed on 10 cases of normal stomach without gastritis. In all cases, C-myc expression was evaluated in the surface, pit, and glandular epithelium separately and graded as positive on a semi-quantitated scale.

Results: C-myc immunohistochemistry of normal stomach demonstrated nuclear expression of the gastric glands only (Figure 1). In cases of gastritis-associated reactive changes, c-myc was expressed in the glandular (100%) and in the pit epithelium (32%), but in the surface epithelium in only 1 case (4%). In contrast, dysplastic epithelium demonstrated expression in the glands (100%), pits (100%), and surface epithelium in almost all cases (85% for low-grade; 100% for high-grade dysplasia) (Table 1). The difference in surface epithelial expression in true dysplastic cases was statically significant compared to non-dysplastic cases ($p < 0.001$). When using c-myc surface epithelial expression to confirm dysplasia, the sensitivity was 93.3%, the specificity was 92.3%, and the accuracy was 92.6%. Differences in expression of c-myc between low and high-grade dysplasia were not statistically significant.

	Non-dysplastic (n=25)	Low grade dysplastic (n=13)	High grade dysplastic (n=3)
Surface epithelium	4%	84.6%	100%
Pit epithelium	32%	100%	100%
Glandular epithelium	100%	100%	100%

Figure 1 - 679



Conclusions: C-myc expression is a useful adjuvant test to help discriminate true dysplasia from dysplasia-like reactive changes in patients with chronic gastritis. Future studies should be done to evaluate c-myc expression patterns in different types of dysplasia and in other dysplastic lesion of the esophagus and intestines.

680 Mutational Profiling of High Grade Appendiceal Mucinous Neoplasms

Xiaoyan Liao¹, Vera Vavinskaya², Katherine Sun³, Yansheng Hao⁴, Xiaodong Li⁵, Mark Valasek⁶, Jane Houldsworth⁷, Noam Harpaz⁸

¹University of Rochester Medical Center, Rochester, NY, ²University of California, San Diego, San Diego, CA, ³NYU Langone Health, New York, NY, ⁴New York, NY, ⁵South Pasadena, CA, ⁶University of California, San Diego, La Jolla, CA, ⁷Icahn School of Medicine at Mount Sinai, New York, NY, ⁸Mount Sinai Medical Center, New York, NY

Disclosures: Xiaoyan Liao: None; Vera Vavinskaya: None; Katherine Sun: None; Yansheng Hao: None; Xiaodong Li: None; Mark Valasek: None; Jane Houldsworth: None; Noam Harpaz: None

Background: Low-grade appendiceal mucinous neoplasm (LAMN) is a well-recognized entity which was included in the WHO 2010 tumor classification. In contrast, high-grade mucinous neoplasm (HAMN), its cytologically high grade counterpart, was largely overlooked in the published literature due to its rarity. As a result, information regarding its natural history, histogenesis and molecular characteristics is incomplete.

Design: Tumors diagnosed as HAMN between 2009 and 2018 were contributed by the pathology departments of three large academic centers (Mount Sinai, UCSD, New York University). Concurrent appendiceal tumors including LAMNs, serrated polyps and colonic-type adenocarcinomas with mucinous features (MACA, >30% mucinous component) served as a source of controls. The slides of each case were re-reviewed to verify fulfillment of the diagnostic criteria (Carr et al., AJSP 2016. 40: 14-26). Relevant clinical and pathological data were obtained from electronic medical records. Representative tumor sections were analyzed by targeted next generation sequencing (NGS) of 50 genes using the Ion AmpliSeq Cancer Hotspot Panel (v2, Thermo Fisher). Chi square statistical analysis employed a significance threshold of $P \leq 0.05$.

Results: We collected 9 cases of HAMN and 23 control tumors comprising 5 serrated polyps, 8 LAMNs, and 10 MACA. The cases and controls had similar gender and age profiles, with an average follow-up of 15 months. All patients survived except one with MACA. NGS revealed high frequencies of KRAS and GNAS mutations in both LAMN and HAMN (KRAS: 100% in both; GNAS: 63% and 56%, respectively), collectively higher than serrated polyps (KRAS: 20%, $P=0.007$, GNAS: 0, $P=0.0396$) and MACA (KRAS: 70%, $P=0.041$; GNAS: 10%, $P=0.012$). No other genetic mutations were detected in LAMN. However, 5 HAMN contained mutations of either TP53 ($n=4$, 44%) and/or ATM ($n=2$, 22%), among which 3 (33%) had concurrent extra-appendiceal adenocarcinomas (EAA). NGS on all 3 EAA detected the same mutations as the corresponding HAMN. Appendiceal MACA harbored similar rate of TP53 mutations ($n=5$, 50%), as well as mutation in APC, FBXW7, PIK3CA, PTEN, and SMAD4 genes that are commonly associated with colorectal carcinoma (Figure 1).

Figure 1 - 680

Genes/group	SP			LAMN				HAMN				MACA			
BRAF															
KRAS															
GNAS															
TP53															
ATM															
PIK3CA															
APC															
FBXW7															
PTEN															
SMAD4															
* Case has concurrent extraappendiceal adenocarcinoma/mucinous carcinoma peritonei															

Conclusions: Our data suggest that HAMN and LAMN are biologically related as they share high rates of KRAS and GNAS mutation that reliably distinguish them from serrated polyps and MACA; however, HAMN contains additional mutations in TP53 or ATM correlating with disease progression.

681 Differential PD-L1 Expression in Post-Transplant Lymphoproliferative Disorder after Solid Organ Transplant

Xiaoyan Liao¹, Yansheng Hao², Abul Ala Syed Rifat Mannan³, Shafinaz Hussein⁴, Noam Harpaz⁵, Huaibin Mabel Ko⁴

¹University of Rochester Medical Center, Rochester, NY, ²New York, NY, ³Perelman School of Medicine at the University of Pennsylvania, Philadelphia, PA, ⁴Icahn School of Medicine at Mount Sinai, New York, NY, ⁵Mount Sinai Medical Center, New York, NY

Disclosures: Xiaoyan Liao: None; Yansheng Hao: None; Abul Ala Syed Rifat Mannan: None; Shafinaz Hussein: None; Noam Harpaz: None; Huaibin Mabel Ko: None

Background: Post-transplant lymphoproliferative disease (PTLD) is a well-recognized EBV-associated organ transplant complication which occurs more frequently after intestinal transplant (ITX, ~20%) than other solid organ transplants (SOT, ~5%). Programmed cell death 1 (PD-1) receptor and its ligand PD-L1 are normally involved in autoimmune regulation but also allow immune escape by tumor cells. Upregulation of PD-L1 is associated with EBV infection and portends a worse outcome in certain tumor types. To date, there is limited data regarding PD-L1 expression in PTLD.

Design: Cases of PTLD following intestinal, liver or kidney transplants diagnosed between 2005 and 2018 were identified from our pathology database. Clinical and pathologic details were collected from electronic medical records. Slides were reviewed to confirm the diagnosis and EBV status (EBER-ISH). IHC staining for PDL-1 (clone 22C3, Dako NA) was performed according to manufacturer's recommendations and was scored positive if ≥5% of the tumor cells showed strong membranous staining. Chi square analysis was performed with a significance threshold of P>0.05.

Results: We identified 21 cases of PTLD including 13 after ITX and 8 after liver (6) and kidney (2) transplants (L/KT). Ten patients (48%) were pediatric and 11 (52%) were adults. There was no significant age difference between patients with ITX vs. L/KT at the time of PTLD diagnosis, however, all L/KT patients were female compared to an even gender distribution in ITX (P=0.018). The median post-transplant interval to PTLD was similar in ITX and L/KT (6 m [range 1-140] vs. 9.5 m [range 5-108]). Nearly all of the lesions involved the gastrointestinal tract (20/21, 95%) (one exception involved bone marrow). Histologically, 6/13 (46%) ITX and 2/8 (25%) L/KT cases were monomorphic-type PTLD and the remainder were polymorphic. EBER-ISH was positive in 17/21 (81%) cases. PD-L1 was expressed more frequently in ITX compared to L/KT (10/13 [77%] vs. 2/8 [25%], p=0.0318). A mean 14-month follow-up in patients with ITX revealed higher mortality with 8 disease-associated deaths (62%) compared to 1 death (13%) in L/KT (P=0.0274) after a mean 71-month follow-up.

Conclusions: PTLD is a serious complication of SOT in both children and adults. We found PTLD post ITX to have a higher expression of PD-L1 and higher mortality rate than PTLD post L/KT. Additional studies are warranted to understand the disease mechanism and explore potential benefits of anti-PD-1/PD-L1 immunotherapy.

682 Mid Esophagus Histological Recovery Lags Behind Distal Esophagus in Remission of Eosinophilic Esophagitis

Bo Lin¹, Raavi Gupta¹, Neha Ahuja¹, Ning Chen¹, Simon Rabinowitz¹

¹SUNY Downstate Medical Center, Brooklyn, NY

Disclosures: Bo Lin: None; Raavi Gupta: None; Neha Ahuja: None

Background: Eosinophilic esophagitis (EoE) is diagnosed based on clinical presentations and esophageal histology with >15 epithelial eosinophils per high power field (hpf). Associated esophageal remodeling is believed to be responsible for EoE complications such as dysmotility, strictures and food impactions. Remodeling includes histologic changes of basal cell hyperplasia, dilated intercellular space and fibrosis. In this study, we showed pathologic features of remodeling recover to baseline levels after treatment when symptoms and eosinophilia normalize.

Design: Three patient cohorts were studied: 1. active EoE patients as determined by clinical features and esophageal biopsies containing >15 eos/hpf (n=36; 76 biopsies, 39 distal, 37 mid). 2. patients in clinical remission after treatment with no mucosal eosinophilia (n=12; 24 biopsies, 12 distal, 12 mid). 3. Patients without EoE as a control group (n=37; 37 distal, 37 mid).

A comprehensive histology scoring system previously described by Cincinnati children's hospital were used to assess: maximum eosinophil count/hpf, basal zone hyperplasia, eosinophil abscesses, eosinophil surface layering, dilated intercellular spaces, surface epithelial alteration, dyskeratotic epithelial cells, and lamina propria fibrosis. Severity (grade) of abnormalities were scored using a 4-point scale and total grade scores were calculated.

Results: Median total grade scores were higher in the mid and distal esophageal biopsies of EoE active patients compared with those in remission as well as to the controls (p < 0.01). The total grade scores in distal esophageal biopsies were not significantly different between remission and control patients (p=0.3); however, they remained higher in the mid esophageal biopsies of patients in remission compared to

controls ($p < 0.01$), indicating the remodeling recovery lagged in the mid than distal esophagus.(Figure 1). Basal zone hyperplasia and dilated intercellular spaces were features still remained in mid esophagus in the remission cohort.

Figure 1 - 682

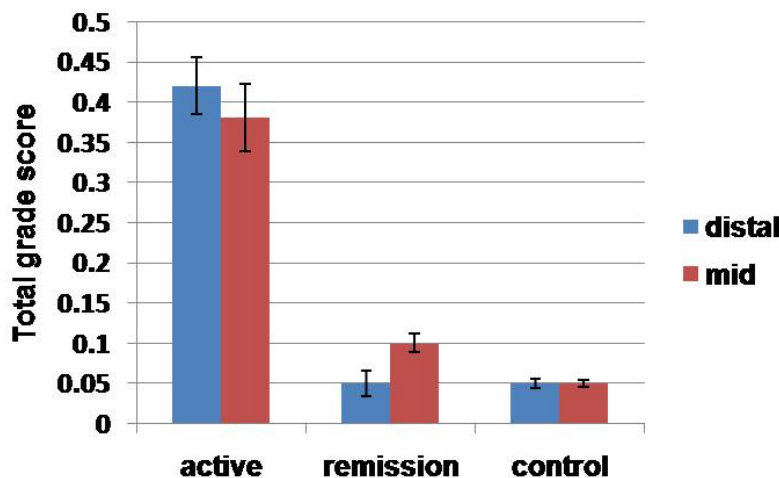


Figure 1. Total grade scores in three cohorts.

Conclusions: The EoE histology scoring system is more effective than eosinophil count in evaluating patients with EoE especially during remission. Patients in remission reached the baseline levels seen in controls in distal esophagus, whereas the recovery of mid esophagus lagged behind distal esophagus with residual basal zone hyperplasia and dilated intercellular spaces after treatment.

683 Human Papillomavirus-Induced Anal Squamous Precancer and Cancer in Patients with Inflammatory Bowel Disease (IBD)

Qingqing Liu¹, Yuxin Liu²

¹Icahn School of Medicine at Mount Sinai, New York, NY, ²Mount Sinai Health System, New York, NY

Disclosures: Qingqing Liu: None; Yuxin Liu: None

Background: Owing to their immunocompromised status, patients with IBD are susceptible to human papillomavirus (HPV) infection in the anal canal and subsequent development of anal squamous precancer (i.e. High-grade squamous intraepithelial lesion, HSIL) and cancer. Using a cohort of IBD patients under longitudinal surveillance via endoscopic biopsy or surgical resection, we aimed to determine the prevalence of HPV-induced anal squamous precancer and cancer as well as associated risk factors.

Design: We searched the pathology database for biopsy or resection specimens from the anal canal for patients with established diagnosis of IBD. Patient demographics were extracted from medical records and multiple clinicopathological parameters were analyzed.

Results: 130 IBD patients met inclusion criteria for this study. Patients had an established diagnosis of Crohn's disease (n=72, 55%), ulcerative colitis (n=50, 39%), or indeterminate colitis (n=8, 6%). 53 patients were female (41%) and 77 patients were male (59%) with a median age of 51 years (range, 19-83). Five male patients were HIV-infected (16%). The average duration since initial IBD diagnosis was 8 years (range, 1-21). The majority of specimens (n=114, 87%) were biopsy samples while 16 (13%) resulted from total proctocolectomy. Overall, HPV-induced squamous lesions were detected in eighteen patients (14%), including LSIL (n=3, 2%), HSIL (n=13, 10%), and invasive squamous cell carcinoma (n=2, 2%). The two cancer patients included a 77-year-old female with 15 years of ulcerative colitis and a 62-year-old male with Crohn's disease for 10 years. Compared to patients with normal mucosa or LSIL, patients with HSIL or cancer were older (median age 62 vs. 50), had diagnosis of ulcerative colitis (63% vs. 29%), and longer periods of IBD (13 vs. 9 years). All 5 HIV-infected IBD patients had HSIL lesions.

Conclusions: IBD patients are at risk of developing anal squamous precancer and cancer. Older patients with prolonged IBD and ulcerative colitis are at greater risk. Our findings warrant the integration of anal cancer screening within routine surveillance for IBD patients. Pathological examination of total proctocolectomy including anus from IBD patients should include careful gross examination and sufficient sampling of the anal squamous mucosa.

684 SOX9 Overexpression Is A Poor Prognostic Indicator in Gastric Cancer

Wenyi Luo¹, Hongxia Sun¹, Lei Zhang², Junsheng Ma¹, Roland Bassett¹, Dongfeng Tan¹

¹The University of Texas MD Anderson Cancer Center, Houston, TX, ²The University of Texas MD Anderson Cancer Center, Gainesville, FL

Disclosures: Wenyi Luo: None; Hongxia Sun: None; Lei Zhang: None; Junsheng Ma: None; Roland Bassett: None; Dongfeng Tan: None

Background: Gastric cancer is a group of common malignancy, resulting in most cancer mortality world-wide only after lung and colorectal cancer. Gastric cancer stem cells were recently identified and associated with increased resistance for chemotherapy- or radiation-induced cell death. SOX9 is a marker for stem cells. Its expression is required for bacteria-induced gastric cancer cell proliferation and correlated with higher tumor stage and lymph node metastasis. However, the survival impact of SOX9 and its correlation with other biomarkers has not been systematically explored. Because SOX9 overexpression is a potential target for cancer treatment, in this study, we aimed to evaluate the expression of SOX9 in a large cohort of patients with gastric adenocarcinoma.

Design: The study included 201 primary gastric cancer patients who underwent surgical resection with no preoperative treatment at our institution between 1987 and 2006. High-density tissue microassays (TMAs) were assembled from selected regions of archived donor tissue containing viable tumor and normal tissue elements. Formalin-fixed paraffin-embedded tissue from these resection specimens were assessed for SOX9 immunohistochemical stains. The nuclear expression of SOX9 in tumor cells were analyzed along with MUC2 (a marker for intestinal differentiation) and HER2/neu expression. Critical clinicopathologic parameters in this study include age, race, gender, tumor differentiation and pathologic stage of the tumor.

Results: Among 201 patients, 64 had high nuclear expression of SOX9; 62 had moderate and 75 had low expression. Higher SOX9 expression was observed in male patients (median=3 vs. 2 for female, $p=0.036$) and tumors with high MUC2 expression (median=6 for high MUC2 expression vs. 4 for moderate and 2 for low, $p=0.031$). There was no correlation between SOX9 with other clinicopathologic parameters identified (table 1). A fitted multivariate Cox model demonstrated that SOX9 was associated with a worse overall survival (HR=1.08, 95%CI: 1.02-1.14, $p=0.009$). In subgroup analyses, higher values of SOX9 were statistically associated with worse overall survival in patients poorly differentiated tumors.

Table 1. Patient characteristics by SOX9 expression

SOX9 expression	Low	High	Moderate	P
Age, Median	62.7	64.7	63.5	0.324
Race, n (%)				0.857
Asian	8 (10.7)	7 (10.9)	12 (19.4)	
Black	9 (12.0)	8 (12.5)	5 (8.1)	
Cacasian	45 (60.0)	38 (59.4)	35 (56.5)	
Hispanic	12 (16.0)	11 (17.2)	9 (14.5)	
Other	1 (1.3)	0 (0.0)	1 (1.6)	
Gender, n (%)				0.062
Female	37 (49.3)	19 (29.7)	24 (38.7)	
Male	38 (50.7)	45 (70.3)	38 (61.3)	
T stage, n (%)				0.279
T1	13 (17.3)	12 (18.8)	13 (21.0)	
T2	8 (10.7)	8 (12.5)	5 (8.1)	
T3	39 (52.0)	32 (50.0)	22 (35.5)	
T4	15 (20.0)	12 (18.8)	22 (35.5)	
N stage, n (%)				0.184
N0	16 (23.9)	15 (23.8)	16 (27.1)	
N1	17 (25.4)	16 (25.4)	5 (8.5)	
N2	16 (23.9)	16 (25.4)	15 (25.4)	
N3	18 (26.9)	16 (25.4)	23 (39.0)	
M stage, n (%)				0.833
M0	63 (84.0)	55 (85.9)	51 (82.3)	
M1	12 (16.0)	9 (14.1)	11 (17.7)	
Tumor differentiation, n (%)				0.253
Poorly differentiated	31 (42.5)	20 (32.3)	25 (41.0)	
Signet ring cell	16 (21.9)	9 (14.5)	14 (23.0)	
Well/Mod. differentiated	26 (35.6)	33 (53.2)	22 (36.1)	
HER2, n (%)				0.191
Negative	72 (97.3)	58 (90.6)	60 (96.8)	
Positive	2 (2.7)	6 (9.4)	2 (3.2)	

Conclusions: Our study demonstrated that SOX9 was associated with the male gender and intestinal differentiation. More importantly, SOX9 overexpression was an independent prognostic indicator of gastric adenocarcinoma and significantly associated with worse overall survival especially in patients with poorly differentiated tumors.

685 Histopathology of Colorectal Cancer in the Context of Consensus Molecular Subtypes and Prognostic Implication

Wenyi Luo¹, Riham Katkhuda¹, Scott Kopetz¹, David Menter¹, Jeffrey Morris¹, Dipen Maru¹

¹The University of Texas MD Anderson Cancer Center, Houston, TX

Disclosures: Wenyi Luo: None; Riham Katkhuda: None; Scott Kopetz: None; David Menter: None; Jeffrey Morris: None; Dipen Maru: None

Background: The gene expression based Consensus Molecular Subtype (CMS) classification has been a landmark development in understanding biology and prioritizing clinical trials for patients with colorectal cancer. Role of histopathology features in predicting a CMS subtype and their contribution in enhancing prognostic and predictive value of a CMS class of colorectal cancer is not yet studied.

Design: H&E slides of 79 primary colorectal cancers that were included in the original study for CMS classification by Guinney et al. (Nature Medicine, Vol. 21, 2015) were reviewed by a gastrointestinal pathologist (W.L.) who was blinded from the CMS subtype and clinical features of these patients. Tumors from CMS 1 were excluded, because most of these tumors were MSI-H and MSI-H CRC has unique histologic features. Pathologic TNM stage, histologic grade, mucinous subtype, infiltrative vs. pushing border, lymphovascular invasion were assessed as per the AJCC/CAP guidelines. Additional histologic features were assessed based on published criteria or criteria generated for this study as shown in Table.

Results: Please see table 1. CMS2 tumors were characterized by high mitotic activity, geographic necrosis and low prevalence of mucinous histology. CMS4 tumors were larger in size, had high N stage, higher prevalence of extramural large vessel invasion, non-glandular growth, infiltrative border, high frequency of tumor budding and poorly differentiated tumor cell clusters. Tumors in CMS3 were more likely to be goblet cell rich and have lower N stage. In the patients with CMS 4 subtype, non-glandular growth was associated with a poor overall survival (101 months vs. 126 months, $p=0.035$) and relapse-free survival (103 months vs. 124 months, $p=0.046$) as compared to patients with CMS 4 subtype with glandular growth only.

Table 1. Histopathological characteristics of patients

	CMS2 (n=45)	CMS3 (n=9)	CMS4 (n=25)	P	
Site, left/right	28/17	5/4	15/9	0.92	
Size (cm), mean±SD	4.4±1.5	5.5±0.8	6±2.6	0.002*	
High grade, n (%)	11 (24.4)	1 (11.1)	9 (36.0)	0.3	
Mucinous adenocarcinoma by 50% cutoff, n (%)	1 (2.2)	4 (50.0)	15 (60.0)	<0.001*	
Mucin percentage, mean±SD	2.7±8.5	60.0±39.7	31.0±37.5	1	
Mitoses/10 HPFs, mean±SD	52.4±23.0	22.2±15.5	34.8±19.4	<0.001*	
Goblet cell-rich by 20/20x cutoff based on average count of ten 20x fields, n (%)	5 (11.1)	7 (77.8)	7 (28.0)	<0.001*	
Nonglandular growth pattern, n (%)	5 (11.1)	1 (11.1)	12 (48.0)	0.001*	
Gegraphic necrosis-high by 10% cutoff, n (%)	24 (53.3%)	1 (11.1)	9 (36.0)	0.004*	
Infiltrative tumor border, n (%)	9 (20.0)	1 (11.1)	12 (48.0)	0.02*	
Tumor budding by 4/20x cutoff based on count of one 20x field at the tumor invasive front with the most tumor buds, n (%)	19 (42.2)	1 (11.1)	18 (72.0)	0.004*	
Poorly differentiated tumor cluster by 10/20x cutoff based on count of one 20x field at the tumor invasive front with the most tumor buds, n (%)	19 (42.2)	1 (11.1)	16 (64.0)	0.02*	
Percentage of stroma, mean±SD	37.0±19.0	28.3±9.4	45.2±17.6	0.04*	
Intramural lymphovascular invasion, n (%)	29 (64.4)	2 (22.2)	21 (84.0)	0.004*	
Extramural large vessel invasion, n (%)	10 (22.2)	1 (11.1)	12 (48.0)	0.04*	
Positive regional nodes, mean±SD	1.7±2.3	0.7±1.1	4.2±6.5	0.02*	
pT	T2 4	0	0	0.02*	
	T3 33	8	12		
	T4 8	1	13		
pN	N0 19	6	7	0.03*	
	N1 19	3	7		
	N2 7	0	11		
pM1	2	0	6		

Conclusions: CMS classes of colorectal cancer demonstrate different histologic patterns. CMS 4 tumors appear to have an aggressive biology and poor patient outcome. Validation of these findings in a larger sample size is warranted.

686 Loss of SMAD4 Expression In Colorectal Carcinoma With Pancreatobiliary-Type Morphology: Important Diagnostic Pitfall

Yamin Ma¹, Burcin Pehlivanoglu², Rebecca Obeng¹, Alyssa Krasinskas¹, Michelle Reid³, Yue Xue³

¹Emory University, Atlanta, GA, ²Adiyaman University Training and Research Hospital, Adiyaman, Turkey, ³Emory University Hospital, Atlanta, GA

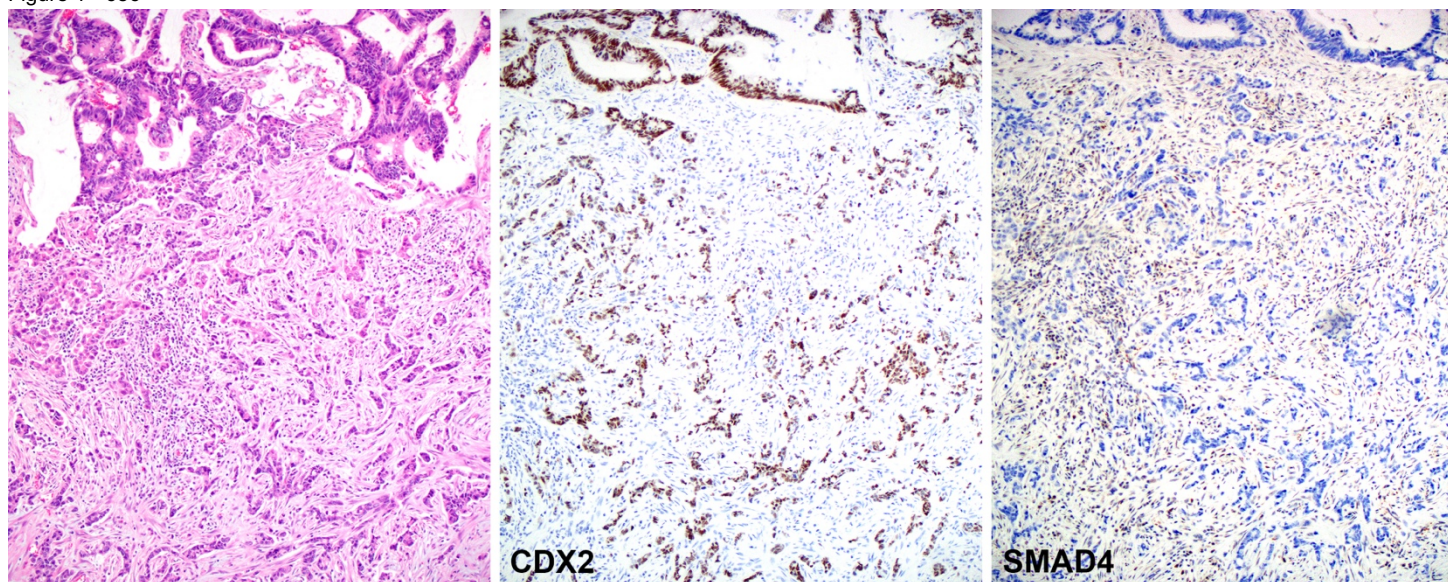
Disclosures: Yamin Ma: None; Burcin Pehlivanoglu: None; Rebecca Obeng: None; Alyssa Krasinskas: None; Michelle Reid: None; Yue Xue: None

Background: Colon cancer typically shows intestinal-type morphology; however, pancreatobiliary-type (PB) morphology has been gradually appreciated. SMAD4 expression in this type of colon cancer has not yet been reported.

Design: We reviewed 275 colorectal carcinoma resection cases from year 2005 to 2010. Cases with PB-type features were selected, which included widely separated small tubular units lined by one or two layers of cuboidal cells. Immunohistochemical stains for CDX2 and SMAD4 were performed on one representative tissue block. Loss of SMAD4 staining with positive internal control was considered positive; and nuclear staining of CDX2 with intensity > 2 was positive.

Results: Twenty-seven cases (9.8%) met the criteria for inclusion (mean age: 66 y; M: F ratio: 4:5; location: 15 in right colon and 12 in left; mean invasive size: 4.6 cm; 13 with lymphovascular invasion; 18 with positive LNs; 19 pT3; 8 developed distant metastasis), which showed PB-type morphology, focally (<25%) in 9, substantially (25-75%) in 10 and diffusely (>75%) in 8 cases. CDX-2 immunolabeling was positive in all foci with PB-type morphology, but only 15 cases (56%) had diffuse strong nuclear staining. On the contrary, SMAD4 immunostain showed complete loss of expression in 22 cases (81%). Among these cases, only half (12/22) diffusely expressed CDX2 protein.

Figure 1 - 686



Conclusions:

The results of our study show that a small subset of colorectal cancers have PB-type morphology and they tend to lose SMAD4 expression. Awareness of this phenomenon is important because loss of SMAD4 expression, possible absence of CDX2 staining, and combined with PB morphology can lead to misdiagnosis of cases particularly in the metastatic sites and in limited samples.

687 Biocartis Idylla™ Microsatellite Instability Assay Shows High Concordance with PCR and IHC for Microsatellite Instability Status in Colorectal Cancer

Alexander Mackinnon¹, Medical College Wisconsin¹, Stephanie Springborn¹

¹Medical College of Wisconsin, Milwaukee, WI

Disclosures: Alexander Mackinnon: None; Medical College Wisconsin: None; Stephanie Springborn: None

Background: Determination of mismatch repair (MMR) and/or microsatellite instability (MSI) status in colorectal cancer (CRC) is recommended to aid in the identification of patients with Lynch Syndrome or as a prognostic indicator. In addition, it is becoming increasingly important as predictive biomarker for cancer immunotherapy. Current molecular testing methods for MSI are often labor intensive and require analysis of paired normal tissue. In this retrospective study, we evaluated and validated the fully automated Biocartis MSI Assay (RUO), which is capable of MSI determination without the need to analyze normal tissue.

Design: 50 archived FFPE CRC specimens with known MSI status were selected for analysis on the Biocartis Idylla system. Both MMR IHC (MLH1, MSH2, MSH6 and PMS2) and a lab-developed PCR assay that targets 5 mononucleotide microsatellites (BAT-25, BAT-26, NR-21, NR-24 and NR-27) were used as reference methods for determination of MSI status on all 50 samples. The Idylla MSI cartridge assesses microsatellite instability at 7 novel loci in the ACVR2A, BTBD7, DIDO1, MRE11, RYR3, SEC31A and SULF2 genes by PCR amplification followed by high-resolution melting curve analysis. MSI-High (MSI-H) is called if 2 or more microsatellite loci demonstrate instability; microsatellite stable (MSS) is called if 0 or 1 microsatellites are unstable. For the two PCR MSI methods (Idylla and the PCR-based assay), analysis was performed from a single 10µm FFPE section. In both cases, a macrodissection was performed. For the LDT PCR method, DNA was extracted and then analyzed; for Idylla, FFPE was inserted directly into the MSI assay cartridge.

Results: 40 samples demonstrated defective MMR (dMMR) by IHC and MSI-H by the PCR-based reference methods, and 10 samples demonstrated proficient MMR (pMMR) by IHC and MSS by the PCR methods. When these 50 samples were analyzed by the Idylla MSI Assay, concordant results were obtained for 40/40 MSI-H/dMMR samples and 10/10 of the MSS/pMMR samples for an overall concordance of 100% (50/50). Additionally, the Idylla system was easy to use, required only 2 minutes of hands on time and produced results in as few as 150 minutes.

Conclusions: The Idylla platform offers a simple and fully automated solution for rapid determination of MSI status in CRC. The Idylla MSI Assay can be easily implemented and validated as part of the routine molecular characterization of CRC.

688 Accuracy of Grading Gastrointestinal Stromal Tumors on Information Available During Biopsy

Zaid Mahdi¹, Raul Gonzalez²

¹Beth Israel Deaconess Medical Center, Newton, MA, ²Beth Israel Deaconess Medical Center, Boston, MA

Disclosures: Zaid Mahdi: None; Raul Gonzalez: None

Background: The risk of progression for gastrointestinal stromal tumors (GISTs) is calculated using tumor site, size, and mitoses per 5 mm². This is generally performed on resection specimens, as biopsy may not sample the most mitotically active area, and radiographic tumor size may differ from gross/pathologic size. Still, the accuracy of risk prediction using data available at time of biopsy has not been assessed.

Design: We identified 38 immunohistochemically confirmed GISTs (c-Kit or DOG1 positivity) with available biopsy and resection specimens and clinical data. Cases that received neoadjuvant therapy were excluded. For biopsies, we recorded site and mitoses per available high-power fields; we extrapolated mitoses to rate per 5 mm² on smaller samples. We also recorded radiographic tumor size at time of biopsy. For resections, we recorded site, size, and mitoses per 5 mm². We performed risk stratification on all samples (using CAP-endorsed criteria) and compared results across matched specimens.

Results: Risk stratification on biopsy and resection was concordant for 27 (71%) GISTs. This included 9 of 10 non-gastric cases (6 duodenum, 3 rectum, 1 jejunum); one duodenal case went from "low risk (8.3%)" to "insufficient data" due to a 1.2 cm size difference. Most gastric biopsies (25/28, 89%) were "no risk (0%)" or "very low risk (1.9%);" the other three measured >5 cm on imaging. This included the most mitotically active biopsy (9 per 5 mm²), which was "high risk (55%)" on biopsy and resection. Six gastric risk-stratification discrepancies were minor, changing from "no risk (0%)" or "very low risk (1.9%)" to "very low risk (1.9%)" or "low risk (3.6%)" due to size differences (generally with gross size barely >2 cm). The other four discrepancies were major; all had mitotic rate discrepancies. Three went from "very low risk (1.9%)" to "moderate risk (16%)" or "high risk (55%/86%)" due additionally to size discrepancy. The fourth only had mitotic discrepancy, going from "moderate risk (16%)" to "high risk (86%)." These four cases had no common distinguishing features on biopsy.

Conclusions: GIST risk stratification is often accurate on data available at biopsy, though occasional cases may harbor much greater risk based on resection data. Such instances appear difficult to predict, indicating that risk stratification on biopsy should be discouraged (or at

least approached cautiously). Risk stratification may be more accurate on biopsies of non-gastric GISTs, though these were a minority in our study.

689 Evaluation for Serrated Epithelial Changes (SEC) in Prior Biopsies of Patients with Inflammatory Bowel Disease (IBD) Associated Flat Dysplasia

Elias Makhoul¹, Zhikai Chi², Deepti Dhall¹, Kevin Waters¹

¹Cedars-Sinai Medical Center, Los Angeles, CA, ²Coppell, TX

Disclosures: Elias Makhoul: None; Zhikai Chi: None; Deepti Dhall: None; Kevin Waters: None

Background: SEC are histologic findings seen in patients with longstanding IBD that have been shown to be associated with a high frequency of dysplasia. To our knowledge, the prevalence of these findings in preceding biopsies of patients with flat dysplasia has not been extensively studied. We retrospectively investigated current and prior samples from IBD patients diagnosed with flat dysplasia in order to assess the prevalence of concurrent and prior SEC.

Design: 167 IBD patients with dysplasia were identified in our departmental archives from 2011-2018. After excluding patients with polypoid dysplasia, our final dataset included 30 patients with flat dysplasia. 18 of these cases had available prior biopsies. For the purposes of this study, we required SEC to extend to the base of the crypts and did not include instances of superficial hyperplastic changes. Basic demographic and clinical variables were collected.

Results: The median age of IBD diagnosis was 34 (range 16-71) and the median age of dysplasia diagnosis was 60 (range 31-71). 56.6% were male, 93% were Caucasian, and 13.3% were taking biologics. 26 patients had ulcerative colitis (UC) and 4 had Crohn's disease (CD). 13.3% of the dysplasia was in the ascending colon, 16.7% in the transverse colon, 10% in the descending colon, 36.7% in the sigmoid, and 23.3% in the rectum. 67% (20/30) of patients had SEC at the time of dysplasia or in a prior biopsy. 67% (12/18) had SEC on prior biopsies. SEC was seen in prior biopsies for 12/16 (75%) of the patients with UC and was seen in the prior biopsies for 0/2 (0%) of the patients with CD. The prior biopsies with SEC occurred a median of 5.5 years (range 1-13) before the development of dysplasia. The SEC seen in prior biopsies was present at the location of dysplasia in all 12 cases and 9 (75%) cases also had SEC at a distant location.

Conclusions: We identified SEC in the majority of IBD patients who developed flat dysplasia. These findings suggest that SEC likely either represent a precursor lesion for flat dysplasia in IBD or signify significant damage to areas of the colon that are at increased risk for dysplasia. We also found that these changes are often present in prior biopsy material perhaps providing an opportunity for either optimizing treatment prior to the development of dysplasia or increased surveillance.

690 Deep Learning Can Recognize Common Patterns of Gastritis

David Martin¹, Joshua Hanson², Ramachandra R Gullapalli³, Frederick Schultz¹, Aisha Sethi³, Douglas Clark¹

¹University of New Mexico, Albuquerque, NM, ²University of New Mexico School of Medicine, Albuquerque, NM,

³Albuquerque, NM

Disclosures: David Martin: None; Joshua Hanson: None; Aisha Sethi: None

Background: The majority of deep learning (DL) studies have focused on neoplastic pathology, with the realm of inflammatory pathology remaining largely untouched. Experienced gastrointestinal pathologists can discriminate between *H. pylori* gastritis, reactive gastropathy, and normal mucosa with relative ease. Accordingly, these patterns are well suited to test the diagnostic capabilities of DL in the realm of inflammatory pathology. We present the first study examining the accuracy of DL in inflammatory gastritis.

Design: Gastric biopsy cases that carried a diagnosis of *H. pylori*-related gastritis (n=100), reactive gastropathy (n=100), and histologically normal gastric mucosa (n=100) were identified from our archives and were confirmed by two gastrointestinal pathologists (reference diagnoses). These cases were scanned with the Aperio VERSA 200 slide scanner (Leica, Wetzlar, Germany). HALO-AI image analysis software (Indica Labs, Corrales NM) was used to perform training and testing. 210 cases (70%) were selected for inclusion in the training set (70 *H. pylori*, 70 reactive gastropathy, 70 normal) and 90 cases (30%) were selected for the test set (30 *H. pylori*, 30 reactive gastropathy, 30 normal). The DL algorithm assigned a colored digital label to each diagnosis in the test set as follows: *H. pylori* = red (Figure 1), reactive gastropathy = yellow (Figure 2), and normal mucosa = green. The labels corresponded to the area of the tissue assigned a diagnostic category by the DL algorithm and was termed Area Distribution (AD). All ADs were quantified as percentages for each case.

Results: Using the 90 test cases, receiver operating characteristics (ROC) curves were generated to determine the AD limits for which the algorithm performed best compared to the reference diagnoses. The ROC curves showed near perfect agreement with the reference diagnoses at an AD percentage cutoff of 50% for normal (area under the curve [AUC]=99.7%) and *H. pylori* (AUC=100%) and 40% for reactive gastropathy (AUC=99.9%). Accuracy metrics using the AD cutoff of 50% for all cases were then calculated with a false positive AD rate defined as >30%. The DL algorithm demonstrated excellent sensitivity/specificity pairings for each diagnosis (Table).

Diagnosis	Sensitivity	Specificity	Accuracy	F-Score
Normal	96.7	86.7	90.0	0.87
Reactive Gastropathy	96.7	96.7	96.7	0.95
H. Pylori Gastritis	100.0	98.3	98.9	0.98

Figure 1 - 690

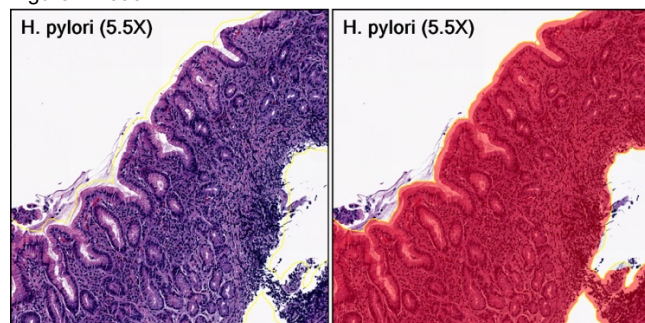
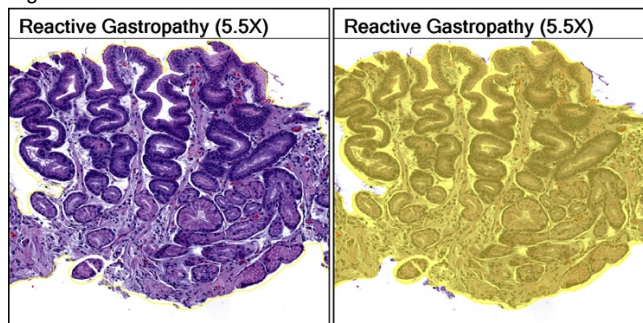


Figure 2 - 690



Conclusions: This is the first study examining the accuracy of DL technology in inflammatory gastrointestinal pathology. This technology demonstrates excellent diagnostic discrimination in a research setting and is especially adept at recognizing the *H. pylori* pattern of gastritis.

691 Paucity of Plasma Cells in the Gut in Patients Following Stem Cell Transplantation

Nana Matsumoto¹, Mina Xu², Joanna Gibson²

¹Yale New Haven Hospital, New Haven, CT, ²New Haven, CT

Disclosures: Nana Matsumoto: None; Mina Xu: None; Joanna Gibson: None

Background: Graft versus host disease (GVHD) of the gastrointestinal (GI) tract is a common clinical concern in patients who undergo allogeneic stem cell transplantation (SCT). Histologic criteria for GVHD and infections are well established. However, the spectrum of other histologic changes post SCT are not well understood. We report 8 patients who present with unusual plasma cell paucity in the GI tract post-SCT.

Design: Patients were identified via a pathology database search over 10 years. Clinicopathologic features recorded included hematologic diagnosis, initial therapy, prior transplant history, degree of HLA match, conditioning regimen, time to engraftment, interval to and indication for GI biopsy, history of prior or subsequent GVHD, and patient outcome.

Results: All patients received reduced-intensity chemotherapy prior to SCT and engrafted within 30 days. Six patients had 10/10 HLA matched donors and 1 patient had a 9/10 matched donor (1 patient had unavailable data). Index GI biopsies were performed 31 to 403 days post SCT (average 229 days). All patients received tacrolimus, alone (1) or with a combination of various immunosuppressants (7). Majority of patients underwent evaluation for possible gut GVHD. Four patients had both upper and lower endoscopy, 2 patients had upper endoscopy alone and 2 patients had colonoscopy alone. Histologic examination of small bowel or colon biopsies revealed a paucicellular lamina propria with near total absence of plasma cells, without villous blunting or architectural change. Features of GI GVHD were seen in 2 patients at the time of the biopsy. On follow-up, 5 patients died with gut GVHD and various complications. Three patients are alive, one with evidence of minimal GVHD of the gut. Only one patient had pre-SCT biopsy, which did not show plasma cell paucity.

Conclusions: We identified 8 patients with GI plasma cell paucity post SCT. Paucity of plasma cells has not been previously described as a feature of GVHD. Similar histologic features can be seen in patients with immune deficiency disorders, such as combined variable immune deficiency syndrome. We speculate that the features observed in this patient cohort are the result of acquired immune deficiency in the setting of post SCT immunosuppression. Plasma cell paucity of the gut may contribute to gut dysfunction and patient morbidity following SCT. Whether this finding is a unique clinicopathologic entity, a drug associated reaction, or an unusual manifestation of GVHD remains to be investigated.

692 INSM1 in Primary Gastrointestinal Tract and Pancreatic Neuroendocrine Neoplasms

Kelsey McHugh¹, Sanjay Mukhopadhyay², Erika Doxtader³, Daniela Allende⁴

¹Cleveland Clinic, Lakewood, OH, ²Cleveland Clinic, Cleveland, OH, ³Cleveland Clinic, Pepper Pike, OH, ⁴Cleveland Clinic, Avon Lake, OH

Disclosures: Kelsey McHugh: None; Sanjay Mukhopadhyay: None; Erika Doxtader: None; Daniela Allende: None

Background: Insulinoma-associated protein 1 (INSM1) has recently been described as a sensitive and specific nuclear marker of neuroendocrine neoplasms. The utility of INSM1 in primary gastrointestinal tract and pancreatic neuroendocrine neoplasms has not been thoroughly investigated. The aim of this study is to ascertain whether INSM1 reliably stains primary gastrointestinal and pancreatic neuroendocrine neoplasms in comparison to traditional neuroendocrine markers (chromogranin and synaptophysin).

Design: Cases were identified through a retrospective pathology database search (2008-2018). A selected formalin fixed paraffin embedded block from ninety primary gastrointestinal and pancreatic neuroendocrine tumors was stained with INSM1 (mouse monoclonal, A-8, Santa Cruz Biotechnology), synaptophysin (mouse monoclonal, Snp88, BioGenex) and chromogranin (mouse monoclonal, DAK-A3, Agilent): 17 gastric, 18 small bowel (16 duodenal, 2 ileal), 16 appendiceal, 21 colonic, and 18 pancreatic. Any nuclear staining for INSM1 or cytoplasmic staining for synaptophysin and chromogranin was considered positive.

Results: INSM1 was positive in 75 of 90 primary gastrointestinal and pancreatic neuroendocrine neoplasms (83%), including 16 gastric (94%), 17 pancreatic (94%), 13 small bowel (72%), 17 colonic (81%), and 12 appendiceal (75%). When divided into well differentiated neuroendocrine tumors (WDNET) and poorly differentiated neuroendocrine carcinoma (PDNEC) primary gastrointestinal and pancreatic neuroendocrine neoplasms, INSM1 was positive in 58 of 70 WDNET (83%) and 17 of 20 PDNEC (85%). INSM1 was negative in 66 of 71 (93%) non-neuroendocrine neoplasms. Positive staining was seen in 0 squamous cell carcinoma (0%), 1 adenocarcinoma (5%), 1 solid pseudopapillary neoplasm (5%), and 3 acinar cell carcinomas (60%). Overall, the sensitivity of INSM1 (83%) was less than that of synaptophysin (99%) and similar to chromogranin (88%) while the specificity of INSM1 (93%) was higher (versus 83% and 85%, respectively). The overall sensitivity, specificity, positive predictive value (PPV) and negative predictive value (NPV) of each of these 3 neuroendocrine markers is detailed in Table 1.

Table 1. Sensitivity and Specificity of INSM1, SYN, CHR for Primary Gastrointestinal Tract and Pancreatic Neuroendocrine Neoplasms

	INSM1	SYN	CHR
Sensitivity	75/90 (83)	89/90 (99)	79/90 (88)
Specificity	66/71 (93)	49/59 (83)	55/65 (85)
PPV	75/79 (95)	89/99 (90)	79/89 (89)
NPV	66/81 (82)	49/50 (98)	55/66 (83)

Abbreviations: INSM1, insulinoma-associated protein 1; SYN, synaptophysin; CHR, chromogranin; PPV, positive predictive value; NPV, negative predictive value.

Conclusions: INSM1 is a useful marker of neuroendocrine differentiation in primary gastrointestinal and pancreatic neuroendocrine neoplasms. When compared to traditional neuroendocrine immunohistochemical stains (synaptophysin, chromogranin), INSM1 demonstrates higher specificity and acceptable sensitivity.

693 Clinicopathological Characteristics of Gastric Cancer after Helicobacter Pylori Eradication

Akio Miyake¹, Shoji Yamanaka², Ohashi Kenichi³

¹Yokohama-shi, Japan, ²Yokohama City University Hospital, Yokohama-shi, Japan, ³Yokohama City University, Kanagawa, Japan

Disclosures: Akio Miyake: None

Background: The incidence of gastric cancer after Helicobacter pylori eradication is increasing. In recent studies, non-neoplastic epithelium was found on the surface of gastric cancer after eradication, but its significance remains unclear.

Design: We enrolled 264 consecutive patients who underwent endoscopic submucosal dissection (ESD) of gastric cancer at Yokohama City University Hospital between 2015 and 2017. After excluding 101 patients who were negative or indefinite for Helicobacter pylori infection, 91 patients and 104 lesions after eradication (eradication group), and 72 Helicobacter pylori-positive patients and 91 lesions

(control group) were enrolled to identify the clinicopathological characteristics, including the incidence of non-neoplastic surface epithelium and the pre-ESD biopsy diagnosis. We additionally investigated MUC-2, MUC-5AC, MUC-6, CDX2, p53 and Ki67 expression in the overlying non-neoplastic epithelium after eradication.

Results: Small (less than 20 mm in each major axis) and depressed-type lesions were significantly more frequent in the eradication group ($P=0.028$, $P<0.001$, respectively). Non-neoplastic epithelium that covered more than 20% of the cancer area was also significantly more frequent in the eradication group ($P<0.014$). Non-neoplastic epithelium noted on 24 lesions in the eradication group exhibited an immunohistochemically gastric-and-intestinal-mixed phenotype, and was negative for p53 and Ki-67. Nineteen lesions in the eradication group and 11 lesions in the control group were classified as “indefinite for neoplasia” by pre-ESD biopsy. Biopsy specimens from 5 out of 19 lesions in the eradication group and none of the 11 lesions in the control group contained a very small amount of atypical epithelium (less than 0.2 mm²), and non-neoplastic tissue comprised more than 90% of the biopsy area.

Conclusions: Non-neoplastic surface epithelium on gastric cancer tissue is frequently present after eradication. This phenomenon may influence the pre-ESD biopsy diagnosis of gastric cancers.

694 Value of Repeat *Helicobacter pylori* Immunohistochemistry: Good Practice or Flogging a Deceased Horse?

Rebecca Molinsky¹, Benjamin Lebwohl², Stephen Lagana³

¹Columbia University Mailman School of Public Health, New York, NY, ²Celiac Disease Center at CUMC, New York, NY,

³New York, NY

Disclosures: Rebecca Molinsky: None; Benjamin Lebwohl: None; Stephen Lagana: None

Background: *Helicobacter pylori* (HP) can be diagnosed in various ways, including by immunohistochemical staining (IHC) of formalin fixed gastric biopsies. Various studies, as well as guidelines by groups of experts have been published regarding proper utilization of HP IHC. Our group generally follows such guidelines, in that HP IHC is ordered only on an as needed basis. It is not uncommon for patients to get multiple upper endoscopies with biopsy (EGDbx), and to the best of our knowledge, no study has addressed the utility of repeating HP IHC in a patient without a history of HP and who has already had negative HP IHC.

Design: We searched the case files of our department for 12 years to identify patients who had >1 EGDbx. Cases were defined as patients whose first biopsy was negative for HP by IHC and then had a subsequent biopsy for which HP IHC was used. Data was tabulated and statistics run through SAS.

Results: 3785 patients had >1 EGDbx. 2930 (77.4%) were diagnosed as negative for HP at first EGDbx, with IHC used in 1283 (42.3%). 932 of those 1283 (75.3%) had HP IHC performed on subsequent EGDbx, and these were the cases. 3 of these 932 (0.32%) had positive HP IHC.

Conclusions: If a first biopsy is HP negative by IHC, the number needed to test on a subsequent biopsy is 311. At 2017 Medicare global rate of \$108.38 per 88342 CPT code, the cost of IHC used per positive result was \$33,706.

695 Villous hypermucinous lesions are genuine precancerous raised lesions in patients with inflammatory bowel disease

Jean-François Mosnier¹, Salim Reis¹, Arnaud Boureille¹, Guillaume Meurette¹, Celine Bossard²

¹Centre Hospitalier Universitaire de Nantes, Nantes, France, ²University Hospital, Nantes, France

Disclosures: Jean-François Mosnier: None; Celine Bossard: None

Background: Although most of these patients with are enrolled in endoscopic program surveillance for dysplasia screening, intestinal carcinomas are always incidentally diagnosed at gross examination of colorectal surgical specimens. The goal of this work was to assess the frequency of incidentally diagnosed intestinal cancer in IBD and the profile of prior lesions.

Design: 796 intestinal resection specimen from 717 patients with IBD (545 Crohn disease and 172 ulcerative colitis) examined in our Pathology Department from 1993 to 2017 were reviewed. Colorectal carcinomas (n = 26), small bowel carcinomas (n = 2) and anal carcinoma (n = 1) were detected in 26 patients. Prior lesion defined as lesion in close vicinity to carcinoma was detected in 18 of 29 carcinomas (62%). All the lesions were histologically reviewed and immunohistochemical study for CDX2, p53, p16, MGMT, mismatch repair protein was performed. DNA was extracted from FFPE blocks and search for KRAS, NRAS, BRAF PIK3CA mutation was undertaken. Charts were reviewed for endoscopic findings before intestinal resection.

Results: Carcinoma diagnosis was incident on examination of surgical specimen in 7 of 26 patients with IBD (27%). All the carcinomas incidentally diagnosed were in specimen showing active colitis background. Carcinomas were adenocarcinomas, NOS (14, 48%), mucinous (12, 42%), clear cell carcinomas (1, 5%) and adenosquamous (1, 5%). The prior lesions were histologically classified as usual in 9 cases, i.e., conventional dysplasia in flat mucosa (n = 1) or raised mucosa (n = 8) and unusual in 9 cases i.e., papillary (2), serrated (2) or villous hypermucinous lesions (6) "indefinite for dysplasia". Genetic and immunohistochemical studies showed that prior lesion harbored similar molecular abnormalities than contiguous carcinomas: p53 overexpression (13/18, %), loss or methylation of CDX2 expression (10/18, 56%), KRAS mutation (5/18), v594 BRAF mutation (1/18) and MSI (1/18). For example, all villous hypermucinous lesions harbored loss of CDX2 expression, overexpression of p53 and in one of these KRAS mutation.

Conclusions: Incidental diagnosis of intestinal carcinomas remains frequent patients with IBD, especially in active colitis background. In these cases, unusual prior lesions are frequent such as papillary, serrated and villous hypermucinous lesions "indefinite for dysplasia" harboring similar molecular abnormalities than contiguous carcinomas, indicating their precancerous nature.

696 Patient Outcome in Disseminated Low Grade Appendiceal Mucinous Neoplasms with Increased Proliferation

Mohamed Mostafa¹, Christopher Hartley², Catherine Hagen²

¹Medical College of Wisconsin, Wauwatosa, WI, ²Medical College of Wisconsin, Milwaukee, WI

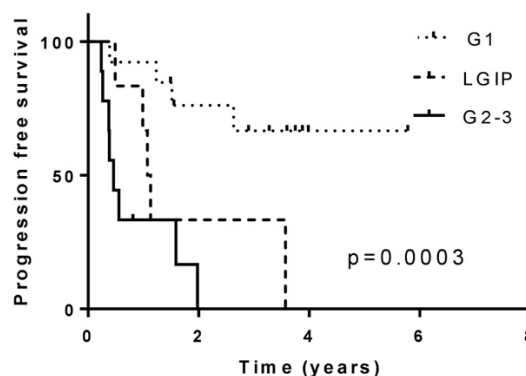
Disclosures: Mohamed Mostafa: None; Christopher Hartley: None; Catherine Hagen: None

Background: Histologic grading of disseminated mucinous appendiceal tumors has been shown to have prognostic significance and is also utilized to dictate treatment. Recent editions of the AJCC staging manual have proposed a three-tier grading system: low grade (G1), high grade (G2), and high grade with signet ring cells (G3). A recent study has identified a minor subset of cases with predominantly low-grade features and focal (<10% of total tumor volume) areas of more prominent atypia which were termed "Low grade mucinous neoplasms with increased proliferation (LGIP)." Little remains known about the prognostic significance of such cases. The goal of this study was to identify cases of LGIP within our institution and determine patient outcome in this cohort.

Design: Cases of disseminated mucinous appendiceal tumors from debulking procedures performed at our institution from 2011-2017 were retrospectively reviewed and graded according to the current AJCC criteria. Cases of LGIP were also identified according to previously described criteria. Clinicopathologic information was collected from chart review.

Results: The study group consisted of 29 patients (M:F 1:1.1, mean age 55.8) with an average follow-up of 3.0 years. Fourteen patients had G1 disease, 6 LGIP, 8 G2, and 1 G3. Five patients (35.7%) with G1, 5 patients (83.3%) with LGIP, and 4/7 patients (57.1%) with G2/G3 had macroscopic evidence of residual disease following surgery. In the remaining 2 patients it was uncertain if there was residual disease. Thirteen G1 patients (92.9%), 3 LGIP patients (50%), and 7 G2 patients (77.8%) received heated intraperitoneal chemotherapy. Five patients (35.7%) with G1 disease, 5 patients (83.3%) with LGIP, and 8 patients (88.9%) with G2/G3 had disease progression/recurrence. Patients with LGIP had significantly worse progression free survival compared patients with G1 disease (HR 4.9, 95%CI 1.9-49.6, p=0.007) and similar progression free survival as patients with G2/G3 disease (HR 2.1, 95%CI 0.7-6.7, p=0.17)(Figure 1). One patient with LGIP and one patient with G2 died of disease progression. All remaining patients were alive at last follow up.

Figure 1 - 696



Conclusions: Patients with LGIP show similar outcome as patients with high grade disease and may be better classified as G2 disease. Further larger studies are necessary to support the findings reported here.

697 Evaluation of the AJCC staging system for low grade appendiceal mucinous neoplasmsMohamed Mostafa¹, Christopher Hartley², Catherine Hagen²¹Medical College of Wisconsin, Wauwatosa, WI, ²Medical College of Wisconsin, Milwaukee, WI**Disclosures:** Mohamed Mostafa: None; Christopher Hartley: None; Catherine Hagen: None

Background: Recently an AJCC staging system has been implemented for low grade appendiceal mucinous neoplasms (LAMN) based on depth of tumor invasion: Tis-tumor confined by muscularis propria; T3-tumor invades through muscularis propria; T4a-tumor invades visceral peritoneum. Staging is based on whichever tumor component (mucin or neoplastic epithelium) extends deeper. Little is known about the prognostic significance of the new LAMN staging system. The goal of this study was to examine the prognostic significance of the new staging system in LAMNs without disseminated peritoneal disease (PD).

Design: All LAMNs resected at our institution from 2012-2017 were reviewed and staged according to the current AJCC system. Clinicopathologic data was collected from chart review.

Results: LAMNs from 13 patients without in initial peritoneal dissemination were included in the study (M:F 1:1.6; mean age 62.4); the average follow-up was 2.5 years. 7 cases were staged as Tis, 4 as T3, and 2 as T4a. Within the T3 tumors, 3 cases had both mucin and epithelium extending into the subserosa, and 1 case had mucin extending into the subserosa and epithelium extending into the muscularis propria. For the T4a tumors, both cases had acellular mucin involving the serosal surface and epithelium limited to the submucosa. The appendix was entirely submitted in 4 of the Tis cases, all grossly lesional tissue was submitted in an additional case, and in 2 cases only representative sections were submitted. The entire appendix was submitted for 3 T3 cases and representative sections were submitted for 1 case. For the T4a cases, one appendix was entirely submitted and the other had representative sections submitted. None of the 13 patients had evidence of disease recurrence during follow-up.

14 patients (M:F 2.5:1; mean age 57.3) with LAMN and low grade PD were identified for survival comparison (average follow-up 3.6 yrs). 5 of the 14 patients (35.7%) with low grade PD had disease recurrence. Patients with disseminated PD were significantly more likely to have disease recurrence compared to patients with LAMN and no peritoneal dissemination ($p=0.04$, HR 6.1, 95%CI 1.04-35.5).

Conclusions: Our results confirm peritoneal dissemination is a risk factor for disease recurrence. However, none of the patients in our cohort with LAMN and lack of PD had evidence of disease recurrence, irrespective of T stage. Further studies are necessary to determine the prognostic significance of the new LAMN T staging system.

698 High Concordance Between Mismatch Repair Protein Immunohistochemistry (MMR IHC) and Microsatellite Instability (MSI) Testing in Colorectal Cancer (CRC)Jonathan Mowers¹, Joel Greenson², Bryan Betz³, Noah Brown⁴¹Ann Arbor, MI, ²University of Michigan Hospitals, Ann Arbor, MI, ³University of Michigan Medical School, Ann Arbor, MI, ⁴University of Michigan, Ann Arbor, MI**Disclosures:** Jonathan Mowers: None; Joel Greenson: None

Background: The sensitivity and specificity of MMR IHC and MSI for detecting defects in MMR (dMMR) in CRC has historically varied widely, but the consensus of studies reports sensitivity and specificity to be in the 90% range. Our experience was that MMR IHC and MSI were much better at predicting dMMR than this at our institution and hence we undertook the following study.

Design: We assembled a cohort of 203 consecutive CRC resection cases with both MMR protein IHC and microsatellite instability testing performed.

Results: Of the 203 patients that had both MMR IHC and MSI testing, 171 (84.2%) were MSI stable by molecular MSI testing; all MSI stable cases had retention of all MMR proteins by IHC except one case, which had loss of MSH6 by IHC, caught at the time of signout, in a patient s/p chemoradiation. 32 (15.8%) cases were MSI high by microsatellite instability testing. No defects in MMR were seen by IHC that were not seen by MSI.

Of microsatellite unstable cases, 20 (9.9%) cases were likely sporadic, whereas 12 (5.9%) cases were most likely Lynch syndrome. Sporadic MSI high colon tumors had defects in MLH1, seen as loss of MLH1 and PMS2 by IHC. Follow up testing showed MLH1 promoter hypermethylation in two cases, BRAF V600E mutations in 17 cases, and both BRAF V600E and MLH1 promoter hypermethylation in one case. Of the 12 likely Lynch syndrome cases, seven (3.4%) had defects in MLH1, seen as loss of MLH1 and PMS2 by IHC. Two cases (1.0%) had defects in MSH2, seen as loss of MSH2 and MSH6 by IHC. One case (0.5%) had a defect in MSH6 with loss by IHC and one case (0.5%) had a defect in PMS2 with loss by IHC. Finally, one case (0.5%) from a Lynch syndrome patient had a MLH1 pathogenic point mutation that was microsatellite unstable and retained all MMR proteins by IHC.

Overall, the sensitivity of IHC for dMMR was 96.8% and the specificity was 99.4%. The positive predictive value was 96.8% and the negative predictive value was also 99.4%. The sensitivity, specificity, positive and negative predictive values of MSI testing for dMMR was 100%.

Conclusions: Our concordance between MMR IHC and MSI is higher than that reported in the literature. There are two main reasons for this (1) continuous improvements in the standardization of the interpretation of PCR peaks and (2) training GI pathologists on the pitfalls of IHC. The cases missed by IHC are attributed to treatment and mutation type. Given the high concordance rate, one could argue that only one modality is necessary for routine use.

699 A series of four patients with oxyntic gland adenoma: deciphering the clinical and histological features of these rare gastric polyps

Jerry Nagaputra¹, Sangeeta Mantoo², Jiezhen Tracy Loh³, Rafay Azhar⁴, Vikneswaran Namasivayam², Wei-Qiang Leow²
¹SGH Anatomical Pathology, Singapore, Singapore, ²Singapore General Hospital, Singapore, Singapore, ³Singhealth, Singapore, Singapore, ⁴Singapore, Singapore

Disclosures: Jerry Nagaputra: None; Jiezhen Tracy Loh: None; Vikneswaran Namasivayam: None; Wei-Qiang Leow: None

Background: Oxyntic gland adenomas are rare lesions of the stomach, composed of oxyntic-type glands. A variety of nomenclatures have been used to designate it, including adenocarcinoma of fundic gland type and oxyntic mucosa pseudo-polyp. We report four cases that demonstrate the spectrum of clinical and morphological variations in oxyntic gland adenoma.

Design: A search of routine histopathology cases from the Singapore General Hospital was conducted to identify cases of oxyntic gland adenoma/polyp between January 2013 to April 2018. Clinical, endoscopic, histological and immunohistochemical information was collated for each case. All the relevant slides from each case were retrieved and reviewed. The measurement of lesion size, morphologic description and immunohistochemical stains were obtained from the microscopic review, where appropriate.

Results: A total of four cases were collated. Age ranged from 55 to 80 years old (mean of 69 years). There was an equal gender distribution. Endoscopically, two lesions were located on the gastric body along the lesser curve while the other two were visualized along the greater curve. One case was incidentally discovered on a routine biopsy for an endoscopic finding of mild gastritis. They measured 0.13cm to 1.5cm (mean 0.7cm) in largest extent. The diagnosis of oxyntic gland adenoma was made on the biopsy specimen for all cases. In three out of the four lesions, endoscopic mucosal resection was subsequently performed. They were composed of irregular, dilated oxyntic glands lined by predominantly chief cells with scattered parietal cells. Mild to moderate nuclear atypia in the form of enlarged nuclei with prominent nucleoli was present in all the four cases. Two of the lesions show clustered and anastomosing glands while the others featured irregular and dilated glands. In one lesion, early submucosal invasion was present. Immunohistochemical staining with synaptophysin was performed in three cases with two showing diffuse, strong reactivity and one exhibiting patchy staining. Ki-67/MIB-1 proliferation index was ~ 3% in three cases in which staining was performed.

Conclusions: Oxyntic gland adenoma is a rare entity with a spectrum of clinical and morphologic presentations. All the lesions in this small series showed chief cell predominance with mild nuclear atypia. Although submucosal invasion was present in one case, no metastatic disease had been observed.

700 Dietary Biotin Deficiency-Induced Colitis as a Novel Model to Study Inflammatory Bowel Disease

Manando Nakasaki¹, Michael Hwang², Jana Chen², Subrata Sabui², Jonathan Skupsky², Hamid Said²
¹University of California, Irvine, Costa Mesa, CA, ²University of California, Irvine, Irvine, CA

Disclosures: Manando Nakasaki: None; Michael Hwang: None; Jana Chen: None; Subrata Sabui: None; Jonathan Skupsky: None; Hamid Said: None

Background: Inflammatory bowel disease develops from complex interactions between the gut microbiome, host genetics and the immune system and it creates a tremendous burden on the healthcare system. To study novel treatments, pre-clinical models are available, but they often don't recapitulate all aspects of the disease. For example, the Dextran Sodium Sulfate (DSS) model for colitis creates mucosal damage, ulceration and crypt destruction that is limited to the large intestine and more closely models ulcerative colitis. On the other hand, the adoptive transfer model can induce transmural inflammation throughout the gastrointestinal tract and models more closely to Crohn's disease. We report on another model for inflammatory bowel disease that develops from dietary biotin deficiency.

Design: Mice are fed a diet absent in biotin with ovalbumin as the protein source to bind biotin produced by the intestinal flora. We have evaluated the histology each week during the development of biotin deficiency and compared with the DSS and adoptive transfer models. In the DSS colitis model, mice received 3% DSS added to their drinking water and were dissected for histologic analysis after 7 days. In the adoptive transfer model, Rag knock-out mice were injected with 1x10⁶ naïve CD4+ T-cells (i.e. regulatory T cell depleted) from

a syngeneic donor and were evaluated after 12 weeks at the peak of disease. Histopathological features included degree of inflammation, goblet cell loss, abnormal crypts, presence of crypt abscesses, mucosal erosion/ulceration, and number of neutrophils.

Results: The biotin deficiency mice develop alopecia between 8 and 10 weeks and have a precipitous decline in body weight from 10 to 14 weeks. The inflammatory changes including architectural distortion and mucosal damage are most prominent in the cecum whereas the DSS model shows significant inflammatory changes in the colon and the adoptive transfer model exhibits inflammatory changes mainly in the small intestine. Most interestingly, the microscopic signs of inflammation from biotin deficiency are present several weeks before symptom development.

Conclusions: Our histological analysis of biotin deficiency mice showed a unique distribution pattern of inflammation and the presence of early inflammatory changes suggesting a wide therapeutic window in which to test novel therapeutics. This novel model will be useful for future experiments focused on identifying treatments and/or a cure for inflammatory bowel disease.

701 **H. pylori Antigen may be Present in Germinal Centers in Gastritis: Biologic and Patient Care Implications**

Nya Nelson¹, Rashmi Tondon¹, Danielle Fortuna¹, Stuti Shroff², Emma Furth³

¹Hospital of the University of Pennsylvania, Philadelphia, PA, ²Massachusetts General Hospital, Philadelphia, PA, ³University of Pennsylvania, Philadelphia, PA

Disclosures: Nya Nelson: None; Rashmi Tondon: None; Danielle Fortuna: None; Stuti Shroff: None; Emma Furth: None

Background: *Helicobacter pylori* (HP) induces gastritis and in a small subset of patients causes adenocarcinoma and lymphoma. Therefore, its detection and treatment are critical. In the setting of gastritis an immunohistochemistry (IHC) for HP is performed if the organisms are not detected on H&E sections. Following this algorithm, we had an index case showing HP IHC staining in germinal centers (GC) of a gastric mucosal biopsy. We aimed to determine the rate of this event.

Design: Stomach biopsy and resection specimens on which HP IHC were performed were identified via a database search. For each year between 01/01/2011 to 5/31/2018, 40-50 biopsy and resection cases were randomly selected to yield a total of 367 cases. For each case, we reviewed the IHC to determine the presence or absence of GC's, HP surface staining, and GC staining. Additional cases with GC HP IHC staining were prospectively collected. Gastric surgical pathology reports from 3/1/18-8/29/18 were reviewed to determine the rate of HP in our patient population.

Results: The overall prevalence of HP in our population is low (7%), with 82% detected by H&E and 18% detected by IHC.

A total of 367 cases and 445 slides were reviewed, with surface HP staining present in 13% of cases (n=46). GCs were present in 92 cases (25% of total cases), HP IHC staining within GCs was seen in 5% of cases with GCs present (n=5). One case demonstrated concurrent GC and surface staining.

An additional 6 cases with GC staining were prospectively identified during the study, for a total of 11 cases with GC HP IHC staining. Five cases showed HP organisms overlying the area of GC staining. Two cases showed GC staining that was distant from the surface staining. Of four cases with only GC IHC staining, 2 patients had a history of HP within the prior 4 months.

Conclusions: HP antigen is present in germinal centers in gastritis in a small group of patients and may not be associated with detectable surface organisms. We hypothesize this immune location may serve as a reservoir for viable organisms within macrophages. There can be geographic discordance between surface and GC HP IHC staining, suggesting that positive IHC in GC may indicate HP infection elsewhere in the stomach. These results provide preliminary evidence of a link between GC HP IHC staining and HP infection, and support further investigation for potential infection in patients that demonstrate GC staining alone.

702 **Neutrophil Gelatinase Associated Lipocalin (NGAL) Is a Valuable Ancillary Marker to Distinguish Dysplasia from Reactive Atypia in Barrett Esophagus**

Recep Nigdelioglu¹, Xianzhong Ding², Stefan Pambuccian³, Xiuzhen Duan³, Yihong Ma⁴

¹Loyola University, Maywood, IL, ²Northbrook, IL, ³Loyola University Medical Center, Maywood, IL, ⁴Loyola University Medical Center, Hinsdale, IL

Disclosures: Recep Nigdelioglu: None; Xianzhong Ding: None; Stefan Pambuccian: None; Xiuzhen Duan: None; Yihong Ma: None

Background: Diagnosis of dysplasia in Barrett esophagus (BE) is a challenge especially in presence of active inflammation with reactive atypia. Immunohistochemical stains for p53 could occasionally be helpful, but are not always reliable. New biomarkers are therefore needed to facilitate the distinction between reactive and dysplastic BE. Neutrophil gelatinase associated lipocalin (NGAL) or Lipocalin-2

(LCN2) is known to limit bacterial growth by sequestering iron and modulating oxidative stress. Studies have shown NGAL expression dysregulation in both benign and malignant conditions. In the gastrointestinal tract, significant upregulation of NGAL has been reported in *H. pylori* associated gastritis, gastric cancer, ulcerative colitis and colorectal carcinoma. However, its role in BE and related dysplasia and/or carcinoma has not been studied. Our goal was to investigate the diagnostic value of NGAL in BE associated dysplasia.

Design: Forty-one cases of gastroesophageal junction biopsy and endoscopic mucosal resection specimens diagnosed from January 2015 to July 2018 were retrieved, including 26 BE with or without dysplasia or adenocarcinoma and 15 cases non-BE with or without active inflammation. Immunohistochemical stain for NGAL was performed and the intensities of NGAL expression within epithelium were scored as 0, 1+, 2+ and 3+. The results were analyzed by t-test and $p < 0.05$ was considered statistically significant.

Results: NGAL was not expressed in squamous epithelium and minimally expressed in deep glands of columnar mucosa (0~1+). Intensive (mostly 3+) NGAL expression was identified in inflamed surface columnar epithelium compared to non-inflamed epithelium (mainly 1+) ($p < 0.0001$). The intensities were high (3+) in all inflammatory reactive atypia either in non-BE cases or non-BE areas of BE cases. In contrast, both BE low- and high-grade dysplastic epithelia showed no or minimal (0-1+) NGAL expression, even in the presence of active inflammation. The t-test between inflammatory reactive atypia and BE dysplasia was statistically significant ($p < 0.0001$).

Conclusions: NGAL expression was markedly elevated in reactive atypia while its expression was inconspicuous in BE dysplastic columnar epithelium. NGAL could be a potential marker to distinguish BE dysplasia from inflammatory reactive atypia.

703 Clinicopathologic Characteristics and Outcomes in Appendiceal Neuroendocrine Tumors: What's In A Name?

Mushal Noor¹, Aaron Huber¹, Justin Cates², Raul Gonzalez³

¹University of Rochester Medical Center, Rochester, NY, ²Vanderbilt University Medical Center, Nashville, TN, ³Beth Israel Deaconess Medical Center, Boston, MA

Disclosures: Mushal Noor: None; Aaron Huber: None; Justin Cates: None; Raul Gonzalez: None

Background: Well-differentiated neuroendocrine tumors (NETs) have widely different behavior depending on site of origin. For example, pancreatic NETs can metastasize and lead to patient death, while appendiceal NETs are often incidental and generally benign. Using the same terminology for lesions at all sites may impact patients' and possibly clinicians' understanding of the disease. A recent large study found size > 1.5 cm, grade 2 status, and lymphovascular invasion related to nodal disease in appendiceal NETs. We similarly reviewed data on appendiceal NETs to determine what factors suggest potential for malignant behavior.

Design: For 139 resected appendiceal NETs, we obtained clinical presentation and follow-up data, including chromogranin A (CgA) levels. We evaluated tumor size, grade (by mitotic rate and/or Ki-67 index), location in the appendix, gross visibility, lymphovascular and perineural invasion, depth of invasion, mesoappendix invasion, and nodal disease. Pathologic factors were compared to nodal status and increased CgA levels using Cox regression, with significance set at $P < 0.05$. We also reviewed appendiceal NET data in the Surveillance, Epidemiology, and End Results (SEER) Program.

Results: In our 139 cases, median patient follow-up was 48 months. Seven patients had positive lymph nodes, and 12 had subsequent CgA elevation; none had distant metastases or died of disease. Four patients had grade 2 NETs; of these, none had nodal disease and only one had increased CgA. Increasing tumor size was associated with increased risk of nodal disease (odds ratio 5.01, $P = 0.004$); all seven node-positive cases were ≥ 1.0 cm. Depth of invasion and mesoappendix involvement did not impact N-status. Factors increasing risk of elevated CgA included size (hazard ratio [HR] 1.92, $P = 0.040$), location in mid-appendix (HR 5.62, $P = 0.035$), mesoappendix involvement (HR 5.78, $P = 0.016$), and AJCC pT4 disease (HR 10.45, $P = 0.020$). For 1,322 cases in the SEER database with N-status data, 108 (8%) were pN1; only four were coded as being < 0.5 cm.

Conclusions: Small (< 0.5 cm) appendiceal NETs not seen grossly that do not invade serosa or mesoappendix appear overwhelmingly benign and low-grade. In such cases, the risk of nodal disease or subsequent increased CgA appears minimal. Unless mitotically active, NETs meeting these criteria likely do not need to be stained for Ki67. Given their benign behavior, more fitting terms for these NETs may be "tumorlet" or "microadenoma," as used for small benign NETs seen in the pancreas.

704 Evaluation of Effect of Carcinoembryonic Antigen Expression on Colorectal Cancer Immune Microenvironment Using Quantitative Multiplex Immunofluorescence Image Analysis

Kenneth Ofori¹, Thomas Hart², Robyn Gartrell³, Yvonne Saenger³, Helen Remotti⁴, Armando Del Portillo¹

¹Columbia University Medical Center, New York, NY, ²Columbia University, New York, NY, ³New York-Presbyterian/Columbia University Medical Center, New York, NY, ⁴Columbia University Medical Center, Dobbs Ferry, NY

Disclosures: Kenneth Ofori: None; Thomas Hart: None; Robyn Gartrell: *Speaker*, PerkinElmer; Yvonne Saenger: *Advisory Board Member*, Amgen; Helen Remotti: None; Armando Del Portillo: None

Background: Colorectal cancer (CRC) is the 3rd most common cancer in men and women and the 2nd leading cause of cancer deaths in the United States. While it is known that tumor infiltrating lymphocytes in CRC impairs tumor growth, it is unclear how the immune microenvironment surrounding CRC may affect the tumor. Carcinoembryonic antigen (CEA) is member of immunoglobulin superfamily of proteins over expressed in a number of malignancies, and has been ascribed a host of functions, including cell adhesion and immune response, and may affect the immune microenvironment through the TGF-beta pathway. This study aims to use multiplexed quantitative multispectral immunofluorescence (qMIF) to characterize and compare the immune microenvironment in CRCs with low and high CEA expression.

Design: Tissue microarrays (TMAs) were constructed from FFPE resection specimens of CRCs from 47 patients, and were stained for CEA by immunohistochemistry. TMAs were then stained using DAPI and Opal 6-plex kits for CD68, HLADR, CD3, CD8, FOXP3, and pan-cytokeratin. Multispectral images were obtained from regions of interest from each core of the TMAs using the Vectra Automated Quantitative Pathology Imaging System. Using inForm software, algorithms were developed to characterize and quantify all cells within the tumor stroma, using both morphology and Opal immunostain profiles. These algorithms included tissue segmentation (tumor vs stroma), cell segmentation, phenotyping, and scoring (marker positivity thresholds). The number of each cell type along with their marker phenotype were batch analyzed from CEA-low and CEA-high tumors using custom R algorithms.

Results: We identified 4 CEA-low and 13 CEA-high CRCs. The average density of CD68+ macrophages, as a proportion of all stromal cells, was higher in CEA-high CRCs than in CEA-low CRCs (13% vs 7%, p=0.03). No significant differences were seen in the density of CD3+FOXP3+ T-cells or CD3+CD8+ T-cells. However, HLADR+CD68+ macrophages and CD3+ lymphocytes may be more abundant in CEA-high CRCs (p=0.13 and p=0.15, respectively, statistically significant using Benjamini-Hochberg procedure, false discovery rate 20%).

Variable	Mean for CEA High Tumors	Mean for CEA Low Tumors	P(T<=t) two-tail	P value Rank	Critical Value
Macrophage density	13.250	4.1984	0.032	1	0.04
FOXP3 lymphocyte density	0.2953	0	0.082	2	0.08
CD8 Lymphocyte density	0.0498	0.0075	0.121	3	0.12
M1 macrophage density	8.7950	5.130	0.125	4	0.16
Lymphocyte density	0.306486923	0.060455	0.146709849	5	0.2

Figure 1 - 704

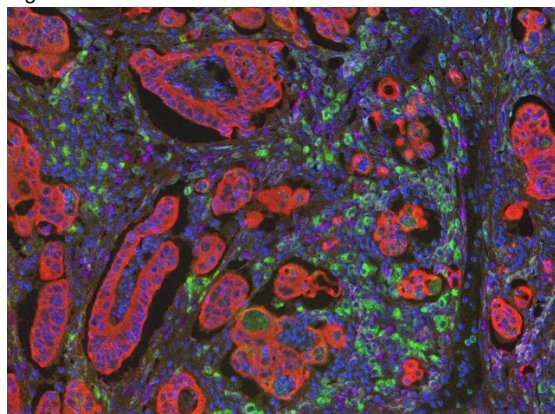
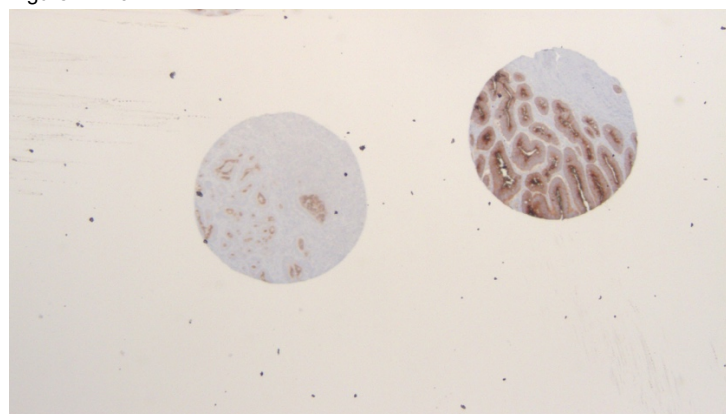


Figure 2 - 704



Conclusions: CEA-low CRCs showed fewer overall CD68+ macrophages, which suggests that these tumors may illicit a different immune response than CEA-high tumors. qMIF is a powerful tool to characterize the tumor microenvironment while maintaining the spatial relationship, and may be able to uncover prognostic information.

705 *Fusobacterium nucleatum* Levels Correlate with Specific Immune Cell Subtypes in the Colorectal Cancer Microenvironment

Shuji Ogino¹, Jennifer Borowsky², Annacarolina Fabiana Lucia Da Silva¹, Andressa Dias Costa³, Kristen Felt³, Mai Chan Lau⁴, Melissa Zhao⁵, Koichiro Haruki³, Tsuyoshi Hamada⁶, Kosuke Mima⁷, Susan Bullman³, Jochen Lennerz⁸, Marios Giannakis³, Charles Fuchs⁹, Jonathan Nowak¹
¹Brigham and Women's Hospital, Boston, MA, ²The Royal Brisbane & Women's Hospital, Brisbane, QLD, Australia, ³Dana-Farber Cancer Institute, Boston, MA, ⁴Boston, MA, ⁵Dana-Farber Cancer Institute, Somerville, MA, ⁶The University of Tokyo, Boston, MA, ⁷Kumamoto University, Kumamoto, Japan, ⁸Massachusetts General Hospital, Harvard Medical School, Boston, MA, ⁹Yale Cancer Center, New Haven, CT

Disclosures: Shuji Ogino: None; Jennifer Borowsky: None; Annacarolina Fabiana Lucia Da Silva: None; Andressa Dias Costa: None; Kristen Felt: None; Mai Chan Lau: None; Melissa Zhao: None; Koichiro Haruki: None; Tsuyoshi Hamada: None; Kosuke Mima: None; Susan Bullman: None; Jochen Lennerz: None; Marios Giannakis: *Advisory Board Member*, AstraZeneca; Charles Fuchs: *Consultant*, Merck & Co., Inc.; *Consultant*, Genentech; *Advisory Board Member*, CytomX; *Consultant*, Eli Lilly; *Consultant*, Sanofi; Jonathan Nowak: None

Background: Mounting evidence suggests a complex interplay between the microbiome, immunity, and carcinogenesis in colorectal cancer (CRC). Notably, *Fusobacterium nucleatum* (*F.n.*) may promote CRC development by suppressing T cell-mediated anti-tumor immunity. We therefore investigated whether higher levels of tumor-associated *F.n.* correlate with specific T cell subtypes in CRC.

Design: Within two U.S. nationwide prospective cohort studies, we measured *F.n.* within CRC tissue using quantitative PCR. To identify T cell subtypes within tumor and stroma, we developed a multispectral fluorescence imaging assay to simultaneously quantitate expression of CD3, CD4, CD8, CD45RO and FOXP3. In a subset of cases (N=415), we conducted whole exome sequencing and calculated neoantigen loads. Multivariable logistic regression analysis was used to assess the association of *F.n.* with T cell subset densities.

Results: *F.n.* was detected in 102 of 752 CRCs. Compared with *F.n.*-negative cases, *F.n.*-high cases were inversely associated with stromal CD3⁺ cell density (multivariable odds ratio (OR) 0.39, 95% confidence interval (CI) 0.20-0.75, P for trend = 0.002 across *F.n.*-high, low, and negative categories), including stromal CD3⁺CD4⁺CD8⁻ cells (multivariable OR 0.41, 95% CI 0.21-0.78, P for trend = 0.001), stromal CD3⁺CD4⁺FOXP3⁻ cells (multivariable OR 0.44, 95% CI 0.23-0.84, P for trend = 0.006) and stromal CD3⁺CD4⁺CD45RO⁺ cells (multivariable OR 0.44, 95% CI 0.23-0.84, P for trend = 0.005). These relationships were not significantly (P>0.3) modified by tumor MSI status or neoantigen loads. For stromal CD3⁺cell density, the corresponding multivariable ORs for *F.n.*-high cases were 0.32 (95% CI 0.13-0.78) for non-MSI-high (MSS) CRCs, and 0.52 (95% CI 0.19-1.45) for MSI-high CRCs. Results were similar for stromal CD3⁺CD4⁺CD8⁻ cells, stromal CD3⁺CD4⁺FOXP3⁻ cells, and stromal CD3⁺CD4⁺CD45RO⁺ cells. Notably, *F. nucleatum* level was not associated with immune cell density in regions of tumor epithelium, or CD3⁺CD8⁺ cytotoxic T cell density in either tumor or stroma.

Conclusions: *F. nucleatum* levels are inversely associated with stromal T cell density, including CD4⁺ memory and effector T cells, along with CD3⁺CD4⁺CD8⁻ T cells. Neither neoantigen load nor MSI status significantly affect this association. Our data provide a compelling rationale for further investigations into interactions between the microbiota and T cells in CRC carcinogenesis, potentially driving novel therapy and prevention strategies.

706 Pathologic Predictors of Pouch Failure: Are We Missing an Elephant in the Room?

Andrea Olivas¹, Kinga Skowron¹, Konstantin Umanskiy¹, Christopher Weber²
¹University of Chicago Medical Center, Chicago, IL, ²Oak Park, IL

Disclosures: Andrea Olivas: None; Kinga Skowron: None; Konstantin Umanskiy: None; Christopher Weber: None

Background: Total abdominal colectomy (TAC) followed by restorative proctectomy with ileal pouch-anal anastomosis (IPAA) is the treatment of choice for patients with refractory ulcerative colitis (UC), and is contraindicated in Crohn's disease (CD). IPAA failure rates are high (10-15%), and there are currently no well-defined pathologic criteria to identify patients at risk for failure. We hypothesize that accurate identification of specific high-risk histologic features in the initial TAC specimen may help predict those patients who are at highest risk of IPAA failure.

Design: A prospectively maintained database was queried for records of patients with a diagnosis of UC who underwent IPAA from 2000-2010. IPAA failure was defined as pouch excision or permanent ileostomy. H&E sections from TACs of patients with pouch failure (n=26) and non-failure matched controls (n=15) were independently reviewed in a blinded fashion and evaluated for features suggestive of Crohn's disease (knife-like ulcers, right-side predominant disease, patchy colonic involvement, ileal disease, and granulomas) and depth of inflammatory infiltrate. Results were correlated with the final pathology report and clinical outcomes.

Results: CD of the pouch was subsequently diagnosed in 58% of patients with IPAA failure (vs 0% non-failures), significantly correlating with IPAA failure (p= 0.0001). However, the final pathology report of the TAC correctly predicted CD in only 33% of these patients. Blinded histologic review revealed that at least one histologic feature suggestive of CD was present in: 50% of all patients with IPAA failure; 67% of

patients with CD and IPAA failure; and 7% of non-failure patients ($p=0.0061$). IPAA failures also had a significantly higher incidence of deep inflammatory infiltrates (muscularis propria or deeper; 50% failure vs 7% non-failure; $p=0.013$).

Conclusions: Careful histologic evaluation of TAC specimens is an important component in the preoperative evaluation of patients for IPAA. We show that the presence of specific histopathologic features suggestive of CD, before a definitive diagnosis of CD can be rendered, can predict IPAA failure. Therefore, a structured final pathologic report highlighting the presence or absence of these high-risk features should be provided, and may aid in the reduction of IPAA failure rates.

707 Can Histologic Features Predict Neoadjuvant Therapy Response in Rectal Adenocarcinoma?

Yuho Ono¹, Justin Cates², Raul Gonzalez¹

¹Beth Israel Deaconess Medical Center, Boston, MA, ²Vanderbilt University Medical Center, Nashville, TN

Disclosures: Yuho Ono: None; Justin Cates: None; Raul Gonzalez: None

Background: Current standard therapy for locally advanced rectal cancer (LARC) is neoadjuvant therapy followed by surgical resection, but there is variability in treatment response among patients. Pathologists are tasked with scoring treatment response on resection specimens, with histology ranging from minimal to complete response. Previous studies have evaluated whether clinical, immunohistochemical (IHC), and molecular parameters can predict neoadjuvant therapy response in LARC. However, few studies have correlated histologic features in patients' initial biopsies to the degree of treatment response in their subsequent post-therapy resection specimens.

Design: This retrospective study included 79 patients with LARC, all of whom received biopsy, then neoadjuvant therapy, then surgical resection. Each patient's initial biopsy was evaluated for tumor grade, budding (using International Tumor Budding Consensus Conference criteria), desmoplasia, adjacent stromal lymphocytes, dirty necrosis, microscopic ulceration, apoptosis, signet ring cells, mucinous features, tumoral Paneth cells, intraepithelial lymphocytes, intraepithelial neutrophils, and prominent lymphoid aggregates. Each patient's post-therapy resection specimen was evaluated for degree of tumor response using the American Joint Committee on Cancer tumor regression grading system. The above histologic features on biopsy, along with patient age at diagnosis, were compared to regression grades in their respective resection specimens by univariate analyses, with significance set at $P<0.05$.

Results: Statistical analyses did not find any significant histologic factors in the tumor biopsies that were predictive of treatment response in the post-therapy resection specimens. However, the presence of increased apoptosis (defined as two or more apoptotic figures in 1 high-powered field) on biopsy trended toward predicting a poor histologic response to neoadjuvant therapy (odds ratio 0.30, 95% confidence interval 0.074-1.21, $P=0.090$).

Conclusions: Histologic features in pretreatment biopsy samples of LARC generally do not appear able to predict response to neoadjuvant therapy. Increased apoptosis did tend to occur more frequently in tumors with a poor response; this contradicts a report that increased IHC staining of apoptosis protease-activating factor 1 predicts favorable response, though other markers of apoptosis have shown no relationship to response. Overall, methods to predict neoadjuvant therapy response in rectal cancer remain elusive.

708 Identifying Predictive Biomarkers of Outcome in Diabetic Colorectal Cancer Patients Treated with Metformin

Christine Orr¹, Christopher Nicol², Harriet Feilotter³, Jim Biagi², Nazik Hammad², Lois Mulligan², Chris O'Callaghan², Ravi Ramjeesingh⁴, Kevin Ren⁵, Kevin Song¹, Kiran Virik², Ami Wang¹, Scott Davey², David Hurlbut²

¹Kingston, ON, ²Queen's University, Kingston, ON, ³Richardson Laboratory, Kingston, ON, ⁴Dalhousie University, Halifax, NS, ⁵Cedars-Sinai Medical Center, Los Angeles, CA

Disclosures: Christine Orr: None; Christopher Nicol: None; Harriet Feilotter: None; Jim Biagi: None; Nazik Hammad: None; Lois Mulligan: None; Chris O'Callaghan: None; Ravi Ramjeesingh: None; Kevin Ren: None; Kevin Song: None; Kiran Virik: None; Ami Wang: None; Scott Davey: None; David Hurlbut: None

Background: Survival of diabetic colorectal cancer (CRC) patients treated with diet or insulin is inferior to that of non-diabetic CRC patients. This decrease in survival is not seen in diabetic CRC patients treated with metformin. Metformin may have antineoplastic effects by activating the AMPK pathway with down-regulation of energy-consuming cellular pathways associated with cancer progression. Our aim is to identify a molecular signature predictive of metformin-mediated favourable clinical outcomes in diabetic CRC patients using a targeted gene expression assay (NanoString).

Design: We retrospectively identified 278 CRC patients with diabetes mellitus. 128 cases were selected based upon availability of primary resection specimens at our institution with ample tumor cellularity. RNA extracted from one FFPE tumour block per case resulted in 99 stage 2 and stage 3 CRC cases suitable for NanoString analysis. Clinicopathologic data were recorded for these cases, and a 153-gene custom panel based on relevant cancer progression and metformin signaling pathways was created for NanoString analysis.

Results: Survival data analysis on the 128 case cohort shows favourable overall survival at 2 years for the metformin-treated CRC diabetic patients (78%) compared with insulin (66%) and diet (71%) groups and this trend continued at 5-year and 10-year follow-up with survival times averaging 4.7, 6.0, and 6.5 years for insulin, diet, and metformin ($p=0.01$ insulin vs. metformin). Stage 3 cases trended towards increased survival with metformin treatment at 5-year follow-up and longer metastasis-free time post tumour resection (table 1). There was no significant difference between treatment groups for sidedness, gender, or age at diagnosis. Nanostring analysis is currently ongoing.

Treatment	Stage 2					Stage 3				
	Min Survival Avg (yrs)	2yr Survival	5 yr Survival	Mets at 5 yr	Avg time to 1st met	Min Survival Avg (yrs)	2 yr Survival	5 yr Survival	Mets at 5 yr	Avg time to 1st met
Metformin	7.4 (n=20)	19 (95%)	15 (75%)	0 (0%)	N/A	7.3 (n=34)	28 (82%)	21 (71%)	9 (26%)	34mo
Diet	7.0 (n=12)	10 (77%)	10 (77%)	1 (8%)	39mo	5.5 (n=19)	15 (79%)	8 (42%)	5 (26%)	25mo
Insulin	5.2 (n=5)	5 (100%)	2 (40%)	2 (40%)	24mo	5.9 (n=9)	8 (89%)	5 (56%)	3 (33%)	19mo

Conclusions: This study provides further evidence for the potential benefit of metformin on survival in stage 3 diabetic CRC patients. Molecular data acquisition of tumour RNA samples using the NanoString platform is currently ongoing and when complete will provide treatment group molecular signatures for clinicopathological and outcome correlation. Based on preliminary data, we anticipate two potential discoveries: 1) tumour molecular profiles of diabetic CRC patient samples that correlate with clinical outcomes; and 2) a gene expression signature predictive of the improved clinical outcome seen with metformin treatment.

709 Reproducibility of AJCC 8th Edition Criteria for Categorizing Deeply Invasive Colon Cancer

Nicole Panarelli¹, Suntrea Hammer², Jingmei Lin³, Purva Gopal², Ilke Nalbantoglu⁴, Lili Zhao⁵, Jerome Cheng⁵, Maria Westerhoff⁵
¹Montefiore Medical Center, Scarsdale, NY, ²University of Texas Southwestern Medical Center, Dallas, TX, ³Indiana University, Indianapolis, IN, ⁴Woodbridge, CT, ⁵University of Michigan, Ann Arbor, MI

Disclosures: Nicole Panarelli: None; Suntrea Hammer: None; Jingmei Lin: None; Purva Gopal: None; Ilke Nalbantoglu: None; Lili Zhao: None; Jerome Cheng: None; Maria Westerhoff: None

Background: The recent AJCC 8th edition defines pT4a colon adenocarcinoma (CAC) as that which directly invades the peritoneum or communicates with the serosa through inflammation. These criteria produce diagnostic confusion among pathologists because fibroinflammatory reactions at the advancing CAC edge and reactive mesothelial proliferation can obscure the relationship between small CAC clusters and the serosal surface. Importantly, the pT category determines overall clinical stage when nodal metastases are absent. We assessed interobserver reproducibility by strictly applying AJCC 8th edition criteria and identified particularly problematic histologic patterns.

Design: 40 cases of CAC present at or near the serosal surface were reviewed by 6 pathologists; low and high power images of the histologic section with deepest invasion in each case were reviewed. Fleiss' Kappa was calculated to assess agreement.

Results: 3 patterns of CAC were observed at the advancing edges of study cases: communication with serosa through inflammation (n=3), pushing border (n=5), infiltrative glands and tumor cell clusters (n=32). Overall agreement for pT category assignment was moderate ($k=0.50$). Agreement was fair ($k=0.21$) when inflammation was present at the advancing tumor edge; all pathologists assigned a pT3 category in one case, whereas the T stage was equally split into T3 or T4a in the other 2 cases. Moderate agreement ($k=0.52$) was achieved for cases with a pushing border; 60% of cases were classified as pT3 by all pathologists. Agreement was also moderate ($k=0.49$) when the advancing edge was infiltrative: 19% were unanimously classified as pT3, and a pT4a designation was agreed upon in 28% of cases.

Conclusions: AJCC 8th edition criteria for staging deeply invasive CAC achieved moderate agreement among 6 pathologists. Although limited in sample size, communication between CAC and serosa via inflammation was the most difficult to reproduce. Pathologists are more likely to agree that cases with a pushing border should be designated as pT3, possibly due to a thin rim of fibrotic tissue between serosa and tumor. Cases with an infiltrative advancing edge also achieved moderate reproducibility, but there was disagreement in more than half of cases. Additional clarification of AJCC criteria for pT categories of transmurally invasive CAC may improve the accuracy of staging.

710 PIK3CA mutations as a prognostic factor in patients with residual rectal cancer after neoadjuvant chemoradiotherapy

Jee Young Park, Kyungpook National University Chilgok Hospital, Daegu, Korea, Republic of South Korea

Disclosures: Jee Young Park: None

Background: This study aimed to investigate the clinical relevance and the prognostic role of PIK3CA mutations in patients with residual rectal cancer who underwent neoadjuvant chemoradiotherapy (NACRT).

Design: Between January 2006 and December 2011, the surgical specimens of 128 patients with residual rectal cancer who underwent NACRT were analyzed. Real-time polymerase chain reaction was performed to evaluate hot spot mutations for exons 9 and 20 of PIK3CA by using formalin-fixed and paraffin-embedded surgical specimens.

Results: PIK3CA mutation was not evaluable in 19 of the 128 cases (14.8%), because of poor DNA quality. Of the other 109 cases, PIK3CA mutant was identified in 3 cases (2.8%). PIK3CA mutant was associated with lymphatic invasion ($P=0.016$), lymph node metastasis ($P=0.034$), and higher pathologic TNM stage ($P=0.040$). Patients with PIK3CA mutant had significantly shorter cancer-specific survival (CSS) ($P<0.001$) and tentatively shorter disease-free survival ($P=0.059$) than those with wild-type. However, PIK3CA mutation was not an independent prognostic factor for CSS ($P=0.166$) in multivariate modeling after adjusting for venous invasion, perineural invasion, lymphatic invasion, tumor regression grade, pathologic T stage, and N stage.

Conclusions: Our findings may aid in understanding the therapeutic approaches targeting PIK3-Akt-mTOR pathway in patients with residual rectal cancer after NACRT. Furthermore, although not an independent prognostic factor, PIK3CA mutation can predict a worse CSS.

711 Persistent Duodenal Mucosal Injury is Common in Follow Up Biopsies from Celiac Disease Patients Despite Strict Adherence to a Gluten Free Diet and Decreases in Anti-IgA Tissue Transglutaminase (tTG) Levels

Natalie Patel¹, Daniel Leffler², Amporn Atsawarungrangkit³, Luca Elli⁴, Alessandro Del Gobbo⁵, Marcela Salomao⁶, Rish Pai⁶, Michael Vieth⁷, Balint Melcher⁸, John Hart⁹, Andrea Olivas¹⁰, Bitu Naini¹¹, Cherise Meyerson¹², Won-Tak Choi¹³, Sanjay Kakar¹³, Maria Westerhoff¹⁴, Jerome Cheng¹⁴, Purva Gopal¹⁵, Mary Bronner¹⁶, Mariana Moreno Prats¹⁷, Marie Robert¹
¹Yale University School of Medicine, New Haven, CT, ²Beth Israel Deaconess Medical Center, Newton, MA, ³Beth Israel Deaconess Medical Center, Boston, MA, ⁴Center for the Prevention and Diagnosis of Celiac Disease, Milano, Italy, ⁵Fondazione irccs ca granda ospedale maggiore policlinico, Milan, Italy, ⁶Mayo Clinic Arizona, Scottsdale, AZ, ⁷Institut fur Pathologie, Bayreuth, Germany, ⁸Institute of Pathology, Bayreuth, Germany, ⁹University of Chicago, Chicago, IL, ¹⁰University of Chicago Medical Center, Chicago, IL, ¹¹UCLA Medical Center, Santa Monica, CA, ¹²UCLA Medical Center, Reseda, CA, ¹³University of California, San Francisco, San Francisco, CA, ¹⁴University of Michigan, Ann Arbor, MI, ¹⁵University of Texas Southwestern Medical Center, Dallas, TX, ¹⁶University of Utah, Salt Lake City, UT, ¹⁷University of Utah Health Sciences Center, Salt Lake City, UT

Disclosures: Natalie Patel: None; Daniel Leffler: Employee, Takeda Pharmaceuticals; Amporn Atsawarungrangkit: None; Luca Elli: None; Alessandro Del Gobbo: None; Marcela Salomao: None; Rish Pai: None; Michael Vieth: None; Balint Melcher: None; John Hart: None; Andrea Olivas: None; Bitu Naini: None; Cherise Meyerson: None; Won-Tak Choi: None; Sanjay Kakar: None; Maria Westerhoff: None; Jerome Cheng: None; Purva Gopal: None; Mary Bronner: None; Mariana Moreno Prats: None; Marie Robert: None

Background: Persistent symptoms despite adherence to a GFD occur in 30% of celiac disease patients. Ongoing inflammation is associated with complications such as lymphoma and osteoporosis. Yet, robust data correlating follow up biopsy findings with symptoms, serology and other associations is lacking. We aimed to define factors associated with persistent villous blunting in a multi-national cohort of patients with initial and follow up duodenal biopsies, in order to better stratify populations who may benefit from adjunctive therapies.

Design: Patients with celiac disease having duodenal biopsies at two timepoints were identified. Initial and follow up biopsies were reviewed blindly by gastrointestinal pathologists to assess Marsh score and intraepithelial lymphocytes (IELs)/100 enterocytes. Biopsy location/number, presenting/persistent symptoms, anti-IgA tTG serology, hemoglobin, diet adherence, and medications were recorded. Descriptive statistics are presented as mean and standard deviation. Initial and follow-up biopsies were compared by paired t-test/Wilcoxon sign rank test.

Results: 144 paired biopsies from 72 patients were retrieved (mean rebiopsy interval of 2.2 years; range 0.32-9.3). Considering all paired biopsies, improvement in Marsh score (41%) lagged behind improvements in IELs (68%) at the second biopsy time point in both proximal and distal duodenum. As expected, improved Marsh scores in 24 patients were associated with a significant decrease in IELs ($p<0.001$), decreased tTG titers ($p<0.001$) and decreased diarrhea ($p=0.049$). However, diarrhea and abdominal pain persisted in 25% and 38% of patients, respectively, while tTG remained positive in 21%. Further, among 41 patients following a strict gluten free diet, 39% showed no improvement in Marsh score, 35% showed no change or increased IELs, 64% had persistent or increased diarrhea, and 4/6 patients had

persistent iron deficiency anemia. Of 95 biopsy samples in which bulb and distal duodenal biopsies were separately submitted, each site was adequately sampled (AGA guidelines) in 59%.

N=72	Time Point-1	Time Point-2	P value
Marsh ? 3 (n, %)	Bulb: 33 (83%) Distal: 58 (89%)	Bulb: 22 (41%) Distal: 30 (48%)	<0.001
IEL/100 enterocytes (Mean)	Bulb: 52 Distal: 50	Bulb: 37 Distal: 41	Bulb: 0.001 Distal: 0.009
Iron deficiency anemia (n, %)	16 (22%)	6 (8%)	0.007
Subgroup with Decrease in MARSH score on follow-up (n=24)			
IEL/100 enterocytes (Mean)	44	24	<0.001
tTG Positive (n, %)	19 (91%)	4 (21%)	<0.001
Abdominal pain (n, (%))	10 (42%)	9(38%)	0.664
Diarrhea (n, %)	13 (54%)	6(25%)	0.049
Strict gluten free diet subgroup (n=41)			
	Increase	No change	Decrease
Marsh Score (n, %)	2 (5%)	14 (34%)	25 (61%)
IEL/100 enterocytes (n, %)	11 (32%)	1 (3%)	22 (65%)

Conclusions: Persistent duodenal inflammation/symptoms are frequent in celiac disease patients on a GFD. In patients showing histologic improvement in follow-up biopsies, amelioration of villous architecture lags behind IEL decreases. In the institutions represented, 59% of biopsies were submitted according to guidelines. These data suggest the need for greater monitoring of mucosal healing in celiac disease and education regarding adequate sampling.

712 Histologic Risk Features in Colorectal Sessile-shaped Malignant Polyps with Submucosal Invasion (pT1) and Nodal Metastasis: A Revisit

Natalie Patel¹, Xuchen Zhang²

¹Yale University School of Medicine, New Haven, CT, ²Yale University School of Medicine, Orange, CT

Disclosures: Natalie Patel: None; Xuchen Zhang: None

Background: It is known that tumor differentiation, lymphovascular invasion (LVI), margin status, polyp shape and size are important risk factors of malignant polyps (pT1) indicating possible nodal metastasis, which justifies a surgery. However, the size, margin and LVI are often unknown or difficult to assess in a piecemeal polypectomy from a sessile-shaped adenomatous polyp (SP). We aimed to identify histologic risk factors in SPs, such as tumor budding (TB, defined as single tumor cell or a cell cluster of up to 4 tumor cells) and poorly differentiated clusters (PDCs, defined as tumor cell clusters composed of ≥5 tumor cells) to determine if these features portend an increase in nodal metastasis potential indicating colectomy.

Design: The pathology database was searched to identify pT1N1 or greater colorectal carcinomas (CRC) arising from SPs from 2005-2018. Malignant SPs and their corresponding resection specimens were reviewed and the age, gender, TB, grade, tumor site, and TNM stage were recorded. Malignant SPs with N0 designation were used as control. Sensitivity (Sn) and specificity (Sp) were calculated for different morphologies and their combinations. A chi-square analysis was used to calculate odds ratio and p values.

Results: 24 cases (11F:13M, average age 62) of nodal positive and 18 cases (11F:7M, average age 68) of nodal negative SPs were identified. Of the nodal positive SPs: 88% were moderately differentiated (low grade), 71% showed high grade TB (HTB), 54% showed PDC, of which 85% of these were associated with HTB. Both HTB and PDC was seen in 46% of cases. Cases with nodal metastasis were more often positive for HTB (71% vs 17%; $P < .001$, PDC (54% vs 22%; $P < .04$), and both HTB and PDC (46% vs 11%; $P < .002$) compared to controls without nodal metastasis. HTB, PDC, and combined HTB and PDC increased the risk of nodal positivity, with odds ratio of and 12.1, 4.1, and 14.3, respectively (see table).

	pT1N≥1 (24)	pT1N0 (18)	P value	OR (95% CI)	Sensitivity, % (95% CI)	Specificity, % (95% CI)	PPV
HTB	71% (17)	17% (3)	0.0005	12.14 (2.74-46.9)	71% (50.8-85.1)	82% (59-94)	85%
PDC	54% (13)	22% (4)	0.0369	4.136 (1.12-13.72)	54% (35-72)	78% (55-91)	76%
HTB and PDC	46% (11)	11% (2)	0.0018	14.3 (2.57-74.26)	67% (42-85)	87% (62-98)	83%

Conclusions:

Our data showed nodal metastasis can be seen in SPs with both low- and high-grade CRCs in the absence of knowledge of polyp size, margin status and LVI. HTB and PDC are important histologic risk factors in predicting metastatic potential with HTB showing more significant risk of nodal metastasis than PDC alone. However, when combined the presence of both HTB and PDC results in an increased risk of nodal metastasis. These histologic risk features should be reported and a colectomy procedure may be warranted when both histologic risk features are present.

713 Gastric Fundic Gland Neoplasms: A multi-institutional study

Natalie Patel¹, Till Clauditz², Mai Iwaya³, Noam Harpaz⁴, Gregory Lauwers⁵, Robert Riddell⁶, Dhanpat Jain¹

¹Yale University School of Medicine, New Haven, CT, ²Hamburg University, Hamburg, Germany, ³Shinshu University Hospital, Matsumoto, Nagano, Japan, ⁴Mount Sinai Medical Center, New York, NY, ⁵H. Lee Moffitt Cancer Center & Research Institute, University of South Florida, Tampa, FL, ⁶Mt. Sinai Hospital, Toronto, ON

Disclosures: Natalie Patel: None; Till Clauditz: None; Mai Iwaya: None; Noam Harpaz: None; Gregory Lauwers: None; Robert Riddell: None; Dhanpat Jain: None

Background: Adenocarcinoma of the fundic gland type is a recently recognized rare gastric neoplasm showing differentiation towards chief and/or parietal cells of the stomach. In contrast to earlier reports, most of which are from East Asia, limited experience from United States suggests that these are benign and term "Oxyntic gland adenoma" has been proposed. The goal of the study is to review the clinicopathologic characteristics of neoplasms showing differentiation towards fundic glands (FGN) within the North America to further characterize this entity.

Design: The pathology databases at 4 institutions were searched for FGN. The slides were reviewed and the diagnosis was confirmed by 4 experienced GI pathologists (DJ, NH, GL, RR) prior to inclusion in the study. The clinical history, patient demographics, tumor characteristics (location, size, depth of invasion, lymph node positivity, and histologic subtype (mixed, parietal, or chief cell predominant) and clinical follow-up were recorded. Detailed histopathologic analysis and review of available immunohistochemical (IHC) stains was performed.

Results: 21 cases (11F: 9M, average age 71) of FGN were identified. The tumor location was body/fundus (18), lesser stomach (1) and cardia (2). The tumors are small (0.1-10cm, mean 0.96cm) and commonest subtype was mixed cell type (47%) followed by chief (43%) and parietal cell predominant (10%). Two cases with only cytologic atypia were considered adenoma, while others were considered invasive carcinoma. Subtle cytologic atypia comprising of enlarged nuclei with tiny nucleoli, multi-layering of cells, anastomosing cords ("endless cord pattern") and stromal changes (myxoid or desmoplasia) were most helpful diagnostic features. All cases were well-differentiated and the diagnosis could be readily established or suspected on H&E sections. IHC markers were performed only on select cases to highlight various cell lineages. Superficial submucosal invasion was identified in 7 cases (33%), one of which led to partial gastric resection with no evidence of nodal metastasis. None of the patients with available follow-up (n=7) had recurrent/residual disease.

Conclusions: Our results suggest that FGNS are distinctive gastric neoplasms that occur mostly in the oxyntic mucosa lined stomach and are generally <1cm in size. These represent a spectrum from adenoma to carcinoma, with about 1/3rd of the cases showing submucosal invasion. The pathogenesis of FGN remains unclear and needs further studies.

714 Immune Microenvironment in Barrett's esophagus, Low-Grade Dysplasia, High-Grade Dysplasia, and Adenocarcinoma of Esophagus

Pallavi Patil¹, Kara Lombardo², Ashlee Sturtevant³, Weibiao Cao⁴

¹Brown University Lifespan Academic Medical Center, Providence, RI, ²Johns Hopkins Medical Institutions, Baltimore, MD, ³Brown University, Providence, RI, ⁴Rhode Island Hospital, Providence, RI

Disclosures: Pallavi Patil: None; Kara Lombardo: None; Ashlee Sturtevant: None; Weibiao Cao: None

Background: Immune microenvironment and immune-based therapies are gaining increasing importance in numerous neoplastic entities for treatment. There are rare studies on PD-L1, PD1 and immune checkpoint therapy in esophageal adenocarcinomas. However, there are no studies on dysplasia and carcinoma post neoadjuvant therapy to our knowledge. We aimed to study the immune microenvironment in Barrett's esophagus (BE), low-grade dysplasia (LG) and high-grade dysplasia (HG) and esophageal adenocarcinoma (EA), and to explore the potential of immune checkpoint-based therapies in patients after chemoradiation therapy.

Design: Our records over past ten years were queried to find cases of BE, LG, HG and EA. Whole slides and existing tissue microarray for some cases were stained by immunohistochemistry for PD-L1 and PD1. Areas of interest were demarcated. PD-L1 was scored as positive or negative in epithelium and white blood cells, <1% cells considered negative. PD1-positive lymphocytes were scored as positive when present and negative when absent.

Results: Squamous epithelium (11 cases), BE (29 cases), LG (9 cases), HG (19 cases), untreated EA (11 cases) and post-treatment EA (12 cases) were included. The expression of PD-L1 in epithelium and white blood cells was noted in a large subset of all above entities as depicted in Table 1, Figure 1. PD-L1 expression in post-treatment adenocarcinomas was higher than in squamous epithelium (p<0.03). Squamous epithelium was less likely to have PD1+ lymphocytes compared to LG (p<0.03), HG (p<0.01), and post-treatment EA (p<0.02). However, there was no significant difference of PD1+ lymphocytes and PD-L1 among BE, LG, HG, untreated EA and treated EA.

Table 1: PD1 and PD-L1 expression in Barrett's esophagus, low-grade dysplasia and high-grade dysplasia and esophageal adenocarcinoma.

	PD1 n (%)	PD-L1 epithelium n (%)	PD-L1 WBCs n (%)
Squamous epithelium n= 11	2 (18%)	7 (64%)	11 (100%)
Barrett's Esophagus n=29	15 (52%)	25 (86%)	26 (90%)
Low Grade Dysplasia n= 9	6 (67%) §	8 (89%)	7 (78%)
High Grade Dysplasia n= 19	13 (68%) §	17 (89%)	16 (84%)
Untreated Adenocarcinoma n=10-11	5/11 (45%)	9/10 (90%)	8/10 (80%)
Post-Treatment Adenocarcinoma n= 12	8 (75%) §	12 (100%) §	12 (100%)

PD1= Programmed cell death protein 1, PD-L1 = Programmed death-ligand 1, WBC= white blood cells

§ P<0.03, compared with squamous epithelium

Figure 1 - 714

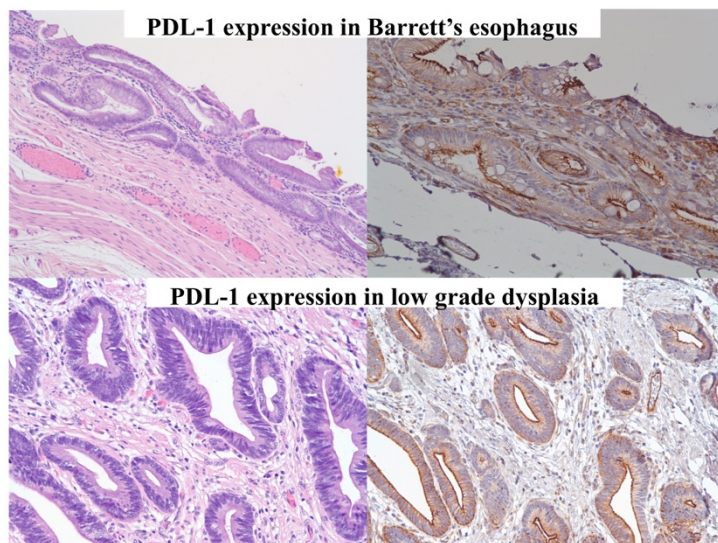
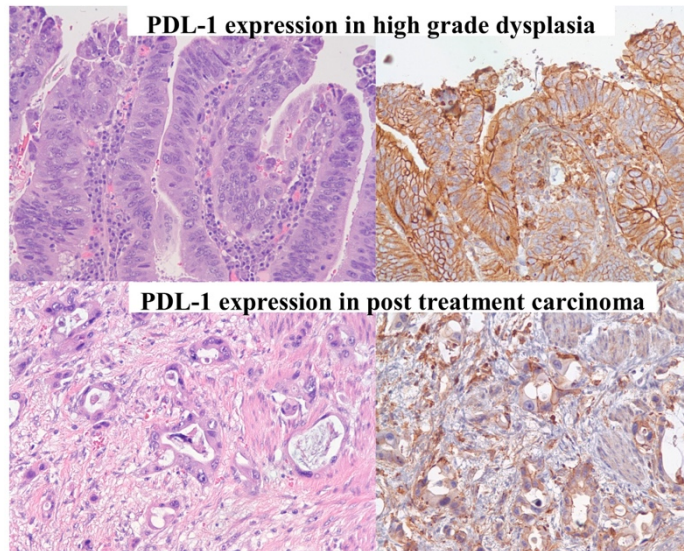


Figure 2 - 714



Conclusions: PD-L1 is expressed in the epithelium and white blood cells in majority of BE, LG, HG, untreated EA and treated EA. The presence of PD1+ lymphocytes in a higher proportion of LG, HG and treated EA, compared to squamous epithelium, suggests a possible association of PD1 in the immune microenvironment of these entities. PD1+ lymphocytes and PD-L1 expression had no significant difference between untreated and treated EA, indicating that immune checkpoint-based therapies may be useful in patients after chemoradiation therapy.

715 Immunohistochemistry Helps Distinguish Signet Ring Cell Carcinoma In-situ from Pseudo-Signet Ring Cells in The Stomach

Pallavi Patil¹, Odise Cenaj², Xiaogang Wen³, Fatima Carneiro⁴, Robert Odze⁵

¹Brown University Lifespan Academic Medical Center, Providence, RI, ²New York University Langone Medical Center, New York, NY, ³Institute of Molecular Pathology and Immunology of the University of Porto (IPATIMUP), Porto, Portugal, ⁴Ipatimup, Porto, Portugal, ⁵Brigham and Women's Hospital, Boston, MA

Disclosures: Pallavi Patil: None; Odise Cenaj: None; Xiaogang Wen: None; Fatima Carneiro: None; Robert Odze: None

Background: We have noted, anecdotally that some benign changes in gastric epithelium develop pseudo-signet ring cell change (pseudo-SRC), sometimes related to inflammation that can mimic in-situ signet ring cell carcinoma (in-situ SRCC). These are difficult to distinguish. The purpose of this study was to evaluate histochemical (mucicarmine, alcian blue, PAS, PAS-D) and immunohistochemical stains (CDX-2, E-cadherin, MIB-1, beta-catenin, p53, MUC1, MUC2, MUC4, MUC6, MUC5AC) that may be useful to distinguish pseudo-SRC from in-situ SRCC.

Design: The study groups consisted of pseudo-SRC cases (n=12), intra-mucosal invasive SRCC controls (n=8), and in-situ SRCC controls (n=2). Pseudo-SRC were defined as cells restricted to intra-epithelial space with nucleus compressed to the edge of the cell membrane by a large cytoplasmic vacuole, have no mitoses, and may show loss of polarity. Clinical and pathological features of cases were recorded. Histochemical and immunohistochemical stains mentioned above were performed and scored as positive or negative in the cells in question.

Results: Pseudo-SRC cases demonstrated chronic gastritis (n=6), active inflammation (n=1), and intestinal metaplasia with chronic gastritis (n=2). Biopsies were from antrum (n=7) and body (n=5). Morphologically, pseudo-SRC were diffusely present in epithelium, noted in foveolae (n=3), neck and glands (n=9). Comparison of groups by expression of stains is shown in Table 1. Immunohistochemically, pseudo-SRC were E-Cadherin and beta-catenin positive, p53 negative, no Ki-67 increase, Figure 1. In-situ SRCC were E-Cadherin, beta-catenin, and p53 negative, no Ki-67 increase, Figure 2. Intramucosal invasive SRCC were E-Cadherin, beta-catenin, and p53 (37%) positive with increased Ki-67 (75%). E-Cadherin and beta-catenin positive in pseudo-SRC was significant than negative in in-situ SRCC, p=0.01 each, p<0.05. Higher Ki-67 and p53 positive intramucosal invasive SRCC was significant than negative in pseudo-SRCC, p=0.007 and p=0.049 respectively, p<0.05. Pseudo-SRC expressed mucins similar to normal gastric mucosa.

Table 1: Comparison of histochemical and immunohistochemical expression of pseudo-SRCC, intramucosal invasive SRCC, and in-situ SRCC.

	Pseudo-SRC n=12, n(%)	Intramucosal invasive SRCC n=8, n(%)	In-Situ SRCC n=2, n(%)
CDX2	0	0	0
E-Cadherin	12 (100)	8 (100)	0**
Mib-1/Ki-67	0	6 (75)*	0
Mucicarmine	0	N/A	N/A
P53	0	3 (37)*	0
Beta-Catenin	12 (100)	7 (87)	0**
Muc1	8 (67)	5/6 (83)	0
Muc2	0	2 (25)	0
Muc4	5 (42)	4/6 (67)	N/A
Muc6	9 (75)	2/7 (28)	0
Muc5AC	10/11 (90)	5/6 (83)	N/A
Alcian Blue	0	N/A	N/A
PAS-D	9/9 (100)	N/A	N/A
PAS	9/9 (100)	N/A	N/A

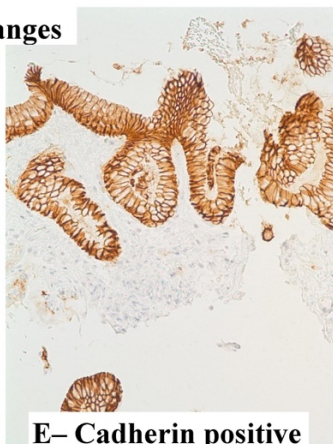
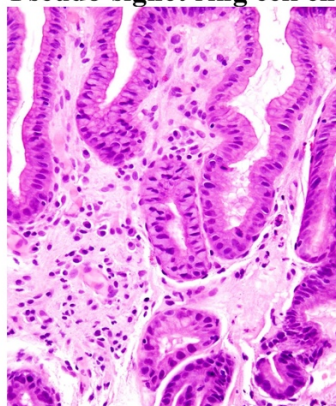
* Significantly higher compared to pseudo-SRC, $p < 0.05$

** Significantly lower compared to pseudo-SRC, $p < 0.05$

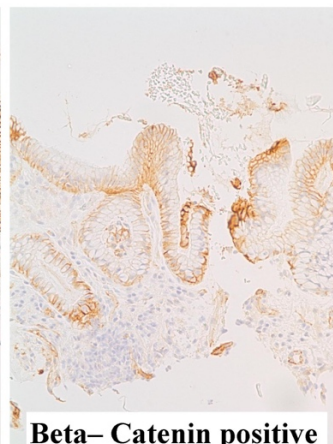
Pseudo-SRC= pseudo signet ring cell changes, SRCC= signet ring cell carcinoma, N/A= not applicable, Muc= mucin, PAS-D= Periodic acid-Schiff-diastase, PAS= Periodic acid-Schiff

Figure 1 - 715

Pseudo-signet ring cell changes



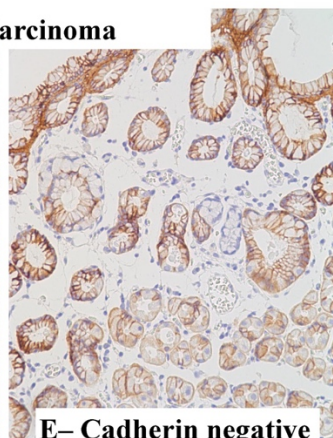
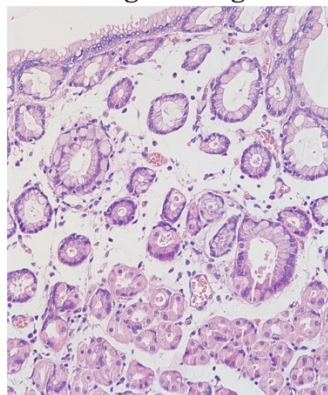
E- Cadherin positive



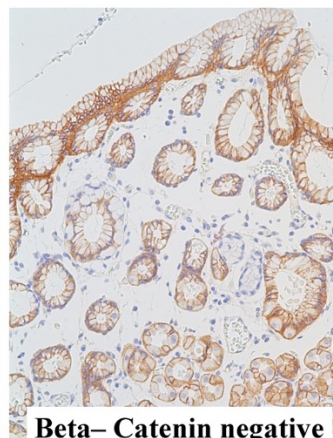
Beta- Catenin positive

Figure 2 - 715

In-situ Signet Ring Cell Carcinoma



E- Cadherin negative



Beta- Catenin negative

Conclusions: Immunohistochemical expression of E-Cadherin and beta-catenin are useful to distinguish pseudo-SRC (positive) from in-situ SRCC (negative). Higher Ki-67 proliferation index and p53 expression may be helpful to distinguish intramucosal invasive SRCC from

pseudo-SRC. Awareness of pathologists' about these entities and their diagnostic tools will help to avoid misdiagnosis, for better patient care.

716 A Comparative Analysis of Immunohistochemical Profile (PDL1, HER2, P53, and CK7) of Primary Gastric Carcinoma, Before and After Administration of Neoadjuvant Chemotherapy

Rugved Pattarkine¹, Qiqi Ye¹, Christopher Gault², Minghao Zhong¹

¹Westchester Medical Center, Valhalla, NY, ²Westchester Medical Center/Mid-Hudson Regional Hospital, New York, NY

Disclosures: Rugved Pattarkine: None; Qiqi Ye: None; Christopher Gault: None; Minghao Zhong: None

Background: Gastric carcinoma comprises 8% of all cancers worldwide and has a high mortality rate when compared to many other cancers. 90% of malignant tumors in the stomach are carcinomas and are often asymptomatic until they are detected at an advanced stage and Neoadjuvant chemotherapy along with immunotherapy with pembrolizumab and trastuzumab (used for PD-L1 expressing and HER-2+ carcinomas respectively) play an important role in pre and post-surgical therapy. Neoadjuvant therapy has been used with locally advanced tumors and those with a high risk of recurrence despite curative surgery. This begs the question of whether the immunohistochemical profile of the tumor is altered after initial administration of neoadjuvant therapy. In particular, are key therapeutic targets like PD-L1 and HER-2 altered in response to neoadjuvant therapy. This study aims to explore this question.

Design: A retrospective review of all gastric carcinoma cases (120 cases) at our institution between 2005 to 2018 was conducted. Nine cases of biopsy-confirmed primary gastric adenocarcinoma were identified in which patients had undergone neoadjuvant chemotherapy prior to resection. A comparative study of immunostaining with CAIX, CK7, PD-L1 and HER-2 (therapeutic markers) expression on pre- and post-treated carcinomas was done.

Results: Tumor specimens obtained pre and post-chemotherapeutic treatment were analyzed (figure 1 and figure 2). A wide range of therapy related changes in the nine cases ranging from mild to significant treatment effect (20-95% response) were present. Two of the cases were positive and 7 were negative for HER2 and showed concordant staining pre and post treatment in 100% cases; 6 cases showed immunopositivity for CK7 and 3 cases were negative for it, and pre- and post-chemotherapy IHC results were concordant in 100% cases; CA 9 was negative in 8 cases and positive in 1 case, and pre- and post-chemotherapy IHC concordance was 100%; PDL1 was negative (using Tumor Proportion Score ≥50% for positivity) in 9 cases, and pre- and post-chemotherapy IHC concordance was 100%.

Figure 1 - 716

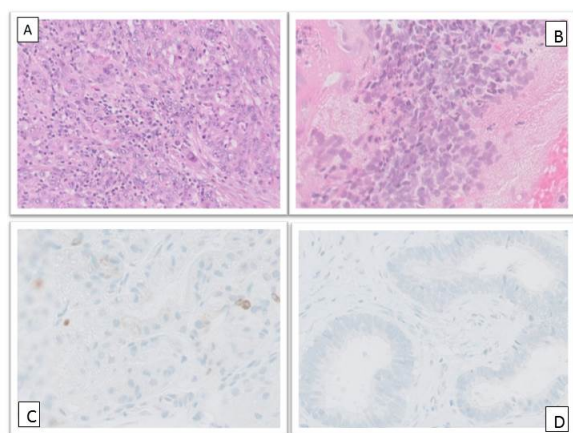


Figure 1 - H&E stain on carcinoma, A) biopsy & B) surgical case.
CK7 stain on carcinoma, A) biopsy & B) surgical case.

Figure 2 - 716

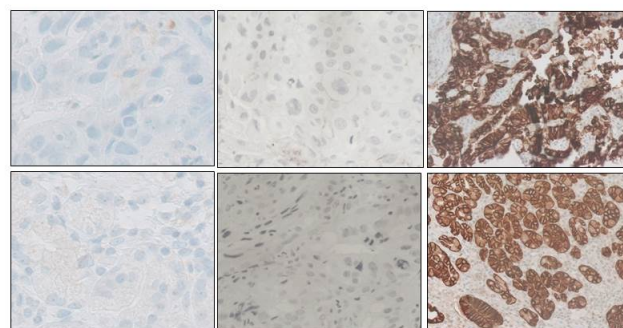


Figure 2- PDL1 on carcinoma A) biopsy & B) surgical case.
HER2 on carcinoma C) biopsy & D) surgical case.
CAIX on carcinoma E) biopsy & F) surgical case

Conclusions: Based on our findings, the Immunoprofile of gastric carcinoma remains consistent pre and post chemotherapy, suggesting there is no change in expression for CAIX, CK7, PDL1 and HER2. Although a study with larger sample size is needed we can conclude that IHC results are reliable to guide clinical management and usability of PDL1 and HER2 even after curative surgical resection for high recurrence risk patients.

717 Molecular Profiling of Neoplastic Progression in Appendiceal Adenocarcinoma Supports Low Grade Appendiceal Mucinous Neoplasm as a Precursor Lesion

Vera Paulson¹, Nemencio Ronquillo², John Thorson³, Mark Valasek³

¹University of Washington Medical Center, Seattle, WA, ²University of Louisville Hospital, Louisville, KY, ³University of California, San Diego, La Jolla, CA

Disclosures: Vera Paulson: None; John Thorson: None; Mark Valasek: None

Background: The relationship between low grade appendiceal mucinous neoplasm (LAMN), high grade appendiceal mucinous neoplasm (HAMN), and appendiceal adenocarcinoma (AAC) is largely unknown; we and others have hypothesized that it is a stepwise progression. To clarify this association, we undertook molecular profiling of invasive AAC arising in a background of LAMN and/or HAMN.

Design: The pathology archives were searched to identify patients with a history of resection for AAC arising in a background of LAMN and/or HAMN. Seven (7) patients with tissue sufficient for molecular testing were identified, comprised of 2 cases each of LAMN/HAMN, HAMN/AAC, and LAMN/HAMN/AAC and one case of LAMN/ACC. Slides were reviewed to confirm diagnosis and to select each component for macrodissection. DNA was then extracted for molecular characterization using targeted next generation sequencing (Illumina HiSeq 2500) performed on libraries prepared with custom designed hybrid capture (Agilent Sure Select) baits of 397 genes to identify mutations, insertion/deletions, and cancer-associated rearrangements. Variants identified were analyzed by an internally developed computational pipeline with manual review by two molecular pathologists.

Results: As previously described, the majority of patients harbored constitutively activating KRAS (6, 86%) and GNAS (3, 43%) mutations; less common findings included an activating NRAS mutation and inactivating TGFRB2 and SMAD4 mutations (1 case each, 14%). Clear evidence of progression was observed in two (2, 29%) cases: (1) a LAMN/HAMN/ACC case demonstrated an increase in mutant PIK3CA and KRAS allele fractions and biallelic inactivation of TP53 (p.G266E with loss of heterozygosity) and (2) a LAMN/AAC case acquired variants in PIK3R1 (p.T576del), CDKN1B (p.I119Mfs*26), and TP53 (p.A159V). Interestingly, the latter case also demonstrated absence of the activating GNAS variant identified in the concurrent LAMN.

Conclusions: Much like the progression of colorectal adenoma to adenocarcinoma, infiltrating AAC can be seen as a distinct lesion arising from appendiceal mucinous neoplasms (LAMN and/or HAMN). These molecular findings support LAMN and HAMN as precursor lesions in a stepwise progression to AAC and suggest molecular events leading to progression include loss of GNAS and TP53, cell cycle dysregulation, and activation of the PI3K signalling pathway. In some cases these events may arise early in the process. Additional studies in larger cohorts are needed to confirm these findings.

718 Diffuse Lymphocytic Esophagitis Is Commonly Associated with Systemic Immune-Mediated Diseases

Meredith Pittman¹, Philip Katz¹, Rhonda Yantiss²

¹New York-Presbyterian/Weill Cornell Medical Center, New York, NY, ²Weill Cornell Medical College, New York, NY

Disclosures: Meredith Pittman: None; Philip Katz: None; Rhonda Yantiss: None

Background: Lymphocytic esophagitis is defined as intraepithelial lymphocytosis (>20/HPF) with rare granulocytes. It is associated with Crohn disease in children but has no established relationship with immune-mediated disorders in adults. In fact, clinicians often ignore a pathologic diagnosis of lymphocytic esophagitis because it lacks specificity. We hypothesize that lymphocytic esophagitis also represents an immune-mediated disorder in adults, but its nature has been masked in prior studies by inclusion of large numbers of patients with other types of esophagitis. We performed this study to refine diagnostic criteria for lymphocytic esophagitis and determine its clinical significance.

Design: We searched our database for adults diagnosed with intraepithelial lymphocytosis (>20/HPF) accompanied by only rare granulocytes. We excluded those with dysmotility, sampling limited to the distal esophagus, and candidiasis in order to eliminate confounding effects of luminal stasis, reflux, and infection. The resultant study group consisted of 54 patients with lymphocytic esophagitis at multiple levels within the esophagus. Data regarding sex, age, endoscopic findings, medications, and other conditions was obtained from the patients' medical records.

Results: Most (68%) patients were women (mean age: 56 years) who presented with dysphagia (60%). The endoscopic appearance mimicked eosinophilic esophagitis in 25 (46%) patients, and featured edema, white plaques, rings, nodularity, and/or linear furrows. The esophagus was normal in 15 (28%) cases. Systemic autoimmune diseases were present in 34 (63%) patients. Most had inflammatory bowel disease (n=14), rheumatoid arthritis (n=6), or psoriasis (n=3); only one had lichen planus. Four (7%) patients were taking sartans. Samples consistently featured mucosal lymphocytosis with clustered lymphocytes, edema, and dyskeratotic cells, regardless of associated disorders.

Conclusions: Esophageal lymphocytosis is a nonspecific manifestation of mucosal irritation. A diagnosis based on histologic features alone is not clinically helpful in most cases; however, excluding patients with motility disorders and sampling confined to the distal esophagus does identify a unique patient group. Diffuse lymphocytic esophagitis is always accompanied by epithelial injury and likely represents an immune-mediated disorder. It is more common among middle-aged women, presents with dysphagia, and frequently simulates the endoscopic features of eosinophilic esophagitis.

719 Histopathological Patterns of Colitis in Patients with Impaired Renal Function: A Retrospective Study of Lower Gastrointestinal Tract Biopsies

Lianqun Qiu¹, Daniel Mais¹, Emily Volk¹

¹The University of Texas Health Science Center at San Antonio, San Antonio, TX

Disclosures: Lianqun Qiu: None; Daniel Mais: None; Emily Volk: None

Background: The most common non-renal site of disorders in patients with impaired renal function is the gastrointestinal tract. The aim of this study was to characterize the range of findings in a population of patients with impaired renal function who presented with colitis, as compared to a concurrent population of patients with normal renal function.

Design: We retrospectively identified consecutive patients who underwent colonoscopic evaluation for colitis between 2010 and 2015 at a single institution with a relatively large population of patients with impaired renal function. Patients were divided into four groups based on their estimated glomerular filtrate rates (group 1 with normal renal function and groups 2, 3, and 4 with mild, moderate and severe impairment according to estimated GFR). All biopsies were reviewed histologically, and, in conjunction with clinical and laboratory data, to determine the etiology.

Results: There were 312 patients in group 1 with normal renal function and 101 patients in groups 2-4 with impaired renal function of varying severity with mean ages of 47 and 64 years in the normal and abnormal renal function groups, respectively ($P < 0.001$). Compared to a preponderance of inflammatory bowel disease (103 cases, 33%) and lymphocytic colitis (30 cases, 9.6%) in group 1 patients, ischemic colitis (59 cases, 58%) was the predominant histopathological pattern in the patients with impaired renal function ($P < 0.001$). Infectious colitis was the second most common colitis pattern in patients with impaired renal function (21 cases, 20.8%); however, only certain infections such as *C. difficile* and CMV infections were more frequently seen in groups 2-4 ($P < 0.001$ and $P = 0.025$, respectively). Medication-induced injury was also more common in impaired renal function groups ($P = 0.001$), with crystal-mediated injury being common in uremic patients, representing 19.7% (11 cases) of histological findings in groups 3-4; whereas only 1 case (0.3%) was identified in group 1 ($P < 0.001$). Subset analysis was conducted using age-matched controls with similar findings to correct for age differences between control and impaired renal function groups.

Conclusions: Colitis in patients with impaired renal function, even after correction for age differences, is etiologically distinct from that seen in patients with normal renal function, and it is most commonly caused by ischemia, infections, and medication.

720 Endoscopic Mucosal Biopsies of Rectal Masses in the Setting of Prior Chemoradiation Therapy – Beware of Male GU Tissues

Whitney Reid¹, Quan Ly¹, Jennifer Leinicke¹, Sean Langenfeld¹, Kelsey Klute¹, Jean Grem¹, Chi Lin¹, Audrey Lazenby¹

¹University of Nebraska Medical Center, Omaha, NE

Disclosures: Whitney Reid: None; Sean Langenfeld: None; Kelsey Klute: None; Audrey Lazenby: None

Background: Routine endoscopic biopsies of rectal masses are most commonly diagnosed as adenoma or carcinoma, with other tissue types rarely identified. We had an unusual finding of scant seminal vesicle amidst inflamed granulation tissue on biopsy of a posterior rectal mass (patient with history of rectal cancer post-surgery and chemoradiation), misdiagnosed as carcinoma. Our study addresses frequency of male GU tissue in mucosal biopsies of the rectum (focusing on patients with prior rectal cancer surgery and chemoradiation), clinical setting, misdiagnoses and IHC markers to establish the correct diagnosis.

Design: Synoptic worksheets for colorectal CA (keywords: "rectum", "male", "low anterior resection") were searched for 10 years, yielding 112 cases (in-house and consults). On these patients, follow-up rectal specimens were found. A search for "colorectal anastomosis" and "prostate or seminal vesicle" in rectal biopsy was also done. 25 cases were found; histories were reviewed, and IHC done on select cases (CK20, CDX2, p40, p63, K903, CK5/6, PSA, NKX3.1).

Results: From the 25 cases identified, 13 were benign colorectal tissue, 9 had recurrent carcinoma, and 3 had male GU tissue. Of the GU tissue, 2 were seminal vesicle and 1 was prostate with focal seminal vesicle. Seminal vesicle stained strongly with a basal cell marker (p40 or P63) and a HMWK (K903 or CK5/6). The prostate tissue had faint staining for PSA, rare cell positive for NKX3.1, but strong staining with K903 and p63. CK20 and CDX2 stained the rectal but not GU tissue. Our incident biopsy, diagnosed as 'carcinoma, NOS, IHC incompatible with colorectal primary' had a re-resection showing the mass was seminal vesicle adherent to posterolateral rectum. The

biopsy with prostate was originally diagnosed as carcinoma by an outside institution, but recognized as atrophic prostate with basal cell hyperplasia on review. All 3 patients had a complicated course after surgery, with deep ulceration of rectal tissue or fistulization after chemoradiation. One patient was on bevacizumab.

Conclusions: 1) Male GU tissue is uncommon in rectal biopsies post rectal cancer surgery and chemoradiation, 2) Male GU tissue is easily misdiagnosed in this setting unless considered and IHC done, 3) Basal cell stains (p40 or p63) or HMWK (K903 or CK5/6) reliably mark male GU tissue, while colorectal markers CK20 and CDX2 are negative, 4) Male GU tissue is usually seen in patients with a more complicated surgical course with deep ulceration after chemoradiation.

721 Periappendiceal Sessile Serrated Adenoma: How Deep Is The Extension Into The Appendix?

Prih Rohra¹, Fatima Mir¹, Shriram Jakate¹
¹Rush University Medical Center, Chicago, IL

Disclosures: Prih Rohra: None; Fatima Mir: None; Shriram Jakate: None

Background: Sessile serrated adenomas (SSAs) preferentially occur in the right colon and are flat fold-like lesions. Larger (>1 cm) lesions are managed by saline lift and endoscopic mucosal resection (EMR). The subsequent surveillance depends upon completeness of excision, the size of SSA and/or presence or absence of dysplasia. When the SSA is present circumferentially along the periappendiceal orifice, its depth of extension into the appendiceal lumen remains endoscopically unknown and all surveillance variables (endoscopic excision, size and dysplasia) are compromised. Surgical removal of the appendix along with a rim of cecum ("cecectomy") remains the best option. We reviewed periappendiceal SSAs treated by cecectomy to evaluate the characteristics of SSA concealed within the appendiceal lumen.

Design: We searched our Medical Center's pathology and endoscopy databases from 2010 to 2018 for endoscopically identified periappendiceal SSAs that were biopsied and subsequently surgically excised by cecectomy. Both the biopsies and the surgical specimens were reviewed to confirm SSA and determine presence or absence of dysplasia and evaluate the extent of SSA within the appendix.

Results: A total of 28 cases (mean age 64; 18 females and 10 males) were identified. Endoscopically, all had polypoid lesions extending around the appendiceal orifice measuring >1 cm in size and not amenable to EMR. Multiple biopsy fragments from these lesions showed SSA with serrated broad-based glands and no dysplasia (Bx 0/28 dysplasia). Subsequent cecectomies showed SSA extending into the upper or basal third of the appendix in 23/28 cases (82%) and the entire appendix in 5/23 cases (18%). 2/5 cases involving the entire appendix (2/28 or 7% total cases) also had low grade dysplasia which was not seen in the endoscopic periappendiceal biopsies.

Conclusions: Endoscopically detected periappendiceal SSAs always extend into the appendix either involving the upper or basal portion (82%) or the entire appendix (18%). Dysplasia may be present in the appendiceal and not the periappendiceal portion of SSA. Cecectomy (appendectomy with excision of the cecal rim) and not EMR, is hence the optimal procedure for managing periappendiceal SSA.

722 Low Incidence Mitotic Activity Best Detected by Manual Count as Compared to Whole Slide Imaging Digital Computer Assessed Counting: Lessons Learned

Sujata Sajjan¹, Yihe Yang², Nasim Mansoor³, Lili Lee⁴
¹Donald and Barbara Zucker School of Medicine at Hofstra/Northwell, New York City, NY, ²Northwell Health Hofstra Northwell School of Medicine, Lake Success, NY, ³Northwell, New Hyde Park, NY, ⁴Northwell Health Hofstra Northwell School of Medicine, New Hyde Park, NY

Disclosures: Sujata Sajjan: None; Yihe Yang: None; Nasim Mansoor: None; Lili Lee: None

Background: Pathologic grading of neuroendocrine tumors (NETs) and carcinomas (NECs) is critical from a prognostic standpoint, but occasionally presents a challenging interpretive dilemma. While Ki-67 is an established proliferation marker in NETs, Ki-67 assessment has limitations due to lack of uniformity and consistency in quantification. These limitations are accentuated in well-differentiated NETs, as slight differences in the value can alter tumor grade. We performed a concordance study to assess different Ki-67 quantification techniques: 1.computer assisted whole slide digital image analysis of Ki-67 (comp-Ki67) and 2.manual count of Ki-67 (MC-Ki67). We also correlated these results with manual mitotic counting on H&E stained slides (MMC).

Design: The study included 134 patients with NETs of the gastrointestinal tract and pancreas from our institution from 2011 to 2017. MC-Ki67 and MMC were retrieved from the pathology report. Ki-67 stained whole slide images were captured and the tumor area with the greatest mitotic activity was manually identified. The Ki-67 positive cells were counted in 0.5 mm² using Ventana Virtuoso software. As per the 2010 WHO criteria, a manual mitotic count is used as the reference against which other techniques are compared. Results were compared by Spearman correlation.

Results: The median age of 134 patients was 65 years (22 to 91 years) and 79 patients were males (58.95%). The locations of the neuroendocrine tumor included stomach (n=6), small bowel (n=64), large bowel (n=6), appendix (n=7), mesentery (n=1) and pancreas (n=50). Out of 134 patients, 108 patients had Grade 1 NETs, 21 had Grade 2 NETs and 5 patients had Grade 3 NECs. Spearman correlation indicates good agreement between MMC versus MC- Ki-67 (correlation coefficient 0.697, $p < 0.001$). However, there was discordance between MMC versus comp-Ki67 (correlation coefficient 0.361, $p < 0.001$). Using MMC as the standard, MC-Ki67 categorized NETs into Grade 1 with a sensitivity of 88.6% and Grade 2 with a sensitivity of 80%. In contrast, the sensitivity of comp-Ki67 was only 31.6% in Grade 1 NETs and 50% in Grade 2 NETs. Notably, in Grade 3 NECs, both MC-Ki67 and comp-Ki67 successfully identified 100% patients (sensitivity = 100%).

Conclusions: We confirm that MMC and MC-Ki67 are acceptable standards for assessment of low and high grade NETs. However, while comp-Ki67 can be used to confirm manual Ki-67 in Grade 3 NECs, there is low concordance with MMC and is an unacceptable method of assessing Grade 1-2 NETs.

723 In Search of Nodular GAVE: Clinico-Pathological Analysis of 70 Gastric Hyperplastic Polyps

Monica Sanchez-Avila¹, Aastha Chauhan², Khalid Amin¹, Shawn Mallory³

¹University of Minnesota, Minneapolis, MN, ²University of Minnesota, Saint Paul, MN, ³UMMC, Minneapolis, MN

Disclosures: Monica Sanchez-Avila: None; Aastha Chauhan: None; Khalid Amin: None; Shawn Mallory: None

Background: Nodular gastric antral vascular ectasia (GAVE) is a recently described entity shown to have a strong association with cirrhosis and autoimmune disorders. Based on a recent study this novel phenotype is mostly diagnosed as hyperplastic polyp (HP) which can cause management challenges since treatment of this entity is focused on ablation rather than polypectomy. This study was undertaken to identify the histological features that can differentiate nodular GAVE from hyperplastic polyps.

Design: Seventy cases of gastric polyps located in the antrum or body with a diagnosis of HP from 61 patients were identified after a retrospective chart review that included retrieval of clinical data. Histology slides were reviewed and following histologic features were scored semiquantitatively on a scale of 0-3 (0=absent, 1= focal/mild, 2= intermediate 3=extensive/diffuse): hyperplastic changes, vascular ectasia, lamina propria smooth muscle proliferation, fibrin thrombi and superficial ulceration with granulation tissue formation. Based on the total score, the cases were divided into three categories: unlikely GAVE (score 0-5), possibly GAVE (score 6-10), likely GAVE (score 11-15) and correlated with clinical features, specifically association with cirrhosis, autoimmune disease and recurrence.

Results: Of the 70 polyps, 48 (68%) were categorized as unlikely GAVE (score 0-5), 13 cases (18%) were in the intermediate, possible GAVE category (score 6-10) while 9 cases (12%) were categorized as likely GAVE (score 11-15). Cirrhosis was present in 3/9 (33%) cases of likely GAVE category, while no case of autoimmune diseases was seen in this group. The intermediate, possible GAVE group, had the highest number of cirrhosis cases, 7/13 (54%) and only one patient with autoimmune disorder. The unlikely GAVE group had 4/48 (8%) patients with cirrhosis and 7/8 patients with autoimmune disorder. Out of the 9 patients with recurrence, 4 were in the intermediate category, 3 in unlikely GAVE category and 2 in the likely GAVE category.

Category (Score)	Unlikely GAVE (0-5)	Possible GAVE (6 - 10)	Likely GAVE (11- 15)
Total Polyps	48 (69%)	13 (19%)	9 (13%)
Cirrhosis	4 (8%)	7 (54%)	3 (33%)
Autoimmune	8 (17%)	1 (8%)	0
Recurrence	3 (6%)	4 (31%)	2 (22%)

Conclusions: Our study found a trend of higher incidence of cirrhosis in HP polyps with GAVE like histologic features. However no such trend was found with autoimmune diseases or recurrence. The histologic features described to be associated with nodular GAVE are not specific enough to render a definite diagnosis and require clinical correlation.

724 Correlation of Clinicopathological Features and LGR5 Expression in Colon Adenocarcinoma

Koichi Sato¹, Takeshi Uehara¹, Tomoyuki Nakajima², Hiroyoshi Ota³

¹Shinshu University School of Medicine, Matsumoto, Japan, ²Shinshu University Hospital, Matsumoto, Japan, ³Shinshu University School of Health Sciences, Matsumoto, Japan

Disclosures: Koichi Sato: None; Takeshi Uehara: None; Tomoyuki Nakajima: None; Hiroyoshi Ota: None

Background: Colorectal cancer is the fourth leading cause of cancer-related death worldwide, with an increasing trend in recent years. Colon cancer stem cells (CSCs) are closely related to tumorigenesis and treatment response. *LGR5* is currently the most robust reliable CSC marker in colorectal cancer. However, *LGR5* expression in the invasive front of colorectal cancer is not well understood. We examined the clinicopathological and prognostic significance of *LGR5* at the invasive front of colorectal cancer.

Design: *LGR5* expression was evaluated by an RNAscope, a newly developed RNA in situ hybridization technique, with a tissue microarray from 59 colon adenocarcinoma (CA) patients selected from the medical archives at our hospital. Patients were stratified into high and low *LGR5* expression groups according to the manufacturer's instructions.

Results: Of the 59 cases, 34 cases contained tumor cells with some *LGR5*-positive dots in the invasive front. Inflammatory cell infiltration was weaker and histological grade was lower in the high *LGR5* expression group compared with the low *LGR5* expression group ($P=0.0075$ and $P=0.0062$, respectively). There were significantly more high stage (Stage IV) tumors, which presents distant metastasis, in the *LGR5* high expression group compared with the *LGR5* low expression group ($P=0.0220$).

Conclusions: *LGR5* expression may be affected by inflammatory cell infiltration in the invasive front of CA. As high *LGR5* expression in the invasion front, which is more frequent in low histological grade CA, is associated with distant metastasis, analysis of *LGR5* expression in the invasive front may have important implications in CSC-targeted therapy.

725 Endoscopic Biopsy Followup of Gastric Intestinal Metaplasia is of no Clinical Benefit in a Low Risk Population

Namrata Setia¹, Lindsay Alpert¹, John Hart¹

¹University of Chicago, Chicago, IL

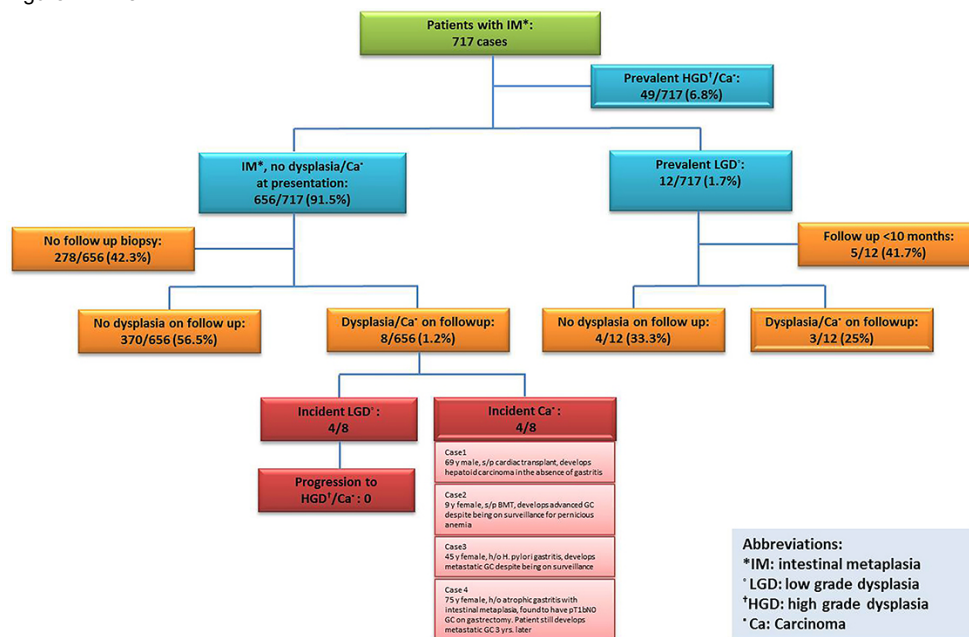
Disclosures: Namrata Setia: None; Lindsay Alpert: None; John Hart: None

Background: The significance of gastric intestinal metaplasia in a low risk population is unclear, and guidelines for surveillance of such cases are not available. The aim of this study is to determine the clinical utility of biopsy followup of intestinal metaplasia encountered in routine practice.

Design: A retrospective study was performed. Pathology reports of endoscopic gastric biopsies from 2005 through 2014 were reviewed. Of the 13,546 cases, 1,816 biopsies from 717 patients showed intestinal metaplasia. Longitudinal followup was conducted to assess the rate of progression to dysplasia or gastric carcinoma (incident dysplasia/carcinoma). Dysplasia or carcinoma at presentation (prevalent dysplasia/carcinoma) in association with intestinal metaplasia was recorded separately.

Results: The mean age of the cohort was 68 years (± 16.5 years, range 3-98 years), the male: female ratio was 1:1.3 and there was a median followup period of 4 years (range 1-36 years). Intestinal metaplasia was present in 5.1% of the entire cohort. Prevalent high grade dysplasia/carcinoma and prevalent low-grade dysplasia comprised 0.35% and 0.09% cases of the entire cohort, respectively. Incident high grade dysplasia/carcinoma and incident low-grade dysplasia developed in 0.01% cases of the entire cohort. None of the incident low grade dysplasia cases progressed to carcinoma despite a mean followup of 2-3 additional upper GI endoscopies with non-targeted biopsies over a mean of 3 years. Surveillance and operative intervention in the patients with incident high grade dysplasia/carcinoma did not prevent the development or progression of gastric carcinoma. Details of incident high grade dysplasia/carcinoma and followup of the entire cohort are shown in Figure 1.

Figure 1 - 725



Conclusions: The risk of incident carcinoma developing in the setting of intestinal metaplasia is extremely low, and follow up of cases with intestinal metaplasia does not prevent the development/progression of carcinoma. Prevalent dysplasia/carcinoma accounts for the majority of gastric neoplasia seen in association with gastric intestinal metaplasia in a population with low risk of gastric carcinoma.

726 Mosaic Expression of 5-Hydroxymethylcytosine (5hmc) In Gastrointestinal Neuroendocrine Neoplasms, Except in Goblet Cell Carcinoids and a Subset of Pancreatic Neuroendocrine Tumors

Aarti Sharma¹, Thomas Krausz², Namrata Setia¹

¹University of Chicago, Chicago, IL, ²University of Chicago Hospital, Chicago, IL

Disclosures: Aarti Sharma: None; Thomas Krausz: None; Namrata Setia: None

Background: Mutation rate in neuroendocrine tumors (NETs) is significantly lower than that in other cancers, indicating a role of epigenetic aberrations in their pathogenesis. However, investigation of epigenetic pathways as a mechanism for understanding the intrinsic characteristics of NETs as a whole has not yet been undertaken. The demethylating agent 5-hydroxymethylcytosine (5hmc) is variably regulated in a variety of normal and neoplastic tissues, and is increasingly used to discriminate biologically relevant groups of tumors. Here, we assessed expression of 5hmc in a cohort of NETs originating from various locations in the gastrointestinal (GI) tract.

Design: 5hmc expression was semi-quantitatively determined by immunohistochemistry for 80 primary neuroendocrine tumors at various sites in the GI tract [13 gastric, 7 duodenal, 15 ileal, 9 colorectal, 11 appendiceal (8 goblet cell carcinoids/adenocarcinoma ex-goblet cell carcinoids and 3 tubular carcinoids), and 25 pancreatic]. Tumors were scored using a numerical system based on the percentage of tumor nuclei with discernable stain uptake (0 - loss to 4 - retention). Comparison between scores of NETs of different sites was accomplished with post-hoc analysis of variance (ANOVA) and t-tests with Bonferroni correction.

Results: The 5hmc scores are shown in Table 1. NETs from the stomach, duodenum, ileum, appendix (tubular carcinoid) and colon/rectum demonstrated a heterogenous and mosaic pattern of 5hmc expression with an average nuclear score of 3 overall. Goblet cell carcinoids (GCC) and adenocarcinoma ex-counterparts (AXGCC), on the other hand, manifested a significant loss of 5hmc expression with an average nuclear score of 1.5 ($p < 0.005$, compared to NETs from the aforementioned sites). Pancreatic NETs demonstrated an intermediate score of 1.9 ($p < 0.05$, compared to NETs other than GCC/AXGCC).

NET Site	5hmc Score \pm SD	p Value					
Stomach	3.2 \pm 1.0	NS*					
Duodenum	3.6 \pm 0.5	NS*					
Ileum	3.1 \pm 0.8	NS*					
Appendiceal tubular carcinoid	4 \pm 0	NS*					
Appendiceal goblet cell carcinoid/adenocarcinoma ex-goblet cell carcinoid	1.5 \pm 0.75	< 0.001**†					
Rectum/Colon	3.4 \pm 0.9	NS*					
Pancreas	1.9 \pm 1.3	< 0.001**‡					
†: p value for comparison between GCC/AXGCC scores from those of stomach, duodenum, ileum, appendix (tubular carcinoid), and rectum/colon							
‡: p value for comparison between pancreatic NET scores from those of stomach, duodenum, ileum, appendix (tubular carcinoid), and rectum/colon							
NS*: Not Significant. Scores from NETs of stomach, duodenum, ileum, appendix (tubular carcinoid), and rectum/colon were not significantly different between groups.							

Conclusions: This study demonstrates an intrinsic loss of expression of 5hmc in not only adenocarcinoma ex-goblet cell carcinoids but also appendiceal goblet cell carcinoids and a subset of pancreatic NETs. Our findings suggest that epigenetic mechanisms involving 5hmc are inherent to the pathogenesis of these tumors.

727 Correlation of missed Giardiasis diagnosis between Histology and Microbiology

Minqian (Jasmine) Shen¹, Lysandra Voltaggio², Scott Robertson³

¹Cleveland Clinic Foundation, Cleveland, OH, ²Baltimore, MD, ³Cleveland Clinic, Cleveland, OH

Disclosures: Minqian (Jasmine) Shen: None; Lysandra Voltaggio: None; Scott Robertson: None

Background: *Giardia duodenalis* is the most common intestinal parasitic infection in the US. It causes diarrhea and is most prevalent among children, travelers and immunocompromised patients. *Giardia* can be detected in the stool—by microscopy or with an immunoassay. *Giardia* trophozoites also can be seen histopathologically in biopsies from the small bowel. Microscopically, the *Giardia* organism is usually found along with the luminal aspect of duodenal epithelium. However, *Giardia* can be difficult to detect, often masquerading as sloughed epithelial cells or luminal contents. Furthermore, the background mucosa can be unremarkable, provided no specific clue pointing to the presence of an infectious organism. We hypothesized that *Giardia* is sometimes missed in small bowel examination. To test this question, we performed a targeted retrospective review of small bowel biopsies from patients with positive stool-based tests. We determined how often *Giardia* is missed and explored what histologic and clinical features were associated with these cases.

Design: We identified all positive *Giardia* stool tests (ova and parasite examination and *Giardia* antigen immunoassay) in our institution from 2002 to 2017. For these patients (n=277), we determined who had a corresponding small bowel biopsy (from 1000 days prior, to 200 days after the positive stool test). These biopsies (n=61) were retrospectively examined for *Giardia* organisms. Histological features and clinical details were recorded for positive cases.

Results: Targeted retrospective review showed *Giardia* in 8 of 61 cases (13.1%). The organism was prospectively identified in 4 of 8 cases (50%) but missed in the remaining 4 cases (50%). A review of clinical history showed 4 of 8 patients were potentially immunocompromised. Clinical history and histological features of all 8 cases are included in Table 1.

Table 1 Clinical History and Histological Features

Case #	Missed	Age/Sex	Predisposing factor	Location	Organism #	Neutrophils	Lymphoid aggregates	Architecture change	Increased intra-epithelial lymphocytes
1	No	7F	N/A	Duodenum	Many	None	Focal	Normal	No
2	No	65F	CVID	Duodenum	Few	Focal	Many	Normal	Yes
3	No	78M	Diabetes	Duodenum	Few	Diffuse	Focal	Expanded villi	Yes
4	No	31M	N/A	Terminal ileum	Few	None	Yes, anatomic	Normal	Yes
5	Yes	42M	HIV	Duodenum	Few	None	None	Expanded villi	No
6	Yes	41M	s/p Liver transplant	Terminal ileum	Few	Focal	Yes, anatomic	Normal	No
7	Yes	58F	s/p Lymphoma	Duodenum	Few	Diffuse	Focal	Expanded villi	No
8	Yes	24F	N/A	Duodenum	Few	Focal	Focal	Expanded villi	No

Conclusions: Even at a large tertiary care center with subspecialty sign-out, *Giardia* was missed in 50% of cases in this study. Our study suggests certain clinical and histologic clues can be used to flag cases with a higher likelihood of *Giardia* infection, and scrutinize them more carefully. Specifically, abnormalities of the duodenal mucosa (acute inflammation, intraepithelial lymphocytosis, villous expansion, prominent lymphoid aggregates) were present in 6 of 8 cases and 4 of 8 patients were immunocompromised. Finally, 2 of 8 cases were terminal ileum biopsies, highlighting the need check for *Giardia* in this site.

728 Chronic Active Enteritis (CAE) in Ileostomy: A Distinct Histologic Pattern Associated with Ulcerative Colitis (UC) with Possible Prediction for Pouchitis

Natallia Sheuka¹, Fernanda Cordeiro-Rudnisky¹, Brandon Koo², Edward Lee¹, Hwajeong Lee³

¹AMC, Albany, NY, ²Albany Medical College, Albany, NY, ³Albany Medical Center, Albany, NY

Disclosures: Natallia Sheuka: None; Fernanda Cordeiro-Rudnisky: None; Brandon Koo: None; Edward Lee: None; Hwajeong Lee: None

Background: Pouchitis is an adverse outcome complicating ileal pouch anal anastomosis (IPAA) following restorative proctocolectomy in inflammatory bowel disease (IBD). Histologic features reflective of the severity of the disease were reported to predict future pouchitis in proctocolectomy specimen. Such histologic features have not been evaluated in ileostomy specimens that are readily available in staged IPAA procedure.

Design: Archived ileostomy specimens from IBD (2014-2017) patients were reviewed. Following histologic features were evaluated: CAE-moderate to marked expansion of the lamina propria by mononucleated cells associated with subtotal villous blunting and variable degree of activity, similar to "chronic active duodenitis" of UC, activity away from the skin, and pyloric metaplasia (PM). Clinical history was obtained by review of electronic medical records. Fisher's exact test was performed to compare the frequencies between parameters and the p value <0.05 was considered statistically significant.

Results: 89 ileostomy specimens (44 end and 45 loop) from 79 IBD patients (48 UC and 31 Crohn's disease (CD)) were reviewed. IPAA was performed in 40 UC and 8 CD patients. 5 of 8 CD patients who underwent IPAA procedure had been initially mis-diagnosed as UC. 10 UC and 4 CD patients developed pouchitis. In 2 (1UC, 1CD) patients, diverting end-ileostomies following chronic pouchitis were examined. 7 (7.9%) ileostomies (1 end and 6 loop) showed CAE, all from UC patients (7 of 55 (12.7%)). The mean age of these patients was 46.6 (range 21 to 74) years, and 4 were female. Among these, 3 developed pouchitis in 4 to 13 months following anastomosis of the pouch, 1 developed pouch dysfunction without evidence of pouchitis in 5 months, and 2 showed no evidence of pouchitis at 10 and 21 months follow-up, respectively. One last UC patient with CAE in the end-ileostomy did not undergo IPAA. In contrast, none of 31 (0%) CD patients showed CAE (p<0.05). Active ileitis with PM was seen in 1 of 55 (1.8%) UC and 7 of 34 (20.1%) CD ileostomies (p <0.01).

Conclusions: Ileostomies from UC and CD demonstrate distinct histologic abnormalities. CAE is identified in about 13% of ileostomies from UC whereas active ileitis with PM is more common in CD. CAE may be an indicator of severe disease and may predict future pouchitis in a subset of patients. Further study is warranted to evaluate whether intensified surveillance for early detection of pouchitis is indicated in IBD patients showing CAE in the ileostomies.

729 A Novel Combined Tumour Budding/Poorly Differentiated Cluster Grading System in Colorectal Cancer: Association with T-stage, N-stage, Venous Invasion and Reduced Disease Free Survival

Sameer Shivji¹, Kai Duan¹, Aysegul Sari¹, Rossi Tomin², Siham Zerhouni³, Erin Kennedy², Mantaj Brar⁴, James Conner², Richard Kirsch²

¹Toronto, ON, ²Mount Sinai Hospital, Toronto, ON, ³Mount Sinai Hospital, Vancouver, BC, ⁴Mount Sinai Hospital, University of Toronto, Toronto, ON

Disclosures: Sameer Shivji: None; Kai Duan: None; Aysegul Sari: None; Rossi Tomin: None; Siham Zerhouni: None; Erin Kennedy: None; Mantaj Brar: None; James Conner: None; Richard Kirsch: None

Background: Histologic grading based on poorly differentiated clusters (PDCs) is emerging as a powerful prognostic tool in colorectal cancer (CRC). Morphologically and biologically, PDCs are closely related to tumour buds (TB) and are distinguished only by an arbitrary numerical threshold that can be difficult to apply in practice. We therefore developed a novel scoring system that counts both PDCs and TB, and evaluated its prognostic significance in a cohort of CRC.

Design: 271 CRC resection specimens (non-neoadjuvant) were included in this study. PDCs were defined as distinct groups of 5 or more tumour cells lacking evidence of gland formation; TB were defined as single cells or clusters of <5 cells as per ITBCC 2016 recommendations. For each case, the 'hotspot' method was used in order to identify the area with the highest density of TB, PDCs, and the two together; a maximum count on a 20x objective for each feature was then obtained. Grade groups for PDC and TB were defined as 0-4(G1), 5-9(G2), and ≥10(G3/high grade [HG]); for the combined score (CS), the threshold for HG was ≥15 buds and/or PDC. The CS, TB and PDC grades were then assessed in relation to other clinical and pathologic features.

Results: The cohort included 63 (23%) stage I, 91 (34%) stage II, 111 (41%) stage III, and 7 (2%) stage IV CRC; 42%, 40% and 35% of cases were classified as HG based on CS, TB and PDC, respectively. 78% of cases classified as HG TB were also HG using the CS system; 74% of HG CS cases were HG TB. CS grade was significantly associated with pT stage, lymph node metastases and venous invasion ($p = <0.00001$, <0.00001 , 0.000045); a similar association was seen when TB and PDC were scored separately ($p=0.00039$ for PDC grade and VI, <0.00001 all other variables). CS, both absolute count and grade, was independently associated with lymph node metastases in multivariable analysis ($p=0.000018$, 0.000015). A preliminary analysis on a subset of cases with clinical follow-up available ($n=137$) found CS to be significantly associated with decreased disease free survival after adjusting for pT and pN stage ($p=0.047$).

Conclusions: This novel scoring system, which incorporates both PDCs and TB to produce a single unified count, was significantly associated with pT-stage, N-stage, VI, and reduced disease free survival. This system avoids the arbitrary (and often challenging) distinction between TB and PDC and, if validated in a larger cohort and by other groups, may be more suited for use in routine pathology practice.

730 CtBP2 Overexpression and Clinical Outcomes in Colorectal Cancer

Irene Shyu¹, Matthew Gayhart², Bryce Hatfield³, Arushi Khurana⁴, Ayesha Chawla⁵, Steven Grossman⁵, Michael Idowu⁴, Bhaumik Patel⁴

¹Richmond, VA, ²VCU School of Medicine, Richmond, VA, ³Virginia Commonwealth University, Richmond, VA, ⁴Virginia Commonwealth University Health System, Richmond, VA, ⁵VCU Health, Richmond, VA

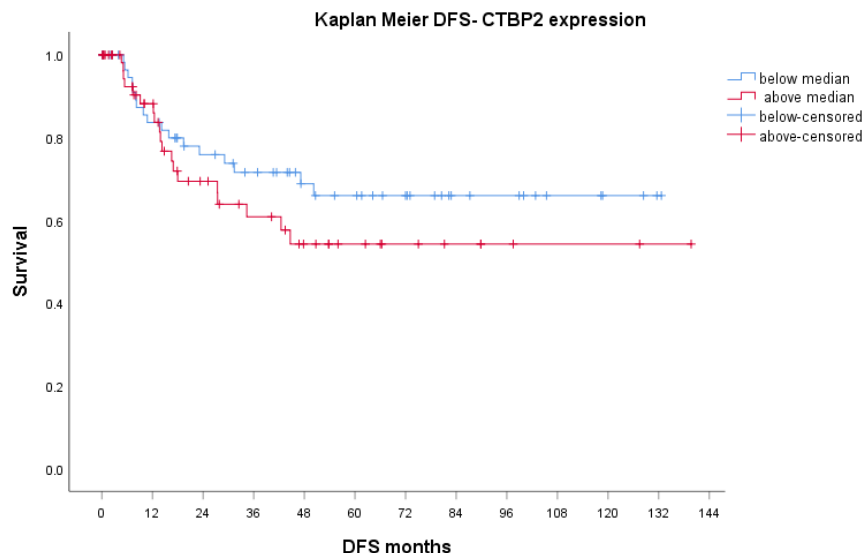
Disclosures: Irene Shyu: None; Matthew Gayhart: None; Bryce Hatfield: None; Arushi Khurana: None; Ayesha Chawla: None; Steven Grossman: None; Michael Idowu: None; Bhaumik Patel: None

Background: Overexpression of C-terminal binding proteins 2 (CtBP2), a paralogous transcriptional coregulator has been associated with poor outcome in several solid tumors. Earlier, we observed that CtBP2 is an important regulator of colon cancer stem cells (CSCs) growth. As CSCs have been implicated in tumor relapse, we sought to determine the association between CTBP2 and clinical outcome in colorectal cancer patients.

Design: Colorectal resections from 123 treatment-naïve patients with stage I-III colorectal adenocarcinoma between 2004-2015 were retrospectively reviewed. Clinicopathologic parameters were collected. A tissue microarray was created using Beecher ATA 27 arrayer. CtBP2 (BD clone 16) immunohistochemistry was performed. Expression of CtBP2 was calculated using H-score ranging from 0-300 (intensity (0-3) and percentage of positive cells). Kaplan Meier analysis and Pearson correlation coefficient were used to correlate the H-score with clinical parameters such as T-stage, N-stage, time to progression, disease-free survival and overall survival.

Results: In time-to-the event endpoint analyses using the median expression as a cutoff value, there was a non-statistically significant trend towards longer disease-free survival with lower CtBP2 expression ($P=0.27$) (Figure 1). However, CtBP2 expression did not influence overall survival in this cohort of colorectal cancer patients. Moreover, H-score of CtBP2 did not correlate with lymph node status (Pearson correlation 0.055) or overall stage (Pearson correlation 0.084).

Figure 1 - 730



Conclusions: CtPB2 overexpression may be associated with a worse progression-free survival. However, it is not correlated with a worse prognosis in colorectal cancer in this cohort. Our findings suggest that further study on the correlation between CTBP2 expression and clinical outcomes, especially that examining the risk of relapse, is needed in colorectal cancer.

731 Prediction of response to 5-FU based neoadjuvant chemotherapy in Esophageal Adenocarcinoma by TFAP2E DNA Methylation analysis

Julia Slotta-Huspenina¹, Marc Tänzer², Raphael Schellnegger², Rupert Langer³, David Horst⁴, Marcus Feith⁵, Roland Schmid², Wilko Weichert⁶, Michael Quante²

¹Technical University of Munich, Muenchen, Germany, ²II. Medizinische Klinik, Klinikum rechts der Isar, Munich, Germany, ³University of Bern, Bern, Switzerland, ⁴Berlin, Germany, ⁵Munich, Germany, ⁶Muenchen, Germany

Disclosures: Julia Slotta-Huspenina: None; Rupert Langer: None; Wilko Weichert: *Speaker*, Lilly, BMS, MSD, Novartis, Roche, AstraZeneca; *Advisory Board Member*, BMS, MSD, Pfizer, Roche, AstraZeneca, Novartis, Boehringer, Merck.; *Grant or Research Support*, Roche, MSD, BMS, Bruker

Background: Esophageal adenocarcinoma (EAC) is one of few cancer entities with rising incidence rates for decades and still has a very poor prognosis. Neoadjuvant chemotherapy with cisplatin and 5-fluorouracil (5-FU) and/or taxol followed by surgery is the current standard approach in treating locally advanced EAC. However, a subset of patients does not respond to CTX. Therefore, molecular predictors of response to systemic treatment are of greatest interest for the management of EAC. Specific DNA methylation patterns could serve as promising biomarkers and while genomic and epigenetic alterations of genes of the AP-2 family are common in human cancers, they have not been investigated in EAC so far. The AP-2 epsilon gene (TFAP2E) has been identified as a mediator of 5-FU resistance in colorectal and gastric cancer. Therefore, we aimed to evaluate the role of TFAP2E as response predictor of EAC to 5-FU based chemotherapy.

Design: We analyzed the methylation of the TFAP2E gene using a methylation sensitive high resolution methylation (MS-HRM) approach followed by bisulfite pyrosequencing in 60 formalin-fixed and paraffin-embedded pretherapeutic biopsies of locally advanced EAC (cT3 and cT4) prior to platin/5-FU based chemotherapy. TFAP2E methylation status was correlated with histopathological response (tumor regression grade and ypT-status) and survival.

Results: Mean TFAP2E methylation was significantly higher in patients without histopathological response to 5-FU based chemotherapy with 34% to 22% ($p < 0.0001$). With a cut-off value of 26,85% methylation ROC calculation showed an area under the curve (AUC) of 0.790 ($p < 0.001$). Considering 5 of 11 CpG islands with binding site characteristics, the accuracy for therapy prediction could be improved to 0.814 (AUC, $p < 0.001$). TFAP2E hypermethylation was also associated with higher ypT stage ($p < 0.04$) and with bad survival ($p < 0.049$).

Conclusions: Our results suggest that TFAP2E DNA methylation status in pretherapeutic biopsies of EAC patients as a biomarker for 5-FU based chemotherapy could predict chemotherapy response and should be tested in prospective cohorts to consolidate this hypothesis.

732 Ileal and Colorectal Endometriosis, a Review of 88 Cases

Anna Sokolova¹, Ian Brown²

¹Queensland Health, Herston, QLD, Australia, ²Brisbane, QLD, Australia

Disclosures: Anna Sokolova: None; Ian Brown: None

Background: Colorectal endometriosis may be an incidental finding, with clinical presentation and histology sometimes mimicking other diseases such as Crohn's disease, mucosal prolapse and even colorectal malignancy.

Design: The aim was to review the clinicopathological features of endometriosis in the ileum and colorectum and to examine the histopathological changes when disease involved the mucosa. Cases were identified using a retrospective database search (2007-2017). Demographic data, clinical presentation, site of involvement and extent of mural disease were recorded. When the mucosa was involved, the presence of erosion, architectural disturbance, active inflammation, chronic inflammation, lamina propria fibrosis and gland atypia were recorded.

Results: There were 88 cases. The median age was 38 years (range 21–81). Ten were discovered on biopsy and 78 were resections. Indications for biopsy were iron deficiency anaemia and colorectal mass. 53% of resections were for known disease. In 4 cases a complication of endometriosis (obstruction x3 (one due to endometrioid carcinoma) and perforation) led to resection without a prior diagnosis. Overall, endometriosis in this series was an incidental finding in 53%. Site of occurrence was rectum (46%), sigmoid (20%), cecum (8%), ileum (8%), ascending colon (5%) and other colon site (13%). Disease was only within or deep to muscularis propria in 48 cases (54%). Fifteen cases (17%) involved the mucosa which displayed erosion/ulceration (67%), crypt architectural disturbance (93%), chronic inflammation (80%), acute inflammation (20%) and fibrosis (87%) adjacent to the endometriosis. The endometriotic glands had marked cytological atypia mimicking colorectal adenocarcinoma in one mucosal case.

Conclusions: Endometriosis was most frequently an incidental finding, including all biopsy diagnoses. Mucosal changes adjacent to endometriosis can mimic Crohn's disease, chronic ischemia or mucosal prolapse. Furthermore, misdiagnosis as malignancy may occur particularly with superimposed cytological atypia. Pathologists should consider endometriosis in young females with mass lesion and mucosal architectural change.

733 Esophageal Ulceration: A 2 Year Comprehensive Clinicopathologic Examination of a Common but Non-specific Finding

Roberto Alvaro Taguibao¹, Maha Guindi², Kevin Waters¹

¹Cedars-Sinai Medical Center, Los Angeles, CA, ²Cedars-Sinai Medical Center, Beverly Hills, CA

Disclosures: Roberto Alvaro Taguibao: None; Maha Guindi: None; Kevin Waters: None

Background: Esophageal ulceration is not infrequently encountered on gastrointestinal (GI) biopsies, but is non-specific as it can occur in many distinct types of injury. Herein we comprehensively examine the clinicopathologic characteristics and histologic findings of all biopsied cases of esophageal ulceration over 2 years at a tertiary hospital.

Design: We identified 120 biopsies with esophageal ulceration from 2015-2016. We collected demographic, clinical, and histologic information to comprehensively study the clinicopathologic characteristics of this cohort.

Results: The mean patient age was 65, 49% were male, 68% were white, and 48% had body mass index (BMI) ≥ 25 . Common symptoms were dysphagia (32%), chest pain (31%), GI bleeding (28%), abdominal pain (26%), nausea/vomiting (28%), and odynophagia (12%). The most common causes were gastroesophageal reflux disease (GERD; 49%), medication 9%, Candida 9%, viral 5%, and idiopathic 23%. No cases were due to eosinophilic esophagitis. There were no cases with concurrent or subsequent carcinoma. The pathologist determined the etiology in 43 cases (24 GERD, 11 Candida, 3 cytomegalovirus (CMV), 2 herpes simplex virus (HSV), and 3 radiation). The histologic findings compatible with GERD were seen in 41% (24/59) of GERD cases. The frequency of ulceration from GERD was similar in older (>60) and younger (≤ 60) patients (50% vs. 41%). All drug related esophagitis needed clinical diagnosis as no pill fragments were seen on biopsy. Aside from GERD therapy, the most common medications were non-steroidal anti-inflammatory drugs (NSAIDs; 31%), psychiatric (23%), chemotherapy (13%), bisphosphonates (8%), and iron (8%). Older patients more frequently had viral esophagitis (9.2%) than younger patients (2.3%). 75% of patients had polypharmacy (≥ 5 drugs). Viral esophagitis was limited to immunocompromised patients. HSV viral inclusions were seen in both positive cases. Immunohistochemical (IHC) stains for HSV-1 and 2 was negative on 83 cases that lacked inclusions on H&E. CMV inclusions were present on H&E in 1 case, but 2.6% (2/78) cases lacking definitive inclusions on H&E were positive by IHC.

Conclusions: Increased BMI and polypharmacy were common in our cohort. As evidenced by GERD and drug esophagitis, clinical/endoscopic correlation is often required for diagnosis. However, treatable causes of esophagitis (particularly viral and Candida in immunocompromised patients) and, though not seen in our cohort, neoplastic processes should be excluded.

734 Inflammatory Bowel Disease (IBD) - Associated Dysplasia Shows An Increased Mutational Load In Comparison To Sporadic Adenomas In Patients With IBD

Roberto Alvaro Taguibao¹, Eric Vail², Elias Makhoul¹, Gaurav Khullar³, Maha Guindi⁴, Kevin Waters¹, Jean Lopategui², Deepti Dhall¹

¹Cedars-Sinai Medical Center, Los Angeles, CA, ²Cedars-Sinai Medical Center, West Hollywood, CA, ³Cedars Sinai Medical Center, Los Angeles, CA, ⁴Cedars-Sinai Medical Center, Beverly Hills, CA

Disclosures: Roberto Alvaro Taguibao: None; Eric Vail: None; Elias Makhoul: None; Gaurav Khullar: None; Maha Guindi: None; Kevin Waters: None; Jean Lopategui: None; Deepti Dhall: None

Background: IBD/colitis-associated dysplasia (CAD) is histologically difficult to distinguish from sporadic adenoma (SA) in biopsies. The diagnosis of CAD warrants close follow-up with high-definition colonoscopy for early detection of carcinoma. Recently, molecular studies have shown that colitis-associated colorectal carcinomas have significantly increased amount of mutations (mutational load) in comparison to sporadic colorectal carcinomas. We evaluated if mutational load can be helpful in differentiating CAD from SA.

Design: Formalin-fixed paraffin embedded blocks with low grade dysplasia (LGD: 6 CAD and 6 SA) from IBD patients were selected for this pilot study from our archives (2015-2018). All SAs were discrete polyps with adenoma-like appearance (top down dysplasia) and normal-appearing background mucosa without active colitis. CAD showed variable atypia with surface maturation, hypermucinous and hyperplastic features in some and were either associated with multifocal dysplasia or with carcinoma in a background of moderately to severely active chronic colitis. The areas with LGD were macrodissected in all cases. After DNA extraction, the Thermo-Fischer Scientific Oncomine Tumor Mutation Load Assay was utilized with library preparation and templating on the Ion Chef platform with subsequent sequencing on the Ion S5-XL platform. Variant calling, analysis and mutational load calculation was performed with Ion Reporter Suite v5.6. Mutational load was reported as the number of non-synonymous mutations per megabase.

Results: The mean age was 62 years for SA and 53 years for CAD while the mean duration of IBD was 12.5 and 17 years respectively. The mutational load for SA ranged from 0 to 5.3 with a mean of 2.9 compared to CAD which ranged from 1.2 to 7.6 with a mean of 4.8. Higher mutational load was seen in the CAD group with a trend towards significance ($P=0.1$, t test), however there were outliers in both groups. Case 6 from SA group with a mutational load of 5.3 was found to have persistent adenoma at the same site for 2 years in follow-up biopsies. Case 7 from CAD group had a mutational load of 1.2. Few crypts were present in the tested portion of the block and the findings may reflect under-sampling.

#	Mutational Load (Mut/MB)	Site	Age	Sex	Duration of IBD	IBD Type: Crohn's Disease (CD), Ulcerative Colitis (UC)	Procedure
Sporadic Adenoma							
1	2.4	Transverse	57	F	16	CD	Biopsy
2	2.4	Rectum	59	M	16	UC	Biopsy
3	2.9	Sigmoid	44	F	4	UC	Biopsy
4	0	Cecum	65	F	21	UC	Biopsy
5	4.1	Ascending	63	M	9	CD	Biopsy
6	5.3	Sigmoid	84	F	8	UC	Biopsy
IBD-Associated Dysplasia							
7	1.2	Sigmoid	61	F	12	UC	Resection
8	5.9	Ascending	48	F	10	CD	Biopsy
9	4.7	Transverse	45	M	22	Indeterminate	Resection
10	4.7	Transverse	71	F	1	UC	Resection
11	7.6	Transverse	30	F	24	CD	Resection
12	4.7	Ascending	64	M	29	CD	Resection

Conclusions: Mutational load may be helpful in differentiating colitis-associated dysplasia from sporadic adenoma. High mutational load in a dysplastic lesion may favor colitis-associated dysplasia over sporadic adenoma.

735 Pathological Prognostic Factors for Survival in Neuroendocrine Neoplasms of Esophagus: Results from the National Cancer Database

Mehran Taherian¹, Shabnam Samankan², Adrienne Groman³, Sai Yendamuri³, Amarpreet Bhalla²

¹University of Buffalo, Buffalo, NY, ²University at Buffalo, Buffalo, NY, ³Roswell Park Comprehensive Cancer Center, Buffalo, NY

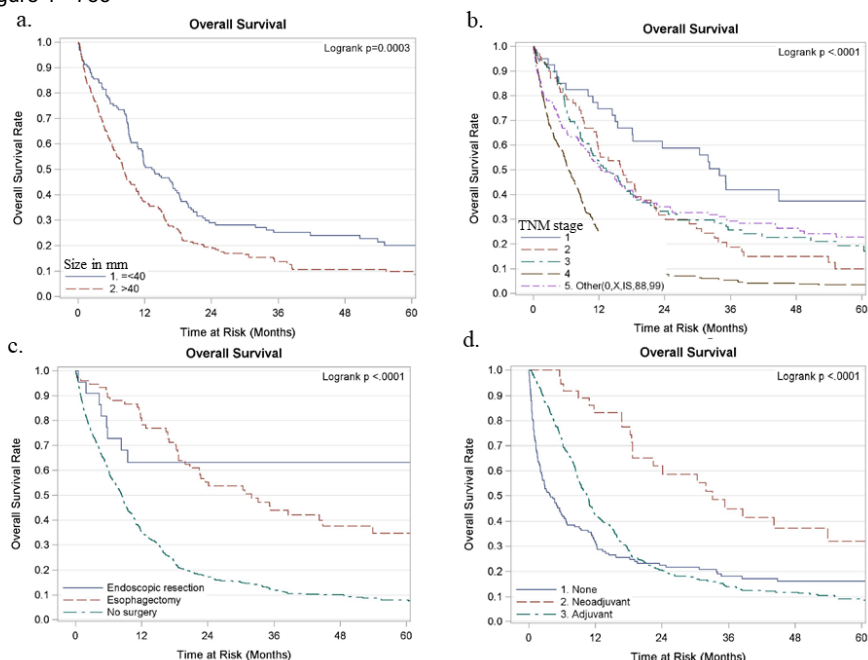
Disclosures: Mehran Taherian: None; Shabnam Samankan: None; Adrienne Groman: None; Sai Yendamuri: None; Amarpreet Bhalla: None

Background: The neuroendocrine neoplasms of the esophagus account for a very small proportion ranging between 0.05% and 7.6% of all esophageal cancers, and include well-differentiated neuroendocrine tumors (NETs) and poorly differentiated neuroendocrine carcinomas (NECs). Limited information is available on survival of these tumors. We sought to define the clinicopathologic features that predict survival in neuroendocrine neoplasms of the esophagus.

Design: Neuroendocrine neoplasms of the esophagus were selected from the National Cancer Database (2004–2013). Univariate and multivariable analyses, and Kaplan–Meier method were performed to compare cohorts and associations between clinicopathologic factors and overall survival (OS). A cutoff of $p < 0.05$ was used for statistical significance.

Results: Of 802 selected patients, 97.5% were NEC and only 2.5% typical NET. The mean age (\pm SD) was 63.9 (\pm 12.3). The tumor location was lower third of esophagus in 55.1%, middle in 20.6%, and upper third in 5.2%. 63.6% of the neoplasms were grade III (poorly differentiated)/IV (undifferentiated or anaplastic). The average tumor size was 6.7 cm (\pm 7.9). The lymph nodes were examined in 11.9%, and 45% of them had at least one positive lymph node. The most frequent metastasis was to the liver (32.2%). Majority of the cases presented at stage IV (47.1%) of the AJCC TNM clinical staging system. 10.7% of patients underwent esophagectomy while 86.5% had no surgery. 68.5% had adjuvant and 6.6% neoadjuvant therapy. Multivariable analyses showed that tumor greater than 4 cm (hazard ratio (HR) 1.45; $P=0.013$), stage III and IV (HR 2.27; $P=0.030$, and HR 4.02; $P<0.001$, respectively) were associated with significantly worse OS, while esophagectomy (HR 0.30; $P=0.019$) and neoadjuvant therapy (HR 0.35; $P=0.006$) were predictors of better survival. The 5-year OS rate was 12% (95% CI, 10–15).

Figure 1 - 735



Kaplan–Meier curves depicting overall survival of patients with neuroendocrine neoplasms of esophagus stratified by: a) tumor size, b) TNM stage, c) type of surgery, and d) chemotherapy.

Conclusions: The neuroendocrine neoplasms of esophagus are exceedingly rare and have a variable clinical behavior. Using the largest dataset of esophageal neuroendocrine neoplasms to date offers valuable information on the tumor characteristics and treatment outcomes. Tumor size, stage, esophagectomy, and chemotherapy are independent predictors of OS. Prospective studies are needed to confirm these findings.

736 Pyloric gland adenomas that develop in the background of normal gastric mucosa are frequently associated with KRAS mutations

Yoko Tateishi¹, Kingo Hirasawa², Chiko Sato², Koji Okudela¹, Mai Matsumura¹, Yoshiaki Inayama², Kenichi Ohashi³
¹Yokohama City University, Yokohama, Japan, ²Yokohama City University Medical Center, Yokohama, Japan, ³Yokohama City University Hospital, Yokohama, Japan

Disclosures: Yoko Tateishi: None

Background: Pyloric gland adenomas (PGAs) are known to occur more commonly in the setting of autoimmune gastritis (AIG). *KRAS* mutations are observed in almost 40% of PGAs, and is often concurrent with *GNAS* mutations. Recently, Choi et al. reported that 35% of PGAs arise against the background of apparently normal gastric mucosa. However, molecular analyses focusing on PGAs in the setting of normal gastric mucosa were not performed. We herein present eight cases of PGA that developed in the setting of normal gastric mucosa, and report the histopathological and molecular findings.

Design: Eight consecutive cases of PGA that developed in the background of normal gastric mucosa from a single institution between 2007 and 2017 were identified. No case occurred in the background of AIG, *Helicobacter pylori* infection or any genetic syndrome, including FAP or Lynch syndrome. Immunohistochemistry for MUC5AC, MUC6, MUC2 and CDX2 was performed. We analyzed mutations in *GNAS*, *KRAS* and *BRAF*, as well as the expression of mismatch repair (MMR) proteins, which is indicative of microsatellite instability.

Results: The patients included 5 females and 3 males with a mean age of 59 years (range: 34–72). The mean size of the PGAs was 3.8 cm (range: 1.0–9.8). The majority of PGAs involved the body/fundus (87.5%). Histologically, the PGAs were composed of closely packed pyloric gland-like cuboidal to low columnar epithelium. PGAs exhibited a tubular (5 cases) or tubulovillous architecture (3 cases). Immunohistochemically, four PGAs (50%) had diffuse MUC6 expression in deeper glands, with MUC5AC expression limited to the superficial foveolar epithelium. Diffuse MUC6 expression was observed in two PGAs (25%), with minor areas of both MUC6 and MUC5AC expression in deeper glands. Two PGAs (25%) had diffuse MUC6 and MUC5AC expression in deeper glands. Activating *KRAS* mutations were found in seven of eight PGAs (87.5%). *GNAS* mutation was found in only one PGA (12.5%) concurrent with *KRAS* mutation. No *BRAF* mutations were observed in any of the PGAs. The loss of MMR protein expression was not noted.

Conclusions: Most PGAs that develop in the background of normal gastric mucosa are caused by activating *KRAS* mutations.

737 P53 Staining as a Marker of Dysplasia Progression Risk in Barrett's Esophagus

Kristen Tomaszewski¹, Steffen Rickelt², William Jeck³, Martin Taylor³, Vikram Deshpande¹, Stuti Shroff⁴
¹Massachusetts General Hospital, Boston, MA, ²David H. Koch Institute for Integrative Cancer Research, Cambridge, MA, ³Boston, MA, ⁴Massachusetts General Hospital, Philadelphia, PA

Disclosures: Kristen Tomaszewski: None; Steffen Rickelt: None; William Jeck: None; Martin Taylor: None; Vikram Deshpande: None; Stuti Shroff: None

Background: Up to 1% of patients diagnosed with Barrett's esophagus (BE) will progress to high grade dysplasia in future esophageal biopsies, but H&E findings on biopsies at initial presentation are not predictive of progression risk. Mutations in tumor suppressor gene *p53* have been associated with progression to dysplasia or malignancy in BE, but the utility of *p53* immunohistochemical staining in predicting dysplastic progression in nondysplastic biopsies at initial presentation has not been widely assessed.

Design: Our pathology case database was queried for esophageal biopsies demonstrating intestinal metaplasia with available follow-up biopsy results. We identified two cohorts of BE patients: those with eventual progression to high grade dysplasia (progressors) and those without progression to dysplasia (non-progressors) on surveillance biopsies. The initial biopsies for both cohorts of patients demonstrating intestinal metaplasia (but no dysplasia) were stained with *p53* immunostain. *p53* staining was scored as a percent of columnar cells with strong nuclear staining. Staining scores were then compared between progressors and non-progressors.

Results: 50 patients with BE on presentation and with follow-up biopsy data available were identified, including 25 cases with dysplastic progression over an average of 3.4 years of follow-up (range: 1.0–9.3 years) and 25 controls with no dysplastic progression over an average of 13 years of follow-up (range: 10–16 years). Of the 25 cases with eventual dysplastic progression, 11 showed *p53* staining of greater than or equal to 5% of columnar cells (range: 5–70%). Non-zero *p53* staining was observed in 3 of the 25 controls, and no control exceeded 5% staining of columnar cells ($p < 0.001$). The sensitivity of *p53* positivity at a cut-off point of 5% in initial biopsies for eventual progression to high grade dysplasia was 44%, while the specificity was 96%.

Conclusions: A cut-off of 5% *p53* staining in initial nondysplastic BE biopsies at presentation is a specific marker and a strong predictor of eventual dysplastic progression.

738 Massive Parallel Sequencing of Neuroendocrine Carcinomas of the Large Bowel Reveals Distinct Molecular Subsets and Patterns of Genomic Evolution

Efsevia Vakiani¹, Timothy Song¹, Cyriac Kandoth¹, Jinru Shia¹, David Klimstra¹

¹Memorial Sloan Kettering Cancer Center, New York, NY

Disclosures: Efsevia Vakiani: None; Timothy Song: None; Cyriac Kandoth: None; Jinru Shia: None; David Klimstra: *Consultant*, Paige.AI; *Consultant*, Merck

Background: Poorly differentiated neuroendocrine carcinomas (NECs) arise infrequently in the large bowel and there is no agreement on the best chemotherapeutic options for adjuvant treatment. Better understanding of the pathogenesis of NECs can enhance the prognostic and therapeutic stratification of these patients.

Design: NECs from 54 patients were retrieved from our institutional archives and classified by morphology as small cell, large cell or mixed NEC. The presence of adenoma and/or adenocarcinoma (ACA) in areas that were not sequenced was recorded and tumors were assessed for mismatch repair deficiency (MMR-D) by immunohistochemistry. Tumors underwent massive parallel sequencing using either a targeted assay of 468 cancer-associated genes or whole exome sequencing. Molecular profiles were compared to conventional ACAs (n=1007) genotyped for clinical purposes. In 8 patients with distinct ACA and NEC components the 2 components were dissected and sequenced separately.

Results: Five (9%) tumors showed MMR-D including 2 small cell carcinomas. The rates of TP53 and KRAS mutations were similar to those observed in conventional ACAs. In contrast, MMR-proficient NECs showed a lower frequency of alterations in APC (59.2% vs 76.1%, p=0.01), SMAD4 (8.2% vs 19%, p=0.06) and PIK3CA (6.1% vs 18.4%, p=0.03) and a higher frequency of aberrations in RB1 (26.5% vs 1.8%, p<0.001), MYC (22.4% vs 6.7%, p<0.001), BRAF (20.4% vs 7.5%, p<0.01) and KMT2D (12.2% vs 3.8%, p=0.01) compared to conventional ACAs. Small cell carcinomas were characterized by the co-existence of RB1 and TP53 alterations. Large cell and mixed NECs were similar to each other in their molecular profile and showed significantly more frequent BRAF V600E mutations and MYC amplifications compared to small cell carcinomas and to conventional ACAs. The concordance in genomic alterations between matched NEC and ACA components ranged from 6% to 84% suggesting marked variability in the molecular time that the 2 components diverge.

Figure 1 - 738

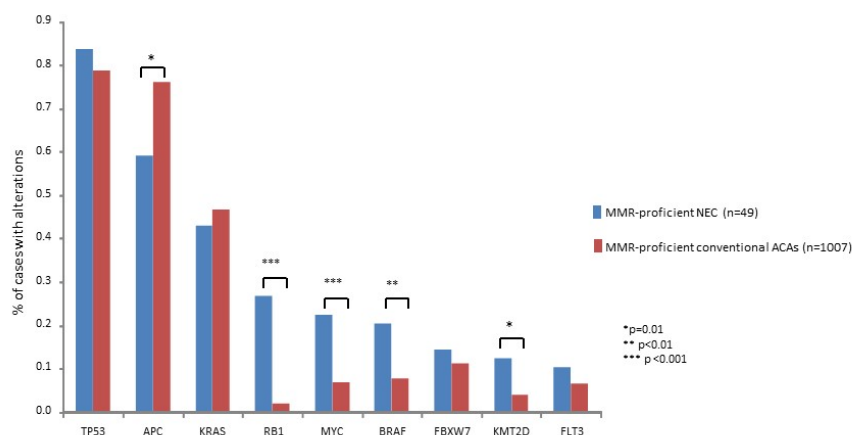
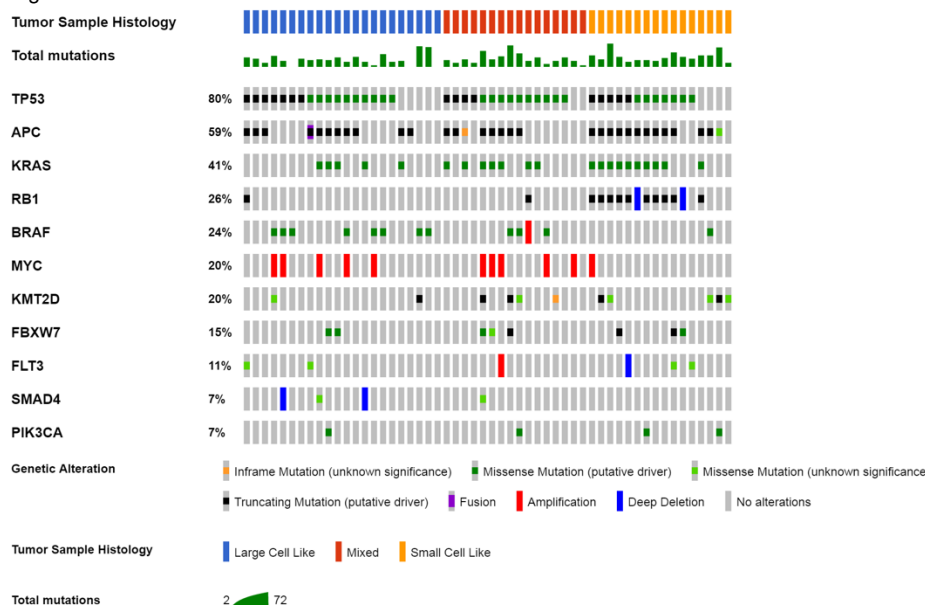


Figure 2 - 738



Conclusions: High grade NECs of the large bowel show morphologic and molecular heterogeneity. Those with large cell morphology show frequent BRAF V600E mutations and/or MYC amplification, while those with small cell morphology are characterized by RB1 alterations. Although as a group NECs share genotypic similarities with conventional ACAs, they show differences in key oncogenes and tumor suppressor genes, some of which have associated prognostic and/or therapeutic implications.

739 Artificial Intelligence-Based Digital Image Analysis for Pathological Categorization of Colonic Polyps

Mark Valasek¹, Eli Brazowski², Maha Al Khawaja³, Ran Shadmi⁴, Roman Gluskin⁴, Yuval Gabay⁴, Ifat Rotbein⁵, Amir Luchtenstein⁴, Israel Ingber⁶, Eliron Amir⁵, Lotan Chorev⁴

¹University of California, San Diego, La Jolla, CA, ²Jerusalem, Israel, ³University of California, San Diego, San Diego, CA, ⁴Nucleai Ltd, Tel Aviv, Israel, ⁵Nucleai Ltd, Kfar Saba, Israel, ⁶Nuclei Ltd, Tel Aviv, Israel

Disclosures: Mark Valasek: *Consultant*, Nucleai Ltd; Eli Brazowski: *Consultant*, Nucleai Ltd; Maha Al Khawaja: *None*; Ran Shadmi: *Employee*, Nucleai Ltd; Roman Gluskin: *Employee*, Nucleai Ltd; Yuval Gabay: *Employee*, Nucleai Ltd; Ifat Rotbein: *Employee*, Nucleai Ltd; Amir Luchtenstein: *Employee*, Nucleai Ltd; Israel Ingber: *Employee*, Nucleai Ltd; Eliron Amir: *Major Shareholder*, Nucleai Ltd; Lotan Chorev: *Employee*, Nucleai Ltd

Background: Digital image analysis has been primarily used for research purposes and for the classification of cytological specimens in clinical settings. However, the potential of digital image analysis to aid in the pathological categorization of colonic polyps (CP) is relatively unknown. Here, we utilized an artificial intelligence based image analysis (AIIA) algorithm for the classification of CP.

Design: A partially annotated set of 417 CP whole slide images (WSI) was utilized to train an AIIA algorithm (Nucleai-CP-Algorithm) based on deep learning convolutional neural networks. Subsequently, we performed a retrospective analysis of a test sample set of 877 WSI including the following diagnoses: 1) normal colonic mucosa (n=87), 2) serrated polyp (i.e. microvesicular hyperplastic polyp and sessile serrated adenoma; n=175), 3) low grade dysplasia (i.e. tubular adenoma; n=577), and 4) high-risk polyp (includes high grade dysplasia and carcinoma; n=38). Alternatively, for binary classification, CP were placed in either non-dysplastic (groups 1 and 2) or dysplastic/malignant (groups 3 and 4) categories. A subset of 219 cases were independently evaluated by multiple (n=3) gastrointestinal pathologists.

Results: Out of the 877 slides, 4.6% (n=40) slides were assessed as “unknown” by the algorithm. After exclusion of these slides, AIIA overall multiclass accuracy with the reference pathologist was 90.2% (ranging from 85% for serrated polyps to 94% for HG/malignant polyps) while binary classification concordance was 96.3% with a sensitivity and specificity of 96.3%. A subset of 219 cases were evaluated by 3 pathologists in which 198 had complete agreement. AIIA concordance with majority agreement diagnoses was 97% (multiclass) and 98% (binary), while concordance with complete agreement cases was 99% (multiclass) and 99.5% (binary). The majority of discrepant cases were between normal colonic mucosa and subtle hyperplastic polyps lacking significant serration.

Conclusions: The findings demonstrate the capability of AIIA to successfully categorize colonic polyps. Therefore, AIIA can have a role not only in research settings, but also in clinical diagnostic workflows involving the pathological categorization of colonic polyps, including triaging cases or quality control.

740 Becoming an Expert in Dysplastic Barrett's Esophagus Assessment: Quantification of Expertise and Continuous Structural Education in the Set-Up of a National Digital Histopathology Review Panel

Myrtle van der Wel¹, Lodewijk Brosens¹, Katharina Biermann², Michael Doukas³, Clement Huysentruyt⁴, A. Karrenbeld⁵, Fiebo Ten Kate⁶, Gursah Kats-Ugurlu⁷, Jaap van der Laan⁸, Ineke van Lijnschoten⁹, Freek Moll¹⁰, George Offerhaus¹¹, Ariadne Ooms¹², C.A. Seldenrijk¹³, Mike Visser¹⁴, Jan Tijssen¹⁵, Jacques Bergman¹⁵, Sybren Meijer¹⁶

¹University Medical Center Utrecht, Utrecht, Netherlands, ²Rotterdam, Netherlands, ³Erasmus Medical Centre, Rotterdam, Netherlands, ⁴Lichtaart, Belgium, ⁵Groningen, Netherlands, ⁶Bergambacht, Netherlands, ⁷UMCG, Groningen, Netherlands, ⁸Haga Ziekenhuis, Den Haag, Netherlands, ⁹PAMM, Eindhoven, Netherlands, ¹⁰Isala, Zwolle, Netherlands, ¹¹AG Biltoven, Netherlands, ¹²Pathan BV, Rotterdam, Netherlands, ¹³St Antonius Ziekenhuis, Nieuwegein, Netherlands, ¹⁴Amsterdam, Netherlands, ¹⁵AUMC, Amsterdam, Netherlands, ¹⁶Academic Medical Center, Amsterdam, Netherlands

Disclosures: Myrtle van der Wel: None; Lodewijk Brosens: None; Katharina Biermann: None; Michael Doukas: None; Clement Huysentruyt: None; A. Karrenbeld: None; Fiebo Ten Kate: None; Gursah Kats-Ugurlu: None; Jaap van der Laan: None; Ineke van Lijnschoten: None; Freek Moll: None; George Offerhaus: None; Ariadne Ooms: None; C.A. Seldenrijk: None; Mike Visser: None; Jan Tijssen: None; Jacques Bergman: None; Sybren Meijer: None

Background: Assessment of Barrett's esophagus (BE) biopsies with low-grade dysplasia (LGD) is subject to observer variability. Various studies show significant downstaging of LGD cases by expert pathologist review. Subsequently, most international guidelines require review of dysplastic cases by BE expert pathologists and in the Netherlands we therefore set up a national digital expert BE review panel. The panel goal is to stratify BE patients according to progression risk, leading to an extended endoscopic surveillance interval and lower health care costs. However, so far no definition of a BE expert pathologist or panel exists. By setting up this panel we aimed to objectively quantify expertise and structurally homogenize assessment within a large group of GI pathologists.

Design: Fifteen pathologists individually assessed 5x60 digitized BE biopsy sets, including the complete spectrum of BE-pathology with both study- and real time panel review cases. At study entrance, participating pathologists were heterogeneous in experience, work setting (community or academic hospital) and weekly BE workload. Outcomes measured were observer agreement; concordance; % of cases diagnosed 'indefinite for dysplasia' or significantly misdiagnosed cases. All outcomes were compared to benchmark values, constructed using a gold standard diagnosis.

Results: In 5 years, 15 pathologists assessed 31500 slides, yielding 6000 individual case diagnoses. After completing each set, pathologists discussed discrepant cases in face to face group discussions, receiving individual performance feedback before proceeding to the next study step. Fig 1 shows the improvement of heterogeneous pathologist expertise related to benchmark values over a timeline of 5 study sets (scale varying from red-orange-yellow to green, with red being least and green being significantly consistent with gold standard diagnosis).

Figure 1 - 740

Figure 1: Improvement of Pathologist Expertise on Assessment of Dysplastic BE Biopsies Related to Benchmark Values Over a Timeline of 5 Study Sets

Pathologist	Study Set Ia	Study Set Ib	Study Set II	Study Set III	Study Set IV	Study Set V
1						
2						
3						
4						
5						
6						
7						
8						
9						
10						
11						
12						
13						
14						
15						

Legend: scale varies from red-orange-yellow to green, with red being least and green being significantly consistent with gold standard diagnosis

Conclusions: After completing all sets, all 15 pathologists met the benchmark values for all outcomes and can be considered BE experts (green). While using a structured approach to form a national digital BE review panel, we show that expertise is reproducible and can be quantified. In our study, a heterogeneous pathologist group evolved into a homogeneous expert panel with reproducible case assessments. The employment of this panel for dysplastic BE cases greatly improves patient care. Potentially, the structure of this training program can be applied to an international setting and other challenging diagnostic pathology areas.

741 Endoscopic resection of early esophageal adenocarcinoma: significant variation in clinical management caused by discrepancies in histological interpretation; recommendations to improve concordance

Myrtle van der Wel¹, Lodewijk Brosens¹, Katharina Biermann², Clement Huysentruyt³, A. Karrenbeld⁴, Fiebo Ten Kate⁵, Gursah Kats-Ugurlu⁶, Jaap van der Laan⁷, Ineke van Lijnschoten⁸, Freek Moll⁹, George Offerhaus¹⁰, Ariadne Ooms¹¹, C.A. Seldenrijk¹², Jan Tijssen¹³, Jacques Bergman¹³, Sybren Meijer¹⁴

¹University Medical Center Utrecht, Utrecht, Netherlands, ²Rotterdam, Netherlands, ³Lichtaart, Belgium, ⁴Groningen, Netherlands, ⁵Bergambacht, Netherlands, ⁶UMCG, Groningen, Netherlands, ⁷Haga Ziekenhuis, Den Haag, Netherlands, ⁸PAMM, Eindhoven, Netherlands, ⁹Isala, Zwolle, Netherlands, ¹⁰AG Bilkhoven, Netherlands, ¹¹Pathan BV, Rotterdam, Netherlands, ¹²St Antonius Ziekenhuis, Nieuwegein, Netherlands, ¹³AUMC, Amsterdam, Netherlands, ¹⁴Academic Medical Center, Amsterdam, Netherlands

Disclosures: Myrtle van der Wel: None; Lodewijk Brosens: None; Katharina Biermann: None; Clement Huysentruyt: None; A. Karrenbeld: None; Fiebo Ten Kate: None; Gursah Kats-Ugurlu: None; Jaap van der Laan: None; Ineke van Lijnschoten: None; Freek Moll: None; George Offerhaus: None; Ariadne Ooms: None; C.A. Seldenrijk: None; Jan Tijssen: None; Jacques Bergman: None; Sybren Meijer: None

Background: Endoscopic resection (ER) is the cornerstone of endoscopic staging of early cancer in Barrett's esophagus (BE). Accurate histological assessment of ER specimens is crucial for deciding on surgical esophagectomy depending on risk factors for distant lymph node metastasis. Relevant histological features are: depth of invasion, differentiation grade, lymphovascular invasion, and R0 excision at the basal margin. Our aim was to assess diagnostic concordance of 13 dedicated BE pathologists scoring these features on scanned images of ER specimens of early BE cancer and evaluate causes of discrepancy.

Design: representative slides each (H&E, desmin, and either D2-40 or CD31), were independently assessed by 13 pathologists from the eight Dutch BE expert centers in one assessment round. Pathologists used an online assessment module that allowed annotations and recording of depth of invasion, differentiation grade, lymphovascular invasion, and the deep margin. For each feature, subclassified concordance and discordance were measured for a subgroup of nine pathologists that were least deviant from the majority diagnosis.

Results: We observed clinically relevant discordances for assessments of all criteria. For differentiation grade, lymphovascular invasion, and R0 excision at the basal margin, the rate of discordance was substantial with 27%, 42%, and 32% of selected cases having ?1 discrepant pathologist, respectively. In x% of cases at least one discordant diagnosis was recorded that changed clinical decision-making. In 45% of specimens ?1 pathologist was discordant regarding 'mucosal vs submucosal' invasion depth. This decreased to 21% when expanded endoscopic treatment criteria were evaluated (grouping m-3 mucosal adenocarcinomas with superficial submucosal sm-1 adenocarcinomas).

Conclusions: Histological assessment of ER specimens of early BE cancer by dedicated GI-pathologists is associated with significant discordances. However, many of these are due to poorly defined diagnostic criteria. We propose 1) review of ER specimens containing high-risk histological features by a second expert pathologist, 2) grouping diagnostic categories into clinically relevant subgroups, and 3) a series of recommendations per feature in order to better define diagnostic criteria and homogenize the challenging assessment of these diagnostic specimens.

742 Multiregional Immunophenotyping Shows Significant Differences in Immune Cell Infiltration Between Barrett's Esophagus and Esophageal Adenocarcinoma

Anuj Verma¹, Edwin Parra¹, Alicia Mejia¹, Zhimin Tong¹, Omkara Lakshmi Veeranki Omkara¹, Barbara Mino¹, Luisa Solis Soto¹, Jaffer Ajani¹, M Blum-Murphy¹, Ignacio Wistuba¹, Riham Katkhuda¹, Dipen Maru¹

¹The University of Texas MD Anderson Cancer Center, Houston, TX

Disclosures: Anuj Verma: None; Edwin Parra: None; Alicia Mejia: None; Barbara Mino: None; Luisa Solis Soto: None; Ignacio Wistuba: None; Riham Katkhuda: None; Dipen Maru: None

Background: Role of microenvironment in understanding risk of progression of Barrett's esophagus (BE) to esophageal adenocarcinoma (EAC) is unknown. In this study, we analyzed similarities and differences in infiltration of immune cell subsets in BE and EAC and assessed heterogeneity in immune cell infiltration in these lesions.

Design: Multiplex immunofluorescence (mIF) was performed in 15 areas (five areas from one patient x 3) of BE and 15 areas of matched EAC in formalin fixed paraffin embedded sections from esophagectomy specimens using the Opal 7-color IHC Kit™ (Perkin Elmer, Waltham, MA). The panel of mIF markers included, CD3, CD8, Granzyme B, FOXP3, CD45RO and pan cytokeratin. The different cell phenotypes were expressed as number of cells per mm², using the InForm™ software program. The phenotype of the cells were determined as follows- 1) Activated Cytotoxic T lymphocytes=CD3+CD8+Granzyme B+ 2) Effector/Memory T lymphocytes=CD3+CD8+CD45RO+ 3) Regulatory T lymphocytes (Tregs) = CD3+FOXP3+CD8-. The analysis of each region was subdivided in to intraepithelial component and stromal component.

Results: Table shows the comparison of immune cell phenotype in a pooled analysis of all regions.

	Intraepithelial			Stromal			Combined		
	Activated cytotoxic T cells	Effector/memory cytotoxic T cells	Tregs	Activated cytotoxic T cells	Effector/memory cytotoxic T cells	Tregs	Activated cytotoxic T cells	Effector/memory cytotoxic T cells	Tregs
BE, Median ±SD	6.42±37	0±73.19	12.18±17	17.87±19	9.61±126	46.94±50	11.95±20	5.97±105	35.87±20
EAC, Median±SD	0±2.71	0±1.20	12.97±12	0±7	0±3	139.83±105	2.98±3	0±2	53.81±41
P value	0.01	0.04	0.17	0.002	0.06	0.009	0.001	0.056	0.057

Higher heterogeneity in immune cell distribution as indicated by higher degree of variation in number of activated cytotoxic T cells (VAR.P=4482 vs. 354), effector/memory cytotoxic cells (VAR.p=41892 vs. 10158) and Tregs (VAR.P=101310 vs. 1798), was observed in EAC as compared to BE. The higher degree of variations in number of these immune cell subset in EAC was also observed with single patient analysis.

Conclusions: Higher infiltration of TReg, lower infiltration of activated and memory T cell and higher variance in distribution of these cells in EAC as compared to BE indicate that immune microenvironment in EAC is different and more heterogeneous than BE.

743 Inter-Tumoral Discordance In Mismatch Repair Protein Expression In Synchronous Or Metachronous Gastrointestinal Tumors: Biological Significance And Clinical Implications

Monika Vyas¹, Zsafia Stadler¹, Jaclyn Hechtman¹, Efsevia Vakiani¹, David Klimstra¹, Jinru Shia¹

¹Memorial Sloan Kettering Cancer Center, New York, NY

Disclosures: Monika Vyas: None; Zsafia Stadler: None; Jaclyn Hechtman: None; Efsevia Vakiani: None; David Klimstra: *Consultant*; Paige.AI, *Consultant*, Merck; Jinru Shia: None

Background: Mismatch repair (MMR) immunohistochemistry (IHC) is used to screen for Lynch syndrome (LS) and determine eligibility for immune checkpoint inhibitor therapy. Discordance of IHC results among different tumors from the same patient is a phenomenon warranting recognition; understanding the potential etiologies for such discordance will facilitate the effective use of IHC and allow appropriate consequent tumor testing or patient management strategies.

Design: Patients with synchronous or metachronous gastrointestinal (GI) tumors that had discrepant MMR IHC results were retrieved from the pathology database and evaluated for their clinico-pathological and molecular characteristics.

Results: Nine of 34 patients (26%) with synchronous/metachronous GI tumors tested had discordant MMR IHC results; 8 of the 9 underwent molecular/genetic testing which revealed a definitive or likely etiology for the discordance. The most common pattern was sporadic MMR inactivation – either *MLH1* promoter hyper methylation (4 patients) or double somatic mutation/inactivation (2 patients, 1 secondary to *POLE* mutation) – resulting in MMR protein loss in 1 tumor and intact MMR expression in the second tumor. Two LS patients had discordant MMR IHC, and their discordance patterns were more complex (cases #1 and 2). Case #2, in particular, had 2 deleterious germline mutations, 1 in *MLH1* and 1 in *MSH2*. In addition to the GI tumors listed in Table 1, this patient also had 35 sebaceous neoplasms (25 adenomas, 6 atypical/borderline neoplasms and 4 carcinomas), 8 of them were *MLH1*/*PMS2* deficient while 27 were *MSH2*/*MSH6* deficient.

Case ID	Age*	Sex	Tumor site	Tumor type	MMR IHC	Explanation (based on germline and somatic mutation data and methylation data)
1	66	M	Ascending colon	Adenocarcinoma	PMS2 loss	PMS2 LS tumor + likely sporadic MSH6 inactivated tumor
	73		Left colon	Adenocarcinoma	MSH6 loss	
2	43	M	Colon	Adenocarcinoma	MSH2/MSH6 loss	Dual MLH1 and MSH2 LS manifesting loss of either MLH1 or MSH2 in different tumors
	43		Colon	Tubular adenoma	MSH2/MSH6 loss	
	63		Stomach	Adenosquamous carcinoma	MLH1/PMS2 loss	
3	46	M	Rectum	Adenocarcinoma	MSH2/MSH6 loss	POLE mutated tumor (with secondary loss of MMR) + sporadic MSS tumor
	45		Sigmoid	Adenocarcinoma	All retained	
4	75	F	Left colon	Adenocarcinoma	All retained	Likely sporadic MSH2 inactivated tumor + sporadic MSS tumor
	79		Right colon	Adenocarcinoma	MSH2/MSH6 loss	
5	43	F	Small bowel	Adenocarcinoma	MLH1/PMS2 loss	Sporadic MLH1 methylated tumor + FAP associated pancreaticoblastoma that was MSS
	43		Pancreas	Pancreatoblastoma	All retained	
6	56	M	Right colon	Adenoma	MLH1/PMS2 loss	Sporadic MLH1 methylated tumor + sporadic MSS tumor
	56		Sigmoid	Adenoma	All retained	
7	85	M	Cecum	Adenocarcinoma	MLH1/PMS2 loss	Sporadic MLH1 methylated tumor + sporadic MSS tumor
	82		Rectum	Adenocarcinoma	All retained	
8	52	M	Rectum	Adenocarcinoma	All retained	Sporadic MLH1 methylated tumor + Sporadic MSS tumor
	52		Stomach	Adenocarcinoma	MLH1/PMS2 loss	
9	71	F	Stomach	Adenocarcinoma	MLH1/PMS2 loss	Pending molecular/genetic testing
	71		Stomach	Mixed acinar and neuroendocrine carcinoma	All retained	

Conclusions: Discordant MMR IHC results are not uncommon in patients with more than one GI tumor, occurring in 26% in our series. While in the majority of cases, the discordance reflects sporadic events, in some, it signifies complex germline deficiency. When considering chemotherapy or therapy with immune-checkpoint-inhibitors in patients with 2 or more tumors, the MMR testing should be performed on the one that is being treated, even when the multiple tumors are all of the same histologic type.

744 Residual Neoplasia Limited To The Mucosa In Rectal Resections For Adenocarcinoma Post-Neoadjuvant Therapy: Frequency, Morphological Spectrum And Potential Clinical Implications

Monika Vyas¹, Martin Weiser¹, Efsevia Vakiani¹, Jaclyn Hechtman¹, David Klimstra¹, Julio Garcia-Aguilar¹, Jinru Shia¹

¹Memorial Sloan Kettering Cancer Center, New York, NY

Disclosures: Monika Vyas: None; Martin Weiser: None; Efsevia Vakiani: None; Jaclyn Hechtman: None; David Klimstra: *Consultant*, Paige.AI; *Consultant*, Merck; Julio Garcia-Aguilar: *Consultant*, Medtronic; *Consultant*, Ethicon Johnson & Johnson; *Consultant*, da Vinci Intuitive Surgical; Jinru Shia: None

Background: Neoadjuvant therapy followed by surgical resection has been the standard of care for locally advanced rectal adenocarcinoma. While the extent of residual disease in the resection has been shown to be predictive of outcome in general, questions remain about the interpretation and significance of residual disease that is limited to the mucosa. In this study, we aim to evaluate the frequency and morphological spectrum of residual intramucosal neoplasia, and provide histological patterns that may facilitate the standardization of assessing pathological response of these lesions.

Design: Clinical and pathological records of all rectal adenocarcinomas treated with neoadjuvant therapy plus surgical resection from 2008 to 2017 were reviewed, and cases that were classified as ypT0 and ypTis were evaluated.

Results: In total, 169 of 984 (17%) rectal resections post-neoadjuvant therapy were staged as ypT0 (146/984, 14.8%) or ypTis (22/984, 2.2%). Pathologic review showed that 34 tumors (34/984, 3.4%) had residual neoplasm limited to the mucosa. 12 of 146 (8%) ypT0 cases contained residual adenoma (7 of 12 had high grade dysplasia with some concerning for intramucosal carcinoma). Of the 22 ypTis tumors, 6 had adenoma with early intramucosal carcinoma (analogous to non-treated malignant polyps, Fig. 1) and 16 had residual carcinoma with treatment effect (some in the form of neuroendocrine differentiation, Fig. 2) limited to the mucosa, 6 of the 16 also had a co-existing adenoma. The reported pathological response for ypTis lesions ranged from 40% to 100% (median, 95%). One case that were reported as having only 40% response had florid adenoma with only focal early intramucosal carcinoma. Positive lymph nodes were observed in 1 ypT0 and 2 ypTis cases.

Figure 1 - 744

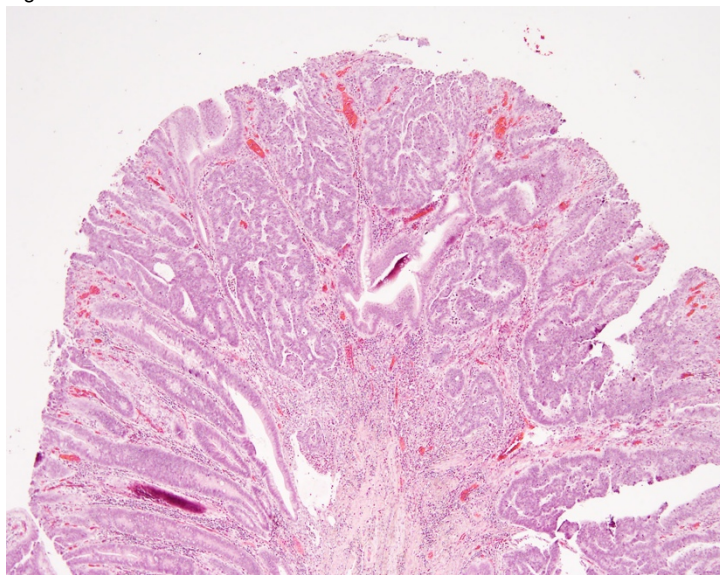
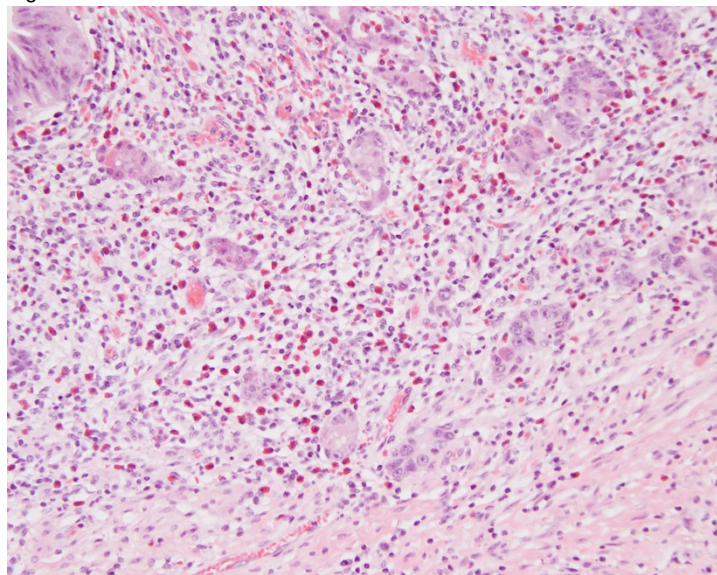


Figure 2 - 744



Conclusions: Residual neoplasia limited to the mucosa occurred in 3.4% of rectal resections for treated adenocarcinomas in our series. The morphological spectrum of these lesions ranges from adenoma to residual invasive carcinoma. At the current time, these lesions are variably graded for pathological response. Further characterization and standardized criteria are needed to ensure consistent and accurate grading and staging of these lesions.

745 A Comprehensive Clinicopathologic and Molecular Analysis of Early Onset Gastroesophageal Adenocarcinomas

Cindy Wang¹, Steven Maron¹, Changqing Ma², Joseph Misdraji³, John Hart¹, Daniel Catenacci¹, Namrata Setia¹

¹University of Chicago, Chicago, IL, ²University of Pittsburgh, Pittsburgh, PA, ³Massachusetts General Hospital, Harvard Medical School, Boston, MA

Disclosures: Cindy Wang: None; Steven Maron: None; Changqing Ma: None; Joseph Misdraji: None; John Hart: None; Daniel Catenacci: None; Namrata Setia: None

Background: Early onset gastroesophageal adenocarcinomas (EO-GECs) are uncommon and account for ~15% of all gastroesophageal carcinomas. The existing literature addresses < 5% of these cases, largely hereditary cancer-predisposing syndromes (HCPS), leaving a wide research gap. This study aims to analyze the clinicopathologic features and genomic alterations in EO-GECs.

Design: 70 patients diagnosed with EO-GECs <50 years of age formed the study cohort. Available clinicopathologic features and reported somatic alterations in the tumors by next-generation sequencing were reviewed. The molecular data were further analyzed by comparing with ClinVar, REPAIRtoire databases, and 47 additional DNA repair genes associated with Fanconi anemia (FA) pathway.

Results: The cohort comprised of 26 gastroesophageal junction carcinomas (GEJCs) and 44 gastric carcinomas (GCs). Of these, 5 (6.67%) cases were in patients with known germline genetic disorders (4 HDGC and 1 JPS). The mean age was 38.6 +/- 8.3 years (42.3 +/- 5.8 yrs GEJCs and 35.8 +/- 8.9 yrs GCs). The male:female ratio was 5:1 for GEJCs and 1:1 for GCs. A family history of cancer was present in 77% of cases. Histologically, signet-ring cell/diffuse component was present in 8% of GEJCs and 63% of GCs. A total of 622 gene mutations were found in 61 patients. The mean number of mutations per patient was 10.2 (range 1-55). The frequency of mutations and gene amplifications/deletions are shown in Figure 1. The most commonly mutated genes include *TP53* (41%), *ARID1A* (23%), *CDH1* (20%), *CDKN2A* (16%), *LRP1B* (18%) and *RUNX1* (18%). Comparison of mutation frequencies with TCGA data is shown in Figure 2. An overall 34.4% (214/622) of mutations were in HCPS genes (31%, 193/622) and DNA repair pathway genes (9.9%, 62/622). Among the mutations in the HCPS genes, 33.1% (71/214) were in gastric HCPS genes, 19.3% (41/214) in GI HCPS genes and 33.6% (72/214) in other HCPS genes (Figure 2). Of the DNA repair pathway genes, mutations in FA/BRCA pathway genes (56.4%) were the most common, followed by mutations in non-homologous end joining repair pathway (14.5%).

Figure 1 - 745

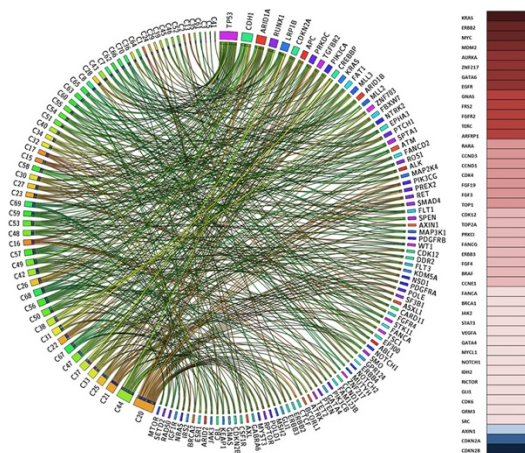


Figure 1 (a): Circos plot showing mutations with a frequency of >2
Figure 1 (b): gene amplifications/deletions with a frequency of >1, top to bottom: amplifications (red) to deletions (blue)

Figure 2 - 745

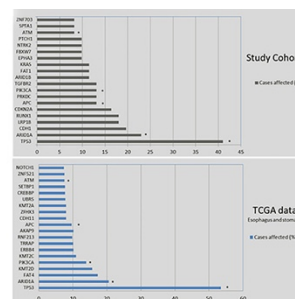


Figure 2 (a): comparative bar chart of most frequently mutated cancer genes

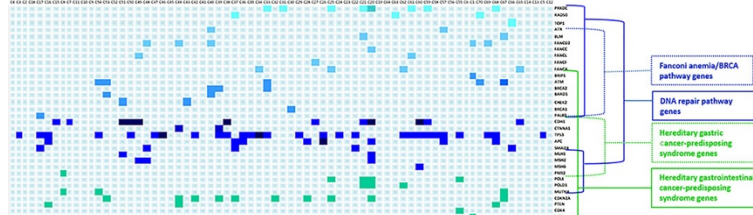


Figure 2 (b): distribution of HCPS and DNA repair pathway genes in the cohort

Conclusions: While the study demonstrates a high frequency of *TP53* and *ARID1A* mutations in EO-GECs as seen in TCGA cohort, it also highlights a significantly different mutational landscape in EOGCs. We also identified a subset of EO-GECs with alterations in the HCPS and DNA repair pathways. Validation of these findings may suggest additional therapy targets in this subset.

746 Detection of Transcriptionally Active Human Papillomavirus in High-grade Squamous Intraepithelial Lesions Arising from Anal Transition Zone

Yan Wang¹, Yiying Wang², Michael Gaisa³, Keith Sigel³, Wenxin Zheng¹, Yuxin Liu⁴

¹University of Texas Southwestern Medical Center, Dallas, TX, ²Henan Provincial People's Hospital, Zhengzhou, China, ³Icahn School of Medicine at Mount Sinai, New York, NY, ⁴Mount Sinai Health System, New York, NY

Disclosures: Yan Wang: None; Yiying Wang: None; Michael Gaisa: None; Keith Sigel: None; Wenxin Zheng: None; Yuxin Liu: None

Background: Human Papillomavirus (HPV)-induced squamous cell carcinoma arising from the anal transition zone has poor prognosis with significantly increased morbidity and mortality. Two distinct cell populations related to anal carcinogenesis have been described for this region: CK7-positive superficial columnar cells and p63-positive basal cells. In this study, we aimed to identify these two cell populations in anal precancerous lesions as well as their co-localization with transcriptionally active HPV in the anal transition zone.

Design: 16 anal high-grade squamous intraepithelial lesions (HSIL) from HIV-infected patients were studied. Two biopsy samples from benign anal transition zone were used as negative control. Immunohistochemistry was performed using antibodies against CK7 and P63. HPV E6/E7 expression was performed on Formalin-Fixed Paraffin-Embedded tissue using RNAscope in situ hybridization (ISH).

Results: All HSIL lesions revealed multilayers of CK7-positive cells in the superficial portion of the dysplastic epithelium as well as p63-positive basal cells above basement membrane (Figure 1). P63-positive cells were arranged in one to four continuous cell layers. Positive HPV 16 E6/E7 signals were detected in all lesions. However, the distribution and cellular location of E6/E7 signals varied significantly among lesions: focal positivity within CK7-positive cells in 5 cases, focal positivity within P63-positive cells in 4 cases (Figure 2), and diffuse positivity involving both CK7 and P63-positive cells in 7 cases. No HPV E6/E7 signals were detected in negative controls.

Figure 1 - 746

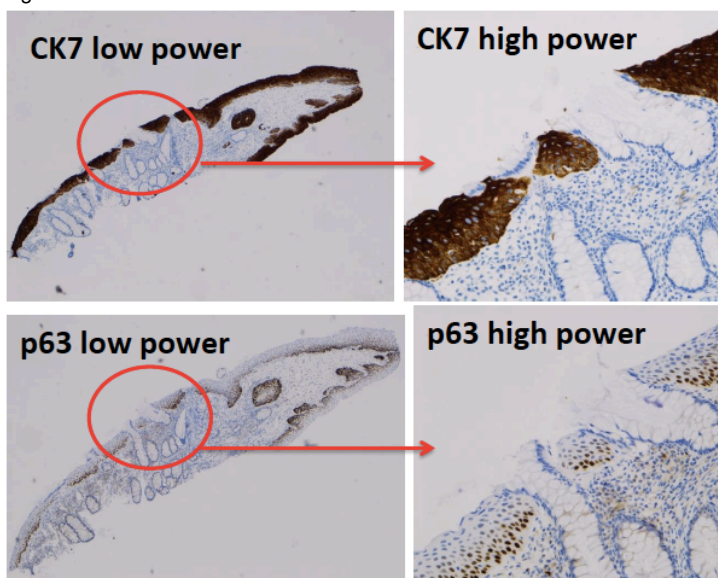
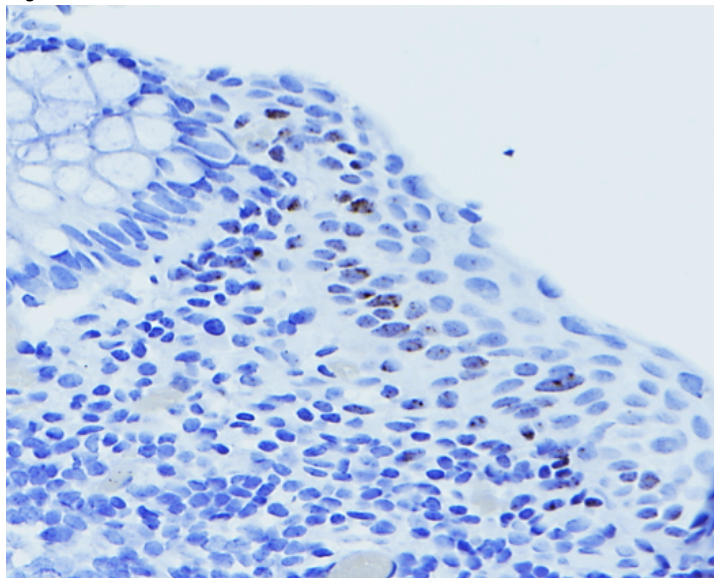


Figure 2 - 746



Conclusions: We confirmed the presence of two distinct cell populations in anal precancerous lesions arising from the transition zone. Both cell populations can harbor transcriptionally active HPV 16 E6/E7 RNA. Further study of the relationships between transition zone cells, HPV 16 E6/E7 localization and lesional progression would be of great value.

747 KRAS Mutation, But Not Mismatch Repair Deficiency, Occurs with Increased Frequency in African American Patients with Colorectal Cancer and Predicts Poor Disease-Free Survival

Donghai Wang¹, Mouyed Alawad¹, Raag Agrawal², M. Haseeb¹, Raavi Gupta¹

¹SUNY Downstate Medical Center, Brooklyn, NY, ²SUNY Downstate, Brooklyn, NY

Disclosures: Donghai Wang: None; Mouyed Alawad: None; Raag Agrawal: None; M. Haseeb: None; Raavi Gupta: None

Background: The incidence and mortality of colorectal cancer (CRC) are higher in African American (AA) patients than white patients. Although socioeconomic factors are involved in this racial disparity, biological differences in CRC in different racial groups remain unelucidated. Deficient Mismatch Repair (dMMR) function has been linked to a better prognosis in CRC. KRAS mutation, another

biomarker, predicts a poor response to EGFR inhibitor therapy. Here we compared profiles of KRAS mutation and MMR status in AA and white patients, and evaluated their prognostic value in CRC.

Design: All CRC cases tested for MMR (n=75) or KRAS mutation (n=110) from 2009 to 2017 at our institution were included in this study. Breakdown of patient population is provided in Table-1. Clinicopathologic variables were recorded for these cases. Chi-square test was used to analyze MMR status and KRAS mutations in different racial groups. Univariate survival analysis was performed with Kaplan-Meier method. Multivariate Cox regression was used to predict hazard ratio (HR) of MMR status and KRAS mutations. Due to limited size of white patient group in our study, we also utilized published data of white patients (Table-1).

Results: There is no significant difference in MMR status between AA and white patients. dMMR is associated with better disease-free survival (DFS) in AA patients with CRC by univariate analysis (p=0.05). However, after adjusting for other factors by multivariate analysis, DFS in AA was not affected. Frequency of KRAS mutation was higher in AA than white patients (57% vs. 21%, p<0.001). Amongst subtypes of KRAS tested, codon 12 mutation was more frequent in AA (85% vs. 69%, p=0.02) (Table-1). KRAS mutation is a significant predictor of poor DFS in both AA (HR=4.67, p<0.001) and other racial groups (HR=4.18, p=0.001) (Fig. 1).

Table 1. Genetic Profiles in AA and White Patients with CRC

Race	MSI	MSS	p value ^a	KRAS-M	KRAS-W	p value ^b	KRAS-12	KRAS-13	KRAS-O	p value ^c
	n (%)	n (%)		n (%)	n (%)		n (%)	n (%)	n (%)	
AA patients, our hospital	9 (16)	49 (84)		54 (57)	41 (43)		46 (85)	6 (11)	2 (4)	
White patients, our hospital	2 (25)	6 (75)	0.87	3 (50)	3 (50)	NA	3 (100)	0 (0)	0 (0)	NA
White patients ^{1,4}	20 (9)	206 (91)	0.14	45 (24)	143 (76)	<0.001	31 (69)	4 (9)	10 (22)	0.019
White patients ^{2,5}	39 (14)	237 (86)	0.78	42 (21)	161 (79)	<0.001				
White patients ³	21 (12)	159 (88)	0.44							

MSI: Microsatellite instability, MSS: Microsatellite Stability, KRAS-M: Mutant KRAS, KRAS-W: Wild-type KRAS, KRAS-O: Other subtypes of KRAS mutation, NA: Not performed due to limited sample size of white patients.

a. Comparison for MMR status.

b. Comparison for KRAS mutation.

c. Comparison for KRAS mutation subtypes.

References: 1 for MSI study: Clin Cancer Res.2014;20:4962.

2 for MSI study: PLoS One. 2014;9:e100461.

3 for MSI study: Clin Gastroenterol Hepatol. 2016;14:1163.

4 for KRAS study: Cancer Biomark. 2013;13:359.

5 for KRAS study: Clin Cancer Res. 2012;18:350.

Figure 1 - 747

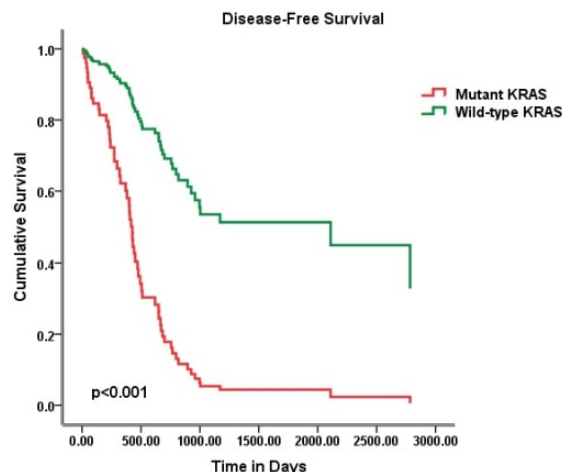


Fig. 1. Disease-free survival in AA patients with and without KRAS mutations

Conclusions: KRAS mutation is strongly associated with poor DFS in CRC in all racial groups. Since frequency of KRAS mutations is higher in AA than white patients, it most likely contributes to their increased mortality.

748 Clinicopathologic Features of Colorectal Cancer in African Americans: A Retrospective Single-Institution Study of 500 Patients

Donghai Wang¹, M. Haseeb¹, Raavi Gupta¹

¹SUNY Downstate Medical Center, Brooklyn, NY

Disclosures: Donghai Wang: None; M. Haseeb: None; Raavi Gupta: None

Background: Colorectal cancer (CRC) has the highest incidence and mortality in African Americans (AA) among all racial groups in the U.S. Although public databases like SEER provide a valuable tool to explore the racial differences in CRC, limitations including regional variation and lack of certain clinicopathologic information exist. We retrospectively analyzed CRC data from our institution with an AA-predominant patient population (86% of all patients), aiming to better define the factors which contribute to racial disparity.

Design: We extracted 33 major demographic, clinical and pathologic features of 500 consecutive cases of CRC diagnosed at our institution from 1/2009 to 12/2017. Tumors from anal canal or appendix, or with histology other than adenocarcinoma are excluded from study. Our data and those from SEER for matched white patients were analyzed by Chi-square test. The significance of individual factors in relation to survival was evaluated with Kaplan-Meier analysis. Multivariate Cox regression model was used to estimate the hazard risk (HR) of independent prognostic factors.

Results: AA are more likely to have advanced stage (25.9% vs. 20.8%, $p=0.041$), low grade (89.2% vs 77.5%, $p<0.001$) tumors in cecum (18.7% vs. 16.2%, $p<0.001$) than white patients. Hypertension and diabetes are more common in AA patients. Compared with other racial groups, AA have worse disease-free survival (DFS) (HR=3.682, $p=0.035$, Fig. 1A). AA patients with CRC in distal or proximal colon have worse overall survival (OS) than those with CRC in middle colon (HR=2.926, $p=0.014$, Fig. 1B), a finding not observed in white patients. In both racial groups advanced stage, perforation and hypertension are independent prognostic factors for OS ($p<0.05$). Similarly, low weight at presentation, mucinous adenocarcinoma, LVI, perineural invasion and KRAS mutations are independent factors significantly associated with poor DFS (Table-1).

Table 1. Multivariate analysis of survival for all races and AA with CRC *

Characteristics		OS for All Races				DFS for All Races				OS for AA				DFS for AA			
		p value	HR	95% CI for HR		p value	HR	95% CI for HR		p value	HR	95% CI for HR		p value	HR	95% CI for HR	
				Low er	Upp er			Low er	Upp er			Low er	Upp er			Low er	Upp er
AJCC Stage	I		1								1						
	II	0.093	3.949	0.793	19.656					0.059	7.903	0.925	67.506				
	III	0.267	2.461	0.502	12.079					0.12	5.359	0.647	44.396				
	IV	0.031	5.96	1.176	30.196					0.014	14.583	1.722	123.512				
Perforation	No		1								1						
	Yes	<0.001	6.323	2.45	16.321					0.002	4.901	1.789	13.432				
HTN	No		1								1						
	Yes	0.005	2.634	1.35	5.142					0.03	2.173	1.076	4.388				
CEA	Normal		1														
	High	0.007	3.194	1.381	7.385												
LVI	No		1				1								1		
	Yes	0.036	2.666	1.067	6.664	0.003	2.549	1.385	4.691					0.004	2.554	1.344	4.853
PNI	No						1								1		
	Yes					<0.001	4.284	2.11	8.697					<0.001	4.847	2.278	10.315
KRAS	Wild-type						1								1		
	Mutant					0.001	4.178	1.787	9.772					<0.001	4.669	1.979	11.015
Histology	Non-mucinous ADC						1								1		
	Mucinous ADC					0.021	2.451	1.146	5.244					0.011	2.743	1.259	5.977
Underweight	No						1								1		
	Yes					<0.001	10.766	4.132	28.05					<0.001	13.066	4.636	36.823
Race	Non-black						1										
	Black					0.035	3.682	1.098	12.346								
Site	Middle parts										1						
	End parts									0.014	2.926	1.24	6.904				

ADC: Adenocarcinoma, HTN: Hypertension, LVI: Lymphovascular invasion, PNI: Perineural invasion.

*Only values of statistically significant factors are listed.

Figure 1 - 748

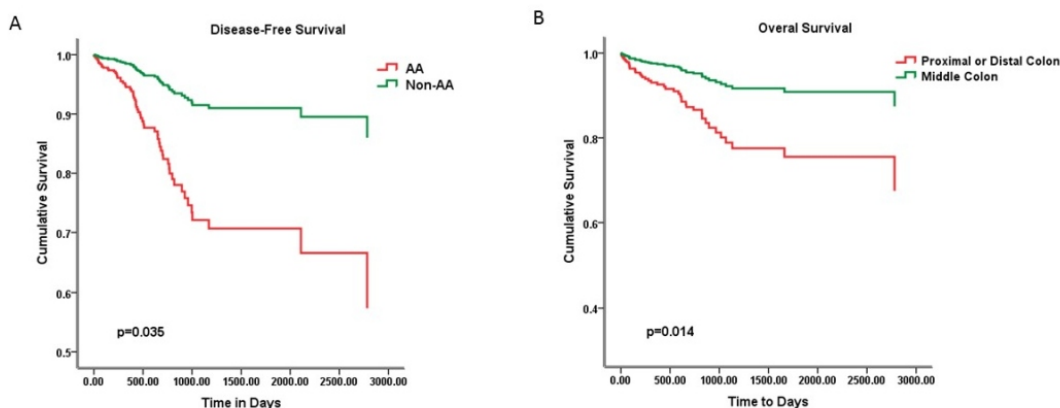


Fig. 1A. Disease-free survival in African American and other racial groups with CRC. 1B. Overall survival of African American patients with CRC arising from middle vs. proximal or distal colon.

Conclusions: After adjusting for other risk factors, we found AA patients with CRC to have worse DFS than other racial groups, indicating a biological basis for this disparity. CRC arising from distal (sigmoid and rectum), or proximal (cecum) colon predicts a poor OS in AA patients.

749 DNA Flow Cytometric and Interobserver Study of “Crypt Cell Atypia” in Inflammatory Bowel Disease

Kwun Wah Wen¹, Sarah Umetsu¹, John Goldblum², Ryan Gill¹, Grace Kim¹, Nancy Joseph¹, Peter Rabinovitch³, Sanjay Kakar¹, Gregory Lauwers⁴, Won-Tak Choi¹

¹University of California, San Francisco, San Francisco, CA, ²Cleveland Clinic, Cleveland, OH, ³University of Washington, Seattle, WA, ⁴H. Lee Moffitt Cancer Center & Research Institute, University of South Florida, Tampa, FL

Disclosures: Kwun Wah Wen: None; Sarah Umetsu: None; John Goldblum: None; Ryan Gill: None; Grace Kim: None; Nancy Joseph: None; Peter Rabinovitch: None; Sanjay Kakar: None; Gregory Lauwers: None; Won-Tak Choi: None

Background: The significance of “crypt cell atypia (CCA)” in inflammatory bowel disease (IBD) is unknown. Pathologists are reluctant to make a diagnosis of dysplasia in this setting. This study evaluates the diagnostic reproducibility and clinical significance of CCA.

Design: DNA flow cytometry (FCM) was performed on 14 cases of CCA from 7 IBD patients (diagnosed at UCSF between 2000 and 2018) using paraffin-embedded tissue. CCA was defined as an area of minimal crypt crowding without architectural atypia showing mild enlargement and hyperchromasia of slightly irregular, but mostly non-stratified nuclei. Atypia is limited to the crypt bases without surface epithelial involvement or significant activity. Seven GI pathologists diagnosed each case as negative (NEG), indefinite for dysplasia (IND), low-grade dysplasia (LGD), or high-grade dysplasia (HGD) by morphology alone, then again with knowledge of FCM results.

Results: None of the patients (male-to-female ratio 5:2; mean age 53 years; mean IBD duration 15 years), except one, had a diagnosis of dysplasia prior to CCA diagnosis. Endoscopically, these were flat lesions (n = 12) or normal appearing mucosa (n = 2). Aneuploidy was detected in all 14 cases. Five (71%) of the 7 patients developed HGD (n = 4) or adenocarcinoma (n = 1) where CCA had been diagnosed within a mean follow-up time of 25 months, whereas one patient had multiple follow-up biopsies showing CCA without a definite diagnosis of dysplasia. No follow-up information was available in the remaining one patient. When diagnoses were grouped as NEG or “atypical” (IND or dysplasia), the overall agreement rate of 76% (kappa = 0.51) improved to 90% (kappa = 0.81) with knowledge of FCM results (Table 1). Even when categorized as NEG or dysplasia groups, the overall agreement rate of 63% (kappa = 0.25) based on morphology alone improved to 73% (kappa = 0.46) with knowledge of FCM results (Table 2). However, when diagnoses were grouped as NEG, LGD, or HGD, the overall agreement rate was < 40% (kappa < 0.09) regardless of knowledge of FCM results.

Table 1. Diagnoses rendered in 14 cases of CCA by 7 pathologists (total of 98 diagnoses).

		"Atypical"			
	NEG	IND	LGD	HGD	Kappa values (% agreement)
Morphology alone	17	49	13	19	0.51 (76%)
With FCM results	5	36	25	32	0.81 (90%)

Table 2. Categorization of NEG or dysplasia groups after reclassification of IND cases*

	Dysplasia*			
	NEG	LGD	HGD	Kappa values (% agreement)
Morphology alone	35	35	28	0.25 (63%)
With FCM results	15	48	35	0.46 (73%)

*If reactive atypia was favored, it was placed into NEG. If LGD or HGD was favored, it was placed into respective category.

Conclusions: The presence of aneuploidy and development of HGD/adenocarcinoma on follow-up indicates that CCA likely represents a dysplastic lesion (at least LGD) and is a histologic marker of neoplastic progression. Although the grading of dysplasia, largely based on cytologic abnormalities, is subject to significant interobserver variability, CCA can be histologically identified and should lead to a recommendation of increased endoscopic surveillance.

750 Intratumoral Budding and Tumor Microenvironment Predict the Response to Neoadjuvant Treatment in Rectal Carcinoma

Xiaoyun Wen¹, Jirong Mass², Katie Louka³, Sui Zee², Daniel Mockler⁴, Kenneth Shroyer⁵, Jela Bandovic²

¹Stony Brook, Stony Brook, NY, ²Stony Brook University Hospital, Stony Brook, NY, ³Stony Brook, NY, ⁴SUNY Stony Brook University Hospital, Kings Park, NY, ⁵Stony Brook Medicine, Stony Brook, NY

Disclosures: Xiaoyun Wen: None; Jirong Mass: None; Katie Louka: None; Sui Zee: None; Daniel Mockler: None; Kenneth Shroyer: None; Jela Bandovic: None

Background: Tumor budding, at the invasive tumor front (peritumoral budding), is an established prognostic parameter in colorectal cancer. However, the significance of intratumoral budding in the pre-treatment biopsies is still uncertain. Our study aims to investigate the correlation of intratumoral budding and the tumor microenvironment in pretreatment rectal cancer biopsies with the response to neoadjuvant treatment.

Design: Pretreatment biopsies of well to moderately differentiated rectal cancer from 13 patients who underwent consecutive resection after neoadjuvant treatment were retrospectively reviewed to evaluate intratumoral budding, type of stroma, and intraepithelial lymphocytes. Pancytokeratin was performed and the number of intratumoral buds was counted on a single hotspot in one high-power field. Intraepithelial lymphocytes (IEL) was graded semiquantitatively as "absent" (less than 2 intraepithelial lymphocytes per high-power field) or "presence" (two or more intraepithelial lymphocytes per high-power field). The tumor stroma was classified as myofibroblastic or myxoinflammatory type.

Results: In pretreatment biopsies, intratumoral budding was observed in 12/13 patients (92%) and ranges from 1 to 28 per hotspot with a median of 8. High-grade intratumoral budding (> 6 buds) was found to be strongly associated with a worse response to neoadjuvant treatment ($P < 0.001$). High-grade intratumoral budding was also found to be strongly associated with myxoinflammatory stroma ($P < 0.001$) and is inversely related to the amount of intraepithelial lymphocytes ($P < 0.001$).

	# of bx fragments	ITB(H&E)	ITB(IHC)	Stroma	IEL	NTR	ypTNM
1	6	(+)	10	MFB	(-)	score 0	T0N0Mx
2	4	(+)	3	MFB	(+)	score 0	T0N0Mx
3	2	(-)	0	Myxoinf	(-)	score 1	T2N0Mx
4	1	(+)	3	Myxoinf	(-)	score 1	T2N0Mx
5	4	(+)	2	MFB	(+)	score 1	T2N1aMx
6	2	(+)	9	Myxoinf	(-)	score 2	T2N0Mx
7	2	(+)	8	Myxoinf	(-)	score 2	T3N0Mx
8	3	(+)	2	MFB	(+)	score 2	T3N0Mx
9	4	(+)	1	Myxoinf	(-)	score 2	T3N1bMx
10	5	(+)	8	Myxoinf	(-)	score 2	T3N0Mx
11	8	(+)	17	Myxoinf	(-)	score 2	T3N0Mx
12	1	(+)	28	Myxoinf	(+)	score 2	T4N2aM1
13	2	(+)	18	Myxoinf	(-)	score 2	T4bN0M1

Abbreviations: ITB = intratumoral budding; "+" = presence of ITB; "-" = absence of ITB;
IEL = intraepithelial lymphocytes: "+" = 2 or more IEL/HPF; "-" = less than 2 IEL/HPF;
Myofibroblastic: MFB; Myxoinflammatory = Myoinf; NTR = neoadjuvant therapy response

Figure 1 - 750

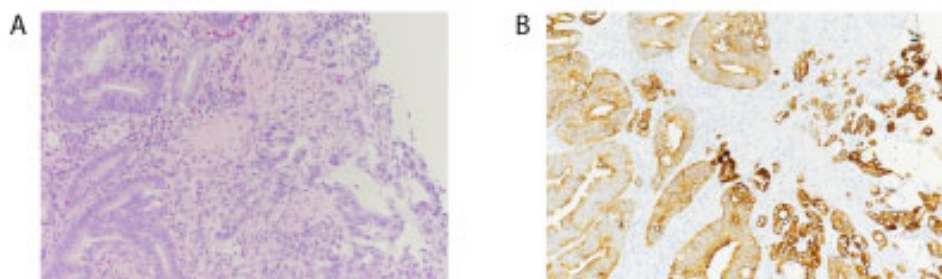


Figure 1. Biopsy specimen with high intratumoral budding. (A) Rectal cancer with small groups and single tumor cells in a myxoinflammatory stroma. (B) Immunohistochemical staining for pan-cytokeratin highlighting the tumor buds.

Figure 2 - 750

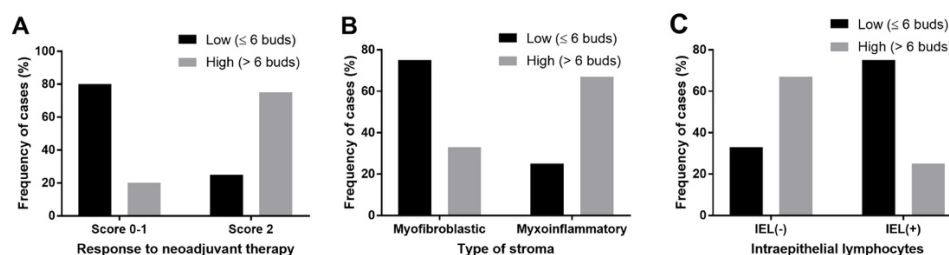


Figure 2. High-grade ITB strongly correlates with a worse response to neoadjuvant therapy, myxoinflammatory type stroma and absence of IEL. (A) Correlation of ITB with pathological response to neoadjuvant therapy. (B) Correlation of ITB with the type of stroma. (C) Correlation of ITB with intraepithelial lymphocytes (IEL). Low ITB was defined as 6 or less buds/HPF and high ITB was defined as greater than 6 buds/HPF. P < 0.001 each.

Conclusions: High-grade intratumoral budding in pretreatment rectal cancer biopsies is strongly associated with myxoinflammatory stroma and absence of intraepithelial lymphocytes, suggesting that the local microenvironment critically influences tumor dissemination. The strong correlation between high-grade intratumoral budding and a worse response to neoadjuvant treatment may help tailor the patient's pre and post resection therapy. Our preliminary results warrant further investigation of intratumoral budding and the tumor microenvironment in a more extensive series of pretreatment rectal cancer biopsies.

751 Varying Practices in Tumor Regression Grading of Gastrointestinal Carcinomas after Neoadjuvant Therapy – Results of an International Survey

Maria Westerhoff¹, Marek Osecky², Rupert Langer³

¹University of Michigan, Ann Arbor, MI, ²Institute of Pathology, University of Bern, Bern, Switzerland, ³University of Bern, Bern, Switzerland

Disclosures: Maria Westerhoff: None; Marek Osecky: None; Rupert Langer: None

Background: Tumor Regression Grading (TRG) is a reliable prognostic tool routinely performed on gastrointestinal (GI) cancers resected after neoadjuvant therapy. Challenges implementing TRG include lack of standardization for grossing treated specimens, multiple grading systems with varying interobserver agreement, and difficulty interpreting therapy-induced changes. We surveyed GI pathologists around the world for their practices in handling neoadjuvant treated GI cancer (CA) specimens and TRG reporting.

Design: A 23-question survey was distributed to GI pathologists through various national and international working groups. TRG-topics addressed grossing, histologic work-up, TRG system used, and degree of difficulty identifying & estimating amount of residual CA within a background of treatment effect.

Results: 132 replies were received from North America (NA) (n=52), Europe (n=56), and other continents (n=24). 93% routinely report TRG and have standardized grossing & histologic work-up. Only 25% always completely embed the entire CA bed, but an additional 55% also completely embed the CA site if it is not a grossly apparent, large mass. In NA, 83% use H&E alone for assessment; 17% add IHC/special stains. In contrast, 44% of non-NA pathologists assess residual CA by H&E only, with 56% using H&E & IHC/special stain. In NA, AJCC/Ryan system is routinely used for gastroesophageal (77%) & rectal CA (86%). Outside of NA, a variety of TRG systems are implemented: for gastroesophageal CA the Mandard system is common (44%), followed by AJCC/Ryan (30%), and Becker (17%); for rectal CA, the AJCC/Ryan (40%) is followed by Mandard (24%), and Dworak system (21%). Overall, most preferred a 4-tiered system (52%) as well as a descriptive estimate of residual CA (27%). The latter, however, was not markedly favored over other TRG system elements such as % fibrosis/CA ratio (26%) or % residual CA (15%). 67% considered that therapy changes in lymph nodes should be part of TRG. Most considered identifying residual CA easy (60%) but estimating therapy-induced fibrosis difficult (44%). Free comments raised issues of costs for detailed pathology work-up & clinical relevance.

Conclusions: This survey provides a comprehensive overview regarding TRG in GI cancer work-ups as performed by multinational surgical pathologists. TRG standardization is high in NA, where national guidelines recommend a specific TRG system (i.e. AJCC/Ryan), but is more heterogenous in other parts of the world according to geographic regions.

752 The Predictive and Prognostic Value of Tumor Infiltrating Lymphocytes in Biopsies of Pre-Neoadjuvantly Treated Colorectal Carcinoma

Kaitlyn Wieditz¹, Paulo Garcia¹, Michael Idowu¹, Melissa Contos²

¹Virginia Commonwealth University Health System, Richmond, VA, ²VCU Health, Richmond, VA

Disclosures: Kaitlyn Wieditz: None; Paulo Garcia: None; Michael Idowu: None; Melissa Contos: None

Background: The current era of immunotherapy has given evaluation of tumor infiltrating lymphocytes (TILs) increased importance in view of potential prognostic and predictive value. The 2017 International Immuno-Oncology Biomarkers Working Group guidelines indicated that the significance of TILs in patients undergoing neoadjuvant therapy has not been adequately investigated using semiquantitative H&E methods. The purpose of our study was to evaluate the predictive or prognostic significance of TILs in biopsies of pretreated colorectal carcinoma using a modified Klintrup-Mäkinen (KM) method.

Design: Pretreated biopsies of patients with rectal carcinoma treated with neoadjuvant chemoradiation (NACR) between 01/2006 and 12/2017 were identified by database search. A modified KM semi-quantitative score examining overall TILs and TILs at the invasive edge was used for evaluation. The original KM score evaluated overall inflammation and individual inflammatory cell lineages; we focused on lymphocytes. Overall TILs were graded on a scale of 0-3 (0= absent inflammatory reaction, 1= weak, 2= moderate, 3= strong). TILs at the invasive edge were graded on a scale of 0-3 (0= no increase, 1= patchy, 2= band-like and 3= prominent or cup-like zone). Post NACR tumor response was studied using a modified Becker grading scale (1= complete response, 2= <10% residual tumor, 3= 10-50% residual tumor and 4= >50% residual tumor). TIL score was correlated to overall survival, response to treatment and distant metastasis using the Chi-Square test and Kaplan-Meier survival estimate.

Results: A total of forty-three colorectal biopsies were available for review. TILs were evaluated on H&E stained histologic sections (Table 1). Less overall TILs in pretreated biopsies were correlated to a better survival ($p=0.038$, Figure 1). Though not statistically significant, our data suggests that increased TILs at the invasive edge tended to a better treatment response ($p=0.066$) and less distant metastasis ($p=0.057$, Figure 2). Overall inflammation was not associated to treatment response or distant metastasis. Inflammation at the invasive edge was not related to overall survival.

		Overall Inflammation		Inflammation at Invasive Edge	
		Absent	Weak	No Increase	Patchy Increase
Total Number	<i>N</i> = 43	24 (56%)	19 (44%)	28 (65%)	15 (35%)
Death across 5 year period	Yes (<i>N</i> =16)	6 (14%)	10 (23%)	6 (14%)	10 (23%)
	No (<i>N</i> =27)	18 (42%)	9 (21%)	22 (51%)	5 (12%)
Tumor Response to NACR Treatment	Complete (<i>N</i> =7)	4 (9%)	3 (7%)	6 (14%)	1 (2%)
	<10% Residual (<i>N</i> =14)	9 (21%)	5 (12%)	10 (23%)	4 (9%)
	10-50% Residual (<i>N</i> =19)	10 (23%)	9 (21%)	12 (28%)	7 (16%)
	>50% Residual (<i>N</i> =3)	1 (2%)	2 (5%)	0	3 (7%)
Distant Metastasis	Yes (<i>N</i> =16)	10 (23%)	6 (14%)	13 (30%)	3 (7%)
	No (<i>N</i> =27)	14 (33%)	13 (30%)	15 (35%)	12 (28%)

Figure 2 - 752

Figure 1 - 752

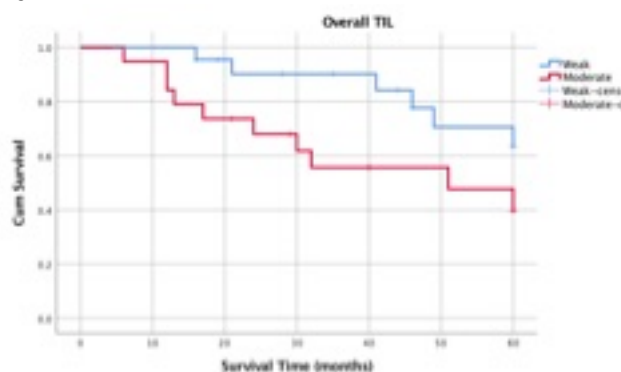


Figure 1: Kaplan-Meier 5-year survival curve for overall TILs ($p=0.038$).

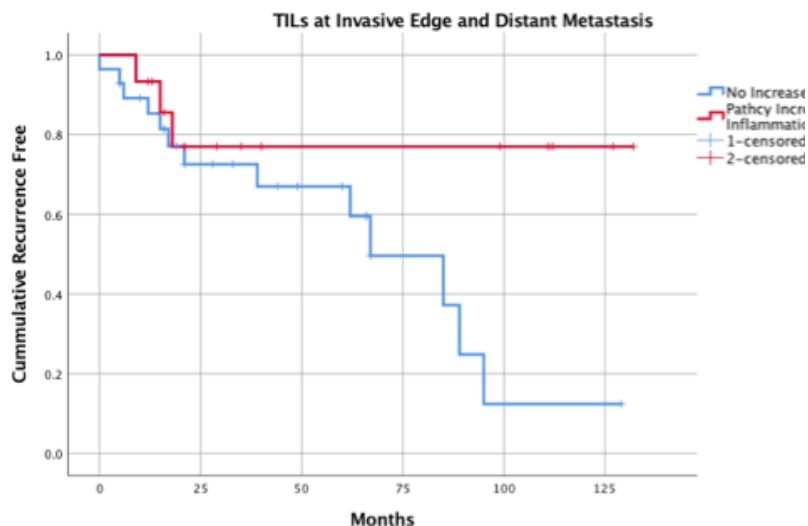


Figure 2: Kaplan-Meier survival curve for invasive edge TIL compared to time to metastasis ($p=0.057$).

Conclusions: Increased overall TILs in pre-NACR treatment rectal cancer is associated shorter survival outcomes. Increased inflammation of the invasive edge trends toward less distant metastasis and better response to treatment which may provide prognostic and predictive value. Further study with a larger cohort will be useful in confirming this observation.

753 The Accuracy of PD-L1 Expression in Endoscopic Biopsy Specimens Versus Resection Specimens in Colonic Adenocarcinoma

Grant Williams¹, Jamie Lombardo², Lynn Messersmith³, Annelies Hickerson³, Jessica Campf⁴, George Peoples⁵, Robert Brady³, Ryan Collins⁶, Guy Clifton⁷

¹San Antonio Uniformed Services Health Education Consortium, Schertz, TX, ²SAMMC, Cibolo, TX, ³SAMMC, Fort Sam Houston, TX, ⁴San Antonio Uniformed Services Health Education Consortium, Fort Sam Houston, TX, ⁵Spring Branch, TX, ⁶Brooke Army Medical Center, JBSA-FSH, TX, ⁷San Antonio Uniformed Services Health Education Consortium, San Antonio, TX

Disclosures: Grant Williams: None; Jamie Lombardo: None; Lynn Messersmith: None; Annelies Hickerson: None; Jessica Campf: None; George Peoples: None; Robert Brady: None; Ryan Collins: None; Guy Clifton: None

Background: Understanding the interaction of the adaptive and innate immune system in tumorigenesis is critical for the development and effective use of immunotherapies. Therapies targeting the Programmed Death-1 (PD-1) receptor have seen success in treating multiple types of cancer. PD-1 ligand (PD-L1) is upregulated by certain tumor cells, including colorectal cancer, and limits the host immune response effectiveness by altering the PD-1/PD-L1 immune axis. Microsatellite instability (MSI) high tumors are known to respond to PD-1 therapy, so are thought to have a higher rate of PD-L1 expression. Understanding the accuracy of PD-L1 expression on endoscopic biopsy can help determine its usefulness in guiding neoadjuvant therapy in trials and in practice.

Design: 96 patients with matched endoscopic biopsies and resected colorectal adenocarcinoma diagnosed between 2006-2016 were selected for retrospective review. Patients who received neoadjuvant therapy were excluded. PD-L1 staining of formalin fixed paraffin embedded tumor cells was interpreted per manufacturer guidelines as negative, low, or high (Figure 1). MSI testing was performed selectively based on modified Bethesda criteria. The PD-L1 status was compared between the biopsy and definitive resection using a Cohen's kappa test.

Results: PD-L1 testing on biopsies was 70/96 negative, 14/96 low, and 12/96 high. On resection, PD-L1 testing was 58/96 negative, 23/96 low, and 15/96 high.

PD-L1 positivity on biopsy weakly correlated with PD-L1 positivity in resection, with 63% of cases in concordance ($k, 0.17$; $p=0.04$). The positive predictive value (PPV) of the endoscopic biopsy was 54% and the negative predictive value (NPV) was 66% compared to the resection. 54% of cases were in concordance ($k, 0.09$; $p=0.10$) when low and high positive were considered.

In the MSI high subset of 6 patients, 5 were PD-L1 negative and 1 was low positive on endoscopic biopsy, while at resection 2 were negative and 4 were positive. PD-L1 positivity on biopsy was in concordance in 50% of cases ($k, 0.18$; $p=0.22$). The NPV was 40% and the PPV was 100%.

Figure 1 - 753

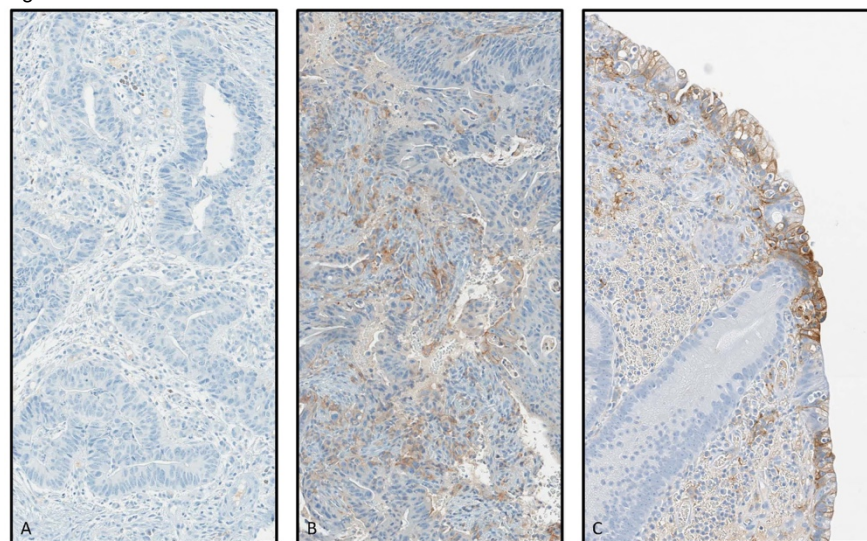


Figure 1: PDL-1 IHC stain of colorectal carcinoma with negative staining (A), low positive (B), and high positive (C).

Conclusions: In this large retrospective study PD-L1 positivity by endoscopic biopsy is weakly correlated to PD-L1 positivity in resection specimens. The concordance of PD-L1 positivity in MSI high subset of patients is poor, although the number of MSI high in this study was small. These data suggest that PD-L1 expression on endoscopic biopsy is not an accurate reflection of the PD-L1 status in the tumor microenvironment.

754 Comprehensive Interrogation of DNA Methylation of Colon Cancers from African Americans

Joseph Willis¹, Alexander Miron², Helen Moinova³, Li Li⁴, Kishore Guda³, Sanford Markowitz⁴, Robin Bissell³

¹University Hospitals Cleveland Medical Center, Cleveland, OH, ²CWRU, Cleveland, OH, ³Case Western Reserve University, Cleveland, OH, ⁴Cleveland Medical Center, Case Western Reserve University, Cleveland, OH

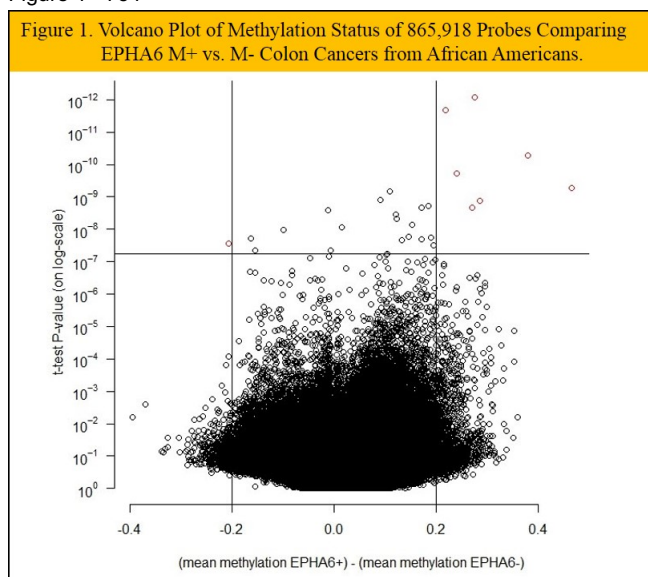
Disclosures: Joseph Willis: None; Alexander Miron: None; Helen Moinova: None; Kishore Guda: None; Sanford Markowitz: None; Robin Bissell: None

Background: Background: The most important epigenetic process in cancer is methylation of CpG islands. In colon cancers (CCs) more genes are silenced by CpG island methylation than by mutation – and some genes are only silenced by methylation. The recognition of co-dependence of genomic and epigenetic has significantly advanced our understanding of carcinogenesis. Our team recently completed the first genome-wide analysis of the mutational landscape of CCs arising in African Americans. We identified a unique mutation signature defined by a mutation in one of 15 signature genes [M+] present in 42% of African American CCs, compared to 15% of Caucasian Americans CCs. M+ CCs had a significantly worse outcome compared to M-. Four genes were mutated solely in African American CCs – with the most common, EPHA6, being present in 6% of African American CCs. EPHA6 mutations signified a markedly worse outcome – even compared to the other M+CCs. An underlying mechanism of mutation causation in this unique population has proved elusive. Direct causation of somatic mutations secondary to epigenetic effects are partially understood and include such processes as epigenetic silencing of DNA repair and chromatin structure modifications. We performed epigenome wide sequencing of these CCs to identify a methylation signature linked to this unique cancer biology.

Design: Design: Using CCs from African Americans with known 15 gene mutation status, we compared genome wide CpG islands methylation status of 31 M+ CCs vs.33 M- CCs as well as methylation status of 236 known CC driver genes using the Infinium EPIC BeadChip 850K Array. We also specifically looked at unique subsets of these CCs, including six EPHA6 M+ vs 58 EPHA6 M- CCs and 38 TP53 M+ vs 26 TP53 M- CCs.

Results: Results: EPHA6 M+ CCs had a highly statistically significant methylation profile after Bonferroni correction for multiple testing based on a subset of probes– upper left and right quadrants of volcano plot Figure 1. Comparisons between M+ vs. M- CCs and TP53 M+ vs TP53 M- CCs did not demonstrate any methylation signature differences either globally or limited to known CC driver genes.

Figure 1 - 754



Conclusions: Conclusion: These data support the uniqueness of CCs with EPHA6 mutations in African American patients. This result is surprising given the number of EPHA6 M+ samples compared to the control group. This highlights the importance of molecular classification of CC to define biologically distinct subsets with potentially unique clinicopathological properties.

755 Interobserver Agreement and the Utility of Immunohistochemistry (IHC) for Assessing Tumor Budding in Colorectal Adenocarcinoma

Mary Wong¹, Maha Guindi², Zhikai Chi³, Deepti Dhall⁴, Stacey Kim⁵, Brent Larson⁴, Richard Mertens⁶, Roberto Alvaro Taguibao⁴, Kevin Waters⁴

¹Arcadia, CA, ²Cedars-Sinai Medical Center, Beverly Hills, CA, ³Coppell, TX, ⁴Cedars-Sinai Medical Center, Los Angeles, CA, ⁵Los Angeles, CA, ⁶Sherman Oaks, CA

Disclosures: Mary Wong: None; Maha Guindi: None; Zhikai Chi: None; Deepti Dhall: None; Stacey Kim: None; Brent Larson: None; Richard Mertens: None; Roberto Alvaro Taguibao: None; Kevin Waters: None

Background: Tumor budding in colorectal carcinoma is a clinically significant predictor of nodal metastases. The International Tumor Budding Consensus Conference (ITBCC) recently published standardized recommendations for assessing and reporting tumor budding. In initiating tumor budding reporting at our tertiary care institution, we evaluated the reproducibility of scoring and the utility of IHC scoring.

Design: Thirty colorectal adenocarcinoma resections (10 each of well, moderate, and poor differentiation) were identified from departmental archives from 2015-2018. H&E and AE1/AE3 stains of a representative section were evaluated for tumor budding by 9 observers (6 faculty, 2 fellows and 1 senior resident) using the ITBCC recommendations. There was a break between H&E and AE1/AE3 scoring of at least 1 day. The median score was used as the adjudicated score for each case. Fleiss Kappa (K) statistics were used to determine the degree of interobserver agreement. A chi-square test was used to compare the distribution of budding categories between H&E and IHC.

Results: The median patient subject age was 69, 50% were male, and 57% were white. Using H&E only, 21 cases had low tumor budding, 6 intermediate, and 3 high. One well differentiated and two poorly differentiated cases comprised the 3 high tumor budding cases. There was moderate agreement (K=0.41) among 9 observers. Agreement was similar among well, moderately, and poorly differentiated cases (K= 0.38, 0.44 and 0.35, respectively). Using IHC to aid in scoring, 8 cases had low budding, 7 intermediate, and 15 high. The change in categories was statistically significant ($p=9.6 \times 10^{-4}$) as 60% of cases were in a higher category of budding and 33% of the low cases on H&E were categorized as high using IHC. No cases were scored in a lower category using IHC compared to H&E only. Agreement was still moderate, but mildly improved (K=0.54), using IHC. Agreement was similar between well, moderately, and poorly differentiated cases (K= 0.54, 0.39, and 0.66, respectively).

Conclusions: Using the ITBCC system with and without IHC, we achieved moderate agreement in categorizing tumor budding among 9 pathologists. While agreement was mildly improved using IHC, tumor budding scores were significantly higher using IHC. As the categories were largely created and validated using H&E, our data strongly suggests that IHC should not be routinely used in the assessment of tumor budding as it could lead to the overestimation of tumor budding using the ITBCC system.

756 Low-grade Appendiceal Mucinous Neoplasms in Association with Serrated Neoplasia

Elizabeth Yiru Wu¹, Reetesh Pai², Michael Drage³, Amitabh Srivastava⁴

¹Rhode Island Hospital/Brown University, Providence, RI, ²UPMC-Presbyterian Hospital, Pittsburgh, PA, ³University of Rochester Medical Center, Rochester, NY, ⁴Brigham and Women's Hospital, Harvard Medical School, Boston, MA

Disclosures: Elizabeth Yiru Wu: None; Reetesh Pai: None; Michael Drage: None; Amitabh Srivastava: None

Background: Low-grade appendiceal mucinous neoplasms (LAMNs) are conventional adenoma-like lesions with expansile growth and propensity for mucin extravasation, perforation, and development of pseudomyxoma peritonei. A subset of LAMNs, however, may be associated with a serrated lesion instead of a conventional adenoma but have not been well characterized. The aim of this study was to describe the morphologic and clinicopathologic spectrum of LAMNs with an associated serrated lesion (serrated LAMNs).

Design: LAMNs from two institutions were retrospectively reviewed for presence of an associated serrated lesion, as defined by prominent serrated crypt profiles or abundant microvesicular mucin with small ovoid basal nuclei reminiscent of a microvesicular hyperplastic polyp (HP) or sessile serrated polyp (SSP), or features similar to a traditional serrated adenoma (TSA). Age, gender, pathologic stage, and outcome were collected for all cases. KRAS mutation status information was also recorded, wherever available.

Results: A total of 88 LAMNs were reviewed, 19 of which were associated with a serrated lesion (21.6%). The median age at diagnosis of serrated LAMNs was 63 yrs (range 25-89 yrs), similar to conventional LAMNs (median 60 yrs; range 24-85 yrs). The male-female distribution was similar between patients with serrated (12/19=63.2% female) and conventional LAMNs (44/69=63.8% female). Most serrated LAMNs had abundant microvesicular mucin similar to HP/SSP (12/19=63.2%), while 3/19 (15.8%) showed TSA-like features; a combination of the two phenotypes was present in the remaining 4/19 (21.1%). Of the LAMNs with available KRAS mutation status, 3/3 (100%) serrated LAMNs and 12/16 (75%) conventional LAMNs were positive for KRAS mutation. A similar proportion of patients with serrated (6/19=31.6%) and conventional LAMNs (19/69=27.5%) presented with disease limited to within the appendiceal wall (pTis(LAMN)).

Conclusions: A significant subset of LAMNs appears to develop through a serrated pathway similar to colorectal neoplasia. The molecular features and prognostic significance of this subset needs to be delineated clearly in future studies.

757 Prognostic value of DNA repair gene based on stratification of gastric cancer

Midie Xu¹, Weiwei Weng¹, Hui Sun², Min Ye², Weiqi Sheng²

¹Shanghai, China, ²Fudan University Shanghai Cancer Center, Shanghai, China

Disclosures: Midie Xu: None

Background: DNA repair genes can be used as prognostic biomarkers in many types of cancer. We aimed to identify prognostic DNA repair genes in patients with gastric cancer (GC).

Design: Global gene expression profiles from altogether 1,325 GC patients samples from six independent datasets were included in the study. Clustering analysis was performed to screen potentially abnormal DNA repair genes related to the prognosis of GC, followed by unsupervised clustering analysis to identify molecular subtypes of GC. Characteristics and prognosis differences were analyzed among these molecular subtypes, and modular driver genes in molecular subtypes were identified based on changes in expression correlation. Multivariate Cox proportional hazard analysis was used to find the independent prognostic gene and development of DNA repair gene signature to calculate the risk score for every patient. Kaplan-Meier method and log-rank test was used to estimate correlations of key DNA repair gene signature with overall survival.

Results: There were 57 key genes significantly associated to prognosis, and GC patients were stratified into three molecular subtypes based on their expression profiles, in which patients in group III showed the best survival ($P < 0.001$). By multivariate Cox proportional hazard analysis, the expression profile of 12 independent key DNA repair genes were identified can classified patients as high risk or low risk by using Youden index. Compared with patients with low-risk score, patients with high risk score in the training set had shorter overall survival ($P < 0.001$). Furthermore, we verified equivalent findings by these key DNA repair genes in the validation set 1 ($P < 0.001$) and the validation set 2 ($P = 0.031$).

Figure 1 - 757

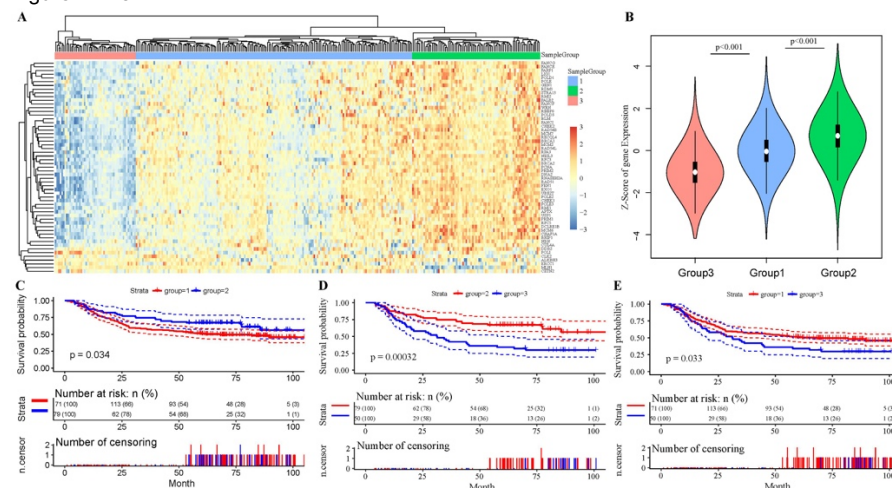
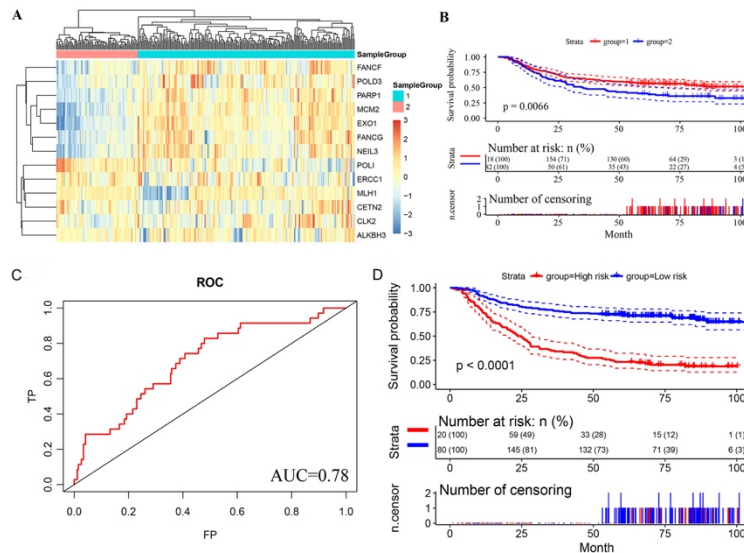


Figure 2 - 757



Conclusions: Identification of GC patients with DNA repair genes signature might be utilised in prognostication and inform treatment decisions for patients at high risk of progression.

758 Genotyping Colon Carcinoma in 3906 Hispanic Patients from Puerto Rico

Zhiwei Yin¹, Khalid Algarrahi², Nawar Matti², Jie-Gen Jiang²

¹Rutgers University-NJMS, Newark, NJ, ²Rutgers New Jersey Medical School - Rutgers University, Newark, NJ

Disclosures: Zhiwei Yin: None; Khalid Algarrahi: None; Nawar Matti: None; Jie-Gen Jiang: None

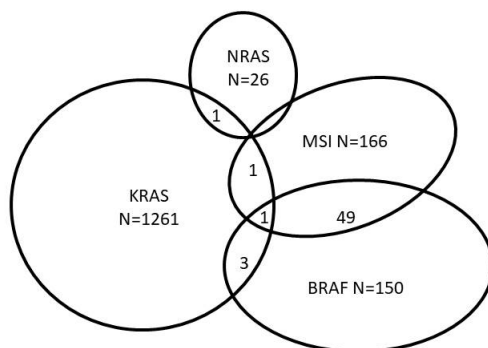
Background: Colon carcinoma is the third most common malignancy in the US, and the second most common cancer in Hispanics. Recent years the EGFR target therapy and anti-PD-1/PDL-1 immunotherapy were developed as promising treatments for colon carcinoma. Evaluating the mutation status of *KRAS*, *MMR/MSI*, *BRAF*, and *NRAS* is essential since these mutations are either used as predictor of EGFR or anti-PD-1/PDL-1 therapy or prognosis factors. As a matter of fact, there are ethnic disparities in the status of these mutations among different racial populations. It has been found that *KRAS* mutation in colon carcinoma has been reported ranging around 30-48% among the North American, Asian, and European populations, and cancers with MSI account for approximately 20% of all colorectal cancers. Unfortunately, the reported data is limited about frequencies of these gene mutations in Hispanics with colon carcinoma. In our study, we evaluate the frequencies of *KRAS* mutation and MSI in Hispanic colon cancer patients from Puerto Rico, and for the first time we report the frequencies of *BRAF* and *NRAS* mutations in this ethnic population.

Design: PCR and NGS results of *KRAS*, *MSI*, *BRAF*, and *NRAS* in 3906 Hispanic patients with colon carcinoma from Puerto Rico between 2008 and 2018 were obtained and analyzed retrospectively.

Results: Foremost, the frequencies of *BRAF* and *NRAS* mutation in Puerto Rican population were assessed: *BRAF* 10.1% and *NRAS* 5.2%. The age (y/o) for *BRAF* is 65.1±13.5, and 63.8±14.2 for *KRAS*. The overall MSI frequency is 9.6%, including sporadic and familial MMR negative colon carcinoma. This is lower than reported frequency (20%) in whites and African American populations. The frequency of *KRAS* mutation was 42.4% (N=2976) with age 64.6±12.7, which is consistent with previously reported frequency (39%). Interestingly, approximately one third of cases with *BRAF* mutation (49/150) also demonstrated overlapped MSI status. There were both of *KRAS* and *BRAF* mutations in 3 cases, and another 3 cases showed overlapped *KRAS* and *NRAS* mutations, *KRAS* mutation and MSI, or *NRAS* mutation and MSI. There were *KRAS* and *BRAF* mutations and MSI identified in 1 case.

Gene	frequency %	Gender (positive patients)		Age (Mean±Stdev)
		Male	Female	
KRAS	42.4(1261/2976)	688	572	64.6±12.7
BRAF	10.1 (150/1485)	51	99	65.1±13.5
NRAS	5.2(26/500)	19	7	63.8±14.2
MSI	9.6(166/1739)	68	98	65.9±12.4

Figure 1 - 758



Conclusions: Hispanic colon carcinoma patients from Puerto Rico demonstrate distinct molecular landscape from other ethnic/racial populations, which might impacts their clinical treatment and outcome.

759 Yes-Associated Protein 1 (YAP1) is a Novel Progressive Marker for Early Stage Esophageal Adenocarcinoma

Feng Yin¹, Dongtao Ann Fu¹, Ashwin Akki¹, Ashwini Esnakula¹, Michael Feely¹, David Hernandez Gonzalo², Jesse Kresak¹, Jinping Lai³, Xiuli Liu¹

¹University of Florida, Gainesville, FL, ²University of Florida-Shands, Gainesville, FL, ³University of Florida College of Medicine, Gainesville, FL

Disclosures: Feng Yin: None; Dongtao Ann Fu: None; Ashwin Akki: None; Ashwini Esnakula: None; Michael Feely: None; David Hernandez Gonzalo: None; Jesse Kresak: None; Jinping Lai: None; Xiuli Liu: None

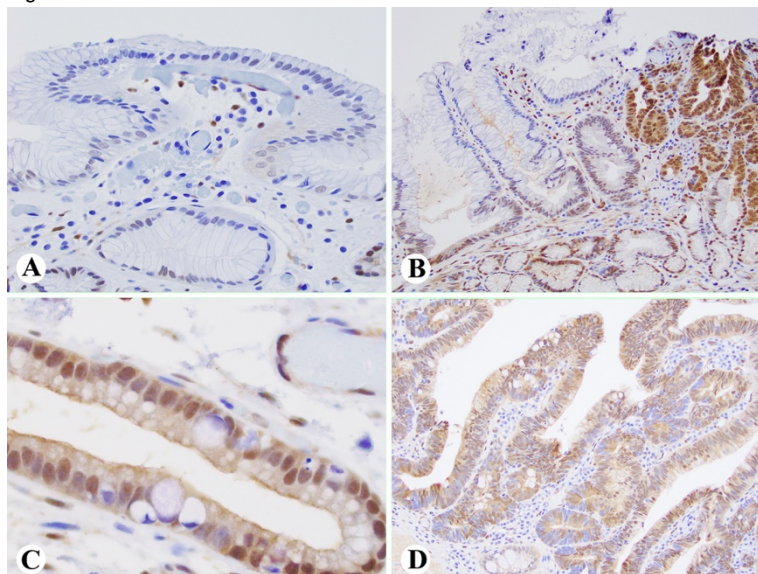
Background: Barrett's esophagus (BE) is a precursor lesion of esophageal adenocarcinoma (EAC). Currently there are no established biomarkers to predict or measure the progression from BE to EAC. YAP1 is the effector of an emerging tumor suppressor Hippo pathway that is involved in organ size control and tumorigenesis. Our current study is designed to evaluate YAP1 expression in early stage EAC including BE with high-grade dysplasia (HGD), intramucosal carcinoma (IMC), and submucosal adenocarcinoma (SAC).

Design: YAP1 expression was assessed using immunohistochemistry in endoscopic submucosal dissection tissues from 58 patients with BE neoplasia (16 HGD, 24 IMC, 18 SAC). The results were scored based on the total percentage of positive cells (0-100%) and intensity of the staining (negative-0, weak-1, intermediate-2, and strong-3). YAP1 expression levels were calculated by multiplying the positive percentage and the intensity score (range: 0-300) and categorized into low (150) expression groups. Statistical analysis was performed using Fisher's exact test.

Results: YAP1 staining was absent on the surface of benign esophageal columnar epithelium (Figure 1A). YAP1 was weakly expressed in the deep crypts of benign esophageal mucus glands and non-dysplastic BE glands (Figure 1A-1B), but absent in the goblet cells within BE glands (Figure 1C). BE with HGD (Figure 1D) and SAC (Figure 1B) showed YAP1 expression in the dysplastic epithelium extending to the surface. 39.7% (23/58) of early stage EAC patients demonstrated low YAP1 expression and 60.3% (35/58) of EAC patients demonstrated high YAP1 expression. High YAP1 expression correlated significantly with the progression of invasion ($p=0.038$), but not with tumor differentiation ($p=0.279$) (Table 1). However, all poorly differentiated SAC (5/5) had high YAP1 expression. Interestingly, EAC with signet ring or mucinous differentiation had absent or very low YAP1 expression.

Category	n	Low YAP1 Expression (%)	High YAP1 Expression (%)	p Value
HGD	16	9 (56.3%)	7 (43.7%)	0.038
IMC	24	11 (45.8%)	13 (54.2%)	
SAC	18	3 (16.7%)	15 (83.3%)	
Differentiation (IMC/SAC):				
G1	20	8 (40.0%)	12 (60.0 %)	0.279
G2	17	6 (35.3%)	11 (64.7%)	
G3	5	0 (0%)	5 (100%)	

Figure 1 - 759



Conclusions: The significance of our study is two-fold. YAP1 is not expressed in goblet cells which makes it a potential biomarker for the initial diagnosis of BE. Early stage EAC demonstrates increased YAP1 expression, and high YAP1 expression might have a prognostic value due to its association with tumor progression.

760 Terminal Ileum Is the Most Sensitive Site for the Histologic Diagnosis of Grade 4 Graft Versus Host Disease (GvHD) in the Lower GI Tract and Is a Harbinger of Poor Outcome

Raymond Yip¹, David Schaeffer², Hui-Min Yang¹

¹Vancouver General Hospital/University of British Columbia, Vancouver, BC, ²Vancouver General Hospital, Vancouver, BC

Disclosures: Raymond Yip: None; David Schaeffer: None; Hui-Min Yang: None

Background: The site of the GI tract where biopsy is most likely to be diagnostic of graft versus host disease (GvHD) remains a controversial topic. The rectosigmoid colon is the preferential site of biopsy for assessment of GvHD as recent reports have indicated equal or higher sensitivity of detection compared to other sites of the lower GI tract, and biopsies can be obtained via a less invasive flexible sigmoidoscopy procedure. It is also known that while histologic grade 1-3 GvHD have correlated poorly with patients' symptoms and the overall clinical grade, patients with histologic grade 4 acute GvHD tend to have more severe clinical manifestations and a poor prognosis.

Design: In our study, we examined cases of lower GI biopsies in the past 2 years at a tertiary center in patients status post stem cell transplantation for the evaluation of graft versus host disease, which included a complete colonoscopy with ileal intubation and biopsies. The site of biopsies and the severity of GvHD were collected from pathology reports.

Results: In 6 of 22 cases, a histologic diagnosis of severe GvHD was rendered. All of these 6 patients showed histologic grade 4 GvHD in terminal ileal biopsies, while only half (3 of 6 patients) showed histologic grade 4 GvHD elsewhere in the GI tract, including the sigmoid colon. One third of patients (2/6) showed no GvHD or rare non-specific enterocyte apoptosis. Significantly, 4 of the 6 patients with histologic grade 4 GvHD diagnosed in ileal biopsies died from complication of severe GI GvHD. 15 of 16 patients without grade 4 GI GvHD are alive at follow-up, and one patient died from respiratory failure from pulmonary GvHD.

Conclusions: In our study cohort, grade 4 GI GvHD was best detected in terminal ileal biopsies, while colonic biopsies alone (including the sigmoid colon) would have detected only 50% of severe GI GvHD cases. While the histologic diagnosis of GI GvHD with the proper clinical correlate typically prompts the clinicians to initiate steroid therapy, given the poor prognosis of histologic grade 4 GvHD in the terminal

ileum, the detection of this finding may also serve to inform the clinicians that escalation or modification of treatment may need to be considered.

761 Ancillary markers for improving reproducibility of “dysplasia” diagnosis in Barrett’s Esophagus

Hira Yousaf¹, Juan Manivel², Carlos Iwamoto³, Brian Hanson⁴, Hector Mesa⁵

¹University of Minnesota, Minneapolis, MN, ²Minneapolis Veterans Administration Med Center, Minneapolis, MN, ³Minneapolis VAHCS, Minneapolis, MN, ⁴Veterans Administration Health Care System, Minneapolis, MN, ⁵Eden Prairie, MN

Disclosures: Hira Yousaf: None; Juan Manivel: None; Carlos Iwamoto: None; Brian Hanson: None; Hector Mesa: None

Background: The WHO classification of Barret esophagus (BE) is stratified into negative, indefinite, low-grade- and high-grade dysplasia/intramucosal adenocarcinoma. Dysplasia is used by gastroenterologists to determine surveillance and/or eradication strategies. Many studies have shown poor reproducibility among pathologists for diagnosing dysplasia and the ancillary studies previously reported to aid in recognizing dysplasia (P53, racemase) are not widely used due to overlapping expression in regenerative and dysplastic processes.

Design: Immunohistochemical markers involved in cell-cycle/division/differentiation and senescence: β -catenin, SATB2, cyclin D1, H2AX, Ki-67, P16, CD44 and OCT4 were applied to selected slides of 20 esophagectomy/endoscopic mucosal resection cases. Forty high-resolution micrographs of optimally oriented areas representative of all WHO classification categories were evaluated by 3 pathologists practicing in a high-volume Barrett’s Hospital. Intensity (0: negative, 1: weak, 2: moderate, 3: strong) and percentage of positive cells (0: none, 1: 1-5%, 2: 6-50%, 3: >50%) were evaluated separately in the surface, neck and crypt regions of the metaplastic glands. A staining score (intensity + % area) ranging from 0-6 was calculated for each immunostain. A consensus diagnosis was considered the gold standard. Student T-test was calculated for the aggregate staining scores of the individual markers by location (surface, neck, crypt) to determine which had the best discriminative power for dysplasia vs. no-dysplasia.

Results: Surface Ki-67 expression showed the greatest mean difference in staining score (2.7) and smallest p-value ($p < 0.001$) for differentiating dysplastic and non- dysplastic BE. Other markers with statistically significant, but lower discriminating power were surface and neck H2AX, surface and neck CD44, surface cyclin D1 and surface P16. By morphology alone, kappa correlation between individual pathologists among themselves and with the consensus diagnosis ranged from fair to substantial (0.396-0.725). Kappa correlation using Ki-67 ranged from substantial to almost perfect (0.70-0.95).

Conclusions: Surface Ki-67 expression showed a high discriminative power to separate dysplastic from non-dysplastic BE and improved greatly the kappa interobserver agreement. A retrospective validation cohort study using this parameter is currently underway.

762 Clinicopathological significance of lymphocytic colitis/collagenous colitis in inflammatory bowel disease

Lin Yuan¹, Tsung-Teh Wu², Vishal Chandan³, Yajue Huang², Lizhi Zhang³

¹Shanghai General Hospital, Shanghai Jiaotong University School of Medicine, Shanghai, China, ²Mayo Clinic, Rochester, MN, ³Rochester, MN

Disclosures: Lin Yuan: None; Tsung-Teh Wu: None; Vishal Chandan: None; Yajue Huang: None; Lizhi Zhang: None

Background: Patients with inflammatory bowel disease (IBD) may occasionally present with lymphocytic colitis/collagenous colitis (LC/CC) either before or after the onset of IBD. Although a few reports have described a small number of such cases, the relationship between these two disorders is still unclear.

Design: Patients with diagnosis of both IBD and LC/CC in last 30 years were collected in our institute. Clinical, endoscopic, and pathological features were reviewed.

Results: 27 patients were identified with both diagnosis of ulcerative colitis (UC) or Crohn’s disease (CD) and LC/CC (Table 1). 10 patients with initial diagnoses of LC (n=2)/CC (n=8) evolved into UC (n=7) or CD (n=3) after a median interval of 14 months (range, 2-44 months). 17 patients with initial diagnosis of UC (n=11) or CD (n=6) developed LC (n=5)/CC (n=12) after a median interval of 139 months (range 15-573 months). Among these, 2 patients with LC eventually evolved into CC and one CC patients changed to LC. IBD patients with initial presentation of LC/CC were significantly older than those who developed LC/CC after onset of IBD (66.5 vs.34.0 years old, $p = 0.001$). The interval time between LC/CC to IBD was significantly shorter than that of IBD to LC/CC (14 vs. 139 months, $p = 0.006$). In IBD patients with later onset of LC/CC, UC with superimposed CC was the most common pattern (n=9). Patients with CD had shorter interval time to develop LC/CC than UC patients although it was not statistically significant (62.5 vs. 158 months, $p = 0.127$). Endoscopically, most of patients started with LC/CC had unremarkable findings, but all patients who developed LC/CC after IBD showed quiescent chronic colitis. Histologically, majority of cases with initial diagnoses of LC/CC (6/10) also showed active inflammation, and when they were diagnosed with IBD, most of biopsy displayed superimposed LC/CC changes (7/10). In IBD patients developing LC/CC, all LC/CC (20/20) showed chronic mucosal injury changes

Table1. Clinical features of 27 cases with both LC/CC and IBD

Patterns	Number of cases	Gender(F/M)	Onset age (years) of initial diagnosis Median/Average(range)	Interval time(months) Median/Average(range)
LC/CC→IBD	10	6/4	*66.5/63(31~76)	#14/17.7(2~44)
LC→UC	2	2/0	69.5/69.5(64~75)	12/12(6~18)
CC→UC	5	2/3	69/64.8(47~76)	13/20(3~44)
CC→CD	3	2/1	62/55.7(31~74)	15/17.7(2~36)
IBD→LC/CC	17	13/4	*34/37.8(15~70)	#139/166.6(15~573)
UC→LC	2	1/1	22/22(21~23)	517.5/517.5(462~573)
UC→CC	9	7/2	34/27.7(15~70)	139/141.3(16~282)
CD→LC	3	2/1	24/28(21~39)	37/68(15~152)
CD→CC	3	3/0	62/58.7(46~68)	77/107(48~196)

*p=0.001, age of onset LC/CC→IBD vs. IBD→LC/CC; #p=0.006, interval time of LC/CC→IBD vs. IBD→LC/CC.

Conclusions: IBD patients with initial presentation of LC/CC tend to occur in older age, with shorter interval time and frequent active inflammation in initial LC/CC. These findings suggest that LC/CC maybe a spectrum of IBD as the initial presentation in a subset of patients with late-onset IBD. On the other hand, IBD patients can develop LC/CC associated with chronic mucosal injury many years after the onset of IBD (typically with >10 years interval time while patients are in remission phase), for which these two processes seem unrelated to each other.

763 Clinicopathological significance of immune checkpoint Inhibitor-induced colitis

Lin Yuan¹, Tsung-Teh Wu², Sarah Jenkins², Vishal Chandan³, Yajue Huang², Lizhi Zhang³

¹Shanghai General Hospital, Shanghai Jiaotong University School of Medicine, Shanghai, China, ²Mayo Clinic, Rochester, MN, ³Rochester, MN

Disclosures: Lin Yuan: None; Tsung-Teh Wu: None; Sarah Jenkins: None; Vishal Chandan: None; Yajue Huang: None; Lizhi Zhang: None

Background: Immune checkpoint inhibitors (ICPIs) are novel effective treatment for advanced malignancies. ICPI-induced colitis is an important side effect of this therapy due to nonspecific immune activation. Recently, Bim has been shown as an important regulator in mediating PD1/PD-L1 interactions in activating T cells and a predictive marker of ICPI treatment. In this study, we sought to investigate the clinical and pathological correlation and the role of Bim+ lymphocytes in ICPI-induced colitis.

Design: Among 276 patients treated with ICPIs in our institute in alst 8 years, 22 patients with ICPI-induced colitis were identified who were confirmed by clinical, endoscopic, and pathological findings. The colitis was pathologically subclassified into: quiescent colitis (QC), focal active colitis (FAC), lymphocytic colitis (LC)-like, inflammatory bowel disease (IBD)-like, and GVHD-like patterns. Immunohistochemical stain of Bim was performed and scored by counting Bim+ cells in lamina propria, crypts, and surface epithelium.

Results: The median age of these 22 cases (M:F=11:11) was 61 years (range 39.3-83.6). The median interval time between starting treatment and onset of symptoms was 58 days (range 14-379). There were 7 cases with QC, 1 FAC, 3 LC-like, 3 GVHD-like, and 8 IBD-like patterns. The number of Bim+ cells in non-QC group was significantly higher than that in QC group (median, 264 vs.59/HPF, p<0.01). The IBD-like group had the highest Bim+ cells in lamina propria compared to non-IBD group (median, 306 vs. 137/HPF, p=0.02). The overall survival of patients with colitis was better than patients without colitis, although the difference was not statistically significant (p=0.08). In

patients with colitis, the prognosis of those with late-onset colitis was significantly better than those who had early-onset colitis after treatment (cutoff interval time was 60 days, $p=0.03$). No association of Bim+ cells count with survival was observed.

Conclusions: The ICPI-induced colitis has several pathologic patterns, and the IBD-like pattern is the most common. There are more Bim+ lymphocytes in the patterns with active inflammation. The survival of patients with colitis tends to be better than those without colitis which is similar to previous reports. However, early-onset colitis is related to significantly worse prognosis. Therefore, early-onset of ICPI-induced colitis is a serious complication of ICPI therapy which needs prompt and proper management.

764 Multi-Institutional Study of Perianal Extramammary Paget's Disease: Clinicopathologic, Immunohistochemical and Molecular Features of 12 Cases

Dongwei Zhang¹, Xiuli Liu², Xuemo (Sean) Fan³, Jinping Lai⁴

¹University of Rochester Medical Center, Rochester, NY, ²University of Florida, Gainesville, FL, ³Cedars-Sinai Medical Center, West Hollywood, CA, ⁴University of Florida College of Medicine, Gainesville, FL

Disclosures: Dongwei Zhang: None; Xiuli Liu: None; Xuemo (Sean) Fan: None; Jinping Lai: None

Background: Extramammary Paget's disease in the perianal region is a rare clinical entity and may be indicative of an underlying carcinoma. It was mostly described in clinical literature as single case reports. The aim of this study was to investigate the clinicopathologic and immunohistochemical features of perianal Paget's disease (PPD).

Design: Twelve cases of PPD from University of Rochester Medical Center, University of Florida College of Medicine, and Cedars-Sinai Medical Center were collected. Clinical presentation, histology, immunohistochemistry, treatment, and outcomes were recorded.

Results: The mean age was 71.8 (range 50-86) years, with 8 males and 4 females. Clinically, the patients presented as itching and irritation of the perianal area. Physical examination showed erythema of perianal area, or mass lesion. Underlying intramucosal or invasive adenocarcinoma in the anorectal region was detected in 8 of 12 (66.7%) patients, some with mucinous or neuroendocrine features. Other tumors were also detected in those patients, including basal cell carcinoma, adrenal cortical adenomas, chronic myeloid leukemia, and follicular lymphoma.

Histologically, perianal skin showed intraepithelial infiltration by sheets and clusters of large atypical neoplastic cells with clear or pale cytoplasm. Mucicarmine stain was positive. By immunohistochemistry, the Paget's cells were positive for CK7, CK20, CDX-2, CEA, MUC1 and MUC2, and negative for GCDFP-15, mammaglobin, p63, PAX8, GATA-3, Melan-A, and SOX-10. Mismatch repair proteins were intact. Molecular studies were performed in the adenocarcinoma with neuroendocrine features. No microsatellite instability was identified by PCR. Next-generation sequencing didn't reveal any mutations. Majority of the patients received local surgical excision, some also received radiation or chemotherapy. Median follow-up was 57 months (range 4-227). Two patients had disease recurrence. Two patients developed distal metastasis. Two patients died, one from adenocarcinoma with liver metastasis, the other from progression of chronic myeloid leukemia.

Conclusions: PPD occurs in older patients with male predominance. Underlying anorectal adenocarcinoma was detected in two thirds of the patients, some with mucinous and neuroendocrine features. A panel of immunohistochemical stains is helpful for the diagnosis of PPD. Wide local surgical excision is the major treatment strategy with good prognosis. Close follow-up is recommended to monitor the disease recurrence and metastasis.

765 Clinicopathological features of Epstein-Barr virus infection, microsatellite instability, and PD-L1 expression in Chinese gastric cancer patients

Li Zhang, Peking University Cancer Hospital, Beijing, China

Disclosures: Li Zhang: None

Background: Gastric cancer is among the most common cancers worldwide. Despite declining incidences, the prognosis remains dismal in China. Recent comprehensive molecular profiling of gastric cancer proposed four molecular subtypes, Epstein-Barr virus-associated, microsatellite instable, chromosomal instable and genomically stable carcinomas. The new molecular classification will spur clinical trials exploring novel targeted therapeutics. Blockade of the programmed death 1 (PD-1) pathway has emerged as a novel therapy for cancer. Therefore, development of biomarkers for response prediction, such as PD-ligand 1 (PD-L1) expression by immunohistochemistry, may help to stratify patients. The aim of this study was to evaluate EBV, MSI, and PD-L1 immunoreexpression in Chinese gastric cancer patients and its relationship with clinicopathological characteristics. This distinction may provide prognostic information and identifies therapeutic targets.

Design: We evaluated 2042 Chinese GC patients who underwent D2-gastrectomy through immunohistochemistry for DNA mismatch repair proteins and PD-L1, and in situ hybridization for EBV detection utilizing Paraffin specimen. PD-L1 expression was classified as expression on tumor cells or on immune cells.

Results: The number of EBV-positive patients is 102 cases, which were identified in 5% of the Chinese GCs. MSI were identified in 7% of the GCs. The number of MSI patients is 143 cases. EBV positivity was associated to male gender ($P = 0.020$), proximal location ($P < 0.001$), poorly differentiated histology ($P = 0.035$) and severe inflammatory infiltrate ($P < 0.001$). PD-L1-positive was seen in 4% of cases, with predominant expression in EBV-positive GC ($P < 0.001$). EBV+ or MSI cancers showed significantly higher rates of PD-L1+ compared with EBV-/MSS cancers ($P = 0.023$). In summary, EBV+ or MSI gastric cancers are more likely to express PD-L1. Our results suggest EBV infection and MSI should be investigated for predicting response to PD-1 blockade.

Conclusions: EBV-positive GCs and MSI GC had increased PD-L1 expression, their recognition is feasible by conventional techniques, and it may help individualize follow-up and guide adjuvant therapy.

766 PD-L1 expression in microsatellite-unstable colorectal cancers

Li Zhang, Peking University Cancer Hospital, Beijing, China

Disclosures: Li Zhang: None

Background: Programmed cell death 1 (PD-1) and its ligand (PD-L1) are key suppressors of the cytotoxic immune response. PD-L1 expression on tumor cells may be induced by the immune microenvironment, resulting in immune escape, and an adverse prognosis in many malignancies. In colorectal carcinoma the response to PD-1/PD-L1 inhibition is correlated with microsatellite instability. However, little is known about the clinicopathologic, molecular, and prognostic characteristics of colorectal carcinoma with PD-L1 expression. The aim of this study was to reveal the clinicopathological characteristics of microsatellite instability-high (MSI-H) colorectal cancers showing PD-L1 positivity, which are good candidates for anti-PD-1/PD-L1 immunotherapy.

Design: The PD-L1 expression status of 84 MSI-H CRCs was retrospectively analysed using immunohistochemistry. PD-L1 positivity in tumour cells were evaluated.

Results: Programmed death ligand-1 positivity in tumour cells were observed in 11 (13%) MSI-H CRCs. Programmed death ligand-1 positivity tumours in MSI-H CRCs were significantly associated with older age ($P = 0.008$), female sex ($P = 0.040$), tumors exhibiting a larger size ($P = 0.020$), advanced TNM stage ($P = 0.030$), non-mucinous-type poor differentiation, tumour budding, and BRAF mutation ($P < 0.001$ for each).

Conclusions: These findings provide a potential mechanistic explanation for the favorable response of microsatellite-unstable colorectal carcinoma to PD-1/PD-L1 pathway blockade, and suggest potential predictive and prognostic roles of PD-L1 immunohistochemistry in colorectal carcinoma.

767 Clinicopathologic Characterization of Gastrointestinal Malakoplakia: A Rare Process Occasionally Associated with Malignancy

Yang Zhang¹, Dora Lam-Himlin², Meredith Pittman³, Kathleen Byrnes⁴, Maryam Pezhoh⁵, Zainab Alruwaili⁶, James Miller⁷, Tatianna Larman⁷, Lysandra Voltaggio¹

¹Johns Hopkins Hospital, Baltimore, MD, ²Mayo Clinic, Scottsdale, AZ, ³New York-Presbyterian/Weill Cornell Medical Center, New York, NY, ⁴Washington University in St. Louis, St. Louis, MO, ⁵Northwestern University Feinberg School of Medicine, Chicago, IL, ⁶Johns Hopkins Medical Institutions, Baltimore, MD, ⁷Johns Hopkins University School of Medicine, Baltimore, MD

Disclosures: Yang Zhang: None; Dora Lam-Himlin: None; Meredith Pittman: None; Kathleen Byrnes: None; Maryam Pezhoh: None; Zainab Alruwaili: None; James Miller: None; Tatianna Larman: None; Lysandra Voltaggio: None

Background: Malakoplakia is a rare inflammatory process presumably related to defective macrophage response to bacterial infection. Most frequently encountered in the genitourinary (GU) tract, involvement of other tissues is well known and the gastrointestinal (GI) tract is the second most common site.

Design: Fifteen cases of malakoplakia involving the GI tract were retrospectively identified from 5 institutions. Pertinent clinicopathologic features were studied.

Results: Nine patients were women (64%). Mean patient age was 66 (range 50-83). Sites included the colorectum (n=13), appendix (n=1), and stomach (n=1). Clinical indications for tissue procurement included routine endoscopic screening (n=8), tumor resection (n=4), diarrhea/weight loss (n=1) and appendicitis (1). Specimen types included 9 biopsies, 5 resections, and 1 appendectomy. All cases were

characterized by histiocytic infiltrates featuring abundant pale eosinophilic cytoplasm focally containing intracytoplasmic targetoid inclusions (Michaelis-Gutmann [MG] bodies). In cases with available stains, MG bodies were highlighted by PAS/D and Von Kossa. The process frequently involved the mucosa (n=11), with effacement of normal glandular architecture in six cases. The submucosa, muscularis propria, and serosa were respectively involved in ten, two, and three cases. All but one case had variable amounts of mononuclear cells; lymphoid aggregates were present in 11. A minority of the cases (n=4) featured a neutrophilic component. Malakoplakia was associated with invasive colorectal adenocarcinoma in 4 cases, one of which additionally showed lesional histiocytes in lymph nodes. Malakoplakia was the only abnormality seen in one appendix. The process was also associated with tubular adenomas (n=1), gastric hyperplastic polyps (n=1), and acute colitis (n=1). All but one patient with available follow up are alive and well with no additional instances of malakoplakia.

Conclusions: Malakoplakia of the GI tract is a benign, typically unexpected finding and, to the best of our knowledge, this is the largest series reported to date at this site. As in the GU tract, it may be associated with malignancy but a cause and effect relationship has not been established. Salient histologic features include a prominent histiocytic infiltrate with occasional targetoid cytoplasmic inclusions, mucosal effacement, and variable degrees of mononuclear and neutrophilic inflammation.

768 Vasculitis Involving the Gastrointestinal System is Often Incidental but Critically Important

Xiaoming Zhang¹, Emma Furth², Rashmi Tondon¹

¹Hospital of the University of Pennsylvania, Philadelphia, PA, ²University of Pennsylvania, Philadelphia, PA

Disclosures: Xiaoming Zhang: None; Emma Furth: None; Rashmi Tondon: None

Background: The clinical diagnosis of vasculitis is challenging due to its wide range of clinical presentations. More challenging is the finding of unexpected vasculitis in the gastrointestinal (GI) pathology specimens with regard to understanding its significance for treatment, outcomes and the possibility of systemic disease. This study aims to identify the significance of GI vasculitis by determining its prevalence and correlation with clinical outcomes.

Design: All GI specimens with histological evidence of vasculitis were identified by retrospective review of the pathology database over a 10-year period (Jan 2008-Aug 2018). Clinical history, treatment and follow-up were reviewed.

Results: A total of 29 cases (mean age: 48.8 years, male-to-female ratio: 1.2:1; Table) were identified (34.5% by biopsy and 65.5% by resection). Abdominal pain was the most frequent (86.2%) symptom and the most common site of involvement was in right colon (27.6%). With a mean duration of follow-up of 25.5 months, 8 (31%, 8/26) patients died, the vast majority of which (7 patients) were secondary to vasculitis related complications.

Importantly, of the 29 total cases, the majority (20/29, 69%) were not suspected clinically (Figure). Interestingly, 20% (4/20) of the patients with unexpected GI vasculitis were subsequently diagnosed with a systemic vasculitis and immunosuppressive treatment was initiated following the initial pathology diagnosis. The vasculitis was restricted to a single GI organ in 8 patients (40%), with only one patient treated with immunosuppressants following the diagnosis. Three of the 20 cases were considered as cancer-related vasculitis, for which no further treatment was given. Three cases were lost to follow-up. Importantly, 24% (4/17) of patients with this unexpected diagnosis died from direct complications of vasculitis (ischemic bowel and/or bowel perforation). Of the 4 patients who died, 2 patients died within 24 hours after the emergent bowel resection and 2 patients died 4 months after this critical diagnosis.

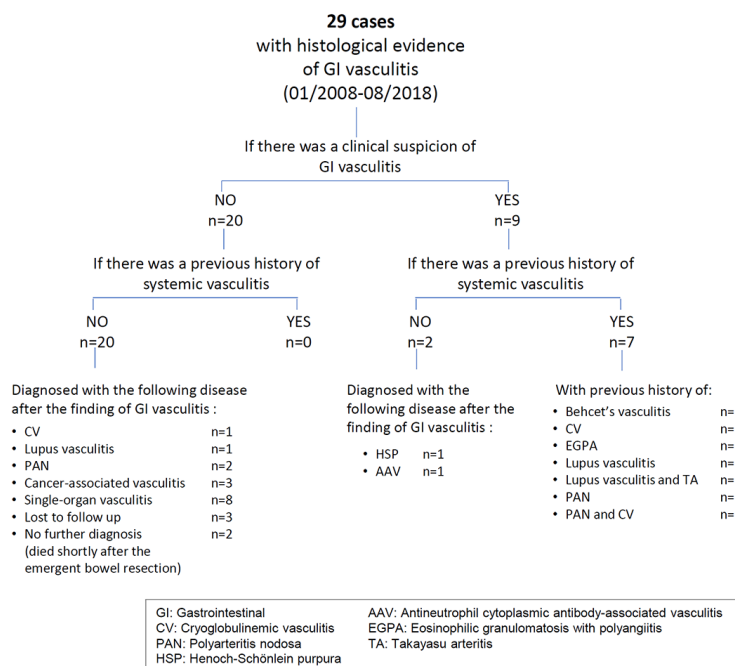
Table. Summary of clinicopathological findings of 29 patients with histological evidence of vasculitis involving the gastrointestinal (GI) system.				
Sex		Site involved by vasculitis		
Male	16/29 (55.2%)	Right colon	8/29 (27.6%)	
Female	13/29 (44.8%)	Ileum	5/29 (17.2%)	
Age		Gallbladder	5/29 (17.2%)	
Mean±SD	48.8±15.4 yrs	Left colon	4/29 (13.8%)	
Range	19-78 yrs	Transverse colon	3/29 (10.3%)	
		Small intestine, NOS	3/29 (10.3%)	
Clinical presentation		Rectum	2/29 (6.9%)	
Abdominal pain	25/29 (86.2%)	Appendix	2/29 (6.9%)	
GI bleeding	7/29 (24.1%)	Jejunum	2/29 (6.9%)	
Nausea/vomiting	5/29 (17.2%)	Sigmoid colon	2/29 (6.9%)	
Diarrhea	4/29 (13.8%)	Stomach	1/29 (3.4%)	
Fever	2/29 (6.9%)	Esophagus	1/29 (3.4%)	
Weight loss	2/29 (6.9%)	Duodenum	1/29 (3.4%)	
Asymptomatic	1/29 (3.4%)	Communication to the clinician		
Jaundice	1/29 (3.4%)	Yes	24/29 (82.8%)	
		Not documented	5*/29 (17.2%)	
Procedure		Prognosis (n=26)		
Biopsy	10/29 (34.5%)	Mean follow-up (months)	25.5±31.9 (0-121)	
Resection	19/29 (65.5%)	Death	8**/26 (30.8%)	

* 1 case didn't have a clinical suspicion of GI vasculitis; 4 cases were clinically suspected;

** The histological diagnosis of GI vasculitis was clinically unexpected in 5 cases (4 cases died from vasculitis related complications and 1 case died from cancer), and clinically suspected in 3 cases (all died from vasculitis related complications).

NOS: not otherwise specified

Figure 1 - 768



Conclusions: The diagnoses of vasculitis in the GI system carries tremendous clinical significance with 24% mortality in the critical diagnosis category. This mortality is essentially identical to that of the patients in our cohort with known vasculitis (28%). Therefore, we affirm that the diagnoses of vasculitis in the GI system continue to be treated as a true “critical value.”

769 Intricate interplay between biomarkers of gastric adenocarcinoma and their implications in prognosis and targeted therapy

Lei Zhang¹, Hongxia Sun², Junsheng Ma², Roland Bassett², Dongfeng Tan², Wenyi Luo²

¹The University of Texas MD Anderson Cancer Center, Gainesville, FL, ²The University of Texas MD Anderson Cancer Center, Houston, TX

Disclosures: Lei Zhang: None; Hongxia Sun: None; Junsheng Ma: None; Roland Bassett: None; Dongfeng Tan: None; Wenyi Luo: None

Background: Gastric cancer is one of the most common human malignancies and the third leading cause of cancer-related deaths worldwide. Despite tremendous progress has been made in understanding the cancer biology and improved clinical surveillance, prognosis remains poor due to the high rate of metastasis and recurrence, the lack of effective therapeutic regimens, and acquired chemoresistance in patients with advanced disease. In this study, we evaluated the expression of multiple biomarkers in one large cohort of patients with gastric adenocarcinoma to define their roles and correlations with disease progression, prognosis, and potential indications for targeted therapy.

Design: The study included 238 primary gastric adenocarcinoma patients who underwent surgical resection with no preoperative treatment between 1987 and 2006. High-density tissue microarrays (TMAs) were assembled from selected regions of archived formalin-fixed paraffin-embedded specimen containing viable tumor and normal tissue elements. The expressions of a battery of biomarkers including HER2, MUC5A, SOX9, CD10, SPOCK1, and PD-L1 (Dako, clone 22C3) were assessed by immunohistochemical stains. We further analyzed the expression characteristics of these biomarkers in correlation with the clinicopathologic parameters including age, race, gender, tumor type, lymph node status, and pathologic stages.

Results: We observed that MUC5AC expression (a marker for gastric foveolar differentiation) was statistically significantly associated with race (high in Asian patients, $p=0.024$) and N stage ($p=0.018$). PD-L1 expression was observed in 8.82% patients and appeared to present more likely in patients with well/moderately differentiated tumors. Interestingly, there is a reverse correlation between expression of PD-L1 and the expression levels of SOX9, a putative stem cell marker for gastric adenocarcinoma. Tumors with low level of SOX9 expression are more likely have PD-L1 positivity ($p=0.034$). Lastly, high level of nuclear expression of SPOCK1, a biomarker that involves in promoting invasion and metastasis of gastric cancer, was associated with worse overall survival (HR 1.47, CI:1.00-2.16, $p=0.05$), and positively correlated with the levels of SOX9 expression ($p=0.029$).

Conclusions: Intricate interplays between different biomarkers in regulating tumor progression are identified in one large cohort study, and these correlations may be instructive to stratify patients into appropriate regimens for more effective targeted therapy.

770 Molecular Study of Gastroesophageal Adenocarcinoma with Chromosomal Microarray and ERBB2 (HER2) FISH Assays

Jianping Zhao¹, Shelby Luikart¹, Gengming Huang¹, Jianli Dong¹

¹University of Texas Medical Branch, Galveston, TX

Disclosures: Jianping Zhao: None; Shelby Luikart: None; Gengming Huang: None; Jianli Dong: None

Background: Gastroesophageal adenocarcinoma (GEA) is often diagnosed at an advanced stage with poor prognosis. Molecular characterization of these tumors will provide important clues for further classification, prognosis, and targeted therapy. Erb-B2 receptor tyrosine kinase 2 (ERBB2/HER2) is an established biomarker for targeted therapy in the patients with advanced GEA. As a standard method to examine *HER2* gene amplification, dual probe *HER2/CEP17* fluorescence in situ hybridization (FISH) has many challenges in GEA specimens, including genetic heterogeneity and polysomy that can limit its accuracy. Chromosomal microarray has been widely used in tumor specimens and may provide an alternative method to examine *HER2* amplification.

Design: To further study molecular characteristics and *HER2* FISH assay in GEA, we performed side by side chromosomal microarray (OncoScan, Affymetrix) and *HER2/CEP17* FISH (PathVysion HER-2 DNA Probe Kit, Abbott) with seven formalin-fixed paraffin embedded (FFPE) GEA specimens. Test results, genetic profiles, and clinical features of these GEA cases were thoroughly evaluated.

Results: Seven cases included three esophageal, two gastric and two gastroesophageal junction adenocarcinomas, four of which had metastasis in lymph nodes or brains. Chromosomal microarray detected several common DNA copy number variations in these cases, including gains in chromosomes 8q/20 (6/7 cases), 2/12p/17q (5/7 cases), 13q (4/7 cases), and losses in chromosomes 18q (6/7 cases) and 9p/16p (4/7 cases). Meanwhile, six of seven cases showed the same results regarding *HER2* amplification (3 amplified, 3 not-amplified) between microarray and FISH assays. There was one case with discordant results on *HER2* status (amplified by microarray, but not-amplified by FISH).

Conclusions: Several DNA copy number variants are detected in GEA samples, which may have prognostic and therapeutic indications. The disagreement of one in seven *HER2* results between chromosomal microarray and FISH assays exemplifies similar challenges of *HER2* testing in GEA as in breast cancer. This discrepancy could be caused by methodological differences, intra-tumor heterogeneity,

and low tumor cell content in the specimen. Further studies are warranted to examine the use of chromosomal microarray in GEA specimens, especially for cases with equivocal FISH results.

771 Retrospective Analysis of Esophageal Squamous Cell Carcinoma in the USA Identified Two Major Patterns of Dysplasia

Lei Zhao¹, Vickie Jo¹, Robert Odze², Agoston (Tony) Agoston²

¹Brigham and Women's Hospital, Harvard Medical School, Boston, MA, ²Brigham and Women's Hospital, Boston, MA

Disclosures: Lei Zhao: None; Vickie Jo: None; Robert Odze: None; Agoston (Tony) Agoston: None

Background: The morphologic spectrum of esophageal squamous dysplasia has been poorly defined in western populations. Histologic criteria for esophageal squamous dysplasia were originally developed in East Asia in the 1980s. However, the spectrum of dysplasia, its morphologic and clinicopathologic correlations have been poorly defined in the USA. The purpose of this study aims to evaluate systematically the spectrum of dysplastic change in a population of patients from the USA to better define the morphologic and clinical associations.

Design: Surgical resection cases for untreated squamous neoplasia were identified from surgical pathology archives (1990-2015), and all slides were reviewed and morphologic features of dysplasia were recorded. Comparison of categorical variables was performed using the Fisher exact test.

Results: 58 esophageal resections of squamous neoplasia without neoadjuvant treatment were identified. The patient group included 30 males and 28 females, with mean age 67.6 years (range 47-81). Overall, two major patterns of dysplasia were observed: non-keratinizing type (N=27 cases, Fig 1) and keratinizing type (N=13, Fig 2). Non-keratinizing type dysplasia appeared as a basaloid proliferation with mild to prominent cytologic atypia. Rare examples of basal discohesion/basal layer splitting (Fig 1D), dysplasia associated with epidermoid metaplasia (Fig 1E) and dysplasia associated with squamous metaplasia of columnar epithelium at GEJ (Fig 1F) were also observed in this category. Non-keratinizing dysplasia was associated with younger age, with smaller tumor size and lower T stage, and basaloid differentiation in the invasive carcinoma (see Table). Keratinizing type dysplasia was characterized by a proliferation of larger atypical squamous cells showing keratinization and marked dyskeratosis/hyperkeratosis. Some cases showed glassy cytoplasmic change (Fig 2E-F) but without significant cytologic atypia. Keratinizing type dysplasia was associated with well-differentiated and verrucoid invasive SCC, and larger tumor size (see Table).

Table: Association between different types of dysplasia and clinicopathological features.

	Non-keratinizing Dysplasia (Odds Ratio)	Keratinizing Dysplasia (Odds Ratio)
Age >70 years	0.16 ***	2.64
Distal location in the esophagus	0.53	4.00
Size of invasive carcinoma (cm)	0.07 ***	5.29 *
Stage of tumor >T2	0.12 ***	0.30
Positive lymph node status	1.18	0.33
Morphology of invasive SCC		
Keratinizing	0.22 *	17.5 ***
Non-keratinizing	0.48	0.48
Basaloid differentiation	>100 ***	<0.01 *
Verrucous/bluntly invasive	<0.01	>100 ***

*p<0.05 **p<0.01 ***p<0.005

Figure 1 - 771

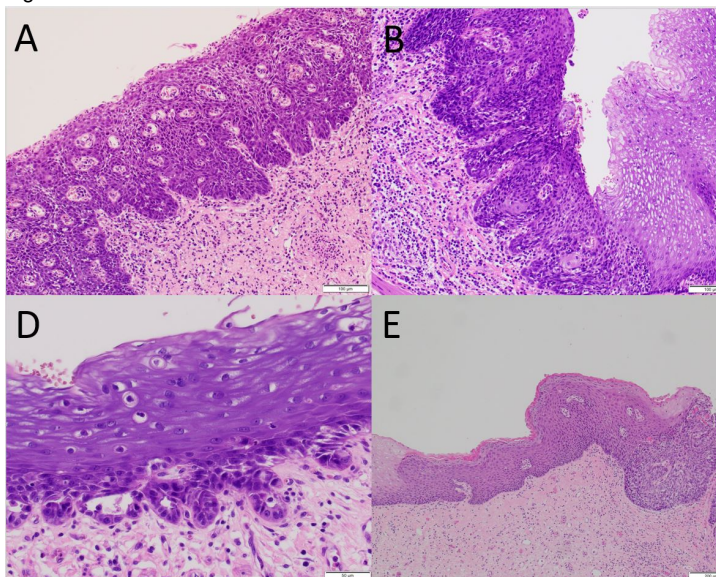
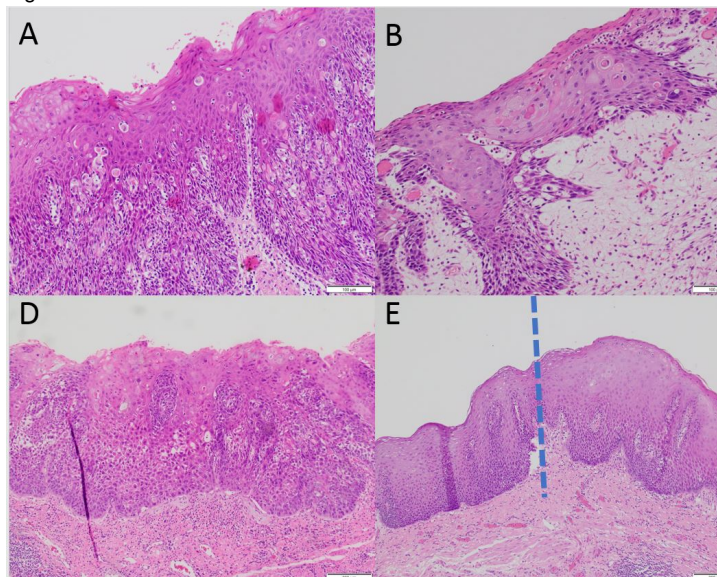


Figure 2 - 771



Conclusions: In this western-based population, squamous neoplasia of the esophagus demonstrates a wide spectrum of precursor changes, analogous to the upper aerodigestive tract. Understanding the range of dysplastic changes facilitates more accurate diagnosis and may provide valuable information about the associated invasive tumor when the latter is not adequately sampled.

772 Prognostic Value and Clinicopathological Correlation of High-Risk HPV in Anal Squamous Cell Carcinoma

Xiaoqin Zhu¹, Azniv Azar², Xiuling Meng³, Karen Dresser⁴, Lloyd Hutchinson⁵, Jacob Bledsoe⁴

¹UMass Memorial Medical Center, Shrewsbury, MA, ²University of Massachusetts Medical School, Worcester, MA, ³UMass Medical School, Worcester, MA, ⁴UMass Memorial Health Care, Worcester, MA, ⁵UMass Memorial Health Care, Worcester, MA

Disclosures: Xiaoqin Zhu: None; Azniv Azar: None; Xiuling Meng: None; Karen Dresser: None; Lloyd Hutchinson: None; Jacob Bledsoe: None

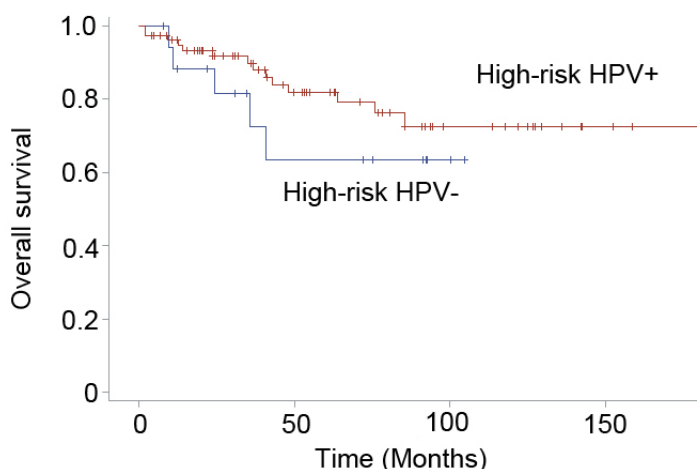
Background: Anal squamous cell carcinoma (SCC) accounts for 1-2% of gastrointestinal malignancies and the incidence has increased 2.2% per year over the last 10 years. Persistent infection with high-risk human papillomavirus (HPV) is strongly associated with the development of anal SCC. We investigated the prognostic value and clinicopathologic correlation of HPV in anal SCC.

Design: 97 cases of anal SCC were identified from 2000 to 2017. FFPE tissue from carcinoma samples was tested for HPV16 or 18 DNA using the Cervista Invader Assay (Hologic). Morphology of 52 cases was reviewed by two pathologists. Multivariable overall survival was performed using Kaplan-Meier method and Cox proportional hazards model. Correlations between high-risk HPV and clinicopathological factors were analyzed by t-test and Chi-square test.

Results: Seventy-nine of 97 (81%) patients with anal SCC were positive for HPV16, and one was positive for both HPV16 and 18. Among the HPV+ cases, 55 were females and 24 were males. Patients with HPV16+ anal SCC were significantly younger than patients with HPV16- anal SCC (mean age of 55 vs. 61; $p = 0.016$). Gender, T stage and disease-free status were not significantly associated with HPV16 status ($p = 0.11$, 0.91 , 0.79 and 0.15 , respectively). A trend toward better overall survival was noted among patients with HPV+ SCC, however multivariable analysis did not reach significance (Figure 1; $p = 0.21$). Fourteen of 15 cases with basaloid morphology were associated with HPV16 and one case with adenoid cystic-like features was associated with non-HPV16/18 high risk HPV. Out of 37 cases of non-basaloid SCC, 29 cases, including 22 cases of conventional non-keratinizing and 7 cases of keratinizing SCC, were HPV16+. Basaloid and non-keratinizing SCC were more likely to be HPV16+ compared to keratinizing SCC ($p = 0.036$).

Figure 1 - 772

Figure 1. Kaplan-Meier Curve for overall survival of patients with high-risk HPV+ vs. HPV- anal squamous cell carcinoma.



Conclusions: Basaloid and conventional non-keratinizing SCC were highly associated with high-risk HPV. A trend toward improved clinical outcome in patients with HPV16 was noted but did not reach statistical significance. Positive HPV is related with younger age but had no impact on clinical stage, disease free status, or overall survival. A significant subset (19%) of anal SqCC cases was negative for HPV16 and 18. Further evaluation of these cases with non-HPV16/18 high-risk HPV testing and genetic analysis is needed for further elucidation of their pathogenesis.

773 Appendectomy Status is Associated with Distinct Molecular and Microbiota Profiles in Colorectal Carcinomas Based on Comprehensive Molecular Testing by Hybridization Capture Next-Generation Sequencing

Menglei Zhu¹, Wei Xin², Sumit Middha¹, Jaclyn Hechtman¹, Maria Arcila¹, Chad Vanderbilt³

¹Memorial Sloan Kettering Cancer Center, New York, NY, ²Case Western Reserve University, Cleveland, OH, ³Memorial Sloan Kettering Cancer Center, Denver, CO

Disclosures: Menglei Zhu: None; Wei Xin: None; Sumit Middha: None; Jaclyn Hechtman: None; Maria Arcila: None; Chad Vanderbilt: None

Background: Recent studies have shown that the appendix plays a key role in immunological processes and microbiome reconstitution in the gastrointestinal system. Preliminary findings from a previous study suggest that patients with history of appendectomy may have higher rates of subsequent right side colorectal carcinoma (CRC) compared to the general population. CRCs diagnosed after appendectomy also shows distinct features with higher proportion of mucinous component, higher rate of mismatch repair deficiency and lower rate of lymph node involvement. Molecular patterns in CRC diagnosed post appendectomy have not been studied.

Design: We reviewed all primary right side colorectal carcinoma resection cases submitted for molecular pathology testing during 2015-2018. Comprehensive molecular profiles including mutations, copy number alteration, MSI status and tumor mutation burden (TMB) of these tumors were analyzed by a hybridization based 468 cancer-associated genes next-generation sequencing (NGS) assay. Hybrid capture Off-Target Mapping to microbial genomes from NGS data, as described in previous study, is used to evaluate microbiota profile.

Results: 26 CRC were diagnosed after appendectomy and 215 CRC without history of appendectomy were identified. 322 and 458 mutations are identified in cases with and without appendectomy, respectively. Mutation rates in CRC diagnosed post appendectomy and without history of appendectomy are as follows: TP53 (73% vs 52%), KRAS (58% vs 49%), FBXW7 (50% vs 21%), BRAF (42% vs 21%), PIK3CA (37% vs 38%), and KMT2D (42% vs 26%). Amplifications in MYC (12%) and FLT3 (8%) were the most frequent copy number alterations in post appendectomy cases. 38.4% of cases with appendectomy were MSI instable comparing with 32.5% in right side CRC without appendectomy. Mean TMB is higher in cases with previous appendectomy (68.6 vs 28.9, $P < 0.01$). A set of 10 microbial genes, which were shown to associate with CRC are evaluated. Significantly more of these microorganisms are identified in cases without previous appendectomy (82 in 215 cases) than cases with appendectomy (4 in 26 cases) ($P < 0.05$).

Conclusions: Conclusion: We observed a different molecular and microbiota profile in primary right side CRC with previous history of appendectomy compared with cases without appendectomy. These results suggest that appendectomy might play a role in CRC pathogenesis by modulating microbiological and immunological microenvironment in gastrointestinal tract.

774 Useful Histomorphologic Features of Gastrointestinal Poorly-Cohesive Carcinomas at the Time of Frozen Section

Xiaoqin Zhu¹, Jacob Bledsoe²

¹UMass Memorial Medical Center, Shrewsbury, MA, ²University of Massachusetts Medical School, Worcester, MA

Disclosures: Xiaoqin Zhu: None; Jacob Bledsoe: None

Background: Frozen section examination of carcinomas with poorly-cohesive growth, including signet ring cell carcinoma, is challenging. Due to their diffuse morphology, the tumor cells may be indistinct and difficult to distinguish between inflammatory or stromal cells. Misdiagnosis may result in significant adverse clinical outcome. We therefore performed a detailed retrospective analysis of such cases to identify features that are helpful to avoid misdiagnosis at the time of frozen section.

Design: We reviewed original frozen section slides from 32 cases (56 distinct specimens) positive for diffuse/poorly-cohesive carcinoma, and frozen section slides of 20 gastroesophagectomy margins negative for carcinoma for comparison. The 32 positive cases comprised 3 lymph nodes, 4 ovaries, 7 gastroesophageal margins and 18 peritoneal biopsies. The origins of carcinoma were stomach (22 cases), appendix (4 cases), colon (3 cases) unknown primary (1 case), and lung (2 cases). Tumor cells and benign inflammatory cells were evaluated for 16 distinct cytologic, 9 architectural, and 3 stromal features (Table 1). Cytologic features were scored by two gastrointestinal pathologists as present (>10% of cells), occasional (<10%), or absent. Architectural and stromal features were scored as present or absent.

Results: Of the 32 cases positive for carcinoma, 4 (12.5%) were misdiagnosed as negative at the time of frozen section. The sensitivity and specificity of histopathologic features for carcinoma are presented in Table 1. Disruption/obliteration of normal structures was the most sensitive (91%) and specific (100%) feature. Other features with 100% specificity for carcinoma included intracytoplasmic mucin vacuoles, foamy cytoplasm, crescent/indented nuclei, hyperchromatic nuclei, prominent nucleoli, multinucleation, nuclei 8x the size of a small lymphocyte, focal gland formation, perineural invasion, and mitotic figures. Other useful features with at least 75% sensitivity and specificity included the presence of many nuclei >4x the size of small lymphocytes, and background fibrosis.

Table 1: Sensitivity and specificity of morphologic features to identify poorly-cohesive carcinomas on frozen sections.

Features		Sensitivity %	Specificity %
Cytoplasmic features	Mucin vacuoles	69	100
	Foamy cytoplasm	53	100
	Pink granular cytoplasm	53	70
	Distinct cell borders	22	65
Nuclear features	Irregular nuclear contours	88	50
	Eccentric nuclei	66	55
	Crescent/indented nuclei	47	100
	Prominent nucleoli	50	100
	Multinucleation	38	100
	Mitotic figures	28	100
	Anisonucleosis (4:1)	47	95
	Many nuclei >4x size of small lymphocytes	75	85
	Occasional nuclei >6x size of small lymphocytes	63	95
	Occasional nuclei >8x size of small lymphocytes	44	100
	Vesicular or finely granular chromatin	81	60
	Hyperchromatic nuclei	44	100
Architecture	Variability in overall cell size	25	90
	Disordered hypercellularity	81	30
	Focal gland formation	22	100
	Short lines of cells	75	15
	Small clusters	94	15
	Retraction features	0	0
	Infiltrating stroma	97	35
	Extracellular mucin	22	85
	Perineural invasion	6	100
Stromal response	Disrupted/obliterated normal structures/stroma	91	100
	Extending through muscularis mucosae (gastric margins)	97	35
	Fibrotic response	75	75

Conclusions: We characterized useful histologic features of poorly-cohesive carcinoma that may serve to avoid false negative interpretation and distinguish between benign inflammatory cells at the time of frozen section. Knowledge of these features may help surgical pathologists avoid misdiagnosis resulting in significant clinical morbidity.

775 Kayexalate Colitis: Correlation of the Pathological, Clinical and Pharmacological Features

Yonah Ziemba¹, Mallorie Angert², Aya Haghamad¹, Dana Razzano³, Hector Chavarria Bernal¹, Aryeh Stock, Kalpana Reddy⁴, Margaret Cho⁵, Taisia Vitkovski⁶, Alex Williamson⁷, Arvind Rishi⁸

¹Northwell Health, New Hyde Park, NY, ²Donald and Barbara Zucker School of Medicine at Hofstra/Northwell, Lake Success, NY, ³New York Medical College, Valhalla, NY, ⁴Northwell Health, Garden City, NY, ⁵Donald and Barbara Zucker School of Medicine at Hofstra/Northwell, Flushing, NY, ⁶Lake Success, NY, ⁷Zucker School of Medicine at Hofstra/Northwell, New Hyde Park, NY, ⁸Northwell Health, New York, Lake Success, NY, Mount Sinai, New York, NY

Disclosures: Yonah Ziemba: None; Mallorie Angert: None; Aya Haghamad: None; Dana Razzano: None; Hector Chavarria Bernal: None; Kalpana Reddy: None; Margaret Cho: None; Taisia Vitkovski: None; Alex Williamson: None; Arvind Rishi: None

Kayexalate, a common therapy for hyperkalemia, has been implicated in bowel necrosis including cases of perforation and death. Despite the seriousness of this effect, the literature describing the pathological and clinical features is very limited, and the dose and time course of the Kayexalate administration is not well characterized. The goal of this study is to assess the association between Kayexalate and the development of bowel necrosis and to describe all cases of Kayexalate-associated injury encountered at our health system.

Design: A retrospective review of electronic medical records was performed in a large health system over a six year period (2012- 2018). Clinical record was reviewed for all patients in whom Kayexalate crystals were identified in their pathology report. Patients were tabulated to analyze clinicopathological features, demographics and patient risk factors. Pharmacy records were reviewed to confirm drug administration and to assess time and number of doses.

Results: 48 patients were identified to have Kayexalate crystals in their pathology report. Only 16 of those had drug administration confirmed in the pharmacy records, (Table 1). 14 were surgical cases and 2 were autopsy cases. The surgical cases all had ileocolonic involvement, while the autopsy cases were both upper GI. All but two cases had Kayexalate-associated injury, including ischemic-colitis pattern, active colitis, and ulcer. In the remaining two, both with multiple doses, crystals were associated with a tubular adenoma and gastric mucosa with no associated injury, respectively. The last dosage was within five days of procedure in 13 cases (80%).

PT	Doses	Most recent dose (days)	Site	Mucosal injury	Indication	Risk factors	Comment
1	4	1	Hepatic flexure	No	Hematochezia	postop	hypothyroid, HTN, Diabetes
2	1	1	Ascending colon	Yes	Weight loss	CKD	Kidney transplant, HTN
3	3	14	Ileocecal valve	Yes	Hematochezia	CKD	Dialysis dependent, CHF, HTN
4	1	4	Colon	Yes	Ischemic bowel status post MI	postop and CKD	recent nephrectomy for malignancy, myocardial infarct during surgery
5	1	2	ileum, cecum, and appendix	Yes	Cecal pneumatosis	postop	Recent bypass revision for PAD
6	1	3	Descending colon	Yes	Abdominal distension and pain, abnormal CT	CKD	CKD, CAD, PVD, diabetes
7	1	2	Ascending colon	Yes	hematochezia	CKD	Chronic renal failure, bladder cancer
8	2	4	Ascending colon and hepatic flexure	Yes	Anemia, fecal occult blood	none	Lung cancer, HTN
9	1	1	Ascending, transverse and descending colon	Yes	Diarrhea, anemia, fecal occult blood	postop and CKD	Kidney transplant, Hep C, PAD
10	1	4	Sigmoid colon	Yes	dysphagia, diarrhea, gastritis	CKD	CKD, diabetes, HTN
11	3	2	Terminal ileum, appendix and portion of colon	Yes	Abdominal pain, pneumatosis seen on CT	postop	Neuroendocrine metastasis to liver and bone s/p chemo, tumor lysis syndrome
12	1	2	Cecum	Yes	GI bleed.	postop and CKD	CAD, Anemia 2/2 CKD, diabetes
13	1	6	Colon, sigmoid and rectum	Yes	anemia GI bleed	postop and CKD	Retroperitoneal mass, malignant pleural effusion, CAD
14	3	7	Hepatic flexure	Yes	n/a	CKD	SLE glomerulonephritis syndrome, Kidney transplant
15	2	2	Stomach	No	Autopsy	none	Diabetes, HTN
16	2	4	Stomach	Yes	Autopsy	CKD	Alcohol dependency, alcoholic hepatitis,

Conclusions: These findings highlight the complexity of Kayexalate diagnosis. Crystal deposition in the GI tract is sometimes a non-pathogenic, incidental finding. The 32 cases in which crystals resembling Kayexalate were found without record of drug administration raise the possibility that there may be unknown drug mimics. Autopsy data is a useful, under-recognized source of information that can be used to determine whether a finding can exist in asymptomatic patients. In our cases, crystals were more likely to be pathogenic when found in the colon and less likely when found in the stomach, but the number of doses did not correlate with extent of injury.